An examination of the neuroimmune interactions of amitriptyline, spinal cord stimulation and opioid therapy in human neuropathic pain

TRINITY COLLEGE DUBLIN

Dr Jonathan Royds

MB, BCh, BAO, BA, MRCS, FCAI, EDRA, FPMCAI, FIPP, MD

A thesis submitted in partial fulfilment of the requirements for the degree of Doctor in Medicine at Trinity College Dublin

Date Accepted: 09/02/2021

Declaration

I declare that this thesis has not been submitted as an exercise for a degree at this or any other university and it is entirely my own work.

I agree to deposit this thesis in the University's open access institutional repository or allow the library to do so on my behalf, subject to Irish Copyright Legislation and Trinity College Library conditions of use and acknowledgement.

Signed _____Jonathan Royds_____

Student Number: 02392569

Date

_____13/02/2021_____

Summary:

Background:

The objective of this thesis was to explore mechanistic processes of amitriptyline, opioids and 'Burst' spinal cord stimulation (SCS) for neuropathic pain *in vivo*. These three therapies are commonly employed for the management of neuropathic pain without a global agreed consensus with regard to mechanism of action. Whilst there is growing body of pre-clinical evidence supporting the concept that chronic neuropathic pain is associated with neuroimmune dysfunction and / or neuroinflammation, this has yet to be translated into the clinical domain. Epidural steroid injections have demonstrated an attenuation of neuroinflammation associated with a short-term reduction in pain. To demonstrate dynamic changes within the neuroimmune interface (neuronal-glia-immune cell communications) we compared the constituents of cerebrospinal fluid (CSF) before and after treatment with amitriptyline and Burst SCS. The mechanisms and side effects of opioids proposed for chronic pain are also related to neuroimmune interactions. Due to the fact many patients were taking opioids before enrolment, we compared the CSF of patients taking and not taking opioids prior to commencing the proposed interventional treatment. Not only would this provide data of confounding variables but give insight into opioid related phenomena and mechanisms. A more detailed characterisation of the effects of currently employed therapies may facilitate better stratification and phenotyping; as well as providing information which may enhance our understanding of the pathophysiology of neuropathic pain.

Methods:

This study involved taking cerebrospinal fluid samples before and after treatment and determining the cellular constituents of central peptides and immune cells. Patients were screened for neuropathic pain at outpatient clinics at St. James's Hospital, Dublin and enrolled according to strict inclusion/exclusion criteria of the individual study. Lumbar radicular pain was the most common diagnosis for enrolled patients. Demographics and pains scores according to numerical rating scale (NRS) were recorded. After a baseline CSF sample the interventional treatment was commenced for 8 weeks. A second sample was subsequently taken after 8 weeks of treatment as well as outcome data. We compared the baseline and post intervention samples examining cellular data of T cells via flow cytometry, specific neuropeptides by ELISA and the proteome via Mass Spectrometry. *In vitro* work was also performed to examine the effect of amitriptyline on T cells directly.

Results:

In a cohort of patients with lumbar radicular pain who were deemed responders to amitriptyline, GO analysis identified immune system process as the most modulated proteins. This was associated with an attenuation of pro-inflammatory pathways, including the MAPK pathway identified by KEGG analysis. The chemokine eotaxin-1 was also significantly reduced in responders to amitriptyline. *In-vitro* work on T cells demonstrated an attenuation of the TH1/Th17 response and a modulation of other cytokine networks. This was largely in naïve populations however postulating that peripheral and central actions of amitriptyline may differ.

According to GO analysis proteins related to synapse assembly were the most modulated after Burst-SCS. This is consistent with neurophysiological data that suggests burst neuronal firing strengthens synaptic transmission and efficacy. Individual protein analysis also indicated that Burst SCS demonstrated potential supraspinal effects and modulation of immune effectors.

GO analysis identified expression of proteins related to positive regulation of nervous system development and myeloid leucocyte activation in patients medicated with opioids. The largest decrease expression of proteins in the patients medicated with opioids related to neutrophil mediated immunity.

Conclusion:

Although effective, no treatment achieved full remission of symptoms in any patient. This would suggest that current therapies only target selective pathways involved in the pathophysiology of neuropathic pain. Although evidence of immuno-modulation was present with all therapies examined; this was not consistent. We have demonstrated that immune effectors or neuro-glial communications are likely contributory in the pathogenesis and attenuation of neuropathic pain. What is also evident was molecular evidence of neuroplasticity which involves many pathways and cells within the central nervous system. The chronicity of pain in humans is inherently complex but advances in technology with CSF analysis and neuroimaging in conjunction with sham/placebo-controlled trials will enable better phenotyping of patients and a better understanding of treatment mechanisms and the pathophysiology of neuropathic pain.

Acknowledgements: I want to give special thanks to my two supervisors Dr Joanne Lysaght and Professor Connail McCrory for their guidance through these last four years. They provided me with continued enthusiasm and support during difficult periods while allowing me to personally work through obstacles and to ensure the work and thinking were my own ideas. I would secondly like to thank all of the patients for taking part in this research and willingly giving spinal fluid samples.

I would like to thank the College of Anaesthesiologists of Ireland for providing me with a grant to carry out this research.

I would like to recognise my collaborators within this work including Dr Hilary Cassidy and her team in Systems Biology Ireland for helping us with proteomic analysis. I also extend equal thanks to Dr Joanne Lysaght's lab in Trinity college for all of their support throughout all of the work within this thesis. This includes Dr Melissa Conroy and Dr Margaret Dunne for their guidance during the critical time of sample analysis. I would also like to thank all of the staff in the day ward in St James's hospital. Their support in allowing me to do assessments and carry out my work was incredibly altruistic and frequently increased their work load on a daily basis. Consideration should also be given to my colleagues including Dr Joseph Fitzgerald, Dr Basabjit Das and Dr Aine O'Gara who covered for me during sample analysis and helped in recruitment of patients for this work.

Lastly, I would like to thank my co-authors who are all mentioned above in the process of getting the work published in peer reviewed journals to contribute to the science of chronic pain.

Funding:

This thesis was supported by an academic grant awarded by the College of Anaesthesiologists of Ireland in 2016.

Quotes:

Civilization no longer needs to open up wilderness; it needs wilderness to help open up the still largely unexplored human mind.

David Rains Wallace *The Dark Range: A Naturalist's Night Notebook (1978)*

I don't see rats in my clinic

Connail McCrory

This thesis is supported by the following research articles:

Published:

Royds J, McCrory C. Neuroimmunity and chronic pain. Bja Education. 2018 Dec 1;18(12):377-83.

Royds J, Cassidy H, Conroy MJ, Dunne MR, Lysaght J, McCrory C. Examination and characterisation of the effect of amitriptyline therapy for chronic neuropathic pain on neuropeptide and proteomic constituents of human cerebrospinal fluid. Brain, Behavior, & Immunity-Health.;10:100184.

Royds J, Conroy MJ, Dunne MR, McCrory C, Lysaght J. An investigation into the modulation of T cell phenotypes by amitriptyline and nortriptyline. European Neuropsychopharmacology. 2020 Feb 1;31:131-44.

Royds J, Conroy MJ, Dunne MR, Cassidy H, Matallanas D, Lysaght J, McCrory C. Examination and characterisation of burst spinal cord stimulation on cerebrospinal fluid cellular and protein constituents in patient responders with chronic neuropathic pain-A Pilot Study. Journal of Neuroimmunology. 2020 Apr 22:577249.

Royds J, Cassidy H, Conroy MJ, Dunne MR, Matallanas D, Lysaght J, McCrory C. An Investigation into Proteomic Constituents of Cerebrospinal Fluid in Patients with Chronic Peripheral Neuropathic Pain Medicated with Opioids-a Pilot Study. Journal of Neuroimmune Pharmacology. 2020 Nov 20:1-7.

Abbreviations:

A: amitriptyline; **AGT**: angiotensinogen; **BBB**: blood brain barrier; **BDNF**: brain derived neurotrophic factor; **CALB1**: calbindin; **CARTPT**: cocaine and amphetamine-regulated transcript protein; **CBLN3**: cerebellin-3; **CCK**: cholecystokinin; **CDC**: centre of disease control; **CGRP**: calcitonin gene related peptide; **CNP**: chronic neuropathic pain; **CNS**: central nervous system; **COX**: cyclo-oxygenase; **CPNP**: chronic peripheral neuropathic pain; **DBI**: acyl-CoA binding protein; **DNA**: deoxyribonucleic acid; **DN4**: dolour neuropathique 4; **DRG**: dorsal root ganglion; **ECT**: electro-convulsive therapy; **EEG**: electroencephalography; **ELISA**: enzyme-linked immunosorbent assay; **EMG**: electromyography; **END3**: endothelin-3; **ERK**: extracellular-signal-regulated kinase; **FACS**: fluorescence-activated cell sorting; **FBSS**: failed back surgery syndrome; **FDR**: false discovery rate; **FGD-PET**: fluorodeoxyglucose positron emission tomography; **FNSS**: failed Neck Surgery Syndrome; **GDNF**: glial cell derived neurotrophic factor; **GO**: gene otology; **HCD**: high-energy collision dissociation; **IPA**: Ingenuity Pathway Analysis; **IPG**: implantable pulse generator; **JAK/STAT**: janus kinases/signal transducer and activator of transcription proteins; **KEGG**: kyoto encyclopaedia of genes and genomes; **KNG1**: kininogen-1; **LCF**: lymphocyte chemoattractant factor; **LP**: lumbar puncture; **MAPK**: mitogen-activated protein kinase; **MME**: milligram morphine equivalent; **MRI**: magnetic resonance imaging; **MS**: mass spectrometry; **N**: Nortriptyline; **NF-kβ**: nuclear factor kappa beta; **NGF**: Nerve growth factor; **NMDA**: N-methyl-D-aspartate; **NNH**: Number needed to harm; **NNT**: Number needed to treat; **NUCB2**: nucleobindin-2; **NRS**: Numerical Rating Pain score; **PBMCs**: Peripheral blood mononuclear cells; **PCSK1N**: proSAAS; **PENK**: proenkephalin-A; **PI:** propidium iodide; **PI3K-Akt**: phosphatidylinositol 3-kinase protein kinase B; **PRL**: growth hormone A1; **PTMs**: post-translational modifications; **QST**: quantitative sensory testing; **RNA**: ribonucleic acid; **SEM**: standard error of means; **SNRI's**: Selective Noradrenaline Reuptake Inhibitors; **SSRI's**: Serotonin reuptake inhibitors; **SST**: somatostatin; **SUV**: standardised uptake value; **TARC**- thymus and activation regulated chemokine; **TMB**: tetramethylbenzidine; **TLR**- toll like receptor; **TSPO**: Translocator Protein; **VAS**: Visual Analogue Scale; **VC:** Vehicle Control; **VEGF**: Vascular epidermal growth factor; **WDR**: Wide dynamic neurons

Table of Contents

List of Figures:

List of Tables:

Chapter 1 Introduction

1.1 Chronic Pain

Chronic pain has been recognized as pain that persists past normal healing time and hence no longer provides the benefit of physiological nociception to aid tissue repair (1). It has become maladaptive and thus is described as a disease of the nervous system (1). Pain is usually regarded as chronic if it has persisted for more than three months (1). Nociception is the process by which peripheral stimulation encodes a neural process of noxious stimuli activation resulting in pain perception (2) [Figure 1].

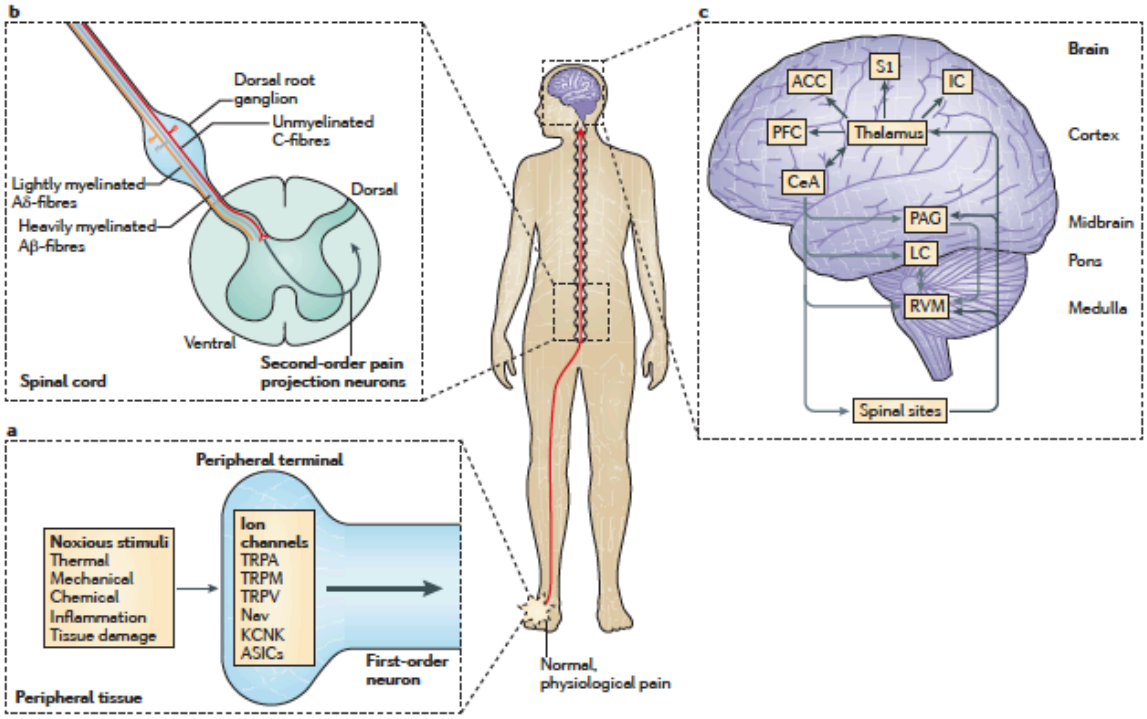

Figure 1: The physiological process of Nociception: A stimulus in the periphery is transduced by clustered ion channels illustrated in (a). Action potentials are then conducted along axons to the soma or Dorsal root ganglion (DRG) which then pass to the dorsal horn and form presynaptic end terminals in image (b) with interneurons and second order neurons. This starts with first order peripheral neurons being activated leading to transmission to the spinal cord where second order neurons are activated. Second order neurons then join ascending fibres in the anterolateral system and project to the brainstem and thalamus. Pain is carried by spinothalamic tracts which decussate several segments after their entry level. Third order neurons then project to several cortical regions via medial and lateral thalamocortical tracts that encode sensory information on pain, e.g. the somatosensory cortex (S1), emotional components of pain: anterior cingulate cortex (ACC) and cognitive: pre-frontal cortex (PFC). Signals undergo modulation at multiple sites to change the nature of a stimulus at the Dorsal Root Ganglion (DRG), dorsal horn and cortical structures. [Figure from Grace et al, Pathological pain and the neuroimmune interface, Nature Reviews, 2014 (3)]

Nociception is defined as the sensory nervous system's response to certain harmful or potentially harmful stimuli (4). Nociceptors are sensory nerve cells that produce a signal to noxious stimuli. Nociceptors are generally silent and will transmit all or none action potentials to higher centres. Nociception can be explained physiologically by activation of first order neurons in response to tissue injury from pressure, temperature, mechanical and chemical receptor activation. A signal is then transduced to second order neurons in the dorsal horn and then to our brain via third order neurons where we experience pain [Figure 2].

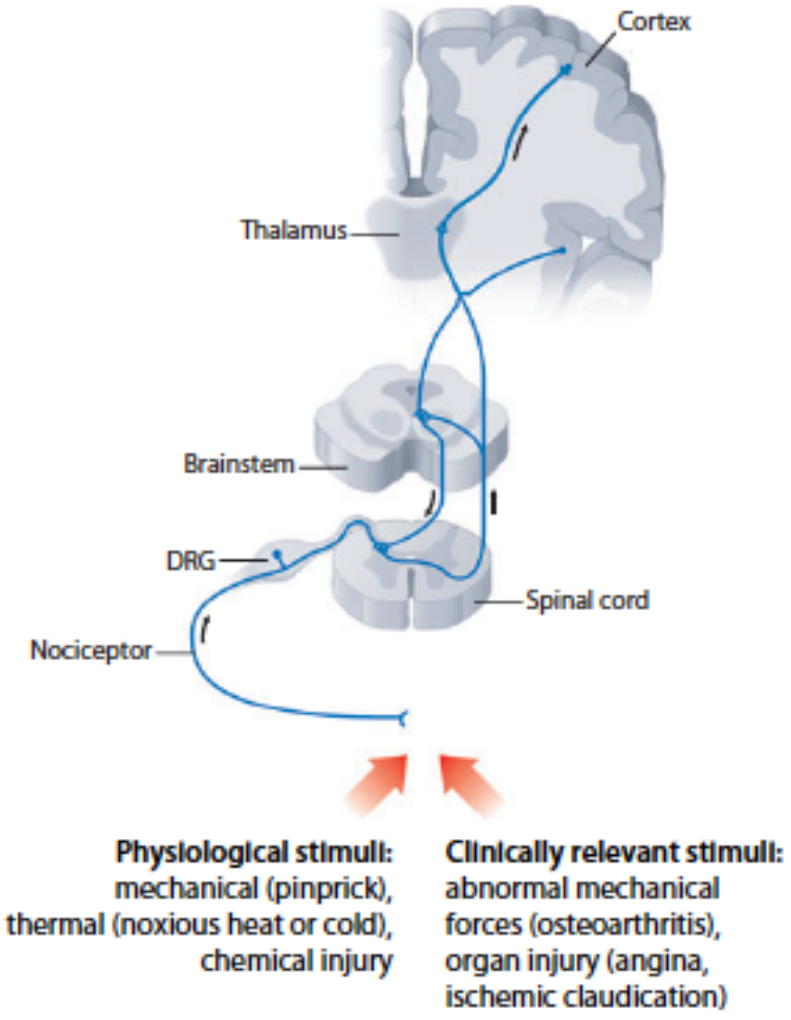

Figure 2: Diagrammatic illustration of nociception: Note descending inhibition from the thalamus that modulates sensory information to higher centres. [Figure from Costigan et al, Annual Reviews in Neuroscience 2009 (5)]

Despite this widely presented representation there are complexities to nociception that are not fully understood. These include mechano-transduction, nociceptor heterogeneity and the modulation of these signals in the dorsal horn and brain particularly in patients with chronic pain (4). Afferent neurons that transmit nociception include C fibres which are unmyelinated and conduct at a slow velocity. C fibres synapse to second order neurons in the dorsal horn and are polymodal, meaning they react to a variety of stimuli from thermal, mechanical and chemical stimuli (6). Other first order neurons include A-delta fibres that are myelinated and have a much higher conduction velocity compared to C fibres (4).
A-delta and C fibres synapse with second order neurons and Wide dynamic neurons (WDR) in the dorsal horn. WDR neurons can induce prolonged responses to different stimuli which are maintained after the stimulus has ended resulting in 'wind up'. This phenomenon is generated by plasticity with synapses that have been implicated in the chronicity of neuropathic pain (7). WDR are thought to trigger the lateral pain pathway to the primary sensorimotor cortex, posterior insular and secondary somatosensory cortex (8). The lateral pain pathway is implicated in our perception of pain while the medial spinothalamic tract (medial pathway) is more associated with the emotional components of pain including fear and avoidance (9, 10). Pain sensations are processed in the spinothalamic tract and thalamocortical projections by medial and lateral pain pathways (10) [Figure 3].

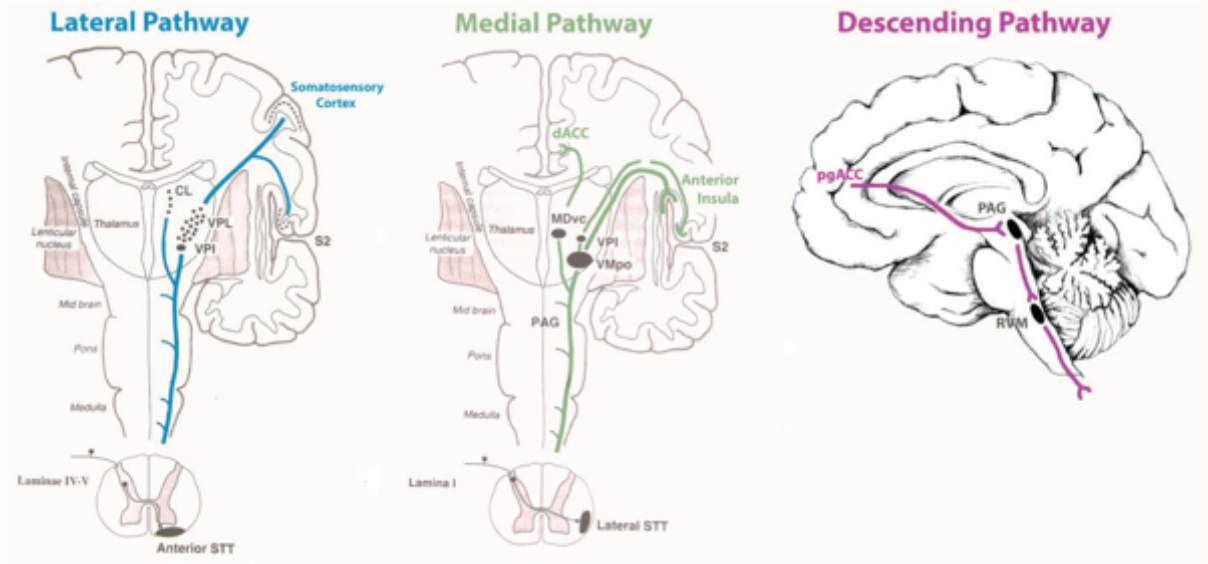

Figure 3: Illustration of the medial and lateral components of the spinothalamic pathways: The lateral ascending pathway processes the discriminatory components of pain through the ventral posterolateral nucleus (VPL) to the somatosensory cortex. The medial pathway processes the motivational, affective and attentional components of pain from the

periaqueductal grey matter, ventral medial nucleus (VMpo), medial dorsal nucleus (MDvc), dorsal anterior cingulate cortex (dACC) and anterior insula. [Figure taken from De Ridder et al, Burst and Tonic Spinal Cord Stimulation, Neuromodulation, 2015 (10)]

Neuropathic pain is different to classical nociceptive pain which is stimulus dependent. Neuropathic pain is spontaneous and not stimulus dependent (11). While neuropathic pain is frequently described in nociceptive pathways, the chronicity of symptoms and their genesis is likely different to nociception. The generation of spontaneous, autonomous signalling without a stimulus resulting in pain perception relies on mechanisms that still lacks a global collaborative consensus (11). This most likely involves a peripheral and central modulation of signals that cause neuropathic pain and these occur from the DRG up to the somatosensory cortex [Figure 4] (5).

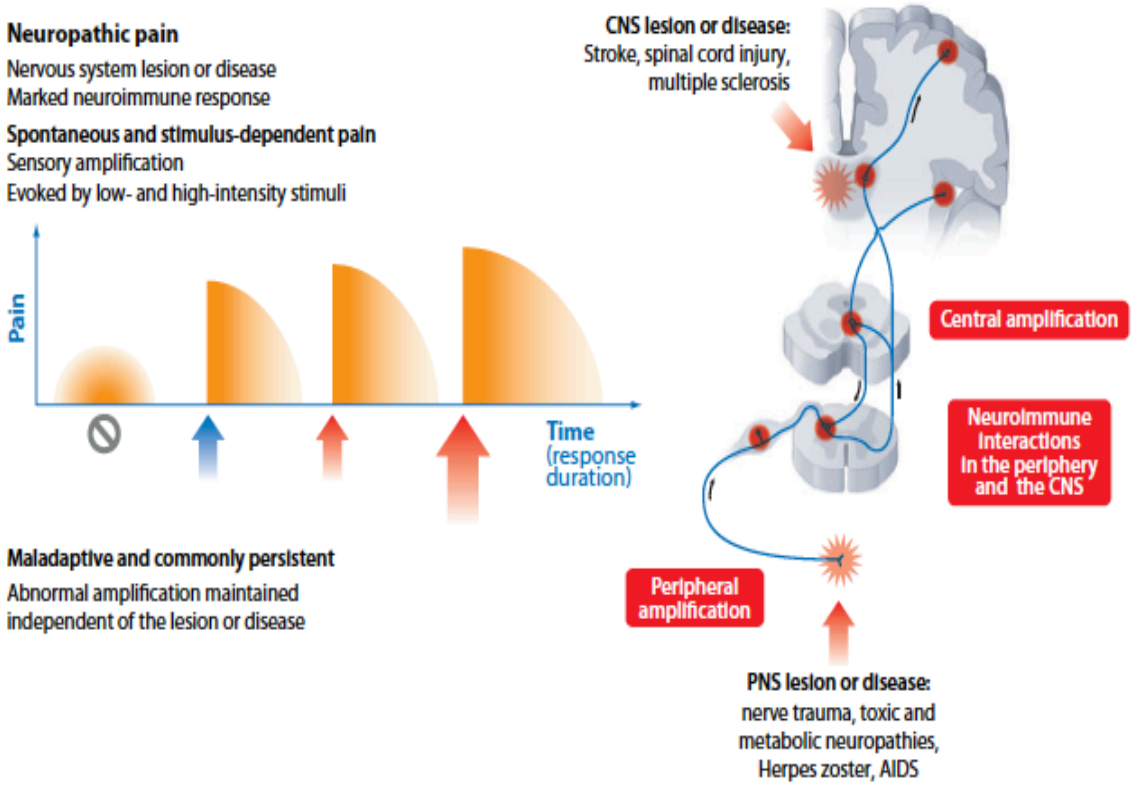

Figure 4: Diagram illustration of amplification of sensory information in patients with neuropathic pain: Graph with pain on the y axis illustrates patients experience pain without a stimulus and the perception of pain is amplified with increasing stimulus. The illustration of the pain pathway shows different anatomical points where modulation or amplification of a stimulus can occur. [Figure taken from Costigan et al, Neuropathic pain: a maladaptive response of the nervous system to damage, Annual Rev Neuroscience, 2009 (5)]

Chronic adult pain is a common problem affecting 19% of Europeans with 61% of these patients being unable to work normally leading to absenteeism, decreased productivity and early retirement with associated negative socio-economic impact and increasing healthcare demands (12). There is a global need to not only enhance our understanding of chronic pain but to develop better diagnostics and treatment to facilitate physicians in the optimisation of care. While nociceptive pain responds to a variety of therapies, neuropathic pain is notoriously resistant to current therapies. Lack of effective affordable treatments for chronic neuropathic pain has contributed to the global rise in the prescription of opioids with devastating consequences for patients and society (13). This is a consequence of managing chronic neuropathic pain with medications we now know have little long-term efficacy but do have significant serious side effects including addiction and overdose leading to fatalities (14-16). This led to the Centre for Disease Control (CDC) publishing specific guidelines for opioid use in 2016 (17). Chronic pain exists in many different entities, whether it be chronic nociceptive pain, neuropathic pain, pain of mixed aetiology or cancer pain (1). Heterogeneity exists in both mechanisms and symptoms, and a one drug treats all approach is ineffective (18). Each is managed differently and needs a high degree of expertise in diagnosis and management to improve outcomes. More research regarding the pathophysiology of pain chronicity, phenotyping and specific treatment is urgently required (5, 19). This demands a greater focus on human research and investigating established efficacious treatments to refine their beneficial properties (20). There is also an inherent urgent need to develop objective measures of diagnosing and quantifying chronic pain; currently clinicians are dependent upon subjective patient reporting with all of its limitations (21, 22).

1.2 Neuropathic pain

Neuropathic pain is defined as pain caused by lesion or disease of the somatosensory system (23). The incidence of neuropathic pain varies between 5-10% of the general population (23). Major challenges in defining neuropathic pain relate to dependence upon subjective symptom reporting and a lack of accurate, user-friendly and cost-effective diagnostic tools (19, 22-24). Different mechanisms of neuropathic pain produce similar subjective descriptions and similarly different symptoms will be experienced emanating from the same diagnosis (25, 26). Neuropathic pain is also associated with a significant

burden of emotional and psychological symptoms which makes treatment all the more challenging (25). Clinical research has moved beyond pre-clinical models to *in vitro* and *in vivo* studies in humans, which has greatly enhanced our understanding of neuropathic pain (23, 27, 28).

The nerve cell body of sensory neurons are located in the DRG which are located on the dorsal root of spinal nerves and are first order neurons (29). These nerves are then relayed to the dorsal horn where neural transmission is heavily modulated (7). Lesions or diseases of this neural system leads to altered transmission of signals to the spinal cord and second order neurons, which may result in pain being perceived in the absence of any stimulus and responses to other stimuli are altered and frequently amplified (30) [Figure 4]. We now know from pre-clinical models and cadavers that the DRG and dorsal horn is where the majority of change in morphology occurs after peripheral nerve injury resulting in chronic neuropathic pain (3, 31, 32). This is caused by multiple aetiologies including mechanical, trauma, metabolic disease, neurotoxic drugs, tumour invasion, infections such as Lymes disease and idiopathic causes (23, 27).

Nerve lesion or dysfunction is not always associated with pain and neuropathic pain will not always become chronic but is variable depending on aetiology (33). Nerve injury after surgery remains one of the easiest to monitor and will vary with nerve involvement, age, cognitive and emotional factors including catastrophising (33, 34). After nerve injury there are compensatory and decompensatory changes to neural function some of which are adaptive and some maladaptive. The balance between these mechanisms after initiation and repair are most likely related to genetic factors which determine if a person develops chronic neuropathic pain (5, 11, 33, 35).

Mechanisms proposed for Neuropathic Pain:

There are many mechanisms proposed for neuropathic pain and all may be relevant and orchestrated in concert to establish chronicity of symptoms. These are the main mechanisms that are frequently implicated:

- Ectopic impulse generation: Ectopic activity in neuropathic pain not only comes from primary sensory neurons but from second order neurons or altered connectivity in the spinal cord (5).

- Ectopic Transduction: Spontaneous activity is observed in nerves at normal temperatures through the TRPV 1 receptor which is usually sensitive at 41 degrees Celsius (5).
- Central Sensitisation: This refers to amplification of pain signals within the central nervous system (CNS). It was initially described within the dorsal horn but now extends further to higher centres in the brain (11).

- Low- Threshold Aβ fibre-mediated pain: Aβ fibres usually signal innocuous sensations but after neural lesions they produce pain. These circuits appear to switch from non-nociceptive signalling to nociceptive circuits. This occurs due to central afferent terminal sprouting, disinhibition and central sensitisation (5).
- Disinhibition: Inhibitory dorsal horn interneurons synapse with central terminals of sensory neurons and modulate afferent input. This is also performed by spinal interneurons. Loss of this stimulus may contribute to the chronicity of neuropathic pain (5).
- Neurodegeneration: Nerves in the periphery and dorsal horn become apoptotic after nerve injury. Spinal neurons die over a period of several weeks which may be related to ectopic activity and glutamate mediated excitotoxicity. This has been demonstrated in many patients with chronic pain conditions including fibromyalgia, migraine, back pain and phantom pain (5, 11, 36).
- Neuroimmune interactions: Neuroimmune interactions occur in the periphery and centrally after nerve injury with glial cells, T-lymphocytes and macrophages all playing a role in repair (3, 37). These cells also produce peptides centrally and maladaptive processes may contribute to the induction and maintenance of neuropathic pain (3, 27, 30, 37, 38).

1.2.1 Diagnosis of Neuropathic pain

Patients with neuropathic pain will often describe their symptoms as burning, electric shocks, shooting and tingling (23). These unpleasant sensations are referred to as dysaesthesia(39). They will also show signs of hypersensitivity, which include hyperalgesia (increased pain to a painful stimulus) and allodynia (pain from a normally non-painful stimulus) (23, 39).

Neuropathic pain can be diagnosed with screening questionnaires including Dolour Neuropathique 4 (DN4), Leeds Neuropathic pain score and Pain Detect (22, 40). While these have their limitations and are based on signs and symptoms, they are easy to perform and are reproducible. The DN4 has become one of the most widely used due to its simplicity and has 86% sensitivity and specificity (41). It can be carried out by any doctor and the result is immediate, however it has a false negative rate of about 10-15% (22, 23, 41).

Diagnostic tests including MRI, nerve conduction studies, skin biopsies and quantitative sensory testing (QST) have also been used to help in diagnosis (22-24). These tests are limited by expense, may not be readily available and have poor diagnostic accuracy (42). Correlation between MRI and symptoms remains extremely poor (43). Nerve conduction studies may detect abnormalities in conduction but this does not correlate well with either symptoms or symptom severity and there remains significant inconsistencies in reporting between centres (22, 23).

1.2.2 Treatment of Neuropathic Pain

Treatment for neuropathic pain is dependent on diagnosis and the severity of symptoms (23, 24, 44, 45). Medications, while sometimes effective, have high NNT (number needed to treat) values. When this is considered with significant deleterious side effect profiles, NNH (number needed to harm), then the NNT/NNH ratio tends to be very high; making stratification of therapeutic options difficult (45). Intervention is effective for some neuropathic pain conditions when single nerves are involved and can be accessed including lumbar radicular pain (46). The poor efficacy and duration of these therapies have led to treating neuropathic pain with a biopsychosocial approach, including pain management programmes where education, acceptance and motivation are emphasised to improve function and quality of life (47, 48). A definitive curative treatment for these patients is rarely achieved.

1.2.3 Medications Utilised for Neuropathic Pain

First line therapy for patients with neuropathic pain have been summarised by as systematic review by Finnerup and colleagues (45). Tricyclic antidepressants including amitriptyline have some of the lowest NNT and NNT/NNH ratios. Other first line drugs include

gabapentin and pregabalin (45, 49-51). Second line therapies include lidocaine patches, which blocks Na channels and capsaicin which acts on the TRPV1 receptor (45). Third line therapies include opioids which should only be prescribed under specialist supervision (45). There are many novel agents developed for neuropathic pain but their true efficacy is yet to be fully established (52-57).

1.2.4 Intervention for Neuropathic Pain

Intervention involves nerve blocks and surgical procedures that deliver drugs, electrical signals or neurolysis to modulate afferent nerve signalling to produce analgesia (58-60). Nerve blocks with steroids seldom work beyond 3 months (46); pulsed radiofrequency to the DRG has prolonged analgesia in a select group of patients (59, 61), but there are no large sham-controlled trials to justify its wide scale use (46, 62, 63). Spinal cord stimulation (SCS) has demonstrated the most promise in treating neuropathic pain predominately in patients with failed back surgery syndrome (FBSS) and complex regional pain syndrome (CRPS) (64-69). FBSS is persistent back and leg pain which is continuous despite one or multiple spinal surgeries to correct potential structural aetiologies(70). CRPS is a neuroinflammatory disease in one or more effected limbs defined by the Budapest criteria (71, 72). Despite this there is morbidity associated with insertion and hardware related problems are common (73). There is also a significant cost in implantation and long-term independent outcome data beyond 24 months is lacking (64, 66). Lack of placebo-controlled trials also create a degree of uncertainty over the true effect of the therapy due to enhanced patient healthcare interactions during SCS implantation. A trial with an adequately blinded cohort of patients demonstrated 30% of patients achieved a reduction of VAS of >20mm with sham SCS (74).

1.3 The Neuroimmune interface:

Neuroinflammation as a contributor to pain chronicity was postulated because neurons alone could not explain the aetiology of neuropathic pain based on early experimental evidence (75). This theory is also thought to explain central sensitisation (11, 27, 30, 35).

Pre-clinical models of neuropathic pain have provided insight into how the chronicity of pain may develop (3, 76). Resident and infiltrating immune cells are implicated in the development of pathological pain signalling through exocytosis of neurotransmitters, dysfunctional glutamate homeostasis, disinhibition and increased synaptic strength of pain pathways (3, 77). Our knowledge of the sciatic nerve ligation and constriction models have illustrated multiple networks within the dorsal horn of resident and infiltrating immune cells (3, 23). These cells with neurons and glia impact neural signalling at the synaptic cleft eloquently termed a part of the 'Neuroimmune Interface'.

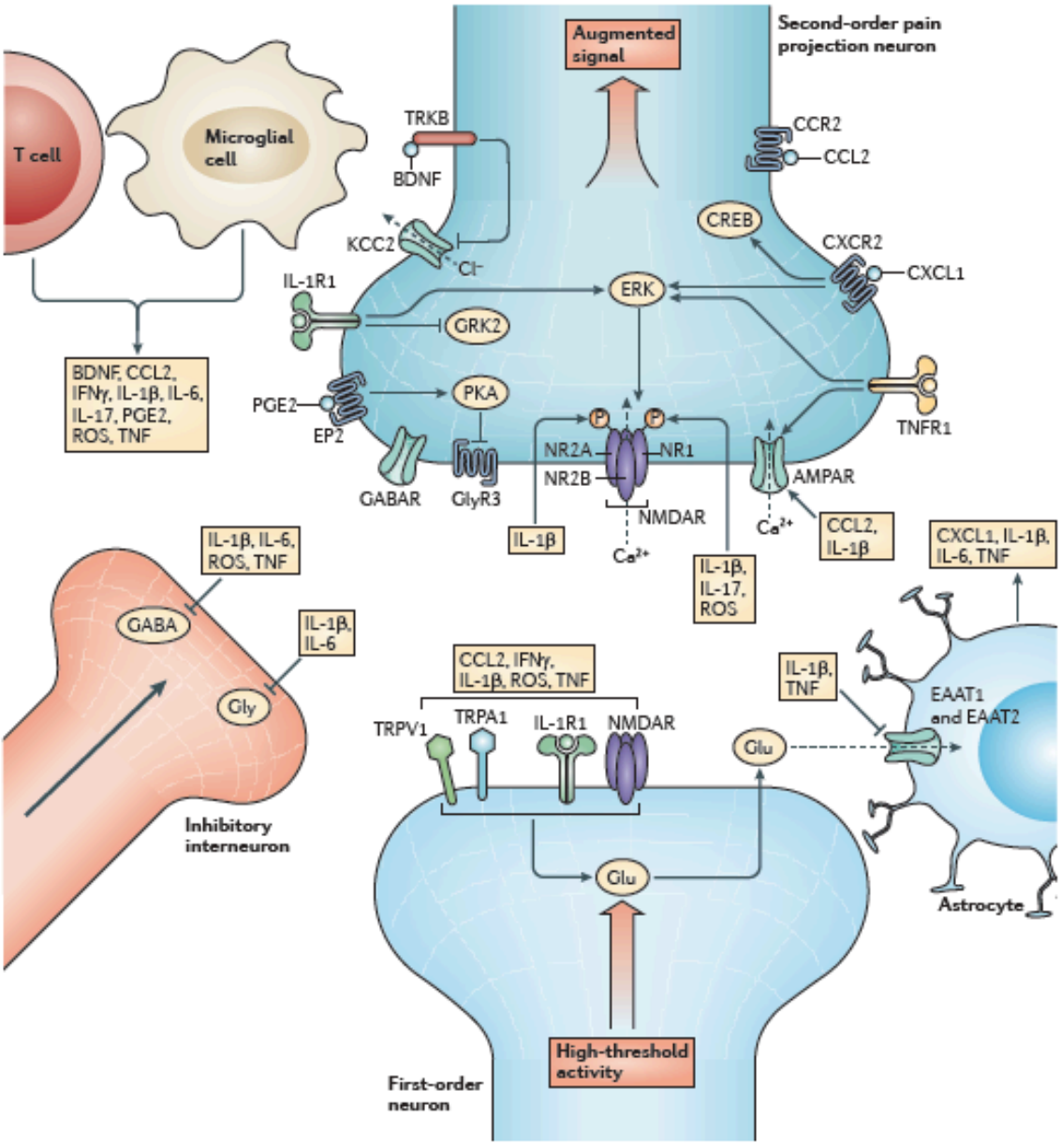

Figure 5: Diagrammatic representation of the Neuroimmune Interface: Neuropeptides from resident Central Nervous System (CNS) cells (Astrocytes and Microglia) can bind to receptors of pre and post synaptic neurons. Neuropeptides are also released from immune cells including T cells that can also modulate pain signalling in first, second and inhibitory interneurons. These neuropeptides can also influence the upregulation of receptors in neuronal structures. This illustrated how synaptic transmission is heavily modulated by a broad range of cells and neuropeptides. [Figure from Grace et al, Pathological pain and the neuroimmune interface, Nature Reviews, 2014 (3)]

This interface extends ortho and antidromically from the DRG to the site of nerve injury or inflammation (3). Orthodromic modulation of pain signals undergo extensive modulation from descending inhibition from the thalamus and higher centres in the brain and are often referred to as the 'pain matrix' or more appropriately neural responses to evoked stimuli (3).

The immune system and the nervous system share a common language of neuropeptides both peripherally and centrally (3, 78). The Neuroimmune interface consists of cytokines, chemokines, neurotrophins and endothelial cell molecules that are secreted by glial cells, macrophages, T- lymphocytes, mast cells and damaged neurons (3, 5, 37, 79, 80). Cross talk exists between all of these modalities, each one stimulating the other in a feed-forward loop enhancing pain signalling (3, 30, 81). This connection not only modulates pain processing but there is now strong pre-clinical evidence demonstrating it can result in dysfunctional signalling contributing to the initiation and maintenance of chronic neuropathic pain (3).

1.3.1 Cytokines and Chemokines

Chemokines are small proteins involved in the chemoattraction of responsive immune cells (82-84). Two chemokines which have been heavily implicated in preclinical models of neuropathic pain are monocyte chemoattractant protein-1 (MCP-1/CCL2) and fractalkine (CX3CL1) via glial cell/ neuronal interactions (82-84). MCP-1 expression is upregulated in the DRG after nerve injury (85). Fractalkine receptor (CX3CR1) is found on microglial cells and activation causes cellular migration and enhanced cytokine production (83, 86). Cytokines are produced both peripherally and centrally as part of a normal immune

response to infection and injury (87). The cytokines implicated in pain chronicity are secreted by T-helper cells and macrophages acting in a cascade synergistically, antagonistically or both (83, 84, 88-93). Centrally microglia and astrocytes are also involved in the production of cytokines and remain active until death (75, 83, 86, 87, 89, 90, 92, 94, 95). This central inflammatory process causes upregulation of NMDA and AMPA receptors (96-99). Electrophysiological testing has demonstrated minor increases in TNF-α boosts the frequency of spontaneous postsynaptic currents and amplifies AMPA and NMDA currents (87, 89, 100). Inhibitory currents and neurotransmitters GABA and glycine are also attenuated by the cytokine IL-6 (100-102). Despite these specific findings, neural signalling is complex and unlikely to be modified by the activity of a single neuropeptide.

1.3.2 Neurotrophins

Neurotrophins are chemicals that stimulate and control neurogenesis promoting survival, development and function (103-105). They are also key players in neuronal plasticity (11, 106, 107). Their activity is vital in development of a functional nervous system but may also lead to maladaptive changes in pain pathways (103, 104, 108, 109). Nerve growth factor (NGF) is an important part of the inflammatory response both centrally and peripherally after tissue and nerve injury (103). NGF levels are elevated in both acute and chronic pain scenarios (103, 110). It acts on TrkA receptors, which are involved in stimulating and maintaining sodium channels which prolong the period of wound sensitivity (111). The TrkA pathway also increases release of pro-nociceptive neurotransmitters centrally including Calcitonin gene related peptide (CGRP), Substance P and Brain Derived Neurotrophic Factor (BDNF) (111). BDNF is an independent contributor to chronic pain hypersensitivity through upregulation of AMPA and NMDA receptors and inhibition of GABAergic signalling in pre-clinical models (112-114). There is also evidence of neuroprotective effects where potential disruptions in its biosynthesis and molecular structure can lead to depression (105, 109, 115). Glial cell derived neurotrophic factor (GDNF) is involved in survival and differentiation of dopaminergic neurons (116). GDNF ligands have attenuated morphological and neurochemical changes in the DRG and behavioural symptoms of nerve injury in pre-clinical models (116).

Vascular epidermal growth factor (VEGF) has functions that extend beyond angiogenesis in the central and peripheral nervous system including neurotrophic and neuroprotective processes (117). VEGF influences microglia, astrocytes and Schwann cells and has many associations to mood, cognition and attenuating neurodegeneration (118, 119). Low levels of VEGF have been found in serum and CSF of people who have committed suicide (120, 121), in patients with FBSS (122) and in patients with neurodegenerative disorders (123). Patients with higher levels of VEGF in CSF have superior cognition and are also less likely to have neurodegenerative disorders including Alzheimer's (123). This adds to the evidence of VEGF's neuroprotective function. It also likely depicts low levels within CSF as being pathological of neurological disorders.

1.3.3 Cellular Participants of the Neuroimmune interface

Mast Cells:

Mast cells are granulated immune cells, which participate in innate host defence and allergic reactions (94, 124, 125). They degranulate immediately after an inflammatory reaction resulting in histamine and bradykinin release which are vasodilators (94). They also release multiple mediators involved the neuroimmune interface including: Il-6, TNF-α, ATP and NGF (94). Mast cells are found close to neurons and contribute to sensitisation (94). The adhesion molecule N-cadherin has been implicated in interaction between nerve terminals and mast cells and is required for degranulation (126). Mast cell degranulation has also been implicated in rapid NGF induced hyperalgesia (127).

Lymphocytes:

T-cells infiltrate nerves and the DRG after nerve injury and contribute towards central sensitisation (128). There is also evidence hyperalgesia and allodynia are attenuated in rodents lacking T cells (128). $CD4^+$ Type 1 Helper T cells (TH1) and (TH2) have different roles in neuropathic pain (81, 128-130). TH1 cells induce neuropathic pain behaviour by releasing pro inflammatory cytokines including IFN-γ and IL-2 (81, 128, 129). TH2 cells attenuate the TH1 response by releasing cytokines (IL-4, IL-10, IL-13) (81, 128, 130). IL-17 is also noted to be raised after peripheral nerve injury within the spinal cord (81). So far there is little pre-clinical evidence linking Natural Killer Cells in chronic pain in rodent models other than neuronal degeneration following nerve ligation (131). $CD8^+$ T cells have been implicated in the initiation (132-134) and the attenuation and repair of neuropathic

pain models (135). As their phenotypes can vary in function more research is required into how they behave and influence pain transmission.

Macrophages:

Macrophages are derived from monocytes and are recruited to injured nerves or tissue and mature in a matter of hours and resident macrophages become phagocytic immediately after tissue injury (136, 137). The presence of macrophages at the site of nerve injury is associated with mechanical allodynia (138). Macrophages are recruited by TNF-α, which is released by Schwann cells on neurons which induces MMP-9. MMP-9 aides in breakdown of the blood brain barrier and allows macrophages to migrate to the injured site or DRG (139). MMP-9 is also activated by IL-15 which not only aids the infiltration of macrophages but induces mechanical hyperalgesia (140). Macrophages also have a role in polymorphonuclear leukocyte infiltration and inflammation. Macrophages move from the satellite cells to the neural cell body and form rings underneath the satellite glial cells after nerve injury in the DRG (136, 137, 139). Following recruitment, macrophages express chemokine macrophage inflammatory protein 1 alpha (MIP1-α) which contributes to the development of neuropathic pain (137).

Microglia:

Microglia are immune cells found throughout the brain and spinal cord (141, 142). They act as resident macrophages within the CNS and are also involved in the homeostasis of neurons (142). Once activated they are termed to be in 'reactive gliosis', where they develop the ability to phagocytose, present antigen to T cells and release cytokines (142-144). After nerve injury adenosine triphosphate (ATP) and chemokines activate this state of reactive gliosis which leads to migration of microglia to the site of injury(142, 145). The proposed theory and body of evidence suggests microglia and their peptides are implicated in the generation and chronicity of neuropathic pain (141, 146). There are multiple interactions through which this is brought about including Neuregulin-1 growth factor and the erB2 receptor; blocking this pathway reduces activation of microglia and MAPK signalling (147). Matrix metalloproteinase-9 (MMP-9) from neurons also activate microglia and is increased in the DRG after nerve injury models and inhibition of MMP-9 delay the onset of neuropathic pain. MMP-2 has been associated with the maintenance of neuropathic pain through IL-1β cleavage (148). The chemokine MCP-1 which binds to microglia is upregulated in many models and leads to excitatory effects (83). Fractalkine

also activates microglia, which results in the activation of the extracellular-signal-regulated kinase (ERK)5 pathway (MAPK family) and hyperalgesia (141). Cytokines TNF-α, IL-1β and IL-6 are released from microglia after activation of Toll like receptor (TLR) 4 and are implicated more in the initiation than maintenance in neuropathic pain models (149, 150). With the wealth of potential pathways in which microglia can create an environment of neuroinflammation or gliosis these pathways can influence and enhance neuroexcitation (142) and synaptic morphology, architecture and transmission (142, 151) [Figure 6]. There is also evidence of cross talk between microglia and astrocytes through cytokines and chemokines and their receptors, including IL-23, IL-18, fractalkine and eotaxin-1. IL-18 activates nuclear factor kappa beta NF-kβ in astroctyes leading to IL-1β, IL-6 and TNF-α upregulation (142).

Astrocytes:

Astrocytes perform many important tasks including maintaining the blood brain barrier (BBB), biochemical support for endothelial cells and repair of damaged neurons (152, 153). Their function is vital towards homeostasis and their role in modulating neural signals is extensive (153-155). Astrocytes have the ability to produce cytokines, chemokines, control ion flux and release neurotransmitters (83, 152, 156, 157). Astrocytes also express an array of receptors including opioid receptors (158, 159). One study demonstrated astrocytes have connections to over thirty thousand cells verifying their ability to influence neuronal signalling on a large scale (156). Astrocytes can switch to a form of reactive gliosis but the exact mechanism of this has not been demonstrated in humans (97, 154). There are two phenotypes of reactive gliosis proposed from pre-clinical evidence which are inflammatory and ischaemic (154). Astrocytes have been implicated in models of neuropathic pain and reactive astrocytes have also been found to extend beyond the source of nerve injury (31). Astrocytes are key players in the architecture of synapses within the CNS and therefor any dysfunction in their supportive processes likely leads to pathology (99, 153). Indeed, pathology within astrocytes has been strongly linked to progression of MS, Parkinson's and other neurodegenerative disorders (160). Astrocyte dysfunction has a profound effect on neuronal function and likely is contributory to pain perception (155).

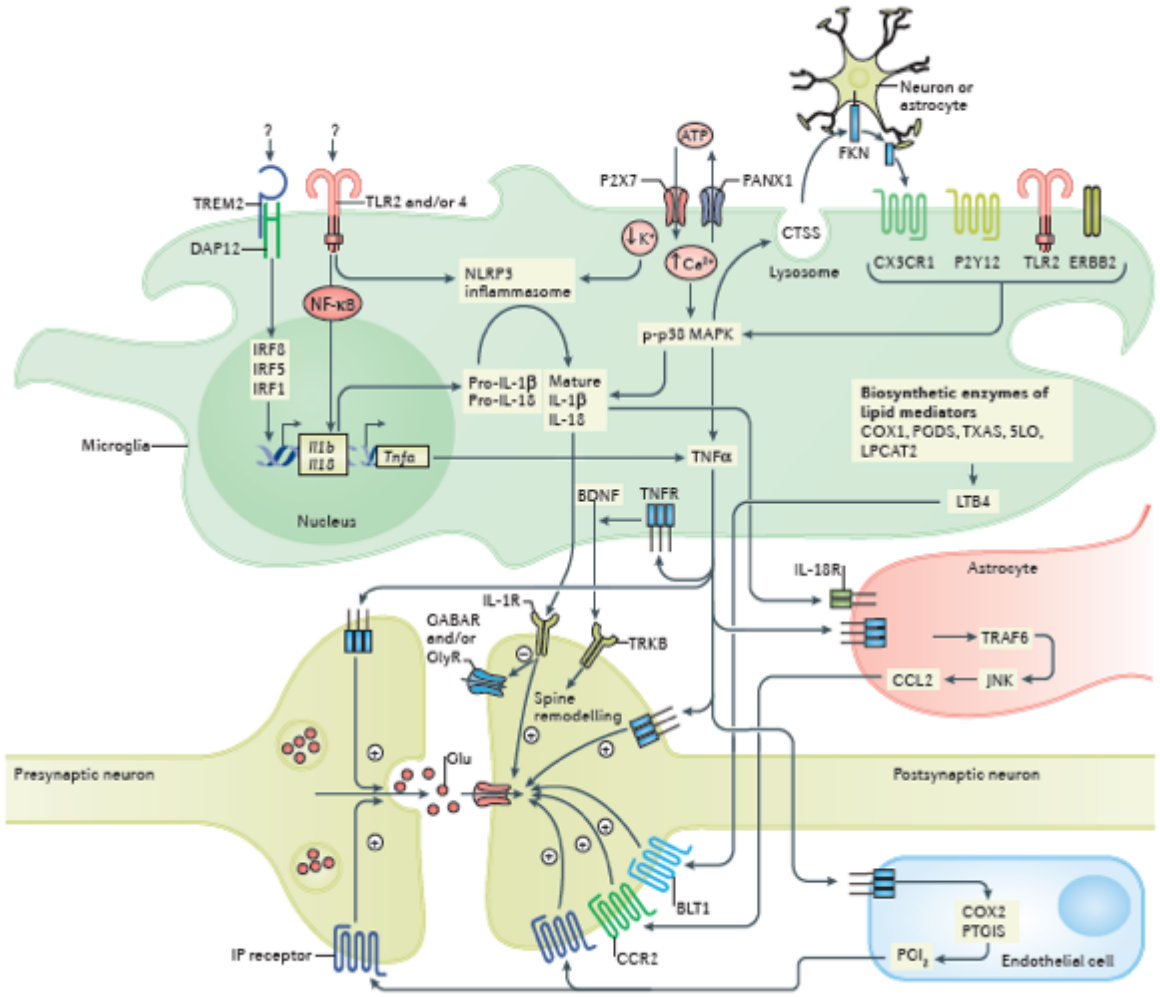

Figure 6: Interaction of Microglia with Neurons encompassing Astrocytes and Endothelial Cells after peripheral nerve injury: Toll like receptors (TLR) are activated to produce pro-inflammatory neuropeptides including TNF-α, IL-1β and BDNF which bind to neurons and increase glutamate mediated neurotransmission and inhibit GABA and glycine mediated synaptic inhibition. Cascades in pathways also lead to neuroinflammatory pathways in astrocytes and endothelial cells modulating signals at the synaptic cleft. [Figure from Inoue et al, Microglia in neuropathic pain, Nature Reviews 2018 (142)]

1.3.4 Summary of evidence of Neuroimmune activation in the chronicity of neuropathic pain

Many models of mice and rats using the sciatic nerve ligation and constriction models have illustrated a multitude of neuroimmune pathways described in the preceding text (3). Although each experiment focuses on a particular pathway it is important to recognise that there are many influential processes in the development of neuropathic pain (3, 5, 79, 161). The persistence of neuropathic pain is a highly complex pathological process involving a multitude of cellular and neuronal pathways. Our understanding of how glial and immune cells behave in these particular environments still requires further work. With the wealth of studies available selective studies with good methodology need to be translated into human experiments to validate findings (76).

1.3.5 Inconsistencies with Pre-clinical Models:

Recent experiments have brought into doubt many of the mechanisms previously championed. A study by Denk and colleagues demonstrated that there was no evidence of systemic infiltrating immune cells after the sciatic nerve ligation model in the dorsal horn (146). There was however a unique molecular signature of microglia from fluorescence-activated cell sorting (FACS) analysis perhaps implicating these cells in the development of neuropathic pain (146). The dorsal horn, where complex networks of neurons exist is thought to be the key location of the generation of autonomous, spontaneous neural firing and the genesis and persistence of neuropathic pain (2). As more advanced techniques are now available, the study of this key anatomical location will grow with other areas of interest including the DRG.

1.3.6 Issues with pre-clinical models and translation research

Rodent models are used extensively in drug research and development (162). Measuring pain in rodent models is problematic; observations can lead to bias. There is also a problem

of creating a true reflective model for the condition in the rodent. A lack of true understanding of mechanisms in humans only adds to this dilemma (20). Observed models in rodents have also led to the theory that different mechanisms exist between sexes (163). This is also observed in human populations where certain conditions have a higher prevalence in one sex (79, 161). Immune based and hormonal mechanisms of pain have been proposed based on these differences (161). This further justifies the need to carry out more clinical based research to enhance understanding and new drug development. So far, many promising pre-clinical experiments have failed to translate (53). Novel drug use including monoclonal antibody to calcitonin gene related peptide (CGRP) for migraine have portrayed some promise in clinical practice but have not been revolutionary (164). Tanuzumab (Anti-NGF) has also meandered through clinical trials and is set to be utilised soon for back and knee pain due to osteoarthritis (111). Neublastin, a glial cell derived neurotrophic factor family member has reduced pain in patients with lumbar radicular pain but only at the lowest and highest doses trialled (165). This unfortunately did not demonstrate a dose-response relationship bringing efficacy into question (165). Interestingly, these drugs are active on peripheral targets and given the central component depicted for CNP, it will be interesting to observe their efficacy over time.

1.3.7 Evidence of Neuroinflammation in chronic pain patients

The concept of neuroinflammation is clear in other neurological conditions including Multiple Sclerosis (MS), Alzheimer's and Huntington's disease (166, 167). This has been portrayed through analysis of cellular profiles and neuropeptide analysis of CSF which is representative of the metabolic processes in the CNS (166, 168). Neuroimaging has also enabled a more detailed localised depiction of the conditions and thus satisfied diagnostic criteria in many circumstances (169). Unfortunately, with chronic pain we currently lack adequate objective diagnostic markers in almost all circumstances. Experimental data into CSF and neuroimaging has been explored however (170-172). The radiolabelled ligand of translocator Protein (TSPO) is highly suggestive of neuroinflammation through upregulation in mitochondria of active cells in the CNS, namely astrocytes and microglia (173). More recently radiolabelled choline has been identified as another target to illustrate neuroinflammation (174). TSPO's true specificity has been questioned however and their still remains debate over whether it represents pathological neuroinflammation in chronic pain patients (76, 175-177). There has also been increased uptake of TSPO within the brain

of patients with depression and a reduction with effective treatment (178, 179). Increased TSPO uptake has been illustrated in the thalamus and brain of patients with chronic low back pain (180, 181), CRPS (182) and fibromyalgia (181). Increased TSPO uptake has also been demonstrated in the spinal cord and neuroforamina (corresponding potentially to the dorsal horn and DRG respectively) in patients with lumbar radicular pain (183). Interestingly, the patients that had evidence of increased TSPO standardised uptake value (SUV) were more likely to respond to epidural steroid injections (183). This generates important questions regarding whether our knowledge of diagnosing the condition needs to change based on this finding as lumbar radicular pain is inherently difficult to accurately diagnose (46). There may also be different phenotypes of the same diagnosis of lumbar radicular pain. The other question is whether gliosis is a temporary phenomenon or protective as many of the patients in initial studies had higher pain scores with a lower level of gliosis (180).

1.3.8 Clinical evidence for role of cytokines, chemokines and neurotrophins in pain chronicity

Whilst the published work to date is observational with small participant numbers it is highly relevant. Increased levels of chemokines and cytokines in cerebrospinal fluid following thoracotomy (peripheral nerve injury) has been demonstrated in 24 patients (184). The magnitude of this response does not correlate with pain scores in the acute setting but demonstrates a central response to peripheral nerve injury *in vivo* (184). The cytokine IL-6 was significantly higher in CSF samples in 30 patients with spinal stenosis compared to ten controls (185). Pain in CRPS has correlated with raised levels of intrathecal and peripheral IL-1β, IL-6 and TNF-α and the anti-inflammatory cytokine IL-10 was lower, negatively correlating with pain intensity (186, 187). This illustrates that increased presence of pro-inflammatory cytokines (TH1 response) and a decrease in TH2 response centrally in CRPS patients (187). Increased number of chemokines have also been demonstrated in patients with chronic lumbar radicular pain versus controls that are thought to be largely produced by glia within the CNS (170). This provides further evidence of neuroinflammation in patients with chronic neuropathic pain (170).

A study within our institution demonstrated higher levels of GDNF and lower levels of VEGF in patients with FBSS (122, 188). Levels of VEGF also decreased on activation of

a spinal cord stimulator after being switched off for 24 hours. There are a multitude of potential explanations for this observation however and it is likely an immediate epiphenomenal event with potentially VEGF binding to more receptors (122). It may also indicate immediate vasodilation and thus analgesia which has been described as a potential mechanistic action of tonic SCS (118, 189). Epidural venous congestion has been hypothesised as being the aetiology of pain in patients with FBSS (70, 190-192). The concept of wash-in and wash-out times of the therapy, as well as the flow of CSF hinders many aspects of this study in conceptualising mechanisms to the true effect of SCS.

To date systemic chemokine and cytokine inhibitors have failed to show any benefit in attenuating pain in clinical trials; this may be related to their inability to effectively cross the blood brain barrier (92, 93, 193). The concept of pro and anti-inflammatory cytokines exclusively modulating pain may be too simplistic. For instance, a rise in cytokines within the CSF is demonstrated in neurosurgical patients having operations on the brain that are frequently painless (194-196). The timing and pattern of event-initiated cytokine biosynthesis is likely a result of a process in the neuroimmune interface which results in central sensitisation and neuroplasticity. Therefore, the expression of cytokine analysis alone within the CSF is unlikely to give a clear picture of the neuroimmune processes involved in chronic pain and needs to be complimented with cellular and proteomic data to provide more information on potential mechanisms (76).

1.3.9 Cellular Analysis of chronic pain in humans

Greater accumulations of activated CD-8 T lymphocytes in CSF samples have been exclusively observed in patients with neuropathy in patients with HIV infection (32). These findings may suggest that migration and accumulation of activated CD-8 T lymphocytes within the CSF is pathological in HIV neuropathy (32). Glial cell changes in the dorsal horn have also demonstrated a positive correlation with painful HIV neuropathy with astrocytes in a reactive state (197). Reactive astrocytes were also found in the dorsal horn of a cadaver of a patient with longstanding CRPS at the level of injury but not at distant sites (31). Increased numbers of CD8+ and CD4+ central memory T cells have been observed in the peripheral blood of CRPS patients versus controls with increased pro-inflammatory signalling pathways (198). Contrary to this finding, peripheral anti-

inflammatory T cell shifts have been observed in 26 patients with neuropathic pain compared to 26 healthy controls (199). The dynamic change in T cells have also been investigated in CSF after PRF to the DRG in one study (60). In responders to PRF the frequency of Natural Killer T cells reduced and the frequency of CD8+ T cells increased after 3 months (60). This study asks many more questions than it answers regarding the dynamic change in cellular constituents to CSF. For one, the DRG lies outside the Blood-Brain barrier and CSF would not reflect the drainage of constituents from the DRG (29, 200-203). Pre-clinical studies have demonstrated altered physiology and neuropeptides in the dorsal horn after PRF (204). These observed phenomena would conclude that the effect of PRF to the DRG would have to be orthodromic. This may alter the physiology of the spinal cord and other components of the CNS changing the potential trafficking of cells and/or altering the phenotype of resident immune cells. As gliosis is associated with neuropathic pain, the alteration in the behaviour of microglia with the dorsal horn may constitute a change in the phenotype of the cellular and molecular component of cells within the CSF (76, 146). This is assuming PRF has an effect within the dorsal horn. These concepts may appear far-fetched but not impossible. Due to the low number of patients and high level of variability of the cell types in the samples, this would bring any conclusions into question. The overall cell numbers were also not measured in this study (60). The cellular constituents of CSF may still be important however; flow cytometry with phenotyped patients including neurodegenerative diseases illustrated clear differences in cellular frequencies (205, 206). Technology examining the cellular constituents of CSF is improving. The introduction of new methods and FACS analysis will elaborate theories further and more information may be obtained (76, 207, 208). There has also been recent research into other chronic pain conditions including rheumatoid arthritis (RA) implicating cellular phenotypes in disease processes (209, 210).

1.3.10 Proteomic Analysis of CSF in chronic pain patients

The study of cytokine and specific neuropeptides in the CSF has its limitations. For instance, despite the change in cytokine profiles we are not sure which cellular structures produce them and whether they are truly reflective and related to the chronicity of neuropathic pain. Proteomic analysis may also have similar flaws but can give a more accurate reflection of potential pain pathways. The proteomic constituents in the CSF of

patients with RA and Fibromyalgia were compared to healthy controls (211). Proteins related to chronic pain were associated with synaptic transmission, inflammatory response, neuropeptide signalling and hormonal activity (211). Another study examined trace elements in patients with FBSS illustrating chronic pain patients have higher levels of Ca, Sr, K, Mg, Ti, P and Na in their CSF compared to controls (212). The concentration of these elements did not reduce after SCS therapy however (212). The proteomic constituents of CSF were also measured before and after SCS in patients with FBSS (213). The top 12 altered proteins were involved in neuroprotection, synaptic plasticity and learning, nociceptive signalling and immune regulation (213).

1.4 Sickness Behaviour

Chronic pain patients will often express signs and symptoms of sickness behaviour by an adaptive reorganisation of priorities (38, 214, 215). These are similar to what one would see during infection; this suggests immune activity. The relationship between pain and the immune system is well established; pain being one of the four cardinal signs of inflammation (216). Depression, lethargy, anxiety, sleep disturbance and hyperalgesia are commonly identified in patients with both chronic pain and sickness behaviour (214). Sickness or pain related behaviour is defined as the interaction between the patient and their environment. Many of these behaviours are learned or conditioned from past experience, can be verbal or non-verbal and involuntary or deliberate (53). Sickness behaviour and psychological disturbances were identified when interferon-α was injected into cancer patients resulting in mood change (217). This is due to cytokines which once detected by neurons in the brain induce vagal nerve afferent stimulation leading to physiological adaptive measures including the need rest in times of infection (91). This is a trait seen in multiple animals and is beneficial to recovery and survival (215). There are incidences when this response can become chronic as seen in inflammatory diseases such as Crohn's and rheumatoid arthritis (218). Symptoms of depression overlap with sickness behaviour and symptoms such as anhedonia, aches and pains, hyperalgesia are also prevalent in chronic pain patients (38).

1.4.1 Pre-clinical Evidence of cytokine induced sickness behaviour

Pre-clinical evidence implicates the direct action of IL-1β and TNF-α in inducing sickness behaviour through feed forward mechanisms (38, 214, 215). These are similar to many pathways highlighted for chronic pain (3, 150). IL-1β activates NF-kβ pathway within microglia which leads to further cytokine production (91, 219). IL-1β acts through the MAPKs, p38 inhibiting neuron potentiation and calcium channels (91). IL-1β may also have a direct excitatory effect on neurons mediated by an increase in ceramide (a family of lipids that act as intracellular signalling molecules) synthesis and subsequent NMDA-mediated calcium influx (220). In contrast, IFNγ, IFNα/β and IL-6 signal primarily through the janus kinases/signal transducer and activator of transcription proteins (JAK/STAT) pathway which induce glia cell secretion of cytokines (91, 219). Other pathways in which sickness behaviour is induced include: TLR4 activated by LPS via induction of Il-6, IL-1β and IFNγ (38, 150, 215, 219). In contrast to the theory on cytokines alone inducing sickness behaviour, Cyclo-oxygenase (Cox-1) inhibits sickness behaviours without decreasing cytokines. Data has also shown either IL-1β or TNF-α must be present to alter sickness behaviour and prostaglandins alone are insufficient (215) .

1.4.2 Depression, Sickness Behaviour and Neuropeptides

Depression is synonymous with many neurodegenerative disorders and pain (38). Much like chronic pain, an agreed pathogenesis of depression in humans has yet to be fully identified (221, 222). Systemic raised levels of IL-6 and TNF-α have been found in depressed patients who are unmedicated versus controls and IL-10 levels were lower and negatively correlated with depression scores (223). Abnormalities in neurogenesis and production of growth factors can also lead to depression (91). In line with this perspective, reduced serum levels and messanger ribonucleic acid (mRNA) expression of BDNF were reported in drug-free depressed patients compared to those treated with antidepressants or healthy controls (224). With respect to the possibility that antidepressants might stimulate BDNF activity (and thus neurogenesis), post-mortem analyses indicated that hippocampal concentrations of the neurotrophins were elevated among depressed individuals who had been treated with antidepressants compared to those who had not been medicated (108, 224). Amitriptyline, a tricyclic antidepressant, has also demonstrated in pre-clinical studies to ability to increase BDNF levels in the brain (225, 226). Furthermore, CSF VEGF levels were lower in medication-free suicide attempters compared to healthy controls and low CSF VEGF levels were negatively correlated with depression severity (120, 121).

Amitriptyline has also demonstrated pre-clinical evidence of increasing VEGF in the hippocampus (227). Raised levels of VEGF have also been found after electro-convulsive therapy (ECT) in a rat hippocampus which is a highly effective treatment for depression (228).

1.5 Amitriptyline

Amitriptyline is widely regarded as one of the first line medications for patients with chronic neuropathic pain and has the lowest NNT figure (45, 50). It is classed as a tertiary amine tricyclic anti-depressant (229). It's utilisation is limited as it is not suitable for patients with ischaemic heart disease, arrhythmias and glaucoma (50). Amitriptyline also has significant side effects which are largely due to its anti-cholinergic effects; these are not necessarily dose dependant and can impact function and driving (50). The NNT for amitriptyline for chronic neuropathic pain from 15 combined studies was 3.6 and the number needed to harm (NNH) was 13.4 (50). Based on the available evidence an initial dose of 10mg can be titrated up with a therapeutic plateau achieved at a dose of 75mg in patients with neuropathic pain (45, 230).

1.5.1 Pharmacokinetics and Pharmacodynamics of Amitriptyline

Amitriptyline is orally absorbed and has a bioavailability of between 30-60% due to first pass metabolism (231). It undergoes demethylation as part of hepatic metabolism which gives rise to the active metabolite nortriptyline (231). It can also undergo hydroxylation but is subject to genetic polymorphism (232, 233). There are other metabolites to amitriptyline including cis- and trans-10-hydroxyamitriptyline and cis- and trans-10-hydroxynortriptyline but these are less active and are present in low amounts in plasma (50). The elimination half-life is reported between 10- 28 hours. The elimination half-life of nortriptyline ranges from 16-80 hours (231). Peak plasma concentrations of the drug are variable; an old study for depression found levels of 60-200 ng/ml were needed to be effective (229). More recent studies at lower doses of 25mg were found to produce a plasma level as low as 26.8ng/ml in healthy volunteers on initial dosing (231). Amitriptyline is highly protein bound in plasma and tissues. However tissue concentrations of other tricyclic compounds in rodent models can be 5-20 times higher than plasma concentrations (234). Toxicology reports in overdose patients in both plasma and CSF show a dose related

concentration in both plasma and CSF demonstrating it penetrates the blood brain barrier to act on the CNS (235). This has also been illustrated in a rodent study illustrating different concentrations of amitriptyline and nortriptyline in the brain and plasma after acute and chronic use (236).

The number of proposed mechanisms of action for amitriptyline in chronic pain are extensive. These largely come from pre-clinical and *in vitro* studies (237, 238). Pharmacological function is inhibition of monoamine reuptake transporters for serotonin and noradrenaline (238). Its active metabolite nortriptyline is more selective to noradrenaline reuptake transporters (238). Selective Serotonin reuptake inhibitors (SSRI's) have been ineffective for chronic pain but Selective Noradrenaline Reuptake Inhibitors (SNRI's) are used for diabetic neuropathy albeit with a higher NNT (45). The site at which these functions occur in modulating chronic pain are thought to be in the dorsal horn and locus coeruleus where noradrenaline is secreted (238). In a mouse model, hyperalgesia was demonstrated if noradrenaline levels decreased in the spinal cord (239). There are also rodent studies displaying increased levels of extracellular noradrenaline in the hypothalamus after amitriptyline. We do not have evidence of increased concentrations of noradrenaline in humans however with tricyclics or duloxetine (240).

Amitriptyline also has affinity for α-adrenergic, histamine, muscarinic cholinergic, 5-HT, N-methyl-D-aspartate (NMDA) and opioid receptors (231, 236-238). Histamine and MAST cells has been heavily implicated in models of chronic pain but whether amitriptyline acts peripherally or centrally on these receptors is currently unknown (94, 124, 125). The binding to NMDA and opioid receptors has been observed in *in-vitro* studies however at therapeutic doses for chronic pain there is much debate on whether this occurs (241, 242). Blockade of the Na+ voltage gated channel in rat skeletal muscle has also been observed via the same subunit used for local anaesthetic with amitriptyline (243). Amitriptyline also interacts with calcium and potassium channels at toxic doses which are thought to be responsible for cardiac related adverse events (238). There is further evidence of amitriptyline inhibiting voltage gated ion channels in the dorsal horn in rodents leading to reduced firing of tonic and adapting neurons in laminae 1-3 (244). The interaction of amitriptyline with these neurons in the dorsal horn at normal therapeutic doses and the specific receptors involved in humans however still needs further research (237).

There is evidence that amitriptyline has trophic like activity as well. A study in rats showed changes in levels of BDNF and GDNF in different areas of the brain after amitriptyline (226). The method by which amitriptyline increases GDNF is through fibroblast growth factor receptor in glial cells (245). In-vitro studies using mice displayed amitriptyline binds to TrkA and TrkB receptors and triggers their dimerization and activation indicating it may possess neurotrophic activity (246). This process involving the TrkA pathway would likely not be related to the analgesic function of amitriptyline as attenuating this pathway is associated with analgesia in many chronic pain conditions (103, 104, 110, 111). Tricyclic antidepressants have also increased levels of VEGF in pre-clinical models in the hippocampus, an area associated with chronic pain (119).

Chronic pain patients are said to be in a state of reactive gliosis from clinical studies and pre-clinical models (183). The anti-inflammatory effect of amitriptyline has been well described. *In vitro* work of astro-glial cell lines in mice displayed that amitriptyline inhibited NF-kβ translocation which resulted in reduced IL-1β protein levels (247). Further studies have demonstrated reduction in pro-inflammatory cytokines in the spinal cord of neuropathic pain models linking it with activation of the A3 adenosine receptor (247, 248). In a clinical setting patients with major depressive disorder demonstrated significantly lower levels of the cytokines IL-1β and Il-6 in plasma correlating with improved symptoms (249).

The link between TLR4 signalling in immune cells and microglia in chronic pain has been widely studied and their interaction enhances pain signalling (150). A study using cell lines with TLR receptors demonstrated amitriptyline likely by binding to the MD2 inhibits TLR 2 and 4 receptors (250). This may also contribute further evidence to amitriptyline's mechanistic action for neuropathic pain. In the same group of experiments however the working group observed oxcarbazepine and carbamazepine exhibited TLR 4 activation. This contradicts this theory to an extent as both of these drugs have a better NNT than amitriptyline for treating trigeminal neuralgia (45, 230). The pathophysiological mechanisms behind different types of neuropathic pain however may explain this analogy (23).

1.6 Spinal cord stimulators

The initial rationale for Spinal cord stimulation (SCS) was based on the hypothesis of gate control theory, depicting modulation of signalling in the spinal cord could reduce the symptoms of neuropathic pain (251, 252). Gate control theory is based on the concept of stimulation and inhibition compete at the dorsal horn to determine if nociception occurs. Therefor non-noxious stimuli are not deemed to be painful (251). Neuromodulation via SCS is based on the hypothesis that structure and function are intertwined in the CNS. The nervous system will respond to the electrical field depending on the frequency or mode of stimulation (189). The location and dynamics of stimulation will code the nervous system to perform a particular function. Electrical signals can be delivered to a particular nerve or structure including the DRG (253). Electrical field can also be delivered to areas of mixed nerve functions (dorsal horn) and the ability to target specific neurons or cellular structures becomes an important factor (254). The first spinal cord stimulator was placed in the intrathecal space and subsequently into the epidural space in order to activate the dorsal columns and modulate pain signalling (255). This replaced pain with paraesthesia and has been termed 'tonic stimulation"(254). It comprised of epidural electrodes connected to an implantable pulse generator (IPG) which can alter the frequency, pulse width and amplitude of the current delivered. SCS was subsequently utilised in other neuropathic pain conditions, predominately failed back surgery syndrome (FBSS), where SCS was superior to re-operation in an open label study with regard to pain scores(64). Subsequent studies showed superiority of SCS to conventional medical management in FBSS in reducing pain intensity (256). The strongest evidence for SCS has been its utilisation for FBSS and Complex regional pain syndrome (CRPS) (65, 213, 256-261). Despite improvements in pain and function, eradication of pain is seldom possible and a positive outcome is accepted as reducing pain by >50% (262).

Conventional tonic stimulation is still used and favoured by many patients with neuropathic pain, however many are intolerant or become intolerant to paraesthesia associated with SCS (263). This has led to the growth of many different waveforms using higher and alternating frequencies that not only provide paraesthesia free stimulation but a higher density of current to the spinal cord (264-266). Two prominent modalities used for FBSS are high frequency (10kHz) (267) and Burst as described by De Ridder (8), that have shown superiority to conventional tonic stimulation in clinical trials (68, 268). There were also

improvements in mood and quality of life within these studies to suggest a different mechanism with the Burst waveform (68, 268).

Tonic SCS

The true mechanism of action of conventional tonic SCS remains to be elucidated but several theories have been proposed (10, 189, 190, 269). These include: inhibition of activation of WDR neurons (WDR neurones are important 'gate-keepers' in the dorsal horn during pain transmission, they may be switched off when stimulated by A-fibres in the DC) (270), activation of GABAergic inhibitory inter-neurons in the dorsal horn, activation of supraspinal mechanisms (descending serotonergic neurones and locus coeruleus neurones), suppression of the neuroimmune response (markers of glial and immune cell activity), suppression of efferent sympathetic fibres and stimulation of peripheral vasodilatory proteins (189, 191, 265, 271-273).

Burst SCS

In burst stimulation 5 pulses are delivered per burst at a frequency of 500 Hz, and 40 bursts are applied per second (8). The cumulative charge of the five monophasic 1 ms spikes is balanced during 5 ms following the spikes, and charge balancing is not completely performed after each individual spike with passive repolarisation [Figure 7].

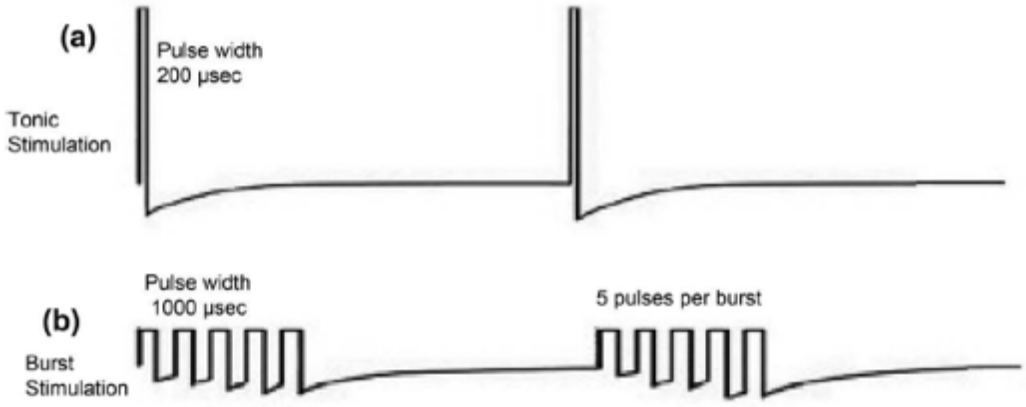

Figure 7: Difference between Tonic and Burst Stimulation: Tonic stimulation has a frequency usually between 40-80Hz, pulse width and amplitude can be modified to get an ideal treatment effect. Burst stimulation has five 1000 microsecond pulses at 500Hz with each train occurring at 40 Hz with passive repolarisation allowed between trains. [Figure from Ahmed at al, Burst and high frequency stimulation: Underlying mechanism of action, Expert Review of medical devices 2017 (272)]

The CNS modulates the frequency and pattern of action potential firing rather than amplitude. Some neurons fire in a tonic pattern of single action potentials but most deploy bursts of action potentials followed by diminished periods of firing (274-277). These bursts ride on an active calcium mediated plateau which differentiates it from tonic firing. This suggests that tonic and burst neuronal firing transmit different types of information (269). Burst stimulation was started based on the dual firing properties of thalamic cells which can fire in tonic or burst modes (275). Burst firing of thalamic cells is a more powerful activator of the cortex, a stronger stimulant than tonic firing (275, 276). This occurs in two ways demonstrated using an animal model. The first, after initial burst firing having a synaptic efficacy greater than that of average cortical firing. Second, due to the efficacy of subsequent impulses nearing the average value further increasing the probability of eliciting neocortical spikes (275). In a clinical study in FBSS, electroencephalogram (EEG) recordings demonstrated a significant increase in neural synchronisation for Burst-SCS compared to tonic in the dorsal anterior cingulate cortex (10). This area of the brain is connected to the medial pain pathway and has previously been implicated in emotion. Including its hippocampus projections this may help control the emotional elements of the chronic pain experience (10, 269). Both tonic and Burst stimulation appear to modulate the lateral and descending inhibitory pathways but Burst-SCS has a potential added feature of modulating the medial spinothalamic tract (10, 278) [Figure 3]. This also demonstrates that stimulation applied at spinal level can provoke changes higher up the pain processing pathway (10).

1.6.1 Evidence of Modulation of the Neuroimmune axis with SCS

Several studies have looked at how tonic spinal cord stimulation affects cytokines, chemokines and neurotrophins in the CSF. An initial study in nine patients demonstrated a significant reduction in VEGF after the patients stimulator was turned on (122). The same patients also had significantly higher levels of MCP-1, GDNF and BDNF compared to

healthy controls (122, 188). Proteomic evaluation of CSF in 15 patients portrayed significant changes in 84 different proteins with stimulator turned on/off (213). These proteins were involved in neuroprotection, nociceptive signalling, immune regulation, and synaptic plasticity (213).

Blister fluid from patients with CRPS taken from the effected limb before and after SCS demonstrated a significant reduction in Eotaxin, IP-10, VEGF and platelet derived growth factor (257). These findings demonstrate the possibility neuromodulation can bring about changes in immune function in the periphery (257). Another study looking purely at Burst stimulation in FBSS noted a significant increase in serum Il-10 levels correlating with reduced pain scores, improved mood and sleep after stimulation (279).

1.7 Cerebrospinal fluid analysis in Chronic Pain

CSF is thought to be produced predominantly from the choroid plexus within the ventricles of the brain. It leaves the brain via the foramina of Luschka and Magendie and circulates in the subarachnoid space around the brain and spinal cord (203, 280). Studies in rats also reveal there is flow of interstitial fluid around neural tissue into CSF (281). There are other theories of CSF production proposed, it may be produced as a consequence of filtration and reabsorption of water through the walls of neural tissue capillaries (202).

The volume of CSF is 150ml in an adult and the rate of production is 600ml per day. It is reabsorbed into the venous sinuses across arachnoid villi (203). CSF provides buoyancy, nourishment (including hormones) and removes endogenous waste products of cellular metabolism from its surrounding structures (282). The metabolic metabolites of neuronal/glial communications are also represented in the CSF so it makes it a valuable entity to analyse (283). A review article has suggested that it remains the best way of analysing astrocytic/microglia/neuronal physiology from the extracellular space of the brain (282). It was also noted that it can take many hours to days for molecular components to equilibrate from CNS tissue to the CSF (284).

CSF is used in medicine for research and for diagnostic purposes. It can be central to the diagnosis of meningitis and cerebrospinal metastasis in cancer (280, 285). It is also increasingly being used to aid diagnosis and further clinical research in multiple sclerosis, Alzheimer's and neurodegenerative disease (105, 110, 286, 287). The total protein content

of CSF is 0.5% of that in plasma making it difficult to study and detect selected proteins. Diffusion of proteins from blood to the CSF is limited by the blood brain barrier (BBB); for this reason there are many proteins unique to the CSF (288). Cytokines, chemokines and neurotrophins can be assessed using enzyme linked immunosorbent assay (ELISA). Mass Spectrometry (MS) can be used for analysing multiple proteins and clustered analysis of selective proteins. The characterisation of neuropeptides for different diseases within CSF is improving and despite a paucity of studies there are definite patterns emerging (211, 288-290). B cell markers including CXCL13 are consistently elevated in autoantibody associated disorders. T-Helper cell subtypes 1 and 17 cytokines are also commonly elevated in multiple sclerosis (168).

Cellular composition of the CSF is assessed using flow cytometry (286). Different neurodegenerative diseases and headache have been characterised by one review demonstrating the cellular constituents differ between different neurological diseases (205). There are clear differences in T helper cell subsets between plasma and CSF (286, 291). There are also distinctive differences in CD4+:CD8+ ratios with different diseases (205). Headache appears to have a higher CD8+ T lymphocyte subset compared to multiple sclerosis (205). More advanced techniques of intracellular analysis including Fluorescence-activated Cell Sorting (FACS) are available at specific sites (76, 146, 292). There are however limitations in the number of cells you collect with a CSF sample and the panel of markers that are utilised to identify specific cells and their different phenotypes. As T cells are the most abundant in the CSF they are an obvious target for analysis (286, 291).

The study of microglia and astrocytes has so far been challenging in chronic pain patients. The study of human astrocytes is at an early stage and is analysed when human brain tissue is excised for epilepsy or tumours (98). Microglia like cells have potentially been detected in CSF samples of patients with HIV using RNA sequencing (208). The authors noted that these are less than 5% of the cells in the CSF and would be very difficult to capture using flow cytometry (208). However, measuring the neuropeptides excreted by cells within the CNS may provide evidence of physiological processes.

Many therapies prescribed to reduce the symptoms associated with chronic neuropathic pain lack a consensual agreement on mechanism of action. The development of drugs for pain emphasises target engagement biomarkers and proof of mechanism in humans by a recent publication by Davis and colleagues (293). This not only increases the chance of

project advancement and success but develops our understanding of the pathophysiology of neuropathic pain. Examination of CSF has improved our understanding of the pathophysiology of neurodegenerative diseases and neurological diseases (207, 211, 294-296). It is therefore essential to explore the pharmacodynamics and mechanisms of therapies already utilised for chronic neuropathic pain to provide information regarding their possible mechanisms of action which will also provide more information on the pathophysiology of chronic neuropathic pain and help stratify medical therapeutic decision making leading to a better outcome for patients.

1.8 Hypothesis:

We hypothesised that the mechanisms of amitriptyline and Burst-SCS involve a modulation in the neuroimmune interface which results in a reduction of perceived neuropathic pain. To explore this dynamic change *in vivo* we analysed CSF samples before and after the intervention.

1.9 Aim:

Our aim was to examine the modulation of the cellular and neuropeptide constituents of CSF in clinical responders to amitriptyline and Burst-SCS (treatments for neuropathic pain). This involved taking CSF before treatment with Burst-SCS and initiation of amitriptyline therapy and after 8 weeks of therapy to examine the CSF T-cell and neuropeptide constituents in responders. Responders were determined by pain scores according to NRS. Lumbar radicular pain was used as a model for the amitriptyline study and suitable patients put forward for SCS were utilised for the Burst-SCS study.

To isolate how amitriptyline modulated T-cells and their exosomes, the most predominant cells with the CSF, we aimed to perform an *in-vitro* analysis of human T-cells from healthy controls to contrast the findings to the CSF analysis. We also planned an ad-hoc study examining the CSF of patients medicated with chronic opioid therapy versus those not medicated with opioids prior to their specified intervention.

Chapter 2

Examination and characterisation of the effect of amitriptyline therapy for chronic neuropathic pain on neuropeptide and proteomic constituents of human cerebrospinal fluid (297)

Highlights:

- The proteome and secretome of cerebrospinal fluid is modulated with amitriptyline
- Immune system process is a key mechanism for amitriptyline in neuropathic pain
- Responders to amitriptyline show a reduction in MAPK and PI3K-Akt pathways
- A pain reduction is associated with a significant reduction of eotaxin in CSF
- Amitriptyline likely has a neurotrophic effect in responders with neuropathic pain

Published :

Brain, Behaviour and Immunity Health (297)

https://doi.org/10.1016/j.bbih.2020.100184

2.1 Abstract:

Introduction: Amitriptyline is prescribed to reduce the intensity of chronic neuropathic pain. There is a paucity of validated *in vivo* evidence in humans regarding amitriptyline's mechanism of action. We examined the effect of amitriptyline therapy on cerebrospinal fluid (CSF) neuropeptides and proteome in patients with chronic neuropathic pain to identify potential mechanisms of action of amitriptyline.

Methods: Patients with lumbar radicular neuropathic pain were selected for inclusion with clinical and radiological signs and a >50% reduction in pain in response to a selective nerve root block. Baseline and 8-week pain scores with demographics were recorded. CSF samples were taken at baseline and 8 weeks after amitriptyline treatment. Proteome analysis was performed using mass spectrometry and secreted cytokines, chemokines and neurotrophins were measured by enzyme-linked immunosorbent assay (ELISA).

Results: A total of 9/16 patients experienced a >30% reduction in pain after treatment with amitriptyline and GO analysis demonstrated that the greatest modulatory effect was on immune system processes. KEGG analysis also identified a reduction in phosphatidylinositol 3-kinase protein kinase B (PI3K-Akt) and mitogen-activated protein kinase (MAPK) signalling pathways in responders but not in non-responders. There was also a significant decrease in the chemokine eotaxin-1 ($p=0.02$) and a significant increase in the neurotrophin VEGF-A ($p=0.04$) in responders.

Conclusion: The CSF secretome and proteome was modulated in responders to amitriptyline verifying many pre-clinical and *in vitro* models. The predominant features were immunomodulation with a reduction in pro-inflammatory pathways of neuronal-glia communications and evidence of a neurotrophic effect.

2.2 Introduction

Amitriptyline is a tertiary amine, tricyclic antidepressant first introduced in 1961 (298). Amitriptyline's mechanism of action in the treatment of depression include re-uptake inhibition of serotonin and noradrenaline from its active metabolite nortriptyline at the synaptic cleft (299). The pharmacodynamics of amitriptyline proposed from pre-clinical and *in vitro* studies are extensive but many have not been validated by *in vivo* evidence in humans (49-51, 225, 226, 237-239, 243-248, 250, 300-307). For this reason, amitriptyline's mechanism of action in many off-label applications including neuropathic pain, fibromyalgia, migraine prophylaxis and complex regional pain syndrome (CRPS) have yet to be defined. Amitriptyline's analgesic effect is achieved using lower doses than is required to treat depression and there are reports of a faster onset of action for alleviation of pain (50, 308). This suggests that at different concentrations amitriptyline targets different pathways and may have a different mechanism of action for off-label applications including chronic neuropathic pain (CNP).

The pathophysiology of neuropathic pain and other neuroinflammatory conditions has been attributed at least in part to pathological changes in the neuroimmune interface (3, 53, 129, 168, 180, 183, 199, 309). This involves a multi-directional communication between neurons, immune cells and glia (3, 30). Many of the mechanisms proposed for the therapeutic action of amitriptyline in CNP relate to pathways within this interface (225, 226, 237, 245-248, 250, 300-305). *In vitro* studies have demonstrated amitriptyline's pharmacodynamic effect on glial cells, which are the predominant cells within the central nervous system with many anti-inflammatory mechanisms described (245, 247, 250, 300, 303, 304). Specifically, amitriptyline has reduced pro-inflammatory cytokines and suppressed ERK 1/2 and MAPK signalling proteins associated with an increase in mechanical withdrawal threshold in mice(248). Amitriptyline has potential neurotrophic activity as well, inducing dynamic changes in brain derived neurotrophic factor (BDNF) (225, 226), and glial cell derived neurotrophic factor (GDNF) *in vitro* (226, 245, 246, 310, 311). Tricyclic compounds have also demonstrated upregulation of vascular endothelial growth factor (VEGF) in the hippocampus of rodents (312).

In vitro studies of human T cells have demonstrated anti-inflammatory properties of amitriptyline by reducing the frequency of IFN-γ producing $CD8^+$ cells and IL-17 producing $CD8^+$ and $CD4^+$ cells (313). Tricyclic antidepressants have also demonstrated prevention of differentiation of monocytes into macrophages *in vitro* (314). CNP conditions

including HIV neuropathy (32, 197, 315), diabetic neuropathy (133, 218) and chronic radicular pain (183, 218) have all implicated neuroimmune dysfunction in their pathophysiology. Although not effective in every case, amitriptyline remains a first line medication for patients with these conditions (23, 45).

Lumbar/sacral radicular pain is neuropathic pain radiating down one or more lumbar/sacral dermatomes. This pain is also described commonly as 'sciatica' or 'nerve root pain'. The point prevalence is 4.6-13.4% and lifetime prevalence is 1.2%-43%, which means it is the most common form of neuropathic pain (316). Acute pain becomes chronic in approximately 30% of patients (46). Diagnosis is made based on history, physical examination and radiological evaluation with confirmation provided by a diagnostic nerve root block (46). Amitriptyline is frequently the first therapy employed to treat chronic radicular pain (317, 318). A randomised controlled trial demonstrated amitriptyline was superior to placebo in patients with sub-acute lumbar radicular pain (317). We hypothesised, assuming a central mechanism of action of amitriptyline, that it modulates the neuroimmune interface alleviating the symptoms of CNP. The examination of neuropeptide and proteomic constituents of cerebrospinal fluid (CSF) has previously been utilised to explore the mechanisms of action of therapies (53, 60, 122, 188, 213). We examined and characterised the cytokine networks and proteomic constituents of CSF before and after amitriptyline treatment using lumbar radicular pain as a clinical model to identify the mechanistic actions of amitriptyline and provide information regarding the pathophysiology of CNP.

2.2.1 Aims:

The aim of this chapter was to explore mechanisms of action of amitriptyline for the treatment of neuropathic pain by examining the cellular, neuropeptide and proteomic constituents of CSF before and after amitriptyline treatment.

2.3 Methods

2.3.1 Location/Ethics/Registration

This was a prospective interventional observational study performed in St James's Hospital, Dublin 8, Ireland; a tertiary referral centre for chronic pain. Ethical approval from the St James's and AMNCH Research Ethics Committee, Dublin, Ireland was sought and obtained. The study was registered online at http://www.isrctn.com/ISRCTN70120536

2.3.2 Participants

Patients attending the pain clinic at St. James Hospital, Dublin were offered inclusion if they met the following inclusion/exclusion criteria. The inclusion criteria were: patients aged 20 -65 years with lumbar radicular pain for >6 months, clinical and radiological evidence of lumbar radicular pain, Douleur Neuropathique (DN4) score of >3 and a reduction in Numerical Pain score (NRS) of >50% after diagnostic nerve root block. Exclusion criteria were: patient refusal, central spinal stenosis, anticoagulant medication, infection, pregnancy, breastfeeding, corticosteroid therapy or NSAID's, stroke, psychiatric history, history of ischaemic heart disease, arrhythmia or heart block, cerebral impairment, current anti-neuropathic medication (excluding opioids) or biologic medication. All patients were given an information leaflet about inclusion in the study. All patients signed a consent form approved by the hospital ethics committee for inclusion in the study. A consent form for the lumbar puncture (CSF sampling) and selective nerve root block was also signed.

2.3.2 CSF Sampling

Under strict asepsis and AAGBI guidelines(319), CSF was obtained between the fourth and fifth lumbar vertebra under fluoroscopic guidance. This occurred at the same time period between 13:00-14:00 hours with the patients fasting for 13-14 hours prior to sample collection. Lidocaine 1%, 2-3ml was infiltrated at the skin for analgesia. An introducer and 25 Gauge Whittacre needle (B braun®) was inserted until resistance entering the dura was felt. 1ml of CSF (2ml in total) was collected in two separate tubes: one for ELISA and one for mass spectrometry. The acquired CSF samples were visually inspected for blood

contamination. The proteomics aliquots were centrifuged for 10 minutes at 2000 g and the supernatant was transferred to a new tube. The tubes were immediately frozen at -20 °C for ELISA and at -80 °C for proteomics. A second consented lumbar puncture (LP) sample was obtained in the same manner after 8 weeks. The time period of 8 weeks was selected to be consistent with the treatment course of anti-neuropathic medications recommended in order to gauge efficacy (45).

2.3.3 Pain Measurement and Diagnosis

Each patient completed an average 24-hour (NRS)(320) and a DN4 score(41) by prior to obtaining the initial CSF sample. After CSF sampling the patients underwent a selective nerve root block. The patients were placed in prone position with pillows to diminish lumbar lordosis. Under strict asepsis and fluoroscopy the vertebra with the corresponding affected nerve was levelled off and rotated to the ipsilateral side so the spinous processes were in line with the contralateral facet column. A 22 Gauge needle was placed inferior to the pedicle and advanced under lateral fluoroscopic guidance to the posterior "safe line" of the epidural space. Iohexol 240mg l/ml (Omnipaque TM, GE Healthcare, Cork, Ireland) 0.5ml was injected to confirm spread along the distribution of the nerve and rule out intravascular placement of the needle. Once in the correct position, 1ml of 1% lidocaine was injected. Patients were again asked to complete a NRS pain score 30 minutes after the diagnostic block. Successful block was determined if the decrease in NRS pain score was >50%.

2.3.4 Intervention

Patients treatment with amitriptyline 10mg nocte was initiated (at night) following the first sample collection. The patients had the option of ceasing the medication and withdrawing from the study at any time. If this occurred, they would have their baseline sample included in the analysis, but a second CSF sample would not be taken. The patients were asked to remain on their other medications including opioids until after the second CSF sample. After one month if tolerated the dose was increased to 25mg. After 8 weeks the patient returned for the second CSF sample with repeat NRS and DN4 scores recorded. Following completion of the study the patients were given the option of staying on the medication or

not. Their answer and reason were also recorded. Successful treatment with amitriptyline was determined by having a >30% reduction in NRS at 8 weeks.

2.3.5 Quantification of soluble mediators in CSF

Glial Cell Derived Neurotrophic factor (GDNF) and Fractalkine singleplex ELISAs (Abcam, Cambridge, UK) were carried out according to the manufacturer's guidelines. Mesoscale Discovery (MSD, Rockville, MD, USA) V-Plex Human Cytokine 30-Plex kit, R-Plex Human Brain Derived Neurotrophic factor (BDNF) antibody set with MSD Gold 96-plate pack and 96- well 4-spot prototype human Nerve Growth Factor (NGF) ELISAs were also carried out according to the manufacturer's instructions. MSD plates were read using MesoScale Diagnostics Sector S600. The sensitivities to the kits are available at www.mesoscale.com, www.abcam.com and in our recent published work (321).

2.3.6 GDNF ELISA:

GDNF singleplex ELISA was carried out according to the manufacturer's guidelines. Briefly, all reagents were allowed to come to room temperature. Assay Diluent B was diluted 5-fold with deionised water. 20ml of wash buffer concentrate was added to 380ml of deionised water to yield 400ml of wash buffer. The Biotinylated anti-Human GDNF detection antibody vial was vortexed. 100 µl of assay diluent B was added and pipetted up and down to mix. The detection antibody was diluted 80 fold with assay diluent B prior to assay procedure. The HRP-Streptavidin concentrate was vortexed and pipetted up and down and diluted with 400-fold assay diluent B.The vial of GDNF Standard was vortexed. The 50ng/ml stock standard was prepared by adding 400 µl Assay Diluent A into the vial. Tubes were labelled #1-7. Standard #1 was prepared by adding 20 µl of the 50ng/ml stock standard to 480 µl of assay diluent A and mixed thoroughly. 400 µl of assay diluent A was placed into the remaining tubes. Standard #2 was prepared by adding 200 µl of Standard #1 and mixed. Standard #3 was prepared by adding 200 µl of Standard # 2 to tube #3 and mixed thoroughly. Serial dilutions were then followed as above until standard #8 which was made up of assay diluent A and served as the zero standard of 0 pg/ml. Samples were left to thaw to room temperature. They were added neat.

Each sample was assayed in duplicate. 100 µl for each standard and 100 µl of each sample was added to each well. The wells were covered and incubated for 2.5 hours in a well plate shaker at room temperature. The solution was discarded and washed 4 times with wash solution of 300 µl using a multi-channel pipette. The plate was then blotted against a clean paper towel. 100 µl of GDNF detection antibody was added to each well and then incubated at room temperature for 60 minutes. The wash was discarded and washed as described above. 100 µl of HRP- Streptavidin solution was added to each well and incubated for 45 minutes at room temperature in a plate shaker. The solution was discarded and washed. 100 µl of tetramethylbenzidine (TMB) one-step substrate reagent was added to each well and incubated for 30 minutes at room temperature in the dark in a plate shaker. 50 µl of stop solution was added to each well and read at 450nm immediately using VersaMax plate reader.

Calculation of the mean absorbance of duplicate standards and samples were obtained. This was subtracted from the average of the zero standard optical density. A standard curve on Excel (Microsoft, USA) was plotted with concentration on the x-axis and the absorbance on the y-axis. The best fit straight line was drawn by Excel to determine the concentrations.

2.3.7 Fractalkine (CX3CL1) ELISA:

All reagents were equilibrated to room temperature. Wash buffer was prepared by diluting the wash buffer solution with ten times deionised water. The antibody cocktail was formed by diluting the capture and detector antibodies in antibody diluent 4BI. The same volume of detector antibody and capture antibody was added to 8-fold antibody diluent 4BI. The fractalkine standard was prepared by adding 1ml of sample diluent and vortexed which contained 5000pg/ml of stock standard solution. Tubes were labelled #1-8 and 285 µl of sample diluent was added to tube #1 and 150 µl sample diluent to tubes #2-8. 15 µl of stock standard solution was added to tube #1 and subsequently 150 µl of tube #1 was added to tube #2. 150 µl of tube #2 was added to tube #3 and the same dilation pattern was repeated to tube #7 giving it a concentration of 3.9 pg/ml. Tube #8 contained no protein.

Samples were left to thaw to room temperature. They were added neat. Each sample was assayed with two replicates. 50 µl of sample or standard was added to appropriate well. The plates were sealed and incubated at room temperature for 1 hour on a plate shaker at 400rpm. Each well was subsequently washed with 3 x 350 µl of wash buffer using a multi-

channel pipette. 100 µl of TMB substrate was added to each well and incubated for 10 minutes in the dark on plate shaker set to 400 rpm. 100 µl of stop solution was added to each well and placed on the plate shaker for 1 minute. The optical density was then recorded at 450nm using a VersaMax platereader. Calculation of the mean absorbance of duplicate standards and samples were obtained. This was subtracted from the average of the zero standard optical density. A standard curve on Excel (Microsoft, USA) was plotted with concentration on the x-axis and the absorbance on the y-axis. The best fit straight line was drawn by Excel to determine the concentrations.

2.3.8 Multiplex ELISAs:

Mesoscale Discovery V Plex plates were used for multiple analyte analysis. All reagents were brought to room temperature. 7 calibrator solutions were prepared plus a zero calibrator. The highest calibrator was prepared (Calibrator 1) by adding 1,000 µL of Diluent 43 to the lyophilized calibrator vial. After reconstituting it was inverted at least 3 times. The reconstituted solution equilibrated to room temperature for 15-30 minutes and then vortexed briefly using short pulses. The next calibrator was prepared by transferring 100 µL of the highest calibrator to 300 µL of Diluent 43 and mixed well by vortexing. Repeated 4-fold serial dilutions 5 additional times were used to generate 7 calibrators. Diluent 43 was used as the zero calibrator.

60 µL of the following SULFO-TAG Anti-hu detection antibodies were added to 2,400 µL of Diluent 3. Each plate was done separately as per panel. Panel 1 (Human Cytokine) contained: GM-CSF, IL-1α, IL-5, IL-7, IL-12/IL-23p40 ,IL-15, IL-16, IL-17A, TNF-β , VEGF-A. Panel 2 (Pro-inflammatory) contained: IFN-γ, IL-1β,IL-2, IL-4, IL-6, IL-8, IL-10,
IL-12p70, IL-13 and TNF-α. Panel 3 (Chemokines) contained Eotaxin-1, MIP-1β, Eotaxin-3, TARC, IP-10, MIP-1α, IL-8 (HA), MCP-1, MDC, MCP-4.

To prepare wash buffer 15 mL of MSD Wash Buffer (20X) was added to 285 mL of deionized water. To prepare read Buffer, 10 mL of Read Buffer T (4X) was combined with 10 mL of deionized water.

The plate was washed 3 times with 150 µl/well of Wash Buffer. 50 µl of prepared samples were added to the well. The plate was sealed with an adhesive plate seal and incubated at room temperature with a plate shaker at 400rpm for 2 hours. The plate was washed 3 times

with 150 µL/well of Wash Buffer. 25 µL of detection antibody solution was added to each well. The plate was sealed with an adhesive plate seal and incubated at room temperature with a plate shaker at 400rpm for 2 hours. The plate was washed 3 times with 150 µL/well of Wash Buffer. 150 µL of 2X Read Buffer T was added to each well. The plate was analysed on the MSD Sector Imager 2400 instrument.

2.3.9 MSD R-Plex plates for NGF and BDNF ELISAs:

200µL of biotinylated capture antibody was added to 3.3 mL of coating diluent and mixed by vortexing. 25 µL of the this solution was added to each well of an MSD GOLD Small Spot Streptavidin plate. This was then tapped gently on all sides. The plate was sealed with an adhesive plate and incubated at room temperature for 1 hour with a shaking plate at 400rpm. Following this the plate was washed 3 times with 150 µL/well of 1X MSD Wash Buffer. The plate was then coated with the capture antibody. The stock calibrator was thawed and keep on ice, then added to assay diluent at room temperature to make the calibration curve solutions. To prepare 7 calibrator solutions plus a zero calibrator for up to 4 replicates: the highest calibrator was prepared by adding 15 µL of stock calibrator to 285 µL of assay diluent and mixed well. The next calibrator was prepared by transferring 50 µL of the highest calibrator to 150 µL of assay diluent and mixed well. 4-fold serial dilutions were repeated 5 times to generate 7 calibrators. The assay diluent was used as the blank. The antibody solution was prepared by adding 60 µL of the supplied 100X detection antibody with 5,940 µL of antibody diluent. The two antibodies in a separate plate were NGF and BDNF.

25µL of assay diluent was added to each well and the plate was tapped gently on all sides. 25 µL of the prepared calibrator standard or sample was added to each well. The plate was sealed with an adhesive plate seal and incubated at room temperature in a plate shaker at 400rpm for 1 hour. The plate was washed 3 times with 150 µL/well of 1X MSD Wash Buffer. 50 µL of detection antibody solution was added to each well; the plate was sealed with an adhesive plate seal and incubated at room temperature with a plate shaker for 1 hour. The plate was washed 3 times with 150 µL/well of 1X MSD Wash Buffer. 150 µL of MSD GOLD Read Buffer was added to each well. Analysis was the carried out on an MSD Sector Imager 2400 instrument.

2.3.10 Sample preparation and protein identification for mass spectrometry

All mass spectrometry (MS) and assistance with data analysis was performed by Dr Hilary Cassidy, Systems Biology Ireland, UCD (University College Dublin). Sample preparation and protein identification have previously been described (321). SP3 preparation was performed according to the protocol of Hughes and colleagues (322). The SP3 protocol utilizes commercially available beads which carry a carboxylate moiety. For this experiment both hydrophobic and hydrophilic Sera-Mag Speed bead Magnetic carboxylate modified particles were employed in a 1:1 mix (GE Healthcare). Prior to use the beads were combined in a ratio of 1:1 (v/v), rinsed and reconstituted in MS grade water (Fisher Scientific) at a stock concentration of 10µg/ml and stored at 4°C until required.

SP3 preparation was performed according to the protocol of Hughes *et al* (322). Briefly, 200µg CSF was resuspended in 100µl lysis buffer [6M urea, 2M thiourea, 50mM MOPS) and centrifuged for 15 minutes at 15,000 RCF at 4ºC to remove any cellular debris. The supernatant was transferred to a fresh Eppendorf tube. The CSF was reduced by adding 0.2M 1,4-dithiothreitol (DTT; Sigma Aldrich) and incubated at 37ºC on a shaker at 700 rpm for 15 minutes. Samples were then alkylated by adding 0.4M iodoacetamide (IAA; Sigma Aldrich). Next acetonitrile (ACN; Sigma Aldrich) was added to each sample to give a final concentration of 70% acetonitrile (v/v) and the prepared SP3 bead mixture was added to each sample and rotated for 18 minutes at room temperature. Subsequently the beads were immobilized by incubation for 2 minutes on the DynaMag-2™ stand (Thermo Fisher). The supernatant was discarded and the pellet was rinsed with 70% (v/v) ethanol in water and 100% ACN. Beads were resuspended in 50 mM ammonium bicarbonate (NH_4HCO_3; Sigma Aldrich). Lyophilised sequence grade trypsin (Promega) was resuspended in 50mM ammonium bicarbonate to a final concentration of 0.5µg/µl and the pH was adjusted to pH 7 before 4µl of trypsin was added to each sample. After overnight digestion at 37°C on a thermoshaker at 500rpm, an additional 8µl of prepared bead mixture was added to the samples and ACN was added to reach a final concentration of 95% (v/v). After mixing and incubation, the supernatant was removed and beads were rinsed with 100% ACN. The peptides bound to the beads were eluted using HPLC grade water with intermittent vortexing. The supernatant containing the purified peptides was transferred into a fresh tube containing 2µl of 10% acetic acid. The samples were placed on the

DynaMag-2™ for 5 minutes before the supernatant was transferred to MS vials for analysis.

2.3.11 LC-MS/MS analysis

Each sample was run in duplicate on a Thermo Scientific Q Exactive mass spectrometer connected to a Dionex Ultimate 3000 (RSLCnano) chromatography system. Each sample was loaded onto a fused silica emitter (75μm ID), pulled using a laser puller (Sutter Instruments P2000, Novato, CA, USA), packed with ReprocilPur (Dr Maisch, Ammerbuch-Entringen, Germany) C18 (1.9μm; 12 cm in length) reverse phase media and were separated by an increasing acetonitrile gradient over 60 minutes at a flow rate of 250 nL/min direct into a Q-Exactive MS. The MS was operated in positive ion mode with a capillary temperature of 320 °C, and with a potential of 2300 V applied to the frit. All data was acquired while operating in automatic data dependent switching mode. A high resolution (70,000) MS scan (300-1600 m/z) was performed using the Q Exactive to select the 12 most intense ions prior to MS/MS analysis using high-energy collision dissociation (HCD).

2.3.12 Data Analysis and Statistics

The ELISA statistical analysis was performed using Prism Graph Pad version 8.0. Fishers exact test was used to compare categorical data. Non-parametric paired and unpaired tests were used where appropriate, Wilcoxon Sign Rank and Mann Whitney respectively for continuous data. Data was expressed in means with standard error of means (SEM). Correlations between the percentage reduction in pain and the difference in the concentration of neuropeptides before and after amitriptyline were calculated using Spearman test with r, confidence intervals (CI) and p values. P values of <0.05 were considered to be significant.

For proteomics, proteins were identified and quantified by MaxLFQ (323) by searching with MaxQuant version 1.5 against the Homo Sapiens reference proteome database which was obtained from Uniprot. Normalisation is conducted through the MaxQuant LFQ algorithm for label-free quantification (323), which has successfully been benchmarked against other software solutions for label-free quantification, independently confirming its

performance. MaxLFQ is a generic method for label-free quantification that can be combined with standard statistical tests of quantification accuracy for each of thousands of quantified proteins (324). In brief, protein abundance profiles are assembled using the maximum possible information from MS signals, given that the presence of quantifiable peptides varies from sample to sample. This is based on the assumption that most proteins do not or only minimally change between conditions, to have a constant baseline (the algorithm still works with (quantitative) changes in about one third of all proteins (323). Once the Maxquant analysis is complete, the individual LFQ intensities for all technical replicates were expressed as a Log_2 value and an average Log_2 value was determined for each of the treatment groups, i.e. responders and non-responders.

For the purposes of identifying proteins which were significantly altered following amitriptyline in the responders and non-responders, strict filtering settings were applied to the proteomics data in order identify proteins which were significantly increased [log fold change (LFC) > 2, false discovery rate (FDR)< 0.05] and decreased (LFC < -2, FDR < 0.05) using Log(p)>1.13 as a cut off following amitriptyline.
Proteins found to be differentially expressed between groups were subjected to pathway mapping analysis and were distributed into categories according to their cellular component, molecular function, and biological process using Ingenuity Pathway Analysis (IPA) [QIAGEN (Redwood City, CA)] or STRING Database (Version 10.5). STRING (www.string-db.org) was used to generate protein-protein interaction networks, which were then imported into Cytoscape for further editing (Version 3.4.0). The NeuroPep database (islab.info/NeuroPep/) and the neuropeptides database (www.neuropeptides.nl) were employed to identify neuropeptides from mass spectrometry. Kyoto Encyclopedia of Genes and Genomes (Kegg) pathway analysis was used to determine increased and decreased expression of proteins.

2.3.13 Flow Cytometry:

After collection, samples were stored at 4°C for no longer than 72 hours in TransFix/EDTA CSF Sample Storage Tubes (CaltagMedsystems Ltd, Buckingham, UK). Samples were allowed to come to room temperature, after which time 2ml of phosphate buffered saline (PBS) solution was added to each tube and centrifuged at 1500 rpm for 3 minutes. The supernatant was discarded and the Transfix tube vortexed. The pellet in the Transfix tube was re-suspended in 200 µl of PBS and divided between three FACS tubes. Three panels

were used, one for T cells, one for Natural Killer (NK) cells and one left unstained as a control. All antibodies were vortexed prior to addition into tubes. Panel 1(T cells) contained: CD-8 (2 µl), CD4(2 µl), CD27(2 µl), CD45(2 µl), CD69(2 µl), CD-45RA(2 µl) (Mitlenyi Biotech, Germany) and CD3 PE-eFluor 610 (2 µl) (eBioscienceThermoFisher Scientific, USA). Panel 2 (NK cells) contained: CD56 (5 µl), CD69 (2 µl), CD45 (2 µl), and CD3-PE- eFluor 610 (2 µl) (Biosciences, Dublin, Ireland). The tubes were vortexed and incubated in the dark for 30 minutes at 4 °C. 2ml of PBS were added to each tube and centrifuged at 1500 rpm for 3 minutes. The supernatant was discarded and the tubes vortexed. The samples were analysed by flow cytometry. Data was acquired using a CyAn™ ADP Analyzer (Beckaman Coulter) and Summit v4.1 and analysed using FlowJo v7.6.1.

2.4 Results

2.4.1 Patient related outcomes

A total of 16 patients entered the study and had a CSF sample taken prior to commencing amitriptyline (pre-treatment sample) (Figure 8). The demographics of the patients including their opioid medications are summarised in Table 1. All patients reported a successful diagnostic nerve root block with a >50% reduction in pain according to NRS and were started on 10mg of amitriptyline (Figure 8, Table 2). One patient reported a lack of efficacy with amitriptyline and problematic anticholinergic side effects at 3 weeks and ceased the medication (Study ID 103). Another patient reported a lack of efficacy with amitriptyline and poor therapeutic regime compliance and was subsequently lost to follow up (Study ID 104) (Figure 1). Fourteen patients (14/16, 87.5%) achieved a dose escalation to 25mg after 4 weeks of treatment (Figure 1). Thirteen patients (13/16, 81%) had a second sample of CSF taken, one patient refused a second CSF sample and was a non-responder to amitriptyline (Study ID 106). In total, there were 16 CSF samples before amitriptyline (pre-treatment samples) and 13 samples after an 8-week course of amitriptyline (post-treatment samples). Nine patients reported a >30% reduction in pain according to NRS after 8 weeks of amitriptyline (9/16, 56%). We performed analysis on the patients who responded to amitriptyline by reporting a >30% reduction in NRS at 8 weeks (n=9),

classified as ‘responders’. We also performed analysis on the ‘non-responders’ (<30% reduction in pain) as a comparative group (n=7), this included 7 “pre-treatment” and 4 “post-treatment” samples. The patients who did not have a second CSF sample taken had their pre-treatment sample included in the analysis on an intention to treat basis, all were non-responders. Patients 103 and 106 had pain scores taken at 8 weeks. No pain score was taken at 8 weeks in patient 104 but there was no reported benefit to the medication before being lost to follow up. There was no difference in demographics, opioid use and pre-treatment neuropeptide concentrations within the CSF of the responder group and the non-responder group (Table 3). Out of the patients that started the study, 10/16 (62.5%) remained on amitriptyline after 8 weeks. The most common reasons given for remaining on amitriptyline were due to pain reduction and improved sleep (Table 2). There was no dose escalation or de-escalation of opioids recorded in any of the patients.

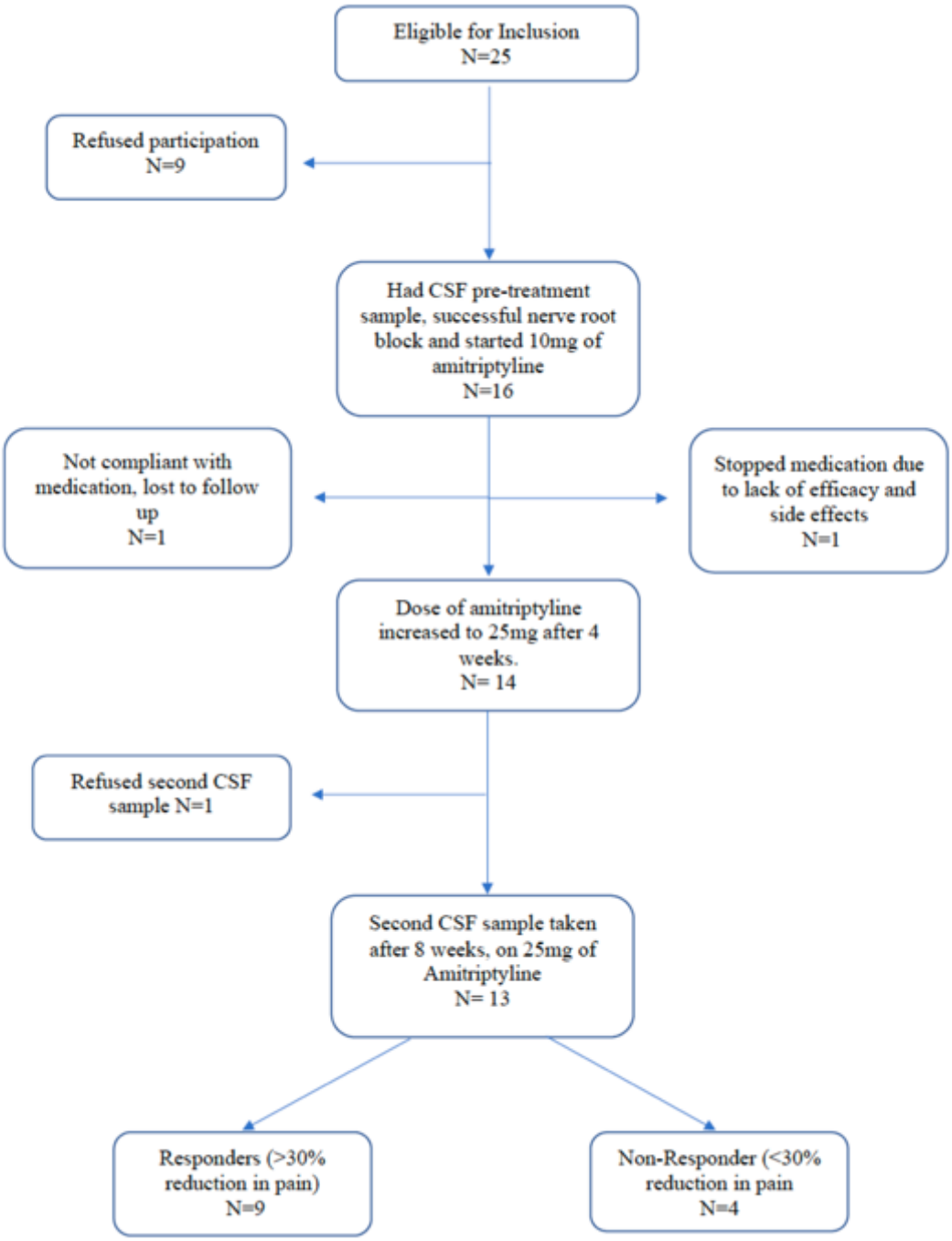

Figure 8: Patient flow and Consort diagram of patients eligible for inclusion for the study, intervention and Cerebrospinal fluid (CSF) sampling

Table 1: Summary of patient demographics including age, gender, nerve root anatomical location of radicular pain, opioids and morphine milligram equivalents (MME).

Study ID	Age	Sex	Affected Nerve Root	Opioid Medication	Type and Dose of Opioid	Morphine milligram equivalents (MME)
101†	63	Female	L5	No	-	-
102†	48	Male	L5	No	-	-
103	61	Female	L5	No	-	-
104	35	Male	S1	No	-	-
105†	56	Male	L5	Yes	Oxycodone 60mg	120mg
106	57	Male	L5/S1	No	-	-
107†	64	Male	L5	Yes	Fentanyl patch 75mcg/hr	270mg
108†	45	Female	L5	Yes	Oxycodone 20mg	40mg
109	50	Female	L5	Yes	Tramadol 100mg	20mg
110	30	Male	L5/S1	No	-	-
111†	53	Female	L4	Yes	Codeine 240mg	24mg
112	40	Female	L5	No	-	-
113†	64	Female	L5	No	-	-
114†	45	Female	L5	Yes	Tramadol 200mg	40mg
115†	42	Female	L5	No	-	-
116	57	Female	L4	No	-	-

† indicates responders to amitriptyline (>30% reduction in pain after 8 weeks).

Table 2: Pain Scores according to numerical rating score (NRS) and Doleur Neuropathique 4 (DN4) at baseline, after selective nerve root block and after amitriptyline

Study ID	NRS	DN4	NRS Post SNRB	NRS Post Amitriptyline	DN4 Post Ami	Stay on Medication	Reason for continued use/cessation
101†	9	8	0	5	8	Yes	Pain reduction and improved sleep
102†	6	4	1	3	4	Yes	Pain reduction and improved sleep
103	9	7	0	-	-	No	Not effective
104	4	6	0	-	-	-	Lost to follow up
105†	9	7	3	5	7	Yes	Pain reduction
106	10	5	5	-	-	No	Not effective
107†	7	4	0	3	3	Yes	Pain reduction
108†	6	8	3	3	4	Yes	Pain reduction
109	6	6	0	7	5	No	Dry mouth/ Fatigue
110	6	5	1	5	5	Yes	Pain reduction
111†	7	6	1	1	3	Yes	Pain reduction and improved sleep
112	4	8	1	6	4	No	Not effective
113†	5	4	1	2	3	Yes	Pain reduction/ Improved sleep
114†	7	8	4	4	4	Yes	Pain reduction

115†	8	6	1	1	5	Yes	Pain reduction/ Improved sleep
116	6	4	1	7	4	No	Not effective

Table 3: Comparison of demographics and baseline neuropeptides between responders to amitriptyline (>30% reduction in pain) and non-responders (<30% reduction in pain)

	Responders	Non- Responders	p-value (Fisher's exact test)
Age	53.33 ± 2.944	47.14 ± 4.595	0.337
NRS	7.11 ± 0.455	6.43 ± 0.87	0.385
DN4	6.22 ± 0.54	5.86 ± 0.51	0.72
Opioids			
Taking opioids	5	1	
Not taking opioids	4	6	0.145
Male	3	3	
Female	6	4	1
Neuropeptides	Mean pg/ml (SEM)	Mean pg/ml (SEM)	p-value (Mann-Whitney test)
Eotaxin-1	29.79 ± 7.48	18.97 ± 3.62	0.47
Eotaxin-3	4.51 ± 1.15	8.29 ± 1.95	0.16
IFN-γ	0.76 ± 0.35	0.34 ± 0.07	0.62

IL-10	0.14 ± 0.03	0.09 ± 0.02	0.31
IL-12/IL-23p40	5.66 ± 0.99	4.75 ± 0.7	0.51
IL-12p70	0.07 ± 0.04	0.05 ± 0.007	0.81
IL-13	2.93 ± 0.29	2.98 ± 0.34	0.89
IL-15	4.96 ± 0.72	4.77 ± 0.62	0.68
IL-16	10 ± 0.86	11.92 ± 1	0.35
IL-17A	0.46 ± 0.12	0.36 ± 0.07	0.78
IL-1α	0.7 ± 0.49	0.39 ± 0.12	0.54
IL-1β	0.23 ± 0.02	0.26 ± 0.05	0.83
IL-4	0.06 ± 0.01	0.07 ± 0.01	0.58
IL-5	0.77 ± 0.09	0.68 ± 0.11	0.4
IL-6	1.3 ± 0.22	1.28 ± 0.27	0.91
IL-7	1.24 ± 0.14	1.12 ± 0.22	0.47
IL-8	15.78 ± 2.37	17.88 ± 6.1	0.75
IP-10	258 ± 40.3	209.8 ± 43.94	0.4
MCP-1	387 ± 46.83	423.9 ± 55.1	0.68
MCP-4	10.58 ± 2.43	8.93 ± 2.69	0.75
MDC	57.16 ± 10.4	44.78 ± 7.87	0.46
MIP-1α	8.38 ± 1.2	5.59 ± 0.65	0.14
MIP-1β	11.19 ± 2.26	14.03 ± 3.72	0.46
TARC	10.99 ± 1.07	8.55 ± 0.46	0.09
TNF-α	0.52 ± 0.05	0.5 ± 0.06	0.91
VEGF-A	3.62 ± 0.53	4.295 ± 1.17	0.99

2.4.2 Cytokines, chemokine and neurotrophin analysis following amitriptyline treatment

There was a significant reduction in the chemokine eotaxin-1 (CCL11) in the post-treatment samples in comparison to the pre-treatment samples [(Pre-treatment) 29.79 ± 7.48 pg/ml vs (Post-treatment) 15.26 ± 1.71 pg/ml, p=0.02, n=9] in patient responders to amitriptyline (Figure 9A, Table 4). There was no significant difference in eotaxin-1 in the non-responders between pre-treatment and post-treatment samples [(Pre-treatment) 18.97 ±3.62 pg/ml vs (Post-treatment) 13.22 ±1.07 pg/ml, p=0.52] (Figure 9B, Table 4). Correlation analysis was performed to determine if levels of eotaxin-1 were related to pain scores and DN4 scores prior to treatment. There was no correlation identified with pain scores according to NRS (r=-0.233, CI -0.66 to 0.3116, p=0.38) and DN4 scores (r=0.27, CI -0.27 to 0.68, p=0.31) to eotaxin-1 levels pre-treatment. Correlation analysis was also performed to determine if there was a relationship between the percentage reduction in pain and change in eotaxin-1 (in the n=13 patients that had pre-treatment and post-treatment samples) after amitriptyline treatment. There was no correlation identified between these two variables (r=0.025, CI -0.5464 to 0.5804, p=0.93).

Significantly higher concentrations of Vascular Endothelial Growth Factor (VEGF-A) were observed in the CSF of responder's post-treatment, compared to pre-treatment [(Pre-treatment) 3.62 ± 0.53 pg/ml vs (Post-treatment) 4.45 ± 0.69 pg/ml, p=0.04, n=9] (Figure 9C, Table 4). There was no significant difference between samples of VEGF-A in the non-responders [Pre-treatment 4.3 ±1.18 pg/ml vs Post-treatment 3.79 ±0.98 pg/ml, p=0.91] (Figure 9D, Table 4) . Correlation analysis was performed to determine if levels of VEGF-A were related to pain scores and DN4 scores prior to treatment. There was no correlation between pain scores (r=-0.2598, CI -0.6902 to 0.3065, p=0.34) and DN4 scores (-0.0128, CI -0.53 to 0.5152, p=0.97) to VEGF-A in the pre-treatment samples. To determine if there was a relationship between VEGF-A and percentage reduction in pain, correlation analysis was performed in the n=13 patients with paired samples. No correlation was identified (r= -0.3019, CI -0.7397 to 0.315, p=0.31).

There was no significant difference in TARC (CCL17) in responders to amitriptyline [(Pre-treatment) 10.99 ±1.07 pg/ml vs (Post-treatment) 12.35 ±1.11 pg/ml, p=0.5] (Figure 9E, Table 4) but there was a significant increase in non-responders [(Pre-treatment, n=7) 8.55

±0.46 pg/ml vs (Post-treatment, n=4) 11.31 ± 0.57 pg/ml, p=0.02] (Figure 9F, Table 4). There was no significant difference in the concentration of IL-12p70 in responders to amitriptyline [(Pre-treatment) 0.05 ±0.03 pg/ml vs (Post-treatment) 0.03 ±0.01 pg/ml, p=0.7] (Figure 9G, Table 4) but there was a significant increase in non-responders [(Pre-treatment, n=7) 0.05 ±0.007 pg/ml vs (Post-treatment, n=4) 0.09 ± 0.01 pg/ml, p=0.03] (Figure 9H, Table 4). The results of the other neuropeptide changes in both groups are available in Table 4. GM-CSF, IL-2,TNF-β, NGF, GDNF and BDNF were undetectable in all samples. To demonstrate the modulation of the individual neuropeptides in each individual patient, a heat map was created to illustrate the ratio of the post-treatment sample in comparison to the pre-treatment sample (Figure 10). Although not significant in every case, there was a downward trend in chemokines within the responders compared to the non-responders.

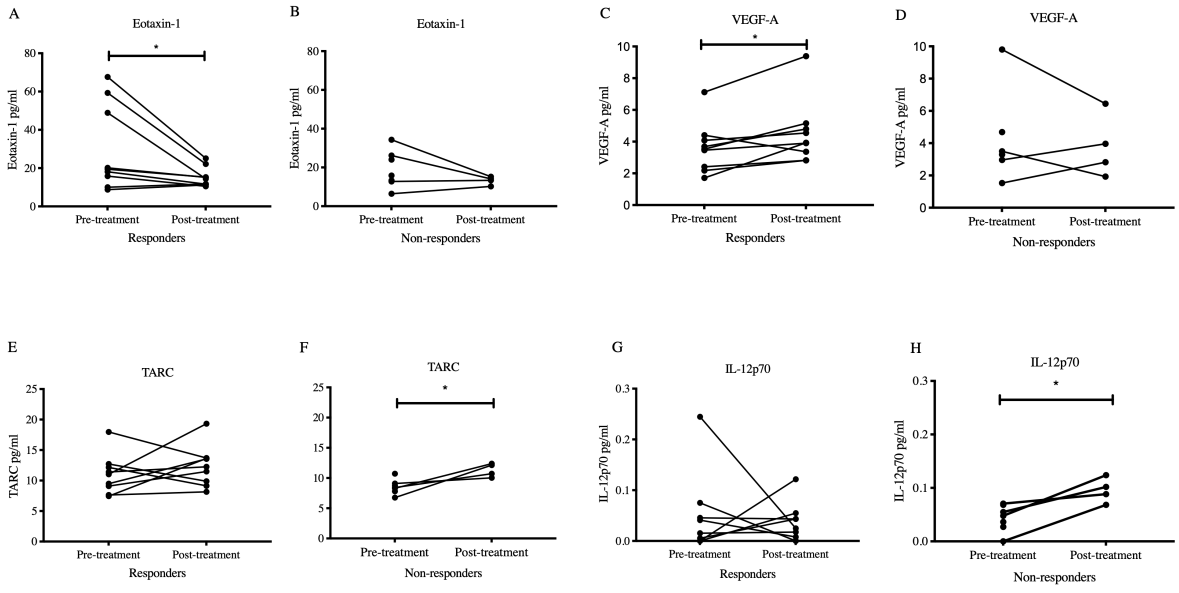

Figure 9: Significant neuropeptide changes: Eotaxin-1 (CCL11) is significantly reduced in the CSF of responders (n=9) after 8 weeks of amitriptyline [(Pre-treatment) 29.79 ±7.48 pg/ml vs (Post-treatment) 15.26 ±1.71 pg/ml, p=0.02] (2A) but not in non-responders [(Pre-treatment) 18.97 ±3.62 pg/ml vs (Post-treatment) 13.22 ±1.07 pg/ml, p=0.52] (2B). Vascular epidermal growth factor A (VEGF-A) is significantly increased in Cerebrospinal fluid (CSF) after eight weeks of amitriptyline in responders (>30% reduction in pain) [(Pre-treatment) 3.62 ±0.53 pg/ml vs (Post-treatment) 4.45 ±0.69, p=0.04] (2C), but not in non-responders [Pre-treatment 4.3 ±1.18 pg/ml vs Post-treatment 3.79 ±0.98 pg/ml, p=0.91] (2D). There is no significant difference in TARC (CCL17) in responders to amitriptyline

[(Pre-treatment) 10.99 ±1.07 pg/ml vs (Post-treatment) 12.35 ±1.11 pg/ml, p=0.5] (2E) but there is a significant increase in non-responders [(Pre-treatment, n=7) 8.55 ±0.46 pg/ml vs (Post-treatment, n=4) 11.31 ± 0.57 pg/ml, p=0.02] (2F). There is no significant difference in the concentration of IL-12p70 in responders to amitriptyline [(Pre-treatment) 0.05 ±0.03 pg/ml vs (Post-treatment) 0.03 ±0.01 pg/ml, p=0.7] (2G) but there is a significant increase in non-responders [(Pre-treatment, n=7) 0.05 ±0.007 pg/ml vs (Post-treatment, n=4) 0.09 ± 0.01 pg/ml, p=0.03] (2H). Non-parametric paired (Wilcoxon Sign Rank) (2A, C, E, G) and unpaired tests (Mann Whitney) (2B, D, F, H) were used with values expressed in means with standard error of means (SEM).

Table 4: Neuropeptide concentrations in pg/ml in Cerebrospinal fluid (CSF) before and after amitriptyline treatment for 8 weeks between responders (>30% reduction in pain) and non-responders (<30% reduction in pain).

	Responders				Non-Responders		
	Mean Pre-Drug (SEM) of neuropetides in pg/ml	Mean Post drug (SEM) of neuropetides in pg/ml	P value		Mean Pre-Drug (SEM) of neuropetides in pg/ml	Mean Post Drug (SEM) of neuropetides in pg/ml	P value
MCP-1	387 ± 46.82	390.5 ± 53.8	0.99		423.9 ±55.1	423.7 ± 20.6	0.52
MCP-4	10.58 ± 2.43	8.85 ± 0.82	0.49		8.94 ± 2.7	11.38 ± 1.85	0.23
Eotaxin-3	4.51 ± 1.15	4.3 ± 1.22	0.99		8.29 ± 1.95	8.3 ± 3.88	0.88
Eotaxin-1	**29.79 ± 7.48**	**15.26 ± 1.71**	**0.02 ***		**18.97 ± 3.62**	**13.22 ± 1.07**	**0.52**
MIP-1α	8.38 ± 1.20	6.08 ± 0.6	0.1		5.6 ± 0.65	6.89 ± 0.75	0.32
MIP-1β	11.19 ± 2.26	9.25 ± 1.45	0.1		14.03 ± 3.72	11.31 ± 0.57	0.93
IP-10	258 ± 40.33	235 ± 15.34	0.65		209.8 ± 43.9	196.8 ± 37.4	0.99
MDC	57.16 ± 10.4	35.02 ± 3.06	0.1		44.78 ± 7.88	39.18 ± 4.84	0.65

TARC	**10.99 ± 1.07**	**12.35 ± 1.11**	**0.5**		**8.55 ± 0.46**	**11.31 ± 0.57**	**0.02 ***
Fractalkine	4.953 ± 1.15	7.182 ± 1.94	0.31		10.9 ± 2.2	6.43 ± 3.1	0.18
IFN-γ	0.38 ± 0.22	0.31 ± 0.14	0.93		0.35 ± 0.07	0.22 ±0.03	0.3
IL-10	0.11 ± 0.03	0.18 ± 0.05	0.11		0.1 ± 0.02	0.11 ± 0.02	0.92
IL-12p70	**0.05 ± 0.03**	**0.03 ± 0.01**	**0.70**		**0.05 ± 0.007**	**0.09 ± 0.01**	**0.03 ***
IL-13	2.9 ± 0.29	3.1 ± 0.22	0.28		2.98 ± 0.34	2.80 ± 0.43	0.61
IL-1β	0.24 ± 0.02	0.31 ± 0.04	0.09		0.26 ± 0.05	0.23 ± 0.06	0.79
IL-4	0.07 ± 0.01	0.08 ± 0.01	0.25		0.07 ± 0.01	0.08 ± 0.03	0.75
IL-6	1.31 ± 0.22	1.5 ± 0.24	0.20		1.28 ± 0.28	1.24 ± 0.09	0.68
IL-8	15.78 ± 2.37	14.95 ± 2.59	0.65		17.8 ± 6.08	12.72 ± 2.44	0.78
TNF-α	0.53 ± 0.0)	0.52 ± 0.05	0.91		0.5 ± 0.06	0.54 ± 0.06	0.79
IL-12/ IL-23p40	5.7 ± 0.99	5.22 ± 1.02	0.36		4.75 ± 0.7	4.70 ± 0.57	0.99
IL-15	4.96 ± 0.72	4.45 ± 0.49	0.16		4.80 ± 0.62	4.61 ± 0.72	0.92
IL-16	10 ± 0.86	10.55 ± 0.81	0.5		11.92 ± 1.02	13.05 ± 1.73	0.41
IL-17A	0.36 ± 0.12	0.46 ± 0.15	0.46		0.36 ± 0.08	0.31 ± 0.11	0.6
IL-5	0.78 ± 0.1	0.81 ± 0.06	0.57		0.69 ± 0.11	0.78 ± 0.11	0.65
IL-7	1.24 ± 0.14	1.30 ± 0.19	0.3		1.12 ± 0.22	1.33 ± 0.39	0.78
VEGF-A	**3.62 ± 0.53**	**4.45 ± 0.69**	**0.04 ***		**4.3 ± 1.18**	**3.79 ± 0.98**	**0.91**

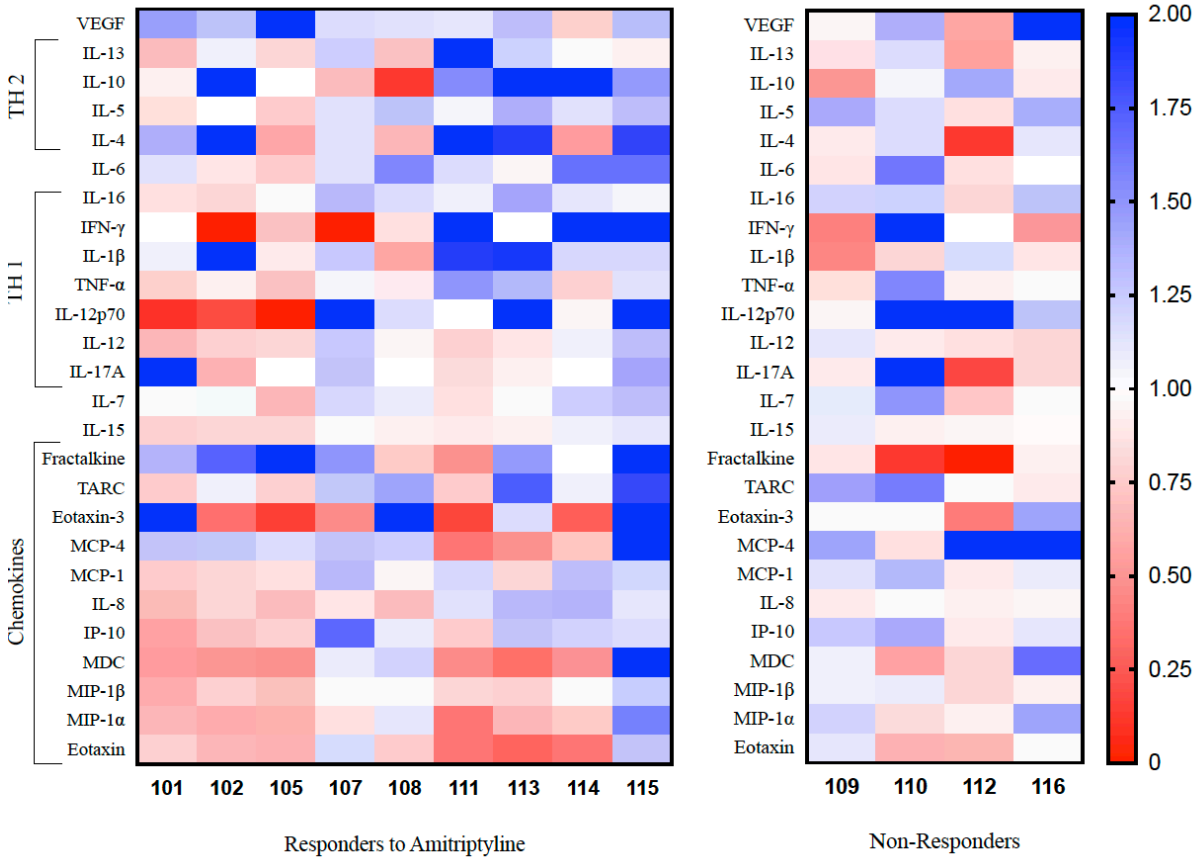

Figure 10: Heat maps of ratios between post-treatment samples (after 8 weeks of amitriptyline) in relation to baseline samples in all patients with paired samples (N=9 in responders, N=4 in non-responders). The fractions are represented by colour according to range, blue being increased and red illustrating relevant decreases in concentration. Values of >2 are illustrated as if they were 2 (dark blue).

2.3.3 Proteomics:

CSF obtained from patients who responded positively to an 8-week course of amitriptyline resulted in the differential expression of 464 proteins compared to pre-treatment samples. Of these 464 differentially expressed proteins, 328 proteins were upregulated and 136 proteins were downregulated following amitriptyline treatment in responders (-2 < LFC > 2) (Figure 11A). The upregulated (Table 5) and downregulated (Table 6) proteins with LFC and FDR values in responders are available as supplementary material. Focusing on these differentially expressed proteins a total of 13 proteins were significantly upregulated (represented by Log(p)>1.13) (Table 7), while 2 proteins were significantly downregulated

after amitriptyline (represented by Log(p)>1.13) (Table 8) (FDR<0.05). The upregulated proteins included Complement C1q tumor necrosis factor-related protein 5, Serine protease inhibitor Kazal-type 6, Tropomyosin alpha-4 chain, Immunoglobulin heavy variable 4-34, Titin, Inter-alpha-trypsin inhibitor heavy chain H3, Cadherin-11, Fibulin-7, Fetuin-B, Immunoglobulin heavy variable 1-18, Immunoglobulin lambda variable 3-16, Epithelial discoidin domain-containing receptor 1 and Semaphorin 6A. The downregulated proteins were Aspartylglucosaminidase and Polypeptide N-acetylgalactosaminyltransferase 2.

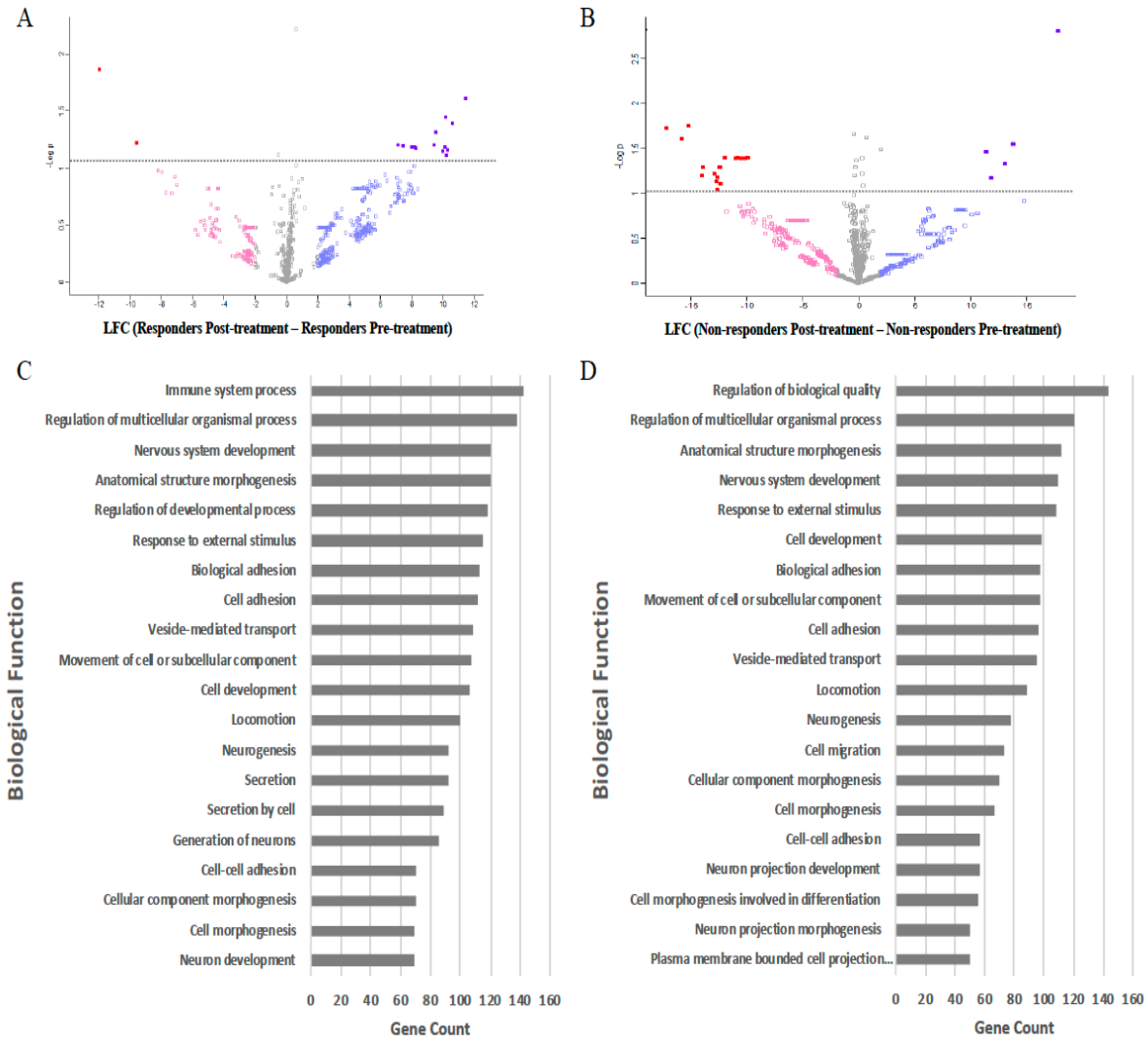

Figure 11: Volcano plots and GO Biological Function: Volcano plots showing differential data of the 464 proteins differentially expressed in responders (11A) to amitriptyline and the 416 differentially expressed proteins in non-responders (11B). Red (decreased) and purple (increased) coloured squares indicate [$-2 \leq$ Log Fold Change (LFC) ≥ 2] with False Discovery Rate (FDR) < 0.05, using Log(p)>1.13 as a cut off for significantly altered proteins. Pink and blue hollow squares indicate ($-2 \leq$ LFC ≥ 2) not significant by FDR. Grey dots are non-significant according to LFC. Proteins taken from Volcano plot with $-2 \leq$ LFC ≥ 2 were further analysed using Gene Otology (GO) analysis to show biological processes in responders (11C) and non-responders (11D). Bar charts illustrate the number of genes involved.

Table 5: All differentially up-regulated proteins in the responders CSF proteome post treatment (Log fold change (LFC) >2) in order of log fold change

Proteins	Gene	LFC	LogP	FDR
Complement C1q tumor necrosis factor-related protein 5	C1QTNF5	11.42819	1.613784	0.046119
Serine protease inhibitor Kazal-type 6	SPINK6	10.61811	1.390578	0.041179
Tropomyosin alpha-4 chain	TPM4	10.31254	1.161122	0.016331
Immunoglobulin lambda variable 3-9	IGLV3-9	10.21451	1.106922	0.000706
Immunoglobulin heavy variable 4-34	IGHV4-34	10.16426	1.44909	0.025403
Titin	TTN	10.15213	1.182481	0.003982
Inter-alpha-trypsin inhibitor heavy chain H3	ITIH3	9.997206	1.146764	0.001663
Cadherin-11	CDH11	9.563253	1.312062	0.035232
Fibulin-7	FBLN7	9.41027	1.199742	0.040171
Immunoglobulin kappa variable 2-30	IGKV2-30	8.406116	0.815816	0.025302
Fetuin-B	FETUB	8.2742	1.171661	0.048387
Immunoglobulin heavy variable 1-18	IGHV1-18	8.185689	1.182731	0.005141
Rab GDP dissociation inhibitor alpha	GDI1	8.181318	1.0182	0.032913
Thymosin beta-4	TMSB4X	8.114562	0.77565	0.035837
Inter-alpha-trypsin inhibitor heavy chain H4	ITIH4	8.056394	0.783139	0.015171
Immunoglobulin lambda variable 3-16	IGLV3-16	8.023568	1.184114	0.000655
Serotransferrin	TF	7.993902	0.819508	0.01003
Spectrin beta chain	SPTBN4	7.960633	0.969096	0.010131
Neutral alpha-glucosidase AB	GANAB	7.907829	0.852551	0.038861
Ephrin type-A receptor 7	EPHA7	7.823435	0.962394	0.039163

Immunoglobulin lambda variable 1-40	IGLV1-40	7.805276	0.8565	0.021371
Cleavage stimulation factor subunit 3	CSTF3	7.760961	0.800228	0.037903
Gamma-enolase	ENO2	7.748377	0.770616	0.027016
Vascular cell adhesion protein 1	VCAM1	7.557629	0.769627	0.030544
Plasma alpha-L-fucosidase	FUCA2	7.541192	0.716678	0.045867
Immunoglobulin kappa variable 1-16	IGKV1-16	7.477572	0.704933	0.024446
Epithelial discoidin domain-containing receptor 1	DDR1	7.47055	1.193837	0.037399
Serum albumin	ALB	7.379386	0.738568	0.004788
N-acetyllactosaminide beta-1,3-N-acetylglucosaminyltransferase 2	B3GNT2	7.254544	0.806971	0.04748
Protein MENT	MENT	7.238085	0.88352	0.045968
Glia-derived nexin	SERPINE2	7.221541	0.753334	0.025806
Heat shock 70 kDa protein 13	HSPA13	7.195482	0.744521	0.034476
Beta-defensin 1	DEFB1	7.175533	0.768265	0.035383
Golgi integral membrane protein 4	GOLIM4	7.172052	0.826421	0.012903
Cathepsin S	CTSS	7.157917	0.738508	0.031956
Sema domain, transmembrane domain (TM), and cytoplasmic domain, (Semaphorin) 6A, isoform CRA_d (Semaphorin-6A)	SEMA6A	7.141019	1.202043	0.002974
Protein disulfide-isomerase A3	PDIA3	7.10535	0.755627	0.032813
Laminin subunit beta-1	LAMB1	7.100268	0.774906	0.013609
Netrin receptor DCC	DCC	7.094054	0.863468	0.011038
Beta-hexosaminidase	HEXA	7.078698	0.720209	0.014768
Netrin-G1	NTNG1	7.054076	0.693102	0.049647
PITH domain-containing protein 1	PITHD1	7.050322	0.910988	0.04622

Leucine-rich repeat and immunoglobulin-like domain-containing nogo receptor-interacting protein 1	LINGO1	6.951312	0.695356	0.044456
Immunoglobulin lambda variable 2-18	IGLV2-18	6.940876	0.766607	0.000605
Twisted gastrulation protein homolog 1	TWSG1	6.656445	0.661405	0.016079
Apolipoprotein B-100	APOB	6.639441	0.603951	0.024093
Dickkopf-related protein 3	DKK3	6.426616	0.886635	0.048085
Scavenger receptor cysteine-rich type 1 protein M130	CD163	6.310534	0.936823	0.01255
Immunoglobulin heavy variable 3-9	IGHV3-9	5.9589	0.848535	0.021875
Matrix Gla protein	MGP	5.83186	0.843416	0.026663
Hyaluronan-binding protein 2	HABP2	5.728062	0.879887	0.03871
CD99 antigen-like protein 2	CD99L2	5.723296	0.574611	0.013861
Haptoglobin-related protein	HPR	5.695962	0.833086	0.019808
Immunoglobulin lambda variable 8-61	IGLV8-61	5.658897	0.452481	0.000454
HCG2044074, isoform CRA_c	MIA-RAB4B	5.645584	0.50891	0.039819
Immunoglobulin kappa variable 1D-16	IGKV1D-16	5.601301	0.467253	0.021018
Latent-transforming growth factor beta-binding protein 4	LTBP4	5.598522	0.827051	0.00499
Complement factor H	CFH	5.587201	0.455301	0.005746
Cysteine-rich secretory protein 3	CRISP3	5.468066	0.505741	0.015675
Adhesion G protein-coupled receptor L1	ADGRL1	5.456646	0.843628	0.018901
Tyrosine-protein kinase receptor TYRO3	TYRO3	5.440636	0.456398	0.014516
Complement C1r subcomponent-like protein	C1RL	5.421855	0.853968	0.047782
Sex hormone-binding globulin, isoform CRA_a	SHBG	5.403968	0.424022	0.015524
Immunoglobulin kappa variable 2-24	IGKV2-24	5.401406	0.479066	0.000907
Immunoglobulin kappa variable 1-17	IGKV1-17	5.35438	0.786853	0.020968

Beta-1,4-galactosyltransferase 1	B4GALT1	5.346389	0.468748	0.029637
Parvalbumin alpha	PVALB	5.320453	0.87417	0.009173
Polypeptide N-acetylgalactosaminyltransferase 6	GALNT6	5.287332	0.465829	0.043044
Lysosome-associated membrane glycoprotein 1	LAMP1	5.273044	0.631152	0.028427
V-set and immunoglobulin domain-containing protein 4	VSIG4	5.269673	0.517698	0.049546
Immunoglobulin kappa variable 1D-39	IGKV1D-39	5.266697	0.820211	0.020917
VPS10 domain-containing receptor SorCS1	SORCS1	5.251321	0.44398	0.043649
Fibulin-2	FBLN2	5.240287	0.796701	0.036442
Neuron-specific vesicular protein calcyon	CALY	5.234496	0.495995	0.047581
Glypican-1 [Cleaved into: Secreted glypican-1]	GPC1	5.215464	0.442803	0.033216
Stanniocalcin-2	STC2	5.211575	0.569803	0.0187
(Death receptor 6) (CD antigen CD358)	TNFRSF21	5.211296	0.788606	0.018397
Immunoglobulin heavy variable 1-69	IGHV1-69	5.210403	0.505993	0.021673
Hypoxia up-regulated protein 1	HYOU1	5.205248	0.832738	0.002218
Immunoglobulin kappa variable 2-40	IGKV2-40	5.185853	0.823654	0.001714
Cell growth regulator with EF hand domain protein 1	CGREF1	5.155449	0.448906	0.045363
Laminin subunit gamma-1	LAMC1	5.133603	0.455035	0.028327
C-C motif chemokine 14	CCL14	5.130085	0.484322	0.039768
Immunoglobulin heavy variable 3/OR16-12	IGHV3OR16-12	5.095563	0.409347	0.001008
CD109 antigen	CD109	5.077099	0.471812	0.041381
Tissue alpha-L-fucosidase	FUCA1	5.029775	0.424189	0.023992
Insulin-like growth factor-binding protein 5	IGFBP5	5.019242	0.729684	0.031855
Semaphorin-3G	SEMA3G	5.009993	0.481919	0.047228
Ryanodine receptor 3	RYR3	5.001	0.823592	0.002268

Protein FAM69C	DIPK1C	4.989687	0.411878	#N/A
Out at first protein homolog	OAF	4.98203	0.745472	0.041734
Intercellular adhesion molecule 5	ICAM5	4.967385	0.467737	0.049093
UDP-glucose 4-epimerase	GALE	4.950185	0.465081	0.040373
Semaphorin-6D	SEMA6D	4.940383	0.481175	0.043196
Follistatin-related protein 5	FSTL5	4.933141	0.432481	0.042843
Collagen alpha-1	COL14A1	4.920002	0.590701	0.037097
Cadherin-6	CDH6	4.919758	0.826578	0.010585
Podocalyxin-like protein 2	PODXL2	4.913977	0.422657	0.047681
Pregnancy zone protein	PZP	4.906181	0.478639	0.030746
Endothelial cell-selective adhesion molecule	ESAM	4.887591	0.438144	0.013105
Thrombospondin-2	THBS2	4.883135	0.44767	0.033266
Carboxypeptidase N subunit 2	CPN2	4.881493	0.707047	0.03125
Folate receptor beta	FOLR2	4.861958	0.732126	0.01124
Stromal cell-derived factor 1	CXCL12	4.85428	0.590177	0.034325
Repulsive guidance molecule A	RGMA	4.85224	0.719941	0.003931
Lactotransferrin	LTF	4.846201	0.387258	0.010988
Testican-2	SPOCK2	4.845342	0.427862	0.043851
SLIT and NTRK-like protein 5	SLITRK5	4.82721	0.445689	0.019052
Immunoglobulin superfamily member 21	IGSF21	4.811787	0.44693	0.044708
Growth/differentiation factor 8	MSTN	4.803275	0.82346	0.017238
Cadherin-15	CDH15	4.798098	0.432784	0.035333
Prosaposin receptor GPR37L1	GPR37L1	4.748311	0.460093	0.018196
Antileukoproteinase	SLPI	4.748151	0.416171	0.02379

Neural cell adhesion molecule L1-like protein	CHL1	4.739815	0.436375	0.002419
CD99	CD99	4.696795	0.823597	#N/A
Protocadherin alpha-C2	PCDHAC2	4.690416	0.412488	0.049798
Alpha-N-acetylgalactosaminide alpha-2,6-sialyltransferase 1	ST6GALNAC1	4.683117	0.496356	0.047278
Transaldolase	TALDO1	4.675637	0.548778	0.012349
Vimentin variant 3	VIM	4.660543	0.823026	0.007863
Secreted and transmembrane protein 1	SECTM1	4.657811	0.515337	0.015927
Protocadherin-10	PCDH10	4.64554	0.822966	0.047984
Cochlin	COCH	4.632325	0.354767	0.013558
Multiple epidermal growth factor-like domains protein 9	MEGF9	4.621635	0.414851	0.04627
Immunoglobulin heavy variable 3-43	IGHV3-43	4.605075	0.390951	0.004335
Neural proliferation differentiation and control protein 1	NPDC1	4.604126	0.46663	0.040423
Junctional adhesion molecule B	JAM2	4.583459	0.560519	0.014315
Contactin-6	CNTN6	4.574779	0.425	0.049395
Polypeptide N-acetylgalactosaminyltransferase 16	GALNT16	4.571223	0.823634	0.042792
Xyloside xylosyltransferase 1	XXYLT1	4.565662	0.405786	0.042893
SH3 domain-binding glutamic acid-rich-like protein 3	SH3BGRL3	4.564519	0.823694	0.040524
Sialic acid-binding Ig-like lectin 14	SIGLEC14	4.555713	0.374308	0.03755
Beta-galactoside alpha-2,6-sialyltransferase 2	ST6GAL2	4.545533	0.821203	0.044758
Peroxiredoxin-6	PRDX6	4.544462	0.823268	0.032661
Protocadherin-1	PCDH1	4.534196	0.413003	0.037349
Dihydrolipoyl dehydrogenase	DLD	4.521311	0.823063	0.011542
Transmembrane glycoprotein NMB	GPNMB	4.516885	0.500012	0.038911

Dyslexia-associated protein KIAA0319	KIAA0319	4.51463	0.823572	0.040675
Neuropilin-1	NRP1	4.471499	0.414869	0.011391
Ephrin-B2	EFNB2	4.465533	0.454502	0.034879
Adhesion G protein-coupled receptor B2	ADGRB2	4.449862	0.370146	0.007258
Sia-alpha-2,3-Gal-beta-1,4-GlcNAc-R:alpha 2,8-sialyltransferase	ST8SIA3	4.444735	0.411258	0.017641
Cerebellin-2	CBLN2	4.439655	0.526334	0.015978
Zona pellucida sperm-binding protein 2	ZP2	4.436124	0.426916	0.037147
4F2 cell-surface antigen heavy chain	SLC3A2	4.431887	0.373736	0.0125
Protein S100-A4	S100A4	4.429987	0.823618	0.032056
Adhesion G protein-coupled receptor B1	ADGRB1	4.401764	0.823217	0.010786
Mannosyl-oligosaccharide 1,2-alpha-mannosidase IC	MAN1C1	4.369495	0.433085	0.047077
Neuroendocrine protein 7B2	SCG5	4.258281	0.403444	0.024899
Sodium channel subunit beta-3	SCN3B	4.229204	0.822942	0.012046
Lysosomal alpha-glucosidase	GAA	4.228729	0.49497	0.027823
C4b-binding protein alpha chain	C4BPA	4.116539	0.535826	0.023841
Phosphoserine aminotransferase	PSAT1	4.094867	0.415361	0.049899
Immunoglobulin lambda-like polypeptide 1	IGLL1	3.773476	0.431085	0.029738
Immunoglobulin lambda variable 3-19	IGLV3-19	3.53469	0.636991	0.021472
Immunoglobulin lambda variable 1-47	IGLV1-47	3.501144	0.555627	0.02127
Decorin	DCN	3.274455	0.602985	0.026159
Immunoglobulin J chain	JCHAIN	3.244743	0.571762	0.020817
Follistatin-related protein 1	FSTL1	3.229605	0.558961	0.037802
Desmocollin-2	DSC2	3.208931	0.335507	0.036794
Cholecystokinin	CCK	3.206945	0.240078	0.025252

Latent-transforming growth factor beta-binding protein 2	LTBP2	3.133864	0.602743	0.013407
Protein NOV homolog	NOV	3.100965	0.560999	0.034576613
Insulin-like growth factor II	IGF2	3.074413	0.499014	0.020766
Reticulon-4 receptor-like 2	RTN4RL2	2.99753	0.295915	0.041835
Delta and Notch-like epidermal growth factor-related receptor	DNER	2.995368	0.299798	0.043145
Ig-like domain-containing protein	n/a	2.981627	0.496303	0.039393489
Immunoglobulin heavy variable 1-2	IGHV1-2	2.978094	0.25598	0.031401
Immunoglobulin kappa variable 2-29	IGKV2-29	2.967857	0.215379	0.007308
Immunoglobulin lambda variable 4-60	IGLV4-60	2.957717	0.225099	0.000504
Protocadherin Fat 2	FAT2	2.940774	0.504804	0.04753
Heparan-sulfate 6-O-sulfotransferase 3	HS6ST3	2.902526	0.307931	0.04254
Probable serine carboxypeptidase CPVL	CPVL	2.892378	0.514199	0.046371
Apolipoprotein M	APOM	2.889507	0.281454	0.019153
EGF-containing fibulin-like extracellular matrix protein 2	EFEMP2	2.887198	0.511931	0.012298
Complement C1q subcomponent subunit A	C1QA	2.87699	0.26346	0.023034
Nectin-1	NECTIN1	2.875081	0.277922	0.039113
ICOS ligand (Inducible T-cell co-stimulator ligand, isoform CRA_b)	ICOSLG	2.846608	0.49537	0.016129
Soluble calcium-activated nucleotidase 1	CANT1	2.824137	0.288835	0.043548
C-type lectin domain family 11 member A	CLEC11A	2.822682	0.29778	0.049496
Phosphoglycerate kinase 1	PGK1	2.820843	0.249104	0.019607
Complement factor H-related protein 2	CFHR2	2.818446	0.51614	0.033518
Kunitz-type protease inhibitor 2	SPINT2	2.813099	0.509133	0.017692
Triggering receptor expressed on myeloid cells 2	TREM2	2.811125	0.206033	0.047732
Sulfhydryl oxidase 2	QSOX2	2.807902	0.219517	0.041482

Myelin-oligodendrocyte glycoprotein	MOG	2.793473	0.223971	0.005796
Selenoprotein P	SELENOP	2.784963	0.455277	0.006552
Cathepsin Z	CTSZ	2.767259	0.481482	0.048185
Coagulation factor XIII B chain	F13B	2.749824	0.289933	0.024849
Protein CutA (Acetylcholinesterase-associated protein)	CUTA	2.747664	0.200404	0.018246
Nidogen-1	NID1	2.737216	0.478418	0.029284
Protein CASC4	CASC4	2.724995	0.478607	0.014415323
Mannosyl-oligosaccharide 1,2-alpha-mannosidase IA	MAN1A1	2.712764	0.257372	0.033115
Lysozyme C	LYZ	2.710925	0.458936	0.035585
Golgi membrane protein 1	GOLM1	2.69706	0.481671	0.042944
Immunoglobulin heavy variable 2-70D	IGHV2-70D	2.688471	0.168082	0.005494
C1QTNF3-AMACR readthrough (NMD candidate)	C1QTNF3-AMACR	2.686661	0.261925	0.011794
Alpha-mannosidase 2	MAN2A1	2.670932	0.198693	0.039869
Immunoglobulin lambda variable 9-49	IGLV9-49	2.658948	0.203054	0.004385
L-selectin	SELL	2.658451	0.26219	0.029183
Protein shisa-7	SHISA7	2.653551	0.200692	0.00751
Lysosomal Pro-X carboxypeptidase	PRCP	2.649717	0.450599	0.033921
Superoxide dismutase	SOD2	2.637111	0.194333	0.0422179
V-set and transmembrane domain-containing protein 2A	VSTM2A	2.623182	0.40899	0.008871
BDNF/NT-3 growth factors receptor	NTRK2	2.619208	0.460349	0.039718
Immunoglobulin lambda constant 7	IGLC7	2.61887	0.179362	0.007056
Gliomedin [Cleaved into: Gliomedin shedded ectodomain]	GLDN	2.615743	0.210857	0.041431
Mitotic spindle assembly checkpoint protein MAD1	MAD1L1	2.613108	0.478607	0.009829

Neurexophilin-1	NXPH1	2.610901	0.188477	0.009627
Nesprin-2	SYNE2	2.59432	0.478607	0.003175
Protein-L-isoaspartate O-methyltransferase	PCMT1	2.591623	0.251897	0.003226
Immunoglobulin lambda variable 6-57	IGLV6-57	2.582448	0.190061	0.021623
UPF0606 protein KIAA1549L	KIAA1549L	2.563533	0.234911	0.014264
Uncharacterized protein KIAA2026	KIAA2026	2.560437	0.478607	0.040272
A disintegrin and metalloproteinase with thrombospondin motifs 4	ADAMTS4	2.556726	0.210405	0.018296
Immunoglobulin kappa variable 1-27	IGKV1-27	2.547243	0.196956	0.000958
Low-density lipoprotein receptor	LDLR	2.543712	0.235158	0.014466
Inositol monophosphatase 3	IMPAD1	2.543062	0.444115	0.047429435
Polypeptide N-acetylgalactosaminyltransferase 1	GALNT1	2.533654	0.280602	0.037702
Growth hormone A1	PRL	2.528425	0.478607	0.020716
Forkhead-associated domain-containing protein 1	FHAD1	2.524438	0.478607	0.007964
Follistatin-related protein 3	FSTL3	2.523193	0.196615	0.019204
Alpha-1,3-mannosyl-glycoprotein 2-beta-N-acetylglucosaminyltransferase	MGAT1	2.511858	0.209734	0.032107
Interleukin-6 receptor subunit beta	IL6ST	2.506559	0.408963	0.033669
Apolipoprotein L1	APOL1	2.504502	0.228614	0.017188
Msx2-interacting protein	SPEN	2.503723	0.478607	0.04506
Granulins	GRN	2.50017	0.478607	0.03246
Eukaryotic translation initiation factor 2 subunit 3B	EIF2S3B	2.4947	0.191611	0.03377
Beta-mannosidase	MANBA	2.494585	0.192063	0.016935
Immunoglobulin heavy constant delta	IGHD	2.483298	0.180974	0.003377
Glucosidase 2 subunit beta	PRKCSH	2.483261	0.426494	0.01623

Immunoglobulin lambda variable 3-1	IGLV3-1	2.479587	0.179397	0.021522
Sonic hedgehog protein	SHH	2.478774	0.478607	0.039214
Junctional adhesion molecule C	JAM3	2.472368	0.208454	0.046069
Osteoclast-associated immunoglobulin-like receptor	OSCAR	2.467715	0.478607	0.001563
Lithostathine-1-beta	REG1B	2.467116	0.478607	0.02495
Adenosine deaminase 2	ADA2	2.466058	0.251314	0.00877
Immunoglobulin kappa variable 6-21	IGKV6-21	2.451476	0.205765	0.00504
Immunoglobulin heavy variable 1-46	IGHV1-46	2.449861	0.263652	0.021724
Calsyntenin-2	CLSTN2	2.444898	0.478607	0.046421
Beta-1,3-N-acetylglucosaminyltransferase lunatic fringe	LFNG	2.442935	0.478607	0.043095
Noelin	OLFM1	2.437302	0.191334	0.045413
Serglycin	SRGN	2.435364	0.279198	0.027722
Heat shock cognate 71 kDa protein	HSPA8	2.424019	0.205323	0.012147
Carbohydrate sulfotransferase 10	CHST10	2.419984	0.200331	0.017843
Protein S100-B	S100B	2.414356	0.478607	0.024345
SPARC-related modular calcium-binding protein 1	SMOC1	2.414143	0.234824	0.046472
CD5 antigen-like	CD5L	2.404987	0.174821	0.017944
Transgelin	TAGLN	2.401188	0.166881	0.036694
Dyslexia-associated protein KIAA0319-like protein	KIAA0319L	2.394599	0.178434	0.008165
Desmocollin-3	DSC3	2.393876	0.478607	0.03876
HLA class I histocompatibility antigen, A-24 alpha chain	HLA-A	2.39099	0.246376	0.025
Immunoglobulin heavy variable 3-64	IGHV3-64	2.389062	0.224358	0.000806
Phospholipase D4	PLD4	2.378785	0.175139	0.012601
Beta-hexosaminidase subunit beta	HEXB	2.37794	0.184693	0.02626

Complement factor H-related protein 3	CFHR3	2.375713	0.478607	0.036946
Lactosylceramide 4-alpha-galactosyltransferase	A4GALT	2.373926	0.478607	0.046976
Neudesin	NENF	2.365416	0.257174	0.049143
Contactin-4	CNTN4	2.364613	0.189003	0.042389
Golgi apparatus protein 1, isoform CRA_c	GLG1	2.357638	0.478607	0.014617
Immunoglobulin lambda variable 5-37	IGLV5-37	2.356011	0.478607	0.000554
Growth arrest-specific protein 6	GAS6	2.347713	0.191653	0.038558
Pro-cathepsin H	CTSH	2.341582	0.384575	0.002319
Chitinase-3-like protein 2	CHI3L2	2.341572	0.478607	0.039365
Group XV phospholipase A2	PLA2G15	2.338137	0.478607	0.014718
Neuroligin-2	NLGN2	2.337719	0.193261	0.043246
Matrix remodeling-associated protein 8	MXRA8	2.33692	0.478607	0.045766
Integrin beta-like protein 1	ITGBL1	2.334031	0.199043	0.019254
Extracellular serine/threonine protein kinase FAM20C	FAM20C	2.331936	0.478607	0.04244
Ephrin-B3	EFNB3	2.327666	0.478607	0.039315
Galectin-1	LGALS1	2.325878	0.478607	0.027117
Retbindin	RTBDN	2.325822	0.478607	0.016179
Piezo-type mechanosensitive ion channel component	PIEZO2	2.325282	0.243486	0.011341
C-type mannose receptor 2	MRC2	2.320588	0.179577	0.048034
Phosphoglycerate mutase 1	PGAM1	2.318655	0.478607	0.030393
Protocadherin-9	PCDH9	2.315718	0.173309	0.009123
Protocadherin-17	PCDH17	2.309916	0.239419	0.017288
Phospholipase D3	PLD3	2.30991	0.178863	0.042188
Connective tissue growth factor	CTGF	2.309777	0.478607	0.032560484

Latent-transforming growth factor beta-binding protein 1	LTBP1	2.285884	0.167376	0.009577
Properdin	CFP	2.282291	0.478607	0.032359
Immunoglobulin heavy variable 2-26	IGHV2-26	2.281675	0.213106	0.004234
Neuropilin-2	NRP2	2.281607	0.24503	0.000252
Exostosin-like 2	EXTL2	2.27606	0.205698	0.048135
N-acetylglucosamine-6-sulfatase	GNS	2.274445	0.478607	0.012651
Cytokine-like protein 1	CYTL1	2.260168	0.157572	0.047177
Proteoglycan 4	PRG4	2.259447	0.362453	0.0063
Plexin-B1	PLXNB1	2.257359	0.478607	0.017591
Calcium/calmodulin-dependent protein kinase type II subunit alpha	CAMK2A	2.255317	0.189784	0.049446
EPHB2 protein (Ephrin type-B receptor 2)	EPHB2	2.254328	0.478607	0.008014
Thioredoxin domain-containing protein 17	TXNDC17	2.251837	0.478607	0.045716
Plexin domain-containing protein 1	PLXDC1	2.242517	0.163638	0.042087
Voltage-dependent calcium channel subunit alpha-2/delta-2	CACNA2D2	2.242261	0.478607	0.009677
C-X-C motif chemokine 16	CXCL16	2.230197	0.218445	0.046321
Protocadherin gamma-C5	PCDHGC5	2.225271	0.223459	0.049748
Low-density lipoprotein receptor-related protein 11	LRP11	2.224691	0.478607	0.040726
Ceroid-lipofuscinosis neuronal protein 5	CLN5	2.22155	0.171885	0.000302
Protein FAM198B	FAM198B	2.214528	0.478607	0.041129032
Thrombospondin-4	THBS4	2.212717	0.178051	0.011089
Insulin-like growth factor binding protein 3 isoform b	IGFBP3	2.205069	0.161065	0.007661
Zinc transporter ZIP10	SLC39A10	2.204511	0.158624	0.048942
Fatty acid-binding protein 5	FABP5	2.203364	0.478607	0.036643
Aminopeptidase N	ANPEP	2.199286	0.478607	0.029536

Cysteine-rich with EGF-like domain protein 1	CRELD1	2.192893	0.478607	0.044607
Cystatin-M	CST6	2.192545	0.225225	0.039466
Apolipoprotein C-III variant 1	APOC3	2.189622	0.151684	0.007813
Complement C2	C2	2.186571	0.372833	0.025504
Adhesion G protein-coupled receptor B3	ADGRB3	2.184578	0.241604	0.017994
ProSAAS	PCSK1N	2.176078	0.149758	0.048488
Protein S100-A6	S100A6	2.173687	0.154335	0.025605
Serpin B6	SERPINB6	2.170479	0.478607	0.000202
cDNA FLJ57652, highly similar to Ephrin-A3	cDNA FLJ57652	2.16808	0.17876	0.008618952
Chloride intracellular channel protein 1 (Chloride channel ABP)	CLIC1	2.158926	0.478607	0.016784
Protein HEG homolog 1	HEG1	2.156519	0.161441	0.048992
ADP-ribosyl cyclase/cyclic ADP-ribose hydrolase 2	BST1	2.154357	0.478607	0.007359
Serum albumin	ALB	2.153855	0.478607	0.014063
Cocaine- and amphetamine-regulated transcript protein [Cleaved into: CART	CARTPT	2.147727	0.149404	0.039617
Seizure 6-like protein 2	SEZ6L2	2.145911	0.321825	0.002117
Protein TMED7-TICAM2	TMED7-TICAM2	2.142035	0.162513	0.004032
Sortilin-related receptor	SORL1	2.133241	0.165384	0.043901
Multiple epidermal growth factor-like domains protein 8	MEGF8	2.131211	0.166287	0.016583
Myocilin	MYOC	2.101603	0.478607	0.045514
Putative phospholipase B-like 2	PLBD2	2.098044	0.478607	0.043347
Lysosomal acid lipase/cholesteryl ester hydrolase	LIPA	2.045292	0.21816	0.003679
Angiopoietin-related protein 2	ANGPTL2	2.042996	0.478607	0.048841
Immunoglobulin heavy variable 3-30-3	IGHV3-30-3	2.042105	0.13862	0.006048

Ephrin-B1	EFNB1	2.019865	0.14488	0.036542
Protein delta homolog 2	DLK2	2.000973	0.182767	0.013962
Metallothionein	MT3	2.000279	0.145022	0.014869

Table 6: All differentially down-regulated proteins in the responders CSF proteome post treatment (Log fold change (LFC) <-2) in order of log fold change.

Proteins	Gene	LFC	LogP	FDR
Aspartylglucosaminidase	AGA	-12.6602	1.771679	0.030948
Polypeptide N-acetylgalactosaminyltransferase 2	GALNT2	-9.60325	1.222043	0.037651
Protein shisa-6	SHISA6	-8.22558	0.975091	0.041532
Acyl-CoA-binding protein	DBI	-7.95918	0.962663	0.003881
Receptor-type tyrosine-protein phosphatase N2	PTPRN2	-7.72644	0.785049	0.044355
Mannan-binding lectin serine protease 1	MASP1	-7.32768	0.779907	0.034526
Peptidyl-prolyl cis-trans isomerase C	PPIC	-7.14398	0.9231	0.034173
Calmodulin-3	CALM3	-7.02432	0.852006	0.014012
Immunoglobulin kappa variable 3D-11	IGKV3D-11	-5.83205	0.453133	0.003327
Proenkephalin-A	PENK	-5.66517	0.417869	0.020665
Low affinity immunoglobulin gamma Fc region receptor II-a	FCGR2A	-5.52249	0.527208	0.028679
Beta-actin-like protein 2	ACTBL2	-5.2778	0.54097	0.040222
IgLON family member 5	IGLON5	-5.24902	0.49407	0.00746
Macrophage colony-stimulating factor 1	CSF1	-5.21601	0.455243	0.027268
Serum amyloid A-1 protein	SAA1	-5.04779	0.820618	0.02752
Histone H2B	H2BC15	-5.03103	0.82253	0.018145
Spondin-2	SPON2	-5.02825	0.823643	0.010333
Basigin	BSG	-4.971	0.823201	0.002873
Myelin-associated glycoprotein	MAG	-4.89095	0.55983	0.030897
Collagen alpha-1(XV) chain	COL15A1	-4.88832	0.409116	0.002369
Brain acid soluble protein 1	BASP1	-4.85925	0.451594	0.036341
Glyceraldehyde-3-phosphate dehydrogenase	GAPDH	-4.84919	0.682624	0.024395
Pyruvate kinase	PKM	-4.83578	0.429305	0.014919
Immunoglobulin kappa variable 6D-21	IGKV6D-21	-4.77294	0.42439	0.00373
OX-2 membrane glycoprotein	CD200	-4.74007	0.521481	0.033821

Multimerin-2	MMRN2	-4.73288	0.48503	0.046673
Renin receptor	ATP6AP2	-4.72947	0.405748	0.006754
Mast/stem cell growth factor receptor Kit	KIT	-4.72721	0.408195	0.028175
Neural cell adhesion molecule 1	NCAM1	-4.6395	0.392346	0.001361
Glutathione S-transferase P	GSTP1	-4.63039	0.407565	0.027067
Immunoglobulin heavy variable 3-38 (non-functional)	IGHV3-38	-4.60007	0.473336	0.005343
Calcium/calmodulin-dependent protein kinase type II subunit beta	CAMK2B	-4.52398	0.392371	0.038155
Soluble scavenger receptor cysteine-rich domain-containing protein SSC5D	SSC5D	-4.52263	0.539295	0.007107
Protein NDRG2	NDRG2	-4.50836	0.463037	0.013458
Nidogen-2	NID2	-4.50685	0.646147	0.038407
Cation-independent mannose-6-phosphate receptor	IGF2R	-4.49586	0.548409	0.028528
Interleukin-1 receptor accessory protein	IL1RAP	-4.40328	0.821889	0.047026
Endoplasmin	HSP90B1	-4.38688	0.64174	0.029435
Xylosyltransferase 1	XYLT1	-4.36094	0.823515	0.041986
Neurexin-3-beta	NRXN3	-4.35024	0.823702	0.004889
Coagulation factor IX	F9	-4.27474	0.453642	0.019859
Carbonic anhydrase 4	CA4	-4.24828	0.349004	0.0312
Hemoglobin subunit alpha	HBA1	-3.47337	0.228658	0.036139
Glutaminyl-peptide cyclotransferase	QPCT	-3.22511	0.571184	0.039919
Proliferation marker protein Ki-67	MKI67	-3.21954	0.217976	0.034224
C-reactive protein	CRP	-3.13636	0.245939	0.022933
Sialate O-acetylesterase	SIAE	-3.09349	0.224935	0.046724
Thioredoxin	TXN	-3.06449	0.244358	0.028024
Pyruvate kinase PKM	PKM	-3.03195	0.537734	0.029335
Immunoglobulin heavy variable 4-4	IGHV4-4	-2.96921	0.483724	0.000857
Double-stranded RNA-specific editase 1	ADARB1	-2.94639	0.231847	0.03624
Immunoglobulin heavy variable 4-4	IGHV4-4	-2.85076	0.221803	0.000857
Fibrillin-1 [Cleaved into: Asprosin]	FBN1	-2.76768	0.204569	0.033317
Immunoglobulin superfamily member 8	IGSF8	-2.7561	0.451409	0.009476
Glutamate receptor 4	GRIA4	-2.75542	0.48125	0.013206
Secreted frizzled-related protein 3	FRZB	-2.74846	0.271682	0.044052
Gamma-glutamyl hydrolase	GGH	-2.74717	0.480914	0.044103
Immunoglobulin kappa variable 1-33	IGKV1-33	-2.7357	0.209784	0.020867
Immunoglobulin heavy variable 3-15	IGHV3-15	-2.73336	0.219064	0.004183
Neurexin-1-beta	NRXN1	-2.70883	0.438147	0.005645
Aspartate aminotransferase, mitochondrial	GOT2	-2.6698	0.222593	0.019556
Cadherin-5	CDH5	-2.66691	0.262746	0.033065
Phosphoinositide-3-kinase-interacting protein 1	PIK3IP1	-2.66426	0.263597	0.044506

Methanethiol oxidase	SELENBP1	-2.64165	0.464427	0.037954
Cerebellin-1	CBLN1	-2.64047	0.465401	0.031552
Leptin receptor	LEPR	-2.6207	0.478607	0.034375
Fc of IgG low affinity IIIa receptor isoform 1	FCGR3A	-2.61339	0.491401	0.006956
Aspartate aminotransferase, cytoplasmic	GOT1	-2.60089	0.412672	0.030141
MANSC domain-containing protein 1	MANSC1	-2.5798	0.214056	0.046623
Sushi, nidogen and EGF-like domain-containing protein 1	SNED1	-2.57015	0.26525	0.043397
ABHD14A-ACY1 readthrough	ABHD14A-ACY1	-2.54107	0.478607	0.006653
Multiple inositol polyphosphate phosphatase 1	MINPP1	-2.53832	0.193708	0.049244
Macrophage mannose receptor 1	MRC1	-2.50812	0.192127	0.031351
Ephrin-A5	EFNA5	-2.50339	0.478607	0.002772
DOMON domain-containing protein FRRS1L	FRRS1L	-2.49743	0.18453	0.047833
Microtubule-actin cross-linking factor 1, isoforms 1/2/3/5	MACF1	-2.49596	0.478607	0.014819
45 kDa calcium-binding protein	SDF4	-2.49579	0.246812	0.045817
Mesothelin	MSLN	-2.49317	0.242061	0.014667
Immunoglobulin lambda variable 1-51	IGLV1-51	-2.48697	0.396368	0.021321
Paired immunoglobulin-like type 2 receptor alpha	PILRA	-2.4861	0.273984	0.009778
NT-3 growth factor receptor	NTRK3	-2.47886	0.222129	0.005696
Tyrosine-protein kinase receptor UFO	AXL	-2.47745	0.411914	0.032863
Hepatocyte growth factor-like protein	MST1	-2.47145	0.26565	0.013659
Collagen alpha-3(VI) chain	COL6A3	-2.46584	0.417639	0.010938
Peroxiredoxin-2	PRDX2	-2.46513	0.212381	0.033014
Neurogenic locus notch homolog protein 3	NOTCH3	-2.44749	0.478607	0.016683
Dipeptidyl aminopeptidase-like protein 6	DPP6	-2.44339	0.267497	0.011442
Immunoglobulin lambda variable 4-69	IGLV4-69	-2.43908	0.177116	0.000403
Neuromodulin	GAP43	-2.43437	0.478607	0.030192
Epsilon-sarcoglycan	SGCE	-2.43282	0.410825	0.008921
WAP four-disulfide core domain protein 2	WFDC2	-2.43186	0.218435	0.038609
EGF-containing fibulin-like extracellular matrix protein 1	EFEMP1	-2.42035	0.249294	0.00625
HLA class I histocompatibility antigen, Cw-6 alpha chain	HLA-C	-2.41788	0.204447	0.006452

Receptor-type tyrosine-protein phosphatase-like N	PTPRN	-2.41709	0.260107	0.03997
Protein Z-dependent protease inhibitor	SERPINA10	-2.40886	0.478607	0.013306
Prosaposin receptor GPR37	GPR37	-2.39706	0.478607	0.01754
Alpha-enolase	ENO1	-2.3931	0.23839	0.025756
Nucleobindin-2	NUCB2	-2.39147	0.276203	0.00121
Stathmin	STMN1	-2.38899	0.478607	0.007157
Tetraspanin	CD81	-2.38226	0.478607	0.007611
Hemoglobin subunit delta	HBD	-2.38211	0.478607	0.022329
Neuroplastin	NPTN	-2.37172	0.478607	0.048337
Elastin	ELN	-2.36773	0.478607	0.008367
Ecto-ADP-ribosyltransferase 3	ART3	-2.3662	0.38671	0.038105
Zinc transporter ZIP12	SLC39A12	-2.36397	0.478607	0.040071
Moesin	MSN	-2.36133	0.478607	0.032006
Fructose-bisphosphate aldolase C	ALDOC	-2.34821	0.359878	0.027369
Endosialin	CD248	-2.3466	0.478607	0.046875
Semaphorin-4B	SEMA4B	-2.33693	0.379717	0.015625
WASH complex subunit 2A	WASHC2A	-2.33669	0.204231	0.002016
Carboxypeptidase N catalytic chain	CPN1	-2.32576	0.183881	0.029587
Protocadherin-7	PCDH7	-2.3168	0.478607	0.018044
Disintegrin and metalloproteinase domain-containing protein 11	ADAM11	-2.31331	0.478607	0.008417
Carbonic anhydrase 14	CA14	-2.31218	0.478607	0.049042
Prosaposin	PSAP	-2.30855	0.478607	0.006149
Endonuclease domain-containing 1 protein	ENDOD1	-2.30357	0.357828	0.018952
Intercellular adhesion molecule 2	ICAM2	-2.29029	0.478607	0.016028
Reticulon-4 receptor-like 1	RTN4RL1	-2.28975	0.243539	0.041784
Integral membrane protein 2B	ITM2B	-2.28202	0.184738	0.049597
Cathepsin L1	CTSL	-2.28035	0.378837	0.02631
Immunoglobulin heavy variable 3/OR15-7	IGHV3OR15-7	-2.27748	0.163593	0.001109
Alpha-N-acetylgalactosaminidase	NAGA	-2.26812	0.478607	0.03004
Malectin	MLEC	-2.26753	0.478607	0.038508
14-3-3 protein zeta/delta	YWHAZ	-2.26106	0.156428	0.035938
Lipolysis-stimulated lipoprotein receptor	LSR	-2.24689	0.478607	0.041935
Complement C1q tumor necrosis factor-related protein 4	C1QTNF4	-2.23709	0.478607	0.046169
Vitamin K-dependent protein Z	PROZ	-2.23593	0.254996	0.0313
Hepatocyte growth factor activator	HGFAC	-2.20818	0.478607	0.010282
Transferrin receptor	TFRC	-2.20731	0.478607	0.013155
UDP-GalNAc:beta-1,3-N-acetylgalactosaminyltransferase 1	B3GALNT1	-2.19175	0.236203	0.018599
14-3-3 protein gamma	YWHAG	-2.16352	0.478607	0.035736
Prolargin	PRELP	-2.11238	0.341692	0.034829
Ephrin-A1	EFNA1	-2.10332	0.161954	0.030847
Carbonic anhydrase 1	CA1	-2.03243	0.213416	0.02006

Cell adhesion molecule 2	CADM2	-2.03145	0.328332	0.042692
Protein FAM19A1	FAM19A1	-2.01999	0.478607	0.041633

Table 7: All significantly differentially up-regulated proteins in the responders cerebrospinal fluid (CSF) proteome post treatment according to Log fold change (LFC) >2, False discover rate (FDR)<0.05 (represented by Log(p)>1.13) in order of LFC.

Proteins	**Gene**	**LFC**	**LogP**	**FDR**
Complement C1q tumor necrosis factor-related protein 5	C1QTNF5	11.42819	1.613784	0.046119
Serine protease inhibitor Kazal-type 6	SPINK6	10.61811	1.390578	0.041179
Tropomyosin alpha-4 chain	TPM4	10.31254	1.161122	0.016331
Immunoglobulin heavy variable 4-34	IGHV4-34	10.16426	1.44909	0.025403
Titin	TTN	10.15213	1.182481	0.003982
Inter-alpha-trypsin inhibitor heavy chain H3	ITIH3	9.997206	1.146764	0.001663
Cadherin-11	CDH11	9.563253	1.312062	0.035232
Fibulin-7	FBLN7	9.41027	1.199742	0.040171
Fetuin-B	FETUB	8.2742	1.171661	0.048387
Immunoglobulin heavy variable 1-18	IGHV1-18	8.185689	1.182731	0.005141
Immunoglobulin lambda variable 3-16	IGLV3-16	8.023568	1.184114	0.000655

Epithelial discoidin domain-containing receptor 1	DDR1	7.47055	1.193837	0.037399
Semaphorin 6A	SEMA6A	7.141019	1.202043	0.002974

Table 8: All significantly differentially down-regulated proteins in the responders cerebrospinal fluid (CSF) proteome post treatment according to Log fold change (LFC) <-2, False discover rate (FDR) <0.05 (represented by Log(p)>1.13) in order of LFC

Proteins	**Gene**	**LFC**	**LogP**	**FDR**
Aspartylglucosaminidase	AGA	-12.6602	1.771679	0.000403
Polypeptide N-acetylgalactosaminyltransferase 2	GALNT2	-9.60325	1.222043	0.000857

In comparison, CSF obtained from patients who did not respond to an 8-week course of amitriptyline (non-responders) resulted in the expression of 415 differentially expressed proteins (Figure 11B), 185 proteins which were found to be upregulated and 230 proteins which were found to be downregulated (-2 < LFC > 2). The upregulated (Table 9) and downregulated (Table 10) proteins with LFC and FDR values in the non-responders are available as supplementary material. Focusing on these differentially expressed proteins in non-responders, a total of 5 proteins were significantly upregulated (represented by Log(p)>1.13) (Table 11), while 20 proteins were significantly downregulated after amitriptyline (represented by Log(p)>1.13) (Table 12) (FDR<0.05).

Table 9: All significantly differentially up-regulated proteins in the non-responders cerebrospinal fluid (CSF) proteome post treatment according to Log fold change (LFC) ≥ 2, in order of LFC

Proteins	Gene	LFC	LogP	FDR
V-type proton ATPase subunit S1	ATP6AP1	17.7330496	2.827164629	0.000714286
Hemoglobin subunit beta	HBB	14.7654748	0.916853442	0.002333333
Phospholipase D4	PLD4	13.82809884	1.543076397	0.000761905
Polypeptide N-acetylgalactosaminyltransferase 2	GALNT2	13.05085897	1.331418633	0.001714286
Vitamin K-dependent protein Z	PROZ	11.81862341	1.173749182	0.00052381
Coagulation factor XIII B chain	F13B	11.35208103	1.458896657	0.00347619
C-X-C motif chemokine 16	CXCL16	10.58946705	0.779384114	0.005238095
Carbonic anhydrase 1	CA1	10.11483301	0.763761581	0.001857143
Immunoglobulin lambda variable 6-57	IGLV6-57	9.526642936	0.816295313	0.001428571
Apolipoprotein B-100	APOB	9.459803377	0.637670617	0.008190476
Transmembrane protein 132D	TMEM132D	9.338163103	0.818080074	0.001190476
Growth/differentiation factor 8	MSTN	9.13526753	0.81789322	0.001285714
Calmodulin-3	CALM3	9.092011315	0.818125411	0.001285714
Phosphoserine aminotransferase	PSAT1	8.904575348	0.816882924	0.001380952
Sodium/potassium-transporting ATPase subunit beta	ATP1B1	8.876823153	0.819146244	0.001095238
Properdin	CFP	8.741453443	0.817537323	0.001333333
Immunoglobulin lambda variable 2-14	IGLV2-14	8.534506525	0.594337708	0.010904762
ProSAAS	PCSK1N	8.363038199	0.573017335	0.011761905
Apolipoprotein C-III variant 1	APOC3	8.120662485	0.619413957	0.009333333
Immunoglobulin heavy variable 3/OR16-12	IGHV3OR16-12	8.118675573	0.48248927	0.009238095
HCG2044074, isoform CRA_c	MIA-RAB4B	8.023610932	0.613593675	0.009761905
Sushi, nidogen and EGF-like domain-containing protein 1	SNED1	7.677152906	0.598988898	0.010571429
Vitamin D-binding protein	GC	7.569223949	0.548967213	0.004095238
Immunoglobulin heavy variable 2-5	IGHV2-5	7.514340264	0.468447446	0.010619048
Immunoglobulin lambda variable 4-69	IGLV4-69	7.445839678	0.443260848	0.015809524
Carboxypeptidase N catalytic chain	CPN1	7.340732506	0.458379973	0.01152381
Follistatin-related protein 3	FSTL3	7.336634636	0.50099463	0.019714286
Ceroid-lipofuscinosis neuronal protein 5	CLN5	7.096825259	0.474514729	0.010238095
Alpha-actinin-2	ACTN2	7.091871262	0.548361172	0.004333333
Neuropilin-2	NRP2	7.066779954	0.476113873	0.01
Protein TMED7-TICAM2	TMED7-TICAM2	7.057989665	0.452669959	0.011904762
Collagen alpha-1(XV) chain	COL15A1	7.056077753	0.453962658	0.011809524
Glutathione S-transferase P	GSTP1	6.920590333	0.426606682	0.016952381
Angiopoietin-related protein 7	ANGPTL7	6.8380129	0.429804911	0.016761905

C-reactive protein	CRP	6.830688136	0.419925642	0.017428571
Leptin receptor	LEPR	6.715878623	0.548839723	0.004190476
Hepatocyte growth factor-like protein	MST1	6.650026321	0.549628117	0.003619048
Ephrin-B1	EFNB1	6.645403181	0.411877943	0.019333333
Protein CutA (Acetylcholinesterase-associated protein)	CUTA	6.634366512	0.749555549	0.016142857
Haptoglobin-related protein	HPR	6.627066748	0.73977755	0.016285714
Immunoglobulin kappa variable 1D-16	IGKV1D-16	6.37615994	0.548918545	0.004142857
Protein disulfide-isomerase A3	PDIA3	6.332456589	0.549142891	0.003952381
Vitamin K-dependent protein C	PROC	6.302891254	0.811739623	0.011095238
Intercellular adhesion molecule 5	ICAM5	6.287291391	0.548417995	0.004285714
Acid sphingomyelinase-like phosphodiesterase 3b	SMPDL3B	6.276886259	0.549114014	0.004
Immunoglobulin heavy variable 3-64	IGHV3-64	6.244223458	0.549585862	0.003761905
Hemoglobin subunit alpha	HBA1;	6.229776723	0.398118721	0.020047619
Apolipoprotein M	APOM	6.195509093	0.730371291	0.016619048
Cathepsin F	CTSF	6.192956924	0.549613221	0.003666667
Immunoglobulin kappa variable 1-8	IGKV1-8	6.180609635	0.830166599	0.010190476
Immunoglobulin heavy variable 1-24	IGHV1-24	6.16588865	0.549328971	0.003809524
Papilin	PAPLN	6.013988291	0.69860971	0.01747619
Cartilage oligomeric matrix protein, isoform CRA_b	COMP	5.987196241	0.549152015	0.003904762
Endoplasmin	HSP90B1	5.907331807	0.706684997	0.017190476
Beta-1,3-N-acetylglucosaminyltransferase lunatic fringe	LFNG	5.897992815	0.549075965	0.004047619
Reticulon-4 receptor	RTN4R	5.849580765	0.682035258	0.019238095
Fc of IgG low affinity IIIa receptor isoform 1	FCGR3A	5.784267426	0.705482828	0.017380952
Cerebellin-3	CBLN3	5.761068889	0.682742674	0.01952381
Alpha-mannosidase 2x	MAN2A2	5.740645681	0.596976377	0.021047619
Immunoglobulin heavy variable 1-69	IGHV1-69	5.641162872	0.297208199	0.023666667
Angiogenin	ANG	5.628179073	0.63261389	0.02047619
Dihydrolipoyl dehydrogenase	DLD	5.579304831	0.549279242	0.003857143
Immunoglobulin heavy variable 3-38 (non-functional)	IGHV3-38	5.457845075	0.312094795	0.022952381
Adhesion G protein-coupled receptor L3	ADGRL3	5.283604213	0.580763835	0.021333333
Ephrin type-B receptor 6	EPHB6	5.271132878	0.309321742	0.023047619
Peroxiredoxin-6	PRDX6	5.061943463	0.293290095	0.022238095
Immunoglobulin kappa variable 2-24	IGKV2-24	5.026254041	0.270859514	0.024904762
Proenkephalin-A	PENK	4.780188833	0.233363727	0.02747619
Neuron-specific vesicular protein calcyon	CALY	4.750963688	0.272408083	0.023

Antileukoproteinase	SLPI	4.5691826	0.256134763	0.025761905
Collagen alpha-2	COL4A2	4.545761926	0.264332197	0.02547619
Hemoglobin subunit delta	HBD	4.37774631	0.319667337	0.013761905
Cystatin-M	CST6	4.310260705	0.246172019	0.026619048
Collagen alpha-2	COL6A2	4.304086753	0.254459302	0.025904762
Sialic acid-binding Ig-like lectin 14	SIGLEC14	4.262669018	0.25365606	0.024142857
Carbonic anhydrase 2	CA2	4.197131838	0.319667337	0.013857143
Tyrosine-protein kinase receptor TYRO3	TYRO3	4.188203812	0.223234079	0.026285714
Alpha-enolase	ENO1	4.182824748	0.227350017	0.027761905
Fibroblast growth factor receptor 3	FGFR3	4.164783137	0.244335446	0.026761905
Calcium/calmodulin-dependent protein kinase type II subunit beta	CAMK2B	4.128267901	0.238390228	0.027190476
Catalase	CAT	4.126898902	0.319667337	0.013666667
Sodium channel subunit beta-3	SCN3B	4.075798852	0.261737055	0.023714286
Cell growth regulator with EF hand domain protein 1	CGREF1	4.070104463	0.2191075	0.026857143
Flavin reductase	BLVRB	4.069440024	0.319667337	0.013
NT-3 growth factor receptor	NTRK3	4.067756925	0.253342166	0.024238095
Hemoglobin subunit gamma-2	HBG2	3.915710722	0.319667337	0.012857143
Proliferation marker protein Ki-67	MKI67	3.892976216	0.319667337	0.012952381
Neuroligin-2	NLGN2	3.880229269	0.219425119	0.026714286
Immunoglobulin lambda variable 2-18	IGLV2-18	3.872142928	0.218576646	0.026952381
Carbonic anhydrase 3	CA3	3.850760324	0.319667337	0.01347619
Calcium/calmodulin-dependent protein kinase type II subunit alpha	CAMK2A	3.804756505	0.211397801	0.027428571
Glutathione hydrolase 7	GGT7	3.798224994	0.225899494	0.026142857
Alpha-1-antitrypsin	SERPINA1	3.754103048	0.189456477	0.02847619
Ankyrin-1	ANK1	3.736327853	0.319667337	0.013190476
Immunoglobulin lambda variable 3-9	IGLV3-9	3.682708127	0.199172748	0.027952381
Phosphoglycerate mutase 1	PGAM1	3.677274295	0.215181944	0.027
Nucleoside diphosphate kinase A	NME1	3.6193864	0.319667337	0.013238095
Bisphosphoglycerate mutase	BPGM	3.610139029	0.319667337	0.013428571
Adenylate kinase isoenzyme 1	AK1	3.56142698	0.319667337	0.013904762
Titin	TTN	3.507405622	0.187706448	0.028666667
Delta-aminolevulinic acid dehydratase	ALAD	3.498456138	0.319667337	0.013285714
Eukaryotic translation initiation factor 5A	EIF5A2	3.474555969	0.319667337	0.014714286
Purine nucleoside phosphorylase (PNP)	PNP	3.43343108	0.319667337	0.013952381
Creatine kinase M-type	CKM	3.422876903	0.319667337	0.01352381
Hsc70-interacting protein	ST13	3.410878045	0.319667337	0.014380952
Spectrin beta chain, erythrocytic	SPTB	3.389299938	0.319667337	0.013380952

Immunoglobulin heavy variable 4-34	IGHV4-34	3.377413886	0.207841224	0.02852381
Msx2-interacting protein	SPEN	3.37459319	0.319667337	0.01247619
Erythrocyte membrane protein band 4.2	EPB42	3.335313252	0.319667337	0.013142857
Retinal dehydrogenase 1	ALDH1A1	3.313064575	0.319667337	0.014
Band 3 anion transport protein	SLC4A1	3.306749616	0.319667337	0.013714286
Cerebellin-2	CBLN2	3.284041132	0.184522015	0.028809524
Immunoglobulin kappa variable 1-12	IGKV1-12	3.274879456	0.319667337	0.015190476
Myosin-7	MYH7	3.256953376	0.319667337	0.013333333
Moesin	MSN	3.242891312	0.319667337	0.013047619
Hemoglobin subunit zeta	HBZ	3.226990564	0.319667337	0.013809524
Sema domain, transmembrane domain (TM), and cytoplasmic domain, (Semaphorin) 6A, isoform CRA_d (Semaphorin-6A)	SEMA6A	3.215990067	0.319667337	0.015380952
Reticulon-4 receptor-like 1	RTN4RL1	3.2011043	0.319667337	0.012619048
Anthrax toxin receptor 1	ANTXR1	3.186499187	0.319667337	0.012285714
Prosaposin	PSAP	3.186161041	0.319667337	0.015095238
GTP-binding nuclear protein Ran	RAN	3.180057798	0.319667337	0.014761905
Nesprin-2	SYNE2	3.160519464	0.319667337	0.015333333
Protein 4.1	EPB41	3.151472364	0.319667337	0.015047619
Chitinase domain-containing protein 1	CHID1	3.134127208	0.319667337	0.012380952
Vimentin variant 3	VIM	3.13274874	0.319667337	0.014952381
Biglycan	BGN	3.127339499	0.319667337	0.013095238
Voltage-dependent calcium channel subunit alpha-2/delta-2	CACNA2D2	3.119617735	0.319667337	0.014666667
Soluble scavenger receptor cysteine-rich domain-containing protein SSC5D	SSC5D	3.114161287	0.187681593	0.028619048
Intercellular adhesion molecule 2	ICAM2	3.098848343	0.319667337	0.014142857
Mesothelin	MSLN	3.098525728	0.319667337	0.014285714
Alpha-N-acetylglucosaminidase	NAGLU	3.08029529	0.319667337	0.012904762
Protein S100-A9	S100A9	3.07059506	0.319667337	0.013571429
Lactotransferrin	LTF	3.060737882	0.319667337	0.014571429
Rho GTPase-activating protein 5	ARHGAP5	3.059758323	0.319667337	0.015285714
Semaphorin-4D	SEMA4D	3.052460534	0.319667337	0.01452381
Elastin	ELN	3.050208228	0.319667337	0.014809524
Folate receptor beta	FOLR2	3.039188521	0.194904771	0.029190476
Chondroitin sulfate proteoglycan 4	CSPG4	3.033057077	0.319667337	0.012666667
Matrix remodeling-associated protein 8	MXRA8	3.028824125	0.319667337	0.012428571
Immunoglobulin lambda variable 3-25	IGLV3-25	3.023512363	0.181672588	0.029571429
Osteoclast-associated immunoglobulin-like receptor	OSCAR	3.014577048	0.319667337	0.015571429

Nebulin	NEB	3.009337561	0.319667337	0.015428571
HCG2044781 (TMEM189-UBE2V1 readthrough)	TMEM189-UBE2V1	2.960947037	0.319667337	0.014190476
Apolipoprotein F	APOF	2.953632627	0.319667337	0.012761905
Integral membrane protein DGCR2/IDD	DGCR2	2.950370244	0.319667337	0.014428571
Palmitoyl-protein thioesterase 1	PPT1	2.942332132	0.319667337	0.01447619
Ribose-phosphate pyrophosphokinase 1	PRPS1	2.942299434	0.319667337	0.014857143
Target of Nesh-SH3	ABI3BP	2.938692365	0.319667337	0.014619048
Complement C2	C2	2.933782373	0.186988089	0.029380952
Cholinesterase	BCHE	2.929139001	0.319667337	0.013619048
Interleukin-1 receptor accessory protein	IL1RAP	2.916219984	0.319667337	0.012238095
Zona pellucida sperm-binding protein 2	ZP2	2.903082166	0.319667337	0.012809524
Mast/stem cell growth factor receptor Kit	KIT	2.902766228	0.195698071	0.029095238
Immunoglobulin heavy variable 3-9	IGHV3-9	2.886199747	0.163831344	0.030809524
Leukocyte-associated immunoglobulin-like receptor 1	LAIR1	2.847871235	0.319667337	0.015142857
Membrane-associated progesterone receptor component 1 (mPR)	PGRMC1	2.8319664	0.319667337	0.014095238
Dyslexia-associated protein KIAA0319	KIAA0319	2.827532904	0.319667337	0.012714286
Procollagen-lysine,2-oxoglutarate 5-dioxygenase 3	PLOD3	2.812179838	0.319667337	0.014238095
EPHB2 protein (Ephrin type-B receptor 2)	EPHB2	2.810941424	0.319667337	0.014904762
Complement C1q tumor necrosis factor-related protein 4	C1QTNF4	2.800175803	0.319667337	0.012333333
Cysteine-rich with EGF-like domain protein 1	CRELD1	2.788597379	0.319667337	0.01252381
ADAM DEC1	ADAMDEC1	2.785990579	0.319667337	0.014047619
Immunoglobulin lambda variable 3-19	IGLV3-19	2.683903899	0.156561474	0.031809524
Angiopoietin-related protein 2	ANGPTL2	2.639735631	0.319667337	0.012190476
Immunoglobulin heavy variable 1/OR15-1	IGHV1OR15-1	2.627850056	0.111442676	0.034190476
ADP-ribosyl cyclase/cyclic ADP-ribose hydrolase 2	BST1	2.603515625	0.319667337	0.015
Peptidyl-prolyl cis-trans isomerase A	PPIA	2.589903014	0.16918915	0.030142857
Ephrin-B2	EFNB2	2.520082542	0.157990932	0.031666667
Neuroendocrine protein 7B2	SCG5	2.501035418	0.15461686	0.032
Peptidyl-prolyl cis-trans isomerase B	PPIB	2.491742202	0.166194609	0.030333333
Immunoglobulin heavy variable 3-64D	IGHV3-64D	2.470560755	0.147379086	0.032619048
Protocadherin-1	PCDH1	2.434499877	0.162878092	0.031047619
Protein S100-A6	S100A6	2.319936889	0.106941093	0.034619048

Matrix Gla protein	MGP	2.26031174	0.127735938	0.034047619
N	AGA	2.244946889	0.143252089	0.032761905
Cochlin	COCH	2.198242051	0.133661232	0.033571429
Podocalyxin-like protein 2	PODXL2	2.176144532	0.138252377	0.033238095
Zinc transporter ZIP10	SLC39A10	2.143930095	0.134474966	0.033428571
Vascular cell adhesion protein 1	VCAM1	2.122811113	0.133555711	0.033619048
Insulin-like growth factor binding protein 3 isoform b	IGFBP3	2.117982251	0.102720954	0.034904762
Laminin subunit gamma-1	LAMC1	2.06313324	0.133007719	0.033761905
Sialate O-acetylesterase	SIAE	2.054455621	0.127116763	0.034142857
UPF0606 protein KIAA1549L	KIAA1549L	2.037216255	0.115539061	0.034809524
Immunoglobulin heavy variable 1-46	IGHV1-46	2.035560949	0.10115746	0.035
Immunoglobulin lambda constant 3	IGLC3	2.032724108	0.092295332	0.035380952

Table 10: All significantly differentially down-regulated proteins in the non-responders cerebrospinal fluid (CSF) proteome post treatment according to Log fold change (LFC) $\leq$ -2, in order of LFC

Proteins	Gene	LFC	LogP	FDR
Double-stranded RNA-specific editase 1	ADARB1	-17.2087869	1.727415111	9.52381E-05
Heat shock cognate 71 kDa protein	HSPA8	-15.82209035	1.612765452	0.000142857
Mannan-binding lectin serine protease 1	MASP1	-15.26076494	1.74757113	4.7619E-05
Protein FAM19A5	TAFA5	-14.02971186	1.201375765	0.000428571
Serotransferrin	TF	-13.95079844	1.289981347	0.000285714
Contactin-4	CNTN4	-12.88501344	1.219143136	0.000380952
Netrin-G1	NTNG1	-12.74417686	1.130274283	0.000571429
Immunoglobulin kappa variable 1-33	IGKV1-33	-12.69562006	1.036308659	0.000666667
Contactin-6	CNTN6	-12.64343766	1.179428872	0.00047619
Semaphorin-3G	SEMA3G	-12.44467851	1.288608643	0.001809524
V-set and immunoglobulin domain-containing protein 4	VSIG4	-12.37137794	1.112227695	0.000619048
Beta-actin-like protein 2	ACTBL2	-11.97152758	1.394164245	0.004809524
Immunoglobulin kappa variable 3D-11	IGKV3D-11	-11.83203895	0.79544591	0.004666667
Ephrin type-A receptor 5	EPHA5	-11.02044582	1.393979428	0.004904762
alpha-1,2-Mannosidase	MAN1B1	-10.86874819	1.394104693	0.004857143
Xyloside xylosyltransferase 1	XXYLT1	-10.64442716	0.862217455	0.003238095
Myelin-associated glycoprotein	MAG	-10.55789995	1.393460684	0.004952381
ZNF511-PRAP1 readthrough	ZNF511-PRAP1	-10.49814292	0.789756711	0.005095238
C-type mannose receptor 2	MRC2	-10.42917606	0.786195248	0.005047619
Netrin receptor DCC	DCC	-10.36592538	0.807453693	0.00452381
SLIT and NTRK-like protein 5	SLITRK5	-10.33363192	0.738262511	0.005761905
Fibrillin-1 [Cleaved into: Asprosin]	FBN1	-10.29858828	0.751509035	0.005666667
Transmembrane glycoprotein NMB	GPNMB	-10.25154924	1.390688251	0.005142857

Spectrin alpha chain, erythrocytic 1	SPTA1	-10.132967	1.390104493	0.005190476
Glypican-1 [Cleaved into: Secreted glypican-1]	GPC1	-9.970864228	0.802395174	0.00152381
Peptidyl-prolyl cis-trans isomerase C	PPIC	-9.96184894	0.775571258	0.005380952
Adhesion G protein-coupled receptor B1	ADGRB1	-9.916713238	1.394168899	0.004761905
Serine protease inhibitor Kazal-type 6	SPINK6	-9.858383724	0.793315005	0.001619048
Secreted frizzled-related protein 4	SFRP4	-9.847377573	0.883573297	0.000857143
Protein HEG homolog 1	HEG1	-9.568422726	0.733865457	0.005857143
Cholecystokinin	CCK	-9.546958923	0.734031886	0.002190476
Beta-mannosidase	MANBA	-9.504348891	0.829070518	0.001047619
Mitotic spindle assembly checkpoint protein MAD1	MAD1L1	-9.424930232	0.670643783	0.008571429
Protocadherin-9	PCDH9	-9.320859909	0.794408112	0.001571429
Contactin-associated protein-like 2	CNTNAP2	-9.249386719	0.708944299	0.002285714
Growth hormone A1	PRL	-8.442205565	0.670371435	0.008619048
Testican-3	SPOCK3	-8.427104201	0.714164085	0.002238095
DOMON domain-containing protein FRRS1L	FRRS1L	-8.412509441	0.640966018	0.008952381
Polypeptide N-acetylgalactosaminyltransferase 6	GALNT6	-8.328299318	0.555926954	0.008095238
WAP four-disulfide core domain protein 1	WFDC1	-8.223711831	0.623258688	0.009571429
Protein delta homolog 2	DLK2	-7.966972283	0.739793262	0.002142857
VPS10 domain-containing receptor SorCS1	SORCS1	-7.924479553	0.626653432	0.009285714
Protocadherin-17	PCDH17	-7.780732155	0.661996425	0.008761905
Extracellular serine/threonine protein kinase FAM20C	FAM20C	-7.74975041	0.612149255	0.009809524
Cadherin-18	CDH18	-7.740121569	0.652409163	0.00252381
Plexin domain-containing protein 1	PLXDC1	-7.733608314	0.611191396	0.009904762
Protein FAM69C	DIPK1C	-7.612144675	0.478729287	0.010666667
Complement C1q tumor necrosis factor-related protein 5	C1QTNF5	-7.607075146	0.599873179	0.010380952
Protein ERGIC-53	LMAN1	-7.604011944	0.464996062	0.011333333
Dyslexia-associated protein KIAA0319-like protein	KIAA0319 L	-7.50304372	0.582919765	0.010714286
Beta-hexosaminidase subunit beta	HEXB	-7.495227337	0.631250613	0.002952381
Lysosomal alpha-glucosidase	GAA	-7.476088864	0.632080457	0.009190476
A disintegrin and metalloproteinase with thrombospondin motifs 4	ADAMTS4	-7.46701295	0.564688679	0.011190476
Sia-alpha-2,3-Gal-beta-1,4-GlcNAc-R:alpha 2,8-sialyltransferase	ST8SIA3	-7.439700603	0.500696171	0.009619048
Tropomyosin alpha-4 chain	TPM4	-7.338697093	0.422970285	0.01652381
Junctional adhesion molecule B	JAM2	-7.230527333	0.607152028	0.010095238
Low-density lipoprotein receptor-related protein 11	LRP11	-7.207210677	0.608560226	0.009952381
Netrin receptor UNC5C	UNC5C	-7.205382483	0.592922124	0.01047619
Cadherin-11	CDH11	-7.190963405	0.573548576	0.010952381
Calnexin	CANX	-7.155601433	0.603356187	0.010142857

Tetratricopeptide repeat domain 7A, isoform CRA_a	TTC7A	-7.111987659	0.452827415	0.011952381
NAD	NAXE	-7.070923397	0.616859375	0.009714286
Neuropilin-1	NRP1	-7.046418122	0.488470551	0.010333333
Follistatin-related protein 5	FSTL5	-7.005941868	0.417417806	0.016857143
Glia-derived nexin	SERPINE2	-6.969583035	0.424984083	0.016380952
Calsyntenin-3	CLSTN3	-6.921108382	0.606538174	0.003
Metallothionein	MT3	-6.91421536	0.435302622	0.016
Ig-like domain-containing protein	n/a	-6.868158	0.530219205	0.005285714
Scrapie-responsive protein 1	SCRG1	-6.863022259	0.440962373	0.015761905
Xylosyltransferase 1	XYLT1	-6.831765652	0.588860966	0.01052381
Chordin-like protein 1	CHRDL1	-6.777474744	0.559736056	0.003333333
Receptor-type tyrosine-protein phosphatase N2	PTPRN2	-6.776586192	0.560417428	0.003380952
Aspartate aminotransferase, mitochondrial	GOT2	-6.7267719	0.42946567	0.016238095
Acid ceramidase	ASAH1	-6.725760392	0.593715894	0.003142857
Protein shisa-6	SHISA6	-6.723671777	0.392282934	0.019428571
Low affinity immunoglobulin gamma Fc region receptor II-a	FCGR2A	-6.670365402	0.559488062	0.003428571
Guanine deaminase	GDA	-6.627694471	0.563704334	0.003285714
Chordin	CHRD	-6.598666668	0.594833754	0.003095238
Polypeptide N-acetylgalactosaminyltransferase	GALNT7	-6.543560982	0.409474884	0.017095238
Out at first protein homolog	OAF	-6.524238041	0.514026478	0.005714286
Beta-1,4-galactosyltransferase 1	B4GALT1	-6.496834959	0.394128656	0.019285714
Golgi integral membrane protein 4	GOLIM4	-6.399989196	0.530323566	0.005333333
Serum albumin	ALB	-6.398368563	0.544868944	0.004428571
Delta and Notch-like epidermal growth factor-related receptor	DNER	-6.356620584	0.496585467	0.006047619
Ryanodine receptor 2	RYR2	-6.338811874	0.698114856	0.018666667
Cadherin-6	CDH6	-6.336361613	0.549470216	0.004238095
Phospholipase D3	PLD3	-6.282430989	0.503528779	0.005952381
Hypoxia up-regulated protein 1	HYOU1	-6.200163228	0.490842118	0.006285714
Immunoglobulin heavy variable 3-15	IGHV3-15	-6.137991973	0.499365413	0.006
Protein CASC4	GOLM2	-6.110157967	0.698114856	0.018761905
Endoplasmic reticulum aminopeptidase 1	ERAP1	-6.003855228	0.698114856	0.017809524
Growth arrest-specific protein 6	GAS6	-5.942723751	0.489024445	0.006380952
Cadherin-5	CDH5	-5.936657906	0.698114856	0.018190476
Thioredoxin	TXN	-5.915117264	0.49022205	0.006333333
Selenoprotein M	SELENOM	-5.728058338	0.698114856	0.019095238
Macrophage mannose receptor 1	MRC1	-5.691224711	0.472828649	0.006619048
Neural cell adhesion molecule 1	NCAM1	-5.689100197	0.445121602	0.006952381
Receptor-type tyrosine-protein phosphatase-like N	PTPRN	-5.686585903	0.698114856	0.018
Coactosin-like protein	COTL1	-5.538314819	0.698114856	0.018095238
Neural cell adhesion molecule L1-like protein	CHL1	-5.511045865	0.47250192	0.006666667
Forkhead-associated domain-containing protein 1	FHAD1	-5.469340801	0.698114856	0.018952381

Lysosomal acid lipase/cholesteryl ester hydrolase	LIPA	-5.443239689	0.698114856	0.019047619
Plastin-2	LCP1	-5.415706294	0.447918598	0.006857143
Malectin	MLEC	-5.380572796	0.698114856	0.018047619
Cation-independent mannose-6-phosphate receptor	IGF2R	-5.369415283	0.698114856	0.018380952
Butyrophilin subfamily 2 member A1	BTN2A1	-5.350942612	0.698114856	0.018857143
Immunoglobulin lambda variable 4-60	IGLV4-60	-5.324790955	0.698114856	0.019142857
Neuromodulin	GAP43	-5.279493332	0.698114856	0.018333333
Microtubule-actin cross-linking factor 1, isoforms 1/2/3/5	MACF1	-5.275220871	0.698114856	0.018714286
Neuroplastin	NPTN	-5.255766392	0.698114856	0.017714286
UPF0454 protein C12orf49	C12orf49	-5.254859447	0.698114856	0.017857143
C-type natriuretic peptide [Cleaved into: CNP-22;CNP-29;CNP-53]	NPPC	-5.234627656	0.293988004	0.024047619
Calsyntenin-2	CLSTN2	-5.21847868	0.698114856	0.017904762
Sodium/potassium-transporting ATPase subunit alpha	ATP1A2	-5.195561886	0.698114856	0.018904762
UDP-GalNAc:beta-1,3-N-acetylgalactosaminyltransferase 1	B3GALNT1	-5.175493717	0.698114856	0.01847619
Macrophage colony-stimulating factor 1	CSF1	-5.156295844	0.289769206	0.023095238
Contactin-3	CNTN3	-5.13400507	0.698114856	0.017761905
Immunoglobulin lambda variable 1-44	IGLV1-44	-5.103190899	0.698114856	0.018428571
Immunoglobulin heavy variable 3-20	IGHV3-20	-5.087020874	0.698114856	0.019
Transmembrane protein 59-like	TMEM59L	-5.066848755	0.698114856	0.017666667
Semaphorin-6D	SEMA6D	-5.049332346	0.310819284	0.023428571
Sodium/iodide cotransporter	SLC5A5	-5.01409483	0.698114856	0.017952381
Chondroadherin	CHAD	-5.004061222	0.698114856	0.01852381
Non-secretory ribonuclease	RNASE2	-4.991362504	0.285910962	0.024428571
Sex hormone-binding globulin, isoform CRA_a	SHBG	-4.991299357	0.301862823	0.023809524
Connective tissue growth factor	CCN2	-4.912896156	0.698114856	0.018238095
Alpha-1,3-mannosyl-glycoprotein 2-beta-N-acetylglucosaminyltransferase	MGAT1	-4.838296618	0.284405125	0.02447619
WW domain-binding protein 2	WBP2	-4.815889495	0.274800999	0.024761905
Chloride intracellular channel protein 1 (Chloride channel ABP)	CLIC1	-4.774667263	0.698114856	0.018571429
Ephrin-A1	EFNA1	-4.738621099	0.285836522	0.024380952
Procollagen-lysine,2-oxoglutarate 5-dioxygenase 1	PLOD1	-4.710621357	0.698114856	0.018142857
Immunoglobulin kappa variable 2-29	IGKV2-29	-4.700024128	0.238457201	0.02552381
Plasma alpha-L-fucosidase	FUCA2	-4.669029372	0.251796477	0.025666667
Aminopeptidase	NPEPPS	-4.644252777	0.698114856	0.018809524
Protocadherin gamma-C5	PCDHGC5	-4.639968804	0.260880522	0.025333333
Cleavage stimulation factor subunit 3	CSTF3	-4.589632239	0.432178734	0.007142857

Beta-Ala-His dipeptidase	CNDP1	-4.500663417	0.22492373	0.005619048
Leucine-rich repeat transmembrane neuronal protein 2	LRRTM2	-4.458975315	0.278282867	0.024619048
Multiple inositol polyphosphate phosphatase 1	MINPP1	-4.441134589	0.442359689	0.007047619
WASH complex subunit 2A	WASHC2 A	-4.435419559	0.263168602	0.025142857
Testican-2	SPOCK2	-4.377730506	0.230407634	0.025857143
Adhesion G protein-coupled receptor B2	ADGRB2	-4.325736795	0.242171746	0.025238095
WAP four-disulfide core domain protein 2	WFDC2	-4.302537509	0.263999194	0.025047619
Immunoglobulin kappa variable 6D-21	IGKV6D-21	-4.280338969	0.245267851	0.026
Transmembrane protein 132A	TMEM132 A	-4.280067171	0.418484252	0.007190476
Sulfhydryl oxidase 2	QSOX2	-4.225917203	0.240475501	0.025380952
Immunoglobulin lambda-like polypeptide 1	IGLL1	-4.2237057	0.255245854	0.025571429
Coagulation factor IX	F9	-4.21966832	0.241075193	0.025285714
Thymosin beta-4	TMSB4X	-4.113992419	0.213201816	0.027095238
Neural cell adhesion molecule L1	L1CAM	-4.100632668	0.389830311	0.007952381
Adhesion G protein-coupled receptor L1	ADGRL1	-4.093407699	0.390182922	0.007857143
Rab GDP dissociation inhibitor alpha	GDI1	-4.079544067	0.229215702	0.025952381
Neurexophilin-1	NXPH1	-3.999327932	0.206137593	0.02752381
Basal cell adhesion molecule	BCAM	-3.991728783	0.253381843	0.025619048
Adipocyte enhancer-binding protein 1	AEBP1	-3.945445946	0.372211016	0.008380952
Thrombospondin-4	THBS4	-3.940882887	0.221122464	0.02652381
Prolow-density lipoprotein receptor-related protein 1	LRP1	-3.923822335	0.377220948	0.008285714
Polypeptide N-acetylgalactosaminyltransferase 18	GALNT18	-3.848302841	0.236403787	0.026571429
Protocadherin Fat 2	FAT2	-3.741374016	0.329352672	0.011714286
Glyceraldehyde-3-phosphate dehydrogenase	GAPDH	-3.723533358	0.329116956	0.011571429
Immunoglobulin superfamily member 21	IGSF21	-3.702085291	0.209832952	0.027285714
Follistatin-related protein 4	FSTL4	-3.68143865	0.338088026	0.010809524
Heparan-sulfate 6-O-sulfotransferase 3	HS6ST3	-3.672327246	0.370803359	0.00847619
Neuronal pentraxin-2	NPTX2	-3.672268867	0.345037673	0.010285714
Inter-alpha-trypsin inhibitor heavy chain H5	ITIH5	-3.636583737	0.318235533	0.015714286
L-selectin	SELL	-3.589487825	0.347736489	0.009857143
Golgi membrane protein 1	GOLM1	-3.57973378	0.339495427	0.010857143
Acyl-CoA-binding protein	DBI	-3.559237821	0.35649969	0.009047619
Neural proliferation differentiation and control protein 1	NPDC1	-3.54023041	0.337655672	0.010761905
Roundabout homolog 1	ROBO1	-3.53718601	0.330444244	0.011380952

Complement C1q subcomponent subunit A	C1QA	-3.494327273	0.306991639	0.016333333
Neutral alpha-glucosidase AB	GANAB	-3.450649534	0.356923238	0.009142857
SPARC-related modular calcium-binding protein 1	SMOC1	-3.439652034	0.335902281	0.011
Mannosyl-oligosaccharide 1,2-alpha-mannosidase IA	MAN1A1	-3.43908017	0.312073977	0.016095238
Stanniocalcin-2	STC2	-3.388532911	0.331343873	0.011619048
Nidogen-2	NID2	-3.385805198	0.323030675	0.012047619
Lysosomal Pro-X carboxypeptidase	PRCP	-3.323272705	0.296399766	0.017333333
Protocadherin alpha-C2	PCDHAC2	-3.286603315	0.317931513	0.015857143
Tenascin-R	TNR	-3.257496561	0.320668592	0.012142857
Cathepsin S	CTSS	-3.226269109	0.320972342	0.015666667
Transgelin	TAGLN	-3.211675985	0.302170188	0.016904762
Proteoglycan 4	PRG4	-3.181848935	0.289329648	0.019619048
Transforming growth factor beta receptor type 3	TGFBR3	-3.140318053	0.289243658	0.019380952
Carbonic anhydrase 4	CA4	-3.109602996	0.300735947	0.017
Fibroblast growth factor receptor	FGFR2	-3.054350649	0.286352759	0.01947619
Integral membrane protein 2B	ITM2B	-3.042938096	0.293945375	0.017619048
Endothelial protein C receptor	PROCR	-3.030934402	0.271515193	0.020428571
C-C motif chemokine 14	CCL14	-3.027749402	0.29507715	0.017285714
Dihydropteridine reductase	QDPR	-2.962807383	0.276973542	0.019904762
Poliovirus receptor	PVR	-2.943588597	0.298442245	0.017142857
Protein/nucleic acid deglycase DJ-1	PARK7	-2.913974217	0.259634845	0.020857143
Complement component C8 gamma chain	C8G	-2.873356206	0.238384617	0.021761905
Thrombospondin-2	THBS2	-2.867097923	0.274242039	0.020380952
OX-2 membrane glycoprotein	CD200	-2.845080512	0.185082266	0.029809524
Multiple epidermal growth factor-like domains protein 8	MEGF8	-2.844053745	0.263737968	0.007619048
Prosaposin receptor GPR37L1	GPR37L1	-2.801086221	0.152790267	0.029761905
Immunoglobulin kappa variable 1-16	IGKV1-16	-2.744635514	0.166754983	0.030714286
Eukaryotic translation initiation factor 2 subunit 3B	EIF2S3B	-2.654777391	0.122476715	0.033952381
Cadherin EGF LAG seven-pass G-type receptor 2	CELSR2	-2.573299408	0.226133376	0.022285714
Secretogranin-1	CHGB	-2.552504744	0.16720634	0.021904762
Epithelial discoidin domain-containing receptor 1	DDR1	-2.517567975	0.167282716	0.03052381
Brain acid soluble protein 1	BASP1	-2.485378197	0.237088871	0.021809524
Beta-galactoside alpha-2,6-sialyltransferase 2	ST6GAL2	-2.474132265	0.164098335	0.031142857
Legumain	LGMN	-2.445262841	0.171111511	0.030190476
Chitotriosidase-1	CHIT1	-2.444283554	0.167764212	0.03047619
Cathepsin O	CTSO	-2.440262794	0.168166481	0.030428571
Immunoglobulin heavy variable 1-2	IGHV1-2	-2.43029901	0.166559451	0.030761905
Immunoglobulin heavy variable 3-13	IGHV3-13	-2.425952366	0.164246903	0.031095238
Spectrin beta chain	SPTBN4	-2.370889187	0.15760389	0.031761905
Protein AHNAK2	AHNAK2	-2.35345711	0.158401641	0.031619048
Protein NDRG2	NDRG2	-2.328153202	0.163578785	0.031238095

Laminin subunit beta-2	LAMB2	-2.327467373	0.180199522	0.03
Complement factor H-related protein 3	CFHR3	-2.325222628	0.15930271	0.03152381
Histone H1.2	H1-2	-2.321843828	0.160586839	0.031428571
Golgi apparatus protein 1, isoform CRA_c	GLG1	-2.321016993	0.164673458	0.031
Sortilin	SORT1	-2.317759923	0.150170825	0.032142857
Tissue alpha-L-fucosidase	FUCA1	-2.317214761	0.110335499	0.034761905
Immunoglobulin lambda variable 5-45	IGLV5-45	-2.279788085	0.158950014	0.031571429
Ryanodine receptor 3	RYR3	-2.243037156	0.152863555	0.032047619
Neurexin-3-beta	NRXN3	-2.152274472	0.149621009	0.00352381
Somatostatin	SST	-2.149101394	0.148217923	0.032380952
Disintegrin and metalloproteinase domain-containing protein 11	ADAM11	-2.137351513	0.138136195	0.032904762
Transmembrane protein 132C	TMEM132C	-2.079115186	0.091664585	0.03552381
Protein FAM198B	GASK1B	-2.071126802	0.154662326	0.031952381
Ectonucleotide pyrophosphatase/ phosphodiesterase family member 5	ENPP5	-2.066145556	0.135168902	0.033142857
PITH domain-containing protein 1	PITHD1	-2.063803264	0.146547182	0.03247619
Cadherin-10	CDH10	-2.054669789	0.148664552	0.032333333
Stromal cell-derived factor 1	CXCL12	-2.029551097	0.145170627	0.032571429
Nucleobindin-2	NUCB2	-2.021849837	0.141120811	0.032666667
Receptor-type tyrosine-protein phosphatase kappa	PTPRK	-2.021718161	0.146872357	0.032428571

Table 11: All significantly differentially up-regulated proteins in the non-responders cerebrospinal fluid (CSF) proteome post treatment according to Log fold change (LFC) ≥ 2, False discover rate (FDR) <0.05 (represented by Log(p)>1.13) in order of LFC

Protein	Gene	LFC	LogP	FDR
V-type proton ATPase subunit S1	ATP6AP1	17.7330496	2.827164629	0.000714286
Phospholipase D4	PLD4	13.82809884	1.543076397	0.000761905
Polypeptide N-acetylgalactosaminyltransferase 2	GALNT2	13.05085897	1.331418633	0.001714286
Vitamin K-dependent protein Z	PROZ	11.81862341	1.173749182	0.00052381
Coagulation factor XIII B chain	F13B	11.35208103	1.458896657	0.00347619

Table 12: All significantly differentially up-regulated proteins in the non-responders cerebrospinal fluid (CSF) proteome post treatment according to Log fold change

(LFC) ≤ -2, False discover rate (FDR) <0.05 (represented by Log(p)>1.13) in order of LFC

Protein	Gene	LFC	LogP	FDR
Double-stranded RNA-specific editase 1	ADARB1	-17.2087869	1.727415111	9.52381E-05
Heat shock cognate 71 kDa protein	HSPA8	-15.82209035	1.612765452	0.000142857
Mannan-binding lectin serine protease 1	MASP1	-15.26076494	1.74757113	4.7619E-05
Protein FAM19A5	TAFA5	-14.02971186	1.201375765	0.000428571
Serotransferrin	TF	-13.95079844	1.289981347	0.000285714
Contactin-4	CNTN4	-12.88501344	1.219143136	0.000380952
Netrin-G1	NTNG1	-12.74417686	1.130274283	0.000571429
Contactin-6	CNTN6	-12.64343766	1.179428872	0.00047619
Semaphorin-3G	SEMA3G	-12.44467851	1.288608643	0.001809524
Beta-actin-like protein 2	ACTBL2	-11.97152758	1.394164245	0.004809524
Ephrin type-A receptor 5	EPHA5	-11.02044582	1.393979428	0.004904762
alpha-1,2-Mannosidase	MAN1B1	-10.86874819	1.394104693	0.004857143
Myelin-associated glycoprotein	MAG	-10.55789995	1.393460684	0.004952381
Transmembrane glycoprotein NMB	GPNMB	-10.25154924	1.390688251	0.005142857
Spectrin alpha chain, erythrocytic 1	SPTA1	-10.132967	1.390104493	0.005190476
Adhesion G protein-coupled receptor B1	ADGRB1	-9.916713238	1.394168899	0.004761905
Double-stranded RNA-specific editase 1	ADARB1	-17.2087869	1.727415111	9.52381E-05
Heat shock cognate 71 kDa protein	HSPA8	-15.82209035	1.612765452	0.000142857
Mannan-binding lectin serine protease 1	MASP1	-15.26076494	1.74757113	4.7619E-05
Protein FAM19A5	TAFA5	-14.02971186	1.201375765	0.000428571

The top 20 GO analysis biological processes involving the differentially expressed proteins in the responders and non-responders are illustrated in Figure 11. The top five biological

processes identified in the responders according to gene count (GC) were: immune system process (GC=142), regulation of multicellular organismal process (GC=138), anatomical structure morphogenesis (GC=121), regulation of nervous system development (GC=121) and regulation of developmental process (GC=118) (Figure 4A). The top five biological processes identified in the non-responders were: regulation of biological quality (GC=144), regulation of multicellular organismal process (GC=120), anatomical structure morphogenesis (GC=112), nervous system development (GC=109) and response to external stimulus (GC=108) (Figure 4B). The clear differential between groups in relation to GO analysis was those proteins related to immune system process in responders but not in the non-responder group.

KEGG analysis was subsequently preformed to identify the up and down regulated high-level functions of biological processes in the responders and non-responder group (Figure 12). The most up regulated proteins according to KEGG analysis were those related to metabolic pathways in the responder (GC=32) and the non-responder (GC=22) groups (Figure 12A, B). The second most upregulated proteins were related to axon guidance in the responders (GC=16) and non-responders (GC=11) (Figure 12A, B). The most down regulated processes in responders according to GC were the PI3K-Akt signalling pathway (GC=8), cell adhesion molecules (CAMs) (GC=6) and mitogen-activated protein kinases (MAPK) signalling pathway (GC=6) (Figure 12C). These pathways were not downregulated in the non-responders (Figure 5D). The most downregulated processes in the non-responders were proteins related to metabolic pathways (GC= 22), lysosome (GC=7) and axon guidance (GC=7) (Figure 12D).

Of the 464 differentially expressed proteins in the responders, the proteins were classified into protein classes as defined by the International Union of Basic and Clinical Pharmacology. Based on the modulation of proteins according to GO and KEGG pathways, we subdivided neuropeptides into neural proteins and immune process proteins to illustrate the dynamic changes of the relevant proteins under these two classes. The expression of neural proteins is illustrated in Figure 13 with the up and down regulated proteins shown in a heat map, pre- and post-treatment in the responders (Figure 13A). The relationship of these neural proteins is illustrated in a K-means clustered protein network of their interactions by biological function (Figure 13B). The majority of proteins modulated were involved in neurogenesis, axonogenesis and regulation of neuronal projections and differentiation.

Similarly, the expression of proteins related to immune processes are summarised in Figure 14. The expression of immune proteins is illustrated with the up and down regulated proteins shown in a heat map, pre- and post-treatment in the responders (Figure 14A). A clustered network of proteins also illustrated the largest concentrations of proteins according to biological function were related to regulation of immune response and leukocyte differentiation, activation and migration.

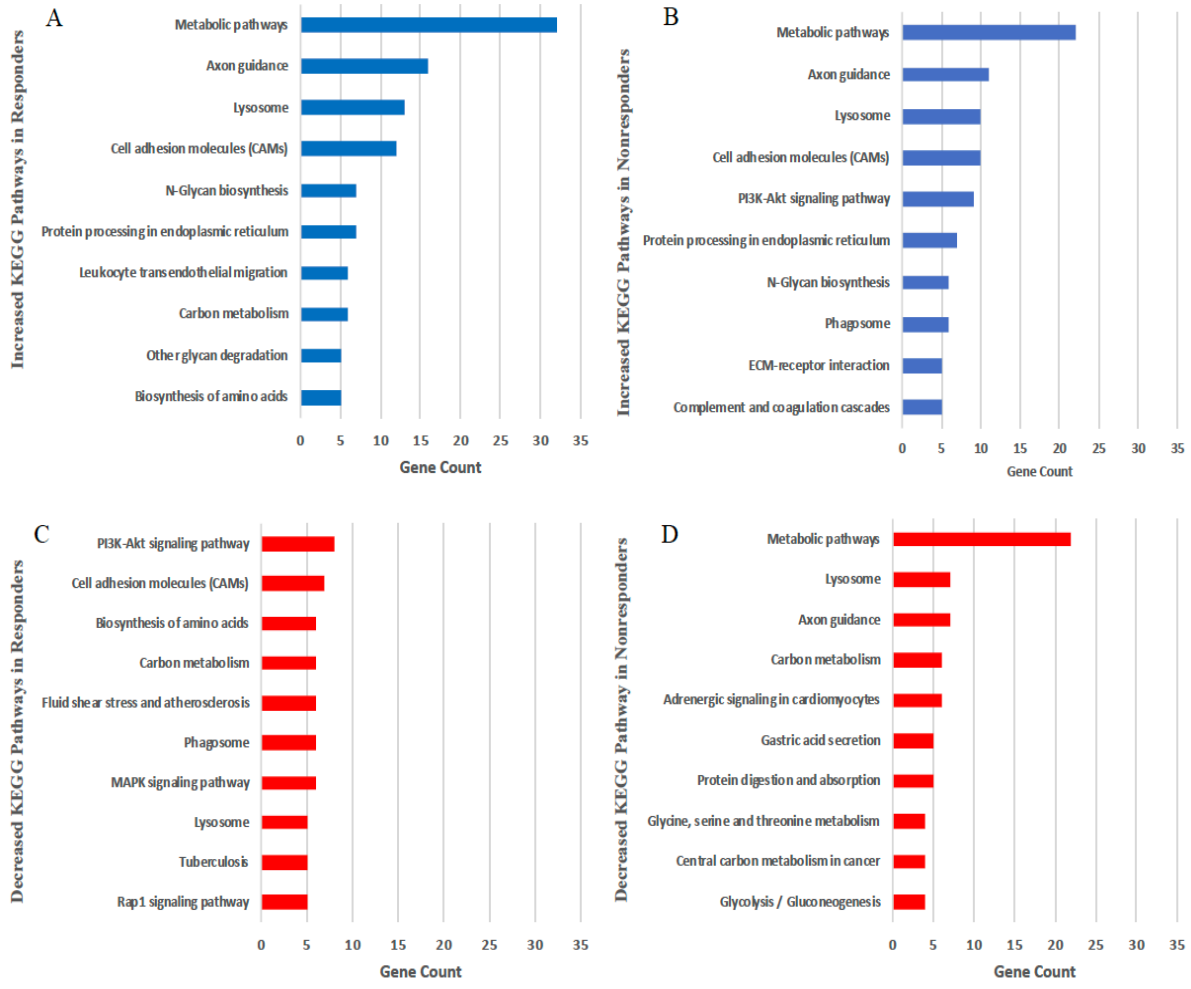

Figure 12: KEGG pathway analysis of up and down regulated proteins: Proteins taken from Volcano plot with LFC ≥ 2 were further analysed using Kyoto Encyclopaedia of Genes and Genomes (KEGG) pathway analysis in responders (12A) and non-responders (12B). Proteins taken from Volcano plot with LFC ≤ -2 were analysed using KEGG pathway analysis in responders (12C) and non-responders (12D). Bar charts illustrate the number of genes involved.

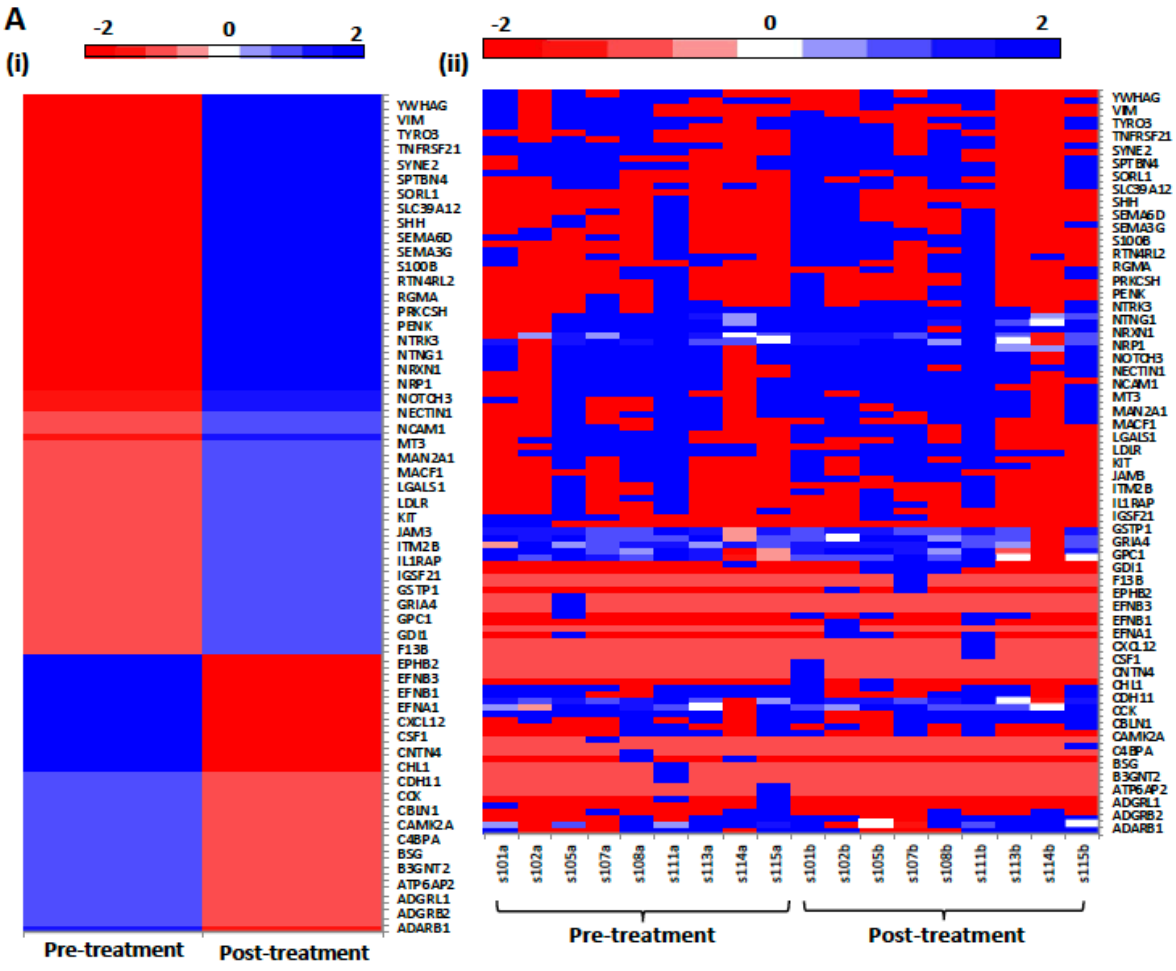
A
(i)
-2
0
2
YWHAG
VIM
TYRO3
TNFRSF21
SYNE2
SPTBN4
SORL1
SLC39A12
SHH
SEMA6D
SEMA3G
S100B
RTN4RL2
RGMA
PRKCSH
PENK
NTRK3
NTNG1
NRXN1
NRP1
NOTCH3
NECTIN1
NCAM1
MT3
MAN2A1
MACF1
LGALS1
LDLR
KIT
JAM3
ITM2B
IL1RAP
IGSF21
GSTP1
GRIA4
GPC1
GDI1
F13B
EPHB2
EFNB3
EFNB1
EFNA1
CXCL12
CSF1
CNTN4
CHL1
CDH11
CCK
CBLN1
CAMK2A
C4BPA
BSG
B3GNT2
ATP6AP2
ADGRL1
ADGRB2
ADARB1
Pre-treatment
Post-treatment
(ii)
-2
0
2
s101a
s102a
s105a
s107a
s108a
s111a
s113a
s114a
s115a
s101b
s102b
s105b
s107b
s108b
s111b
s113b
s114b
s115b
Pre-treatment
Post-treatment

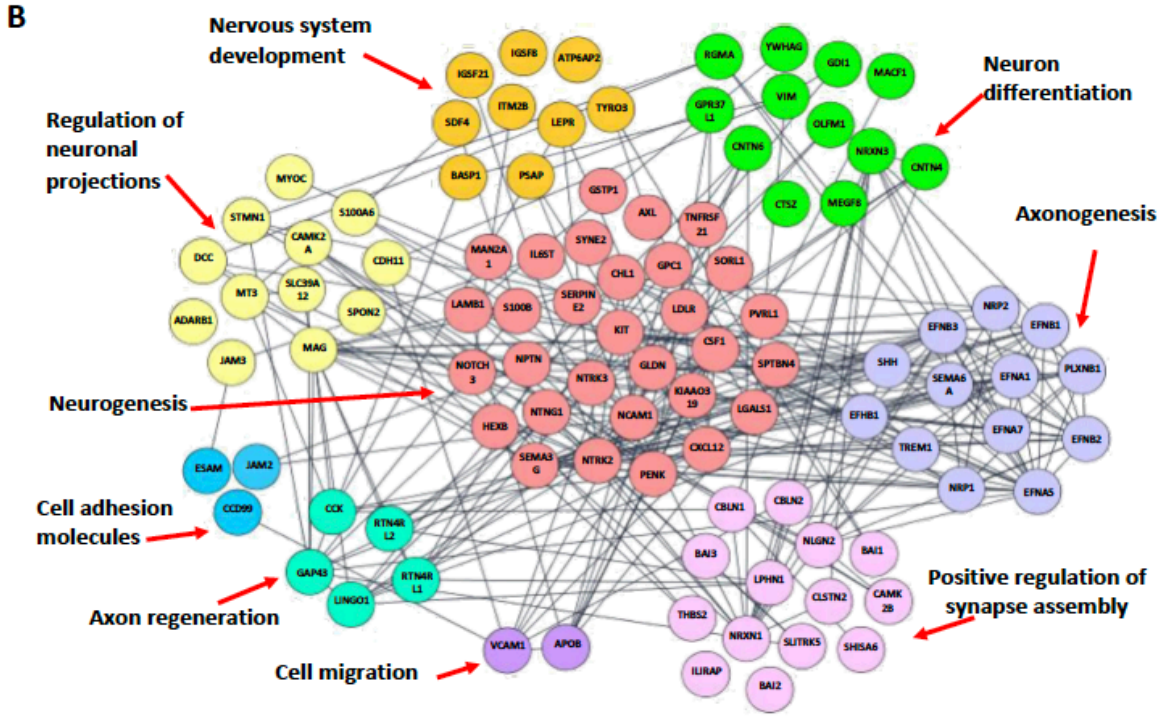
B
Nervous system development
Regulation of neuronal projections
Neurogenesis
Cell adhesion molecules
Axon regeneration
Cell migration
Neuron differentiation
Axonogenesis
Positive regulation of synapse assembly

Figure 13: Heat map and clustering of neural proteins in responders: Proteins taken from Volcano plot with $-2 \leq LFC \geq 2$ were used to create heatmaps of the neural proteins in responders only. [13A(i)] Panel shows the heatmap for all responder samples simply divided before (pre-treatment) and after 8 weeks of amitriptyline. [13A(ii)] Panel breaks this heatmap down to illustrate each individual samples expression profile. (13B) Clustering of the neuronal process protein network by biological function: Proteins taken from Volcano plot with $-2 \leq LFC \geq 2$ were input into string where K-means clustering was performed to create this clustered network of biological processes.

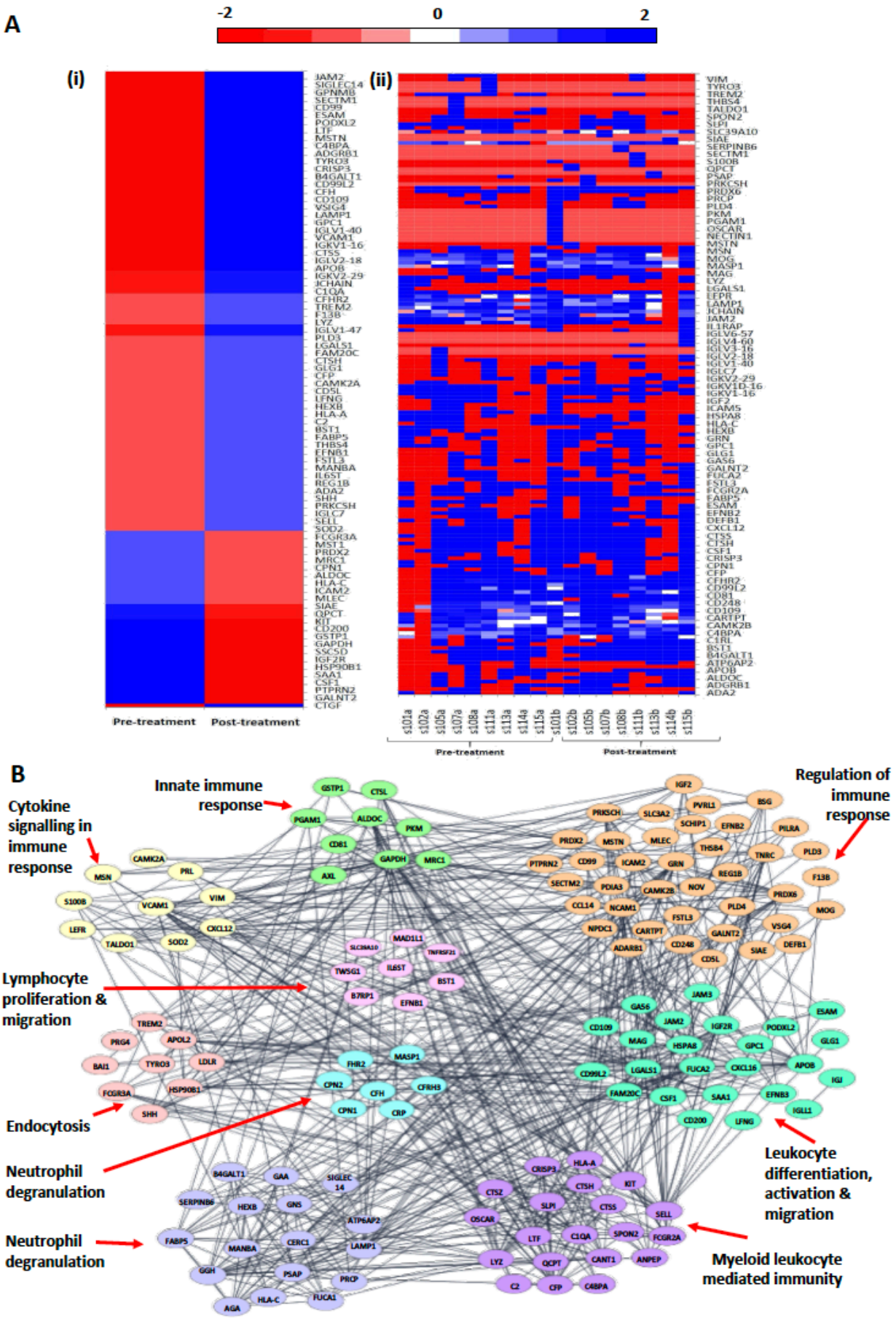
A
-2
0
2
(i)
(ii)
Pre-treatment
Post-treatment
B
Innate immune response
Cytokine signalling in immune response
Regulation of immune response
Lymphocyte proliferation & migration
Endocytosis
Neutrophil degranulation
Neutrophil degranulation
Leukocyte differentiation, activation & migration
Myeloid leukocyte mediated immunity

Figure 14: Heat Map and clustering of immune mediated proteins in responders: Proteins taken from Volcano plot with $-2 \leq LFC \geq 2$ were used to create heatmaps of the immune process proteins in responders only. [14A(i)] Panel shows the heatmap for all responder samples simply divided before (pre-treatment) and after 8 weeks of amitriptyline. [14A(ii)] Panel breaks this heatmap down to illustrate each individual samples expression profile. (14B) Clustering of the immune related protein network by biological function: Proteins taken from Volcano plot with $-2 \leq LFC \geq 2$ were input into string where K-means clustering was performed to create this clustered network according to biological processes.

2.3.4 Cellular Flow cytometry data:

There were no significant differences in the percentage frequencies of T cells in the CSF of responders and non-responders after amitriptyline. The individual dot plots of the different phenotypes of T cells are illustrated in Figure 15 in all of the patients. The data from $CD4^+$ cells was excluded as it is likely that the antibody were not functioning correctly and therefore the data was not reliable. The data from the $CD56^+$ cells were also excluded as they were not detected in 25/37 (67%) of samples. There were also no paired samples from any patients with regard to $CD56^+$ cells and therefore no meaningful insights could be gained.

We obtained data for n=6 patients within the responder group. Within the responders to amitriptyline the frequencies of $CD3^+$ cells and activated $CD3^+$ cells reduced after amitriptyline (Pre vs Post amitriptyline: $CD3^+$ cells: 69.47% ±6.79% vs 42.22% ±14.72%, p=0.22), (Pre vs Post amitriptyline: activated $CD3^+$ cells: 42.84% ±19.19% vs 31.77% ±16.59%, p=0.99). There was also a reduction in the frequency of $CD8^+$ cells (Pre vs Post amitriptyline: activated $CD8^+$ cells: 65.27% ±7.412% vs 40.28% ±15.38%, p=0.22). Within the subsets of T cells there was a reduction of the frequencies of central memory cells after amitriptyline in responders (Pre vs Post amitriptyline: $CD45RA^-CD27^+$ cells: 33.68% ±10.95% vs 13.07% ±7.56%, p=0.22). There was an increase in the frequency of effector memory T cells (Pre vs Post amitriptyline: $CD45RA^-CD27^-$ cells: 34.95% ±11.75% vs 48.44% ±15.12%, p=0.44) and terminally differentiated (Pre vs Post amitriptyline: $CD45RA^+CD27^-$ cells: 18.42% ±13.01% vs 33.71% ±15.5%, p=0.22). There was also a decrease in the frequency of naïve cells after amitriptyline in responders (Pre vs Post amitriptyline: $CD45RA^+CD27^+$ cells: 12.94% ±7.99% vs 5.287% ±2.85%, p=0.44).

We obtained data for n=3 patients within the non-responder's cohort. Within the non-responders to amitriptyline the frequencies of $CD3^+$ cells reduced after amitriptyline (Pre vs Post amitriptyline: $CD3^+$ cells: 73.87% ±13.24% vs 57.97% ±14.16%, p=0.4) and the

frequencies of activated $CD3^+$ cells increased (Pre vs Post amitriptyline: activated $CD3^+$ cells: 40.6% ±20.93% vs 49.6% ±20.87%, p=0.71). There was also an increase in the frequency of $CD8^+$ cells (Pre vs Post amitriptyline: activated $CD8^+$ cells: 36.10% ±6.185% vs 45.48% ±15.16%, p=0.99). There was an increase in the frequency of effector memory T cells (Pre vs Post amitriptyline: $CD45RA^-CD27^-$ cells: 26.45% ±21.27% vs 48.66% ±25.6%, p=0.86) and terminally differentiated (Pre vs Post amitriptyline: $CD45RA^+CD27^-$ cells: 14.55% ±5.5% vs 32.78% ±20.65%, p=0.62). There was also a decrease in the frequency of naïve cells after amitriptyline in non-responders (Pre vs Post amitriptyline: $CD45RA^+CD27^+$ cells: 27.28% ±22.2% vs 18.29% ±17.18%, p=0.4). Analysis was not possible on the central memory cells in the non-responders as there was only 1 sample that recorded a result in the B samples (post amitriptyline).

A

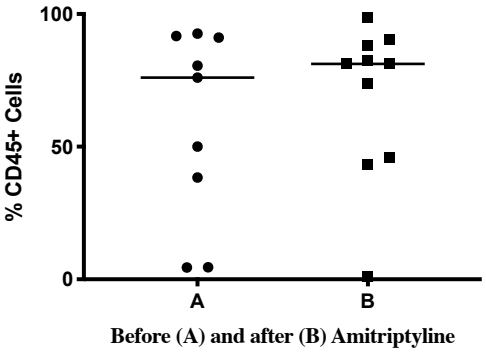
%CD45+ Amitriptyline A vs B
% CD45+ Cells
100
50
0
A
B
Before (A) and after (B) Amitriptyline

B

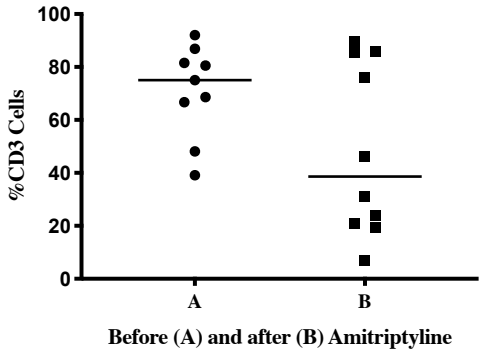
%CD3+ Amitriptyline A vs B
%CD3 Cells
100
80
60
40
20
0
A
B
Before (A) and after (B) Amitriptyline

C

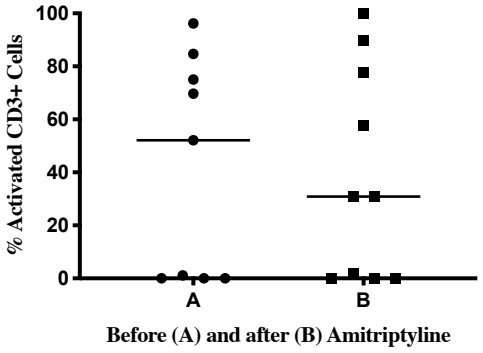
% Activated CD3+ Amitriptyline A vs B
% Activated CD3+ Cells
100
80
60
40
20
0
A
B
Before (A) and after (B) Amitriptyline

D

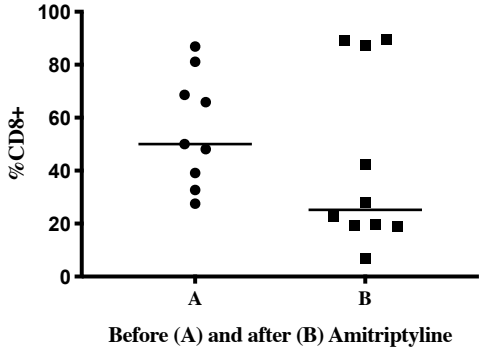
%CD8+ Amitriptyline A vs B
%CD8+
100
80
60
40
20
0
A
B
Before (A) and after (B) Amitriptyline

E

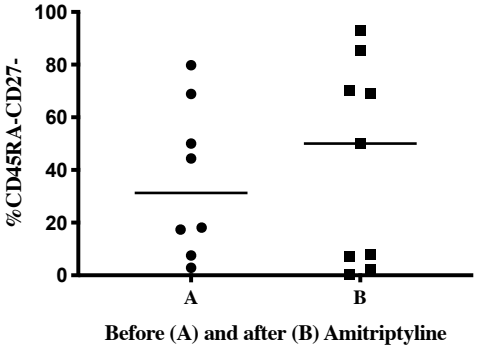
%Effector Memory Amitriptyline A vs B
%CD45RA-CD27-
100
80
60
40
20
0
A
B
Before (A) and after (B) Amitriptyline

F

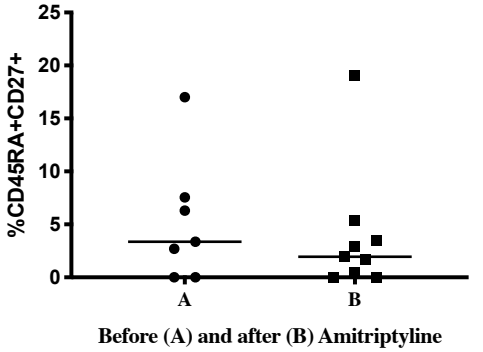
% Naive Amitrityline A vs B
%CD45RA+CD27+
25
20
15
10
5
0
A
B
Before (A) and after (B) Amitriptyline

G

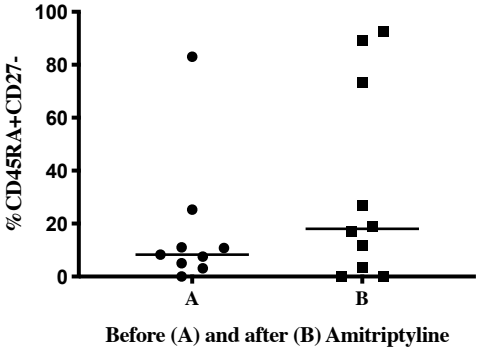
% Terminally Differentiated Amitrityline A vs B
%CD45RA+CD27-
100
80
60
40
20
0
A
B
Before (A) and after (B) Amitriptyline

H

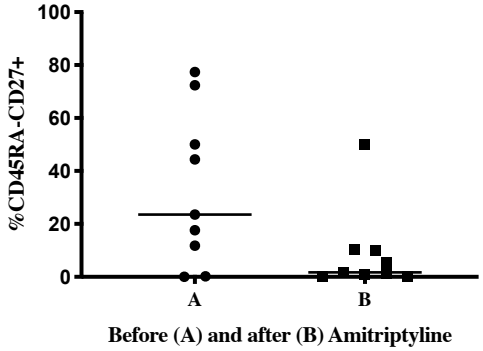
% Central Memory Amitrityline A vs B
%CD45RA-CD27+
100
80
60
40
20
0
A
B
Before (A) and after (B) Amitriptyline

Figure 15: Individual dot plots of cellular flow cytometry data of cerebrospinal fluid before and after amitriptyline: Comparison of (a) the percentage of $CD45^+$ cells, (b) the percentage of $CD3^+$ cells, (c) the percentage of $CD8^+$ cells and (d) the percentage of $CD3^+$ $CD69^+$ cells before and after amitriptyline. The phenotype of the percentage of $CD8^+$ cells in the CSF before and following amitriptyline: (e) Effector Memory cells (f) Naive cells before and after burst stimulation (g) terminally differentiated cells before and after (h) Central memory cells before and after amitriptyline.

2.5 Discussion

We present the first *in vivo* study examining the effect of amitriptyline on the CSF secretome and proteome in patients treated with amitriptyline as therapy for CNP. Amitriptyline therapy resulted in 56% (9/16) of patients achieving a 30% reduction in pain which is concordant with other studies published (45, 50, 317). A high response rate is due to deeming a >30% reduction as success, as opposed to 50% utilised in other selective studies (45, 50). The reason why patients respond to tricyclic antidepressant medication likely relates to genetic polymorphisms (232, 233) and to phenotypical characterisations of neuropathic pain (325). The choice to include patients in the non-responder group who had not provided a post treatment CSF sample was based on intention to treat.

The results from the proteomic GO and KEGG analysis illustrate many of the same active processes in both the responders and non-responders. For instance, nervous system development was one of the highest modulated processes according to GO analysis in both groups. KEGG analysis demonstrated that proteins related to axon guidance were the second most upregulated proteins after amitriptyline therapy in responders and non-responders. . The neurotrophic effect of amitriptyline has been described, associated with increases of GDNF (226, 245, 310), BDNF (225, 226) and VEGF (117, 118, 227, 312). While we did not detect BDNF and GDNF within our samples, VEGF-A was significantly upregulated in responders suggesting a potential pathway of analgesic efficacy. While some of the processes listed in both groups may still be contributory to the analgesic effect of amitriptyline in neuropathic pain, the differences are likely to be more representative of this effect. Modulation of proteins related to immune system process were the most differentiated after amitriptyline in responders and did not feature in the top 20 processes of non-responders. This provides more compelling evidence that amitriptyline exerts its analgesic effect at least in part by immunomodulation. The immunomodulatory effects of amitriptyline have been described in microglia (225, 247, 250), astrocytes (300) and

peripheral immune cells including T cells (313) which can infiltrate the CNS after nerve injury and can be pathognomonic of neuropathic pain (129). Although we did not observe statistical significance regarding modulation of cytokines from our data, definite trends were identified particularly a reduction in chemokines in responders.

The PI3K-Akt signalling pathway is implicated in many cellular processes including trafficking, immunity, proliferation and metabolism (326, 327), which we report here as the most downregulated pathway in responders. Specifically, there is *in vitro* evidence of PI3K inhibitors modulating the secretion of cytokines including IL-6 and TNF-α in LPS stimulated monocytes and macrophages (326). The PI3K-Akt signalling pathway has also been implicated in the development of neuropathic pain and hyperalgesia in sciatic nerve ligation models, diabetic neuropathy, bone cancer pain, spinal cord injury and inflammatory pain (328). Furthermore, inhibition of PI3K in the spinal cord prevented pain behaviours in mice induced by planter incision (329). Given the PI3K-Akt signalling pathway was upregulated in non-responders, this enhances the evidence that downregulation of this pathway is instrumental in the analgesic effect of amitriptyline for neuropathic pain.

Responders to amitriptyline had a significant decrease in the chemokine eotaxin-1 in CSF. While there was no healthy control arm in this study, raised eotaxin-1 levels in the CSF have already been demonstrated in patients with lumbar radicular pain compared to healthy controls (170). Increased levels of eotaxin-1 in blood samples have also been reported in patients suffering from depression but larger studies have found no difference compared to controls (330). However, eotaxin-1 within CSF is raised compared to controls in other neurodegenerative diseases including Alzheimer's, Huntington's and multiple sclerosis (MS) (331). American football players with chronic post traumatic encephalopathy also had elevated levels of eotaxin-1 in the brain and CSF on autopsy (287). Based on our inclusion and exclusion criteria we do not believe any of these conflicting variables were relevant in our patient cohort. Eotaxins are a subfamily of eosinophil chemokines which have been implicated in allergic inflammation, inflammatory bowel disease and asthma (88, 331, 332). Eosinophils are not prevalent within the CSF except for infection or the presence of blood; this suggests that eotaxin-1 is secreted by other cells within the CNS and likely carries out a different function (333). Chemokines in the CSF are thought to be produced primarily by glial cells and are referred to as glial-transmitters (3, 82-84, 89, 170,

331). Within the central nervous system (CNS) neurons, oligodendrocytes and astrocytes express receptors for eotaxin-1, indicating it is a participant in neuronal-glial communication (334). Furthermore, network analysis of IL-1β/ TNF-α stimulated human astrocytes *in vitro* resulted in secretomes of not only eotaxin-1, but PI3K and ERK 1/2 pathways which were all downregulated in responders within our study (335). Astrocytes and microglia's production of eotaxin-1 in an inflammatory environment also leads to immune cell trafficking (334, 335). Eotaxin-1 specifically recruits microglia and increases reactive oxygen species inducing excitotoxic neuronal cell death (336). From our cluster analysis of immune proteins, leukocyte differentiation, activation and migration were one of the highest modulated clusters after amitriptyline therapy in responders (Figure 7B). This also suggests that amitriptyline may modulate the trafficking of immunocompetent cells within the CNS.

Pre-clinical and *in vitro* attenuation of glial inflammatory pathways with amitriptyline has been reported but not with eotaxin-1 directly (247, 250, 300, 301). However, to our knowledge there are no studies examining the effect of amitriptyline on chemokines within the CNS thus far. Reactive glial cells have been illustrated in patients with lumbar radicular pain using radiolabelled translocator protein (TSPO), (a marker of gliosis), compared to controls in the dorsal horn and neuroforamina (183). TSPO is a more specific marker for microglia and astrocytes (173). From our data in responders, proteins related to immune system processes were modulated to the greatest extent and this was also associated with a decrease in proteins related to MAPK signalling pathways. Semaphorin 6A, a significantly upregulated protein, negatively regulates the ERK1 and ERK2 cascade which are part of the MAPK signalling pathway and have been associated with pain hypersensitivity (337). ERK is upregulated in neurons, microglia and astrocytes after neuronal injury in rodent models and may be implicated in the pathogenesis of neuropathic pain (338). Amitriptyline has been shown to inhibit both the ERK and MAPK pathways in neuropathic pain models in rodents (248). Our data adds to the available evidence that amitriptyline attenuates pro-inflammatory pathways within the CNS. Pre-clinical studies also indicate that these are established pathways relating to pathological pain within the neuroimmune interface (3).

Levels of VEGF-A increased in responders to amitriptyline after 8 weeks of treatment. Without a control arm we cannot compare baseline (pre-treatment) levels to normal subjects. However, patients with Failed Back Surgery Syndrome (FBSS), who have a

similar pain distribution, have lower levels of VEGF in CSF compared to healthy controls (122). There is also evidence of a reduction in VEGF levels within CSF in patients suffering from stress, depression and after a suicide attempt (119-121), which are synonymous with the CNP experience. Depletion of VEGF can lead to dysfunction of the nervous system (117, 118, 123, 228, 339) and injection of VEGF into the spinal cord of rats has demonstrated activation of neural stem cells after spinal cord injury (340). The significant increase in VEGF-A suggests amitriptyline may induce restorative repair mechanisms as a consequence of nerve dysfunction in chronic neuropathic pain.

VEGF expression after the application of amitriptyline has been uniquely demonstrated in animal models in the hippocampus (227, 312, 341). RNA sequencing analysis also indicates VEGF-A is produced predominately by astrocytes and microglia and also by neurons, oligodendrocytes and endothelial cells (342). The role of VEGF-A within the CNS involves neurogenesis, axon outgrowth, neuronal migration, gliogenesis and glia survival (117, 118). Outside of the CNS, VEGF predominant role is in angiogenesis. However, VEGF has demonstrated an improvement in nerve blood flow in models of diabetic and peripheral neuropathies (117, 343). Sensory neuropathy also improves with intramuscular injection of plasmid DNA encoding VEGF in diabetic patients (344). Further evidence to elicit mechanisms outside of angiogenesis include intramuscular VEGF gene transfer improving sensory deficits without angiogenesis in the sciatic nerve of mice suggesting a different mechanism in neurons (345). Other potential mechanisms of VEGF include neuroprotective effects in DRG cell bodies which have multiple receptors for VEGF (117-119). There is pre-clinical evidence that amitriptyline, likely via TrkA phosphorylation, regenerated DRG neurons in a dose dependent manner in rodents (346). This provides further evidence that amitriptyline can enhance neuronal growth and redevelopment. Pathological nerve damage is synonymous with lumbar radicular pain and neuropathic pain (23, 185), and amitriptyline's function may partially reverse this process.

The increase in concentration of TARC and IL-12 in the non-responders may be explained by severity or progression of pathology. Both neuropeptides have been associated with an increase in neurodegeneration and neuroinflammation within the CSF of patients with MS (347, 348). Furthermore, attenuation of the GM-CSF/TARC pathway is under investigation as a potentially novel analgesic for osteoarthritis (349).

While this study offers valuable insights into a vastly understudied area, there are limitations which include a relatively small number of participants and a confounding variable of opioid medications in some of the patients. For this reason, the results of this study, although informative, should be taken as preliminary evidence in humans. Although CSF analysis of patients medicated with opioids correlated level of pain to levels of IL-6 and IL-10, these cytokines were not significantly altered in our cohort (350). A study of CSF in patients with CRPS demonstrated no difference in the level of cytokines with patients on or not on opioids (187). We still do not have sufficient evidence to determine how opioids effect cytokines, chemokines and the proteomic constituents in CSF. There is however some *in vitro* data to suggest amitriptyline may restore the analgesic effect of opioids by inhibiting Toll like receptor (TLR)-2 & -4 signalling (250).

The reduction in pain in responders with the associated change in neuropeptides may not be attributable to amitriptyline alone. Improved sleep was also reported by 5/9 (56%) of responders which may be a confounding variable. Quality of sleep has been reported as a potential confounding variable in other studies examining neuropeptides and cytokines in chronic pain patients (170). The impact of sleep on neuropeptides as an independent variable is yet to be defined however. There are also many limitations to CSF analysis that are discussed in other publications (213, 321, 351). These include blood contamination(351), rostral-caudal gradient of protein concentrations(351) and inability to detect specific neuropeptides implicated in CNP (213). There is also the confounding variable of differentially expressed proteins that have a high individual variance between samples (352), however, none of these proteins were significantly altered in our cohort.

2.5.1 Flow Cytometry data

No difference was observed from our cellular data and this was likely related to large variance. Large SEM's were noted between samples, some markers were also undetectable in some samples. There are a number of explanations for the large variance in outcomes. Early on in the study, samples were analysed at different time points ranging from hours to 7 days post acquisition, this likely contributed to variability in cell viability. Novel data has also suggested certain cells including monocytes undergo apoptosis after 2-3 hours after collection. Furthermore, mid-way through the project the company manufacturing the Transfix storage tubes (Cytomark) for CSF altered their recommendations for storage from

7 days to 3 days. The majority of our samples were stored for 7 days prior to this new recommendation and as such the samples in this study were stored for varying periods of time. More stringent, completely homogenous timing of sample analysis would need to be performed in the future. Some studies have also excluded samples outside of a range of cells (>5 μ/l) (206, 207), counting beads were not used in our study so we were unable to make comparisons. The error bars in some published studies have also been high making it difficult to draw any firm conclusions from flow-cytometry data of CSF published so far (60, 286, 291, 353). Larger studies will be required to determine what effect amitriptyline has on lymphocyte subsets.

2.6 Conclusion

In summary, we have demonstrated the dynamic modulation of the proteomic and neuropeptide constituents of CSF *in vivo* in patients medicated with amitriptyline for the treatment of CNP. The predominant differential pathways were related to immune activity with a reduction of neural-glial pro-inflammatory pathways and a neurotrophic effect. These findings support pre-clinical and *in vitro* work with amitriptyline which demonstrated pharmacodynamic changes within inflammatory and VEGF pathways in particular. This provides information regarding the mechanism of action of amitriptyline in vivo in humans and also insights into the pathophysiology of CNP.

Chapter 3:

An investigation into the modulation of T cell phenotypes by amitriptyline and nortriptyline(313)

Highlights:

- Neuropathic pain may be related to T cell dysfunction
- Amitriptyline and nortriptyline modulate the function of T cell *in vitro*
- Amitriptyline and nortriptyline can attenuate the T_H1/T_H17 immune response and modify immunomodulatory pathways *in vitro*

Published in journal 'European Neuropsychopharmacology' (354)
https://doi.org/10.1016/j.euroneuro.2019.12.106

3.1 Abstract:

Amitriptyline is prescribed for treating the symptoms of neuroinflammatory disorders including neuropathic pain and fibromyalgia. As amitriptyline has evidence of modulating the neuroimmune interface; the effects of amitriptyline treatment on T-cell phenotype and function were examined *in vitro*. Peripheral blood mononuclear cells(PBMCs) were isolated and treated with amitriptyline, nortriptyline and a combination of both drugs. Toxicity for T-cells was assessed by Annexin V/Propidium Iodide staining. Activation status and cytokine expression by T-cells post treatment was assessed by flow cytometry. The levels of secreted cytokines, chemokines and neurotrophins were measured by ELISA in the supernatants. There was no significant increase in T-cell death following 24 or 48 hours compared to controls. There were significantly lower frequencies of $CD8^+$ T-cells after treatment with amitriptyline, nortriptyline and a combination of both compared to a Vehicle Control(VC)($p<0.001$). The frequencies of naive $CD8^+CD45RA^+$ cells were significantly lower after amitriptyline, nortriptyline and a combination of both ($p<0001$). The frequencies of $CD27^+CD4^+$($p<0.05$) and $CD27^+CD8^+$($p<0.01$) T-cells were also significantly lower following combination drug treatment. Significantly lower frequencies of IFN-γ-producing $CD8^+$ T-cells were observed with all treatment combinations($p<0.05$) and frequencies of IL-17-producing $CD4^+$ and $CD8^+$ T-cells were significantly lower following amitriptyline treatment ($p<0.05$). Frequencies of Natural Killer T-cells were significantly higher following treatment with nortriptyline($p<0.05$). Significantly higher levels of IL-16 ($p<0.001$) and lower levels of TNF-β ($p<0.05$) were observed in supernatants. This data indicates that both amitriptyline and nortriptyline modulate the phenotype and function of T-cells and this may have clinical relevance in the pathologies of its off-label applications.

3.2 Introduction:

Amitriptyline has a broad range of clinical indications but is most frequently prescribed for chronic neuropathic pain, depression, chronic widespread pain, fibromyalgia and migraine prophylaxis (45, 49, 50, 237). Unlike most analgesic medication it takes time to establish efficacy potentially indicating that its mechanism of action involves a period of modulation or plasticity (230, 241). It is classed as a tertiary amine tricyclic anti-depressant, and central and peripheral mechanistic actions have been proposed (238). Toxicology reports of overdose in plasma and cerebrospinal fluid (CSF) demonstrate a dose related concentration in both compartments, illustrating that amitriptyline penetrates the blood brain barrier and works both peripherally and centrally (235).

Numerous mechanisms of action of amitriptyline have been derived from pre-clinical and *in vitro* studies. Pharmacological function includes inhibition of monoamine reuptake transporters for serotonin and noradrenaline (231, 238, 239, 355). Its active metabolite nortriptyline is more selective for noradrenaline reuptake transporters (355). Amitriptyline also has affinity for α-adrenergic, histamine, muscarinic cholinergic, 5-hydroxytryptamine (HT), N-methyl-D-aspartate (NMDA) and opioid receptors (49, 231, 237, 238, 241, 243, 248, 303, 355). Blockade of the Na^+ voltage gated channels has also been reported (243). Toxic doses of amitriptyline interact with calcium and potassium channels, which are thought to be responsible for cardiac related adverse events (238). Nortriptyline is also a medication prescribed solely due to decreased side effects (229, 231).

The anti-inflammatory effect of amitriptyline has been well described. *In vitro* work with astro-glial cell lines from mice demonstrated amitriptyline inhibited NF-kβ translocation, which resulted in a reduction of interleukin IL-1β (300). Reductions in pro-inflammatory cytokines were demonstrated in the spinal cord of neuropathic pain models linking it with activation of the A3 adenosine receptor (247, 248). A study using cell lines expressing TLRs demonstrated amitriptyline inhibits TLR-2 and TLR-4 signalling, likely by binding to MD2 (250).

There is growing clinical evidence that chronic neuropathic pain, fibromyalgia and chronic widespread pain are neuroinflammatory disorders associated with changes in the neuroimmune interface (30, 180, 181, 183, 309, 356-359). The neuroimmune interface is a complex system involving a bi-directional communication between glia, immune cells and

neurons (3). Messengers within this system include cytokines, chemokines and neurotrophins secreted predominately by leucocytes and glial cells. Dysfunctional or maladaptive processes involving T cells (129, 199), macrophages (136, 137) and monocytes (84) have all been implicated in the chronicity of neuropathic pain. Immune cells are present both peripherally and centrally and while there have been many *in vitro* experiments in glial cells, there are few on immune cells involving the application of amitriptyline (238, 247, 250, 300, 301, 303, 304).

Painful and non-painful peripheral neuropathy, including diabetic (133), chemotherapy (135, 360) and HIV (32) induced have been linked to T cell dysregulation (129). The effect of amitriptyline on the symptoms of peripheral neuropathy therefore may be mediated via T cells. There is strong evidence that patients suffering from chronic pain express altered levels of cytokines in their blood and CSF compared to controls including interferon (IFN)-γ, IL-10, IL-4 and IL-17 suggesting neuroinflammation (168, 171, 199, 218, 223, 309, 350, 359-365). This may be part of the explanation for the benefit accrued by patients with chronic pain from amitriptyline prescription. Individual serum cytokines *in vivo,* including IL-6 in major depressive disorder, are reduced following treatment with tricyclic antidepressants, correlating with improved mood (249).

Previous *in vitro* experiments have demonstrated that the tricyclic antidepressant trimipramine can suppress IFN-γ production in T helper (T_H)1 cells and T cell proliferation (366). This suggests that the immunomodulatory effects with tricyclic antidepressants may be related to their direct biological effects on immune cells (366).

3.2.1 Aims

This study aimed to determine the effects of amitriptyline and nortriptyline on T cell activation and cytokine production on human PBMCs *in vitro.*

3.3 Experimental Procedures:

3.3.1 Sample Preparation

Nine healthy donors aged between 33-65 years of age had 18ml of whole blood taken under aseptic conditions in EDTA tubes (Grenier Bio One, Essen, Germany) after informed consent. The blood was immediately brought to the laboratory for analysis. Peripheral blood mononuclear cells (PBMCs) were isolated by density centrifugation using Ficoll-Paque™ Plus (GE Healthcare, Sweden). Cells were resuspended in Roswell Park Memorial Institute (RPMI) medium supplemented with 10% (v/v) foetal calf serum (FCS) and 1% (v/v) pen-strep (50U/ml penicillin and 100µg/ml streptomycin) and plated.
Amitriptyline (A) and Nortriptyline (N) hydrochloride (Sigma-Aldrich, Missouri, USA) powder was suspended in sterile de-ionised water and added at the following concentrations singly and in combination: 50 ng/ml (A=159.3 nM, N=166.8 nM), 100 ng/ml (A=318.6 nM, N=333.6 nM), or 200 ng/ml (A=637.2 nM, N=667.1 nM), for 24 and 48 hours for 3 donors. Vehicle controls (VC) contained the equivalent amount of de-ionised water as the 200 ng/ml treatment.

3.3.2 Cell death analysis

PBMCs from 3 healthy volunteers were transferred to FACS tubes and resuspended in 1ml of binding buffer and stained with a pre-optimised concentration of Annexin V (IQ Products, Netherlands) at 4°C for 15-20 minutes in the dark. Cells were re-suspended in 500 µl of binding buffer and immediately before 500 µl propidium iodide (PI) (1:4000 dilution of 1 mg/ml stock) was added. PBMCs from an additional donor were included who was prescribed 25 mg Amitriptyline as a control.

3.3.3 Flow cytometry analysis

Data was acquired on a CyAn™ ADP Analyzer (Beckman Coulter) using Summit v4.1 acquisition software and analysed using FlowJo v7.6.1 software (TreeStar, USA).

3.3.4 Analysis of T cell activation following amitriptyline and active metabolite nortriptyline treatment

PBMCs were isolated from 6 healthy controls and seeded in RPMI media. Amitriptyline and Nortriptyline hydrochloride (Sigma-Aldrich, Missouri, USA) was added at a concentration of 100 ng/ml separately and in combination for 24 hours at 37°C. A VC containing the same volume of de-ionised water was also included. The cells were washed with FACS buffer and blocked for 5 mins with blocking buffer (FACS buffer containing 50% FCS) at room temperature to ensure the Fc receptors were saturated in order to prevent non-specific binding of antibodies. Antibodies against CD3-APCVio770, CD4-VioBlue, CD8-PerCP, CD56-PEVio770, CD27-FITC VioBright, CD69-PE and CD45RA-VioGreen (Miltenyi Biotech, Bergisch Gladbach, Germany) were added and incubated for 30 min at 4°C protected from light. Cells were washed and resuspended in 500 µl of FACs buffer, and were analysed by flow cytometry immediately

3.3.5 T cell cytokine expression following amitriptyline and active metabolite nortriptyline treatment

PBMCs from 6 healthy volunteers were treated with 100 ng/ml of Amitriptyline, Nortriptyline, a combination of both or none (as VC) for 24 hours at 37°C. Nortriptyline was used as it is an active metabolite of nortriptyline to replicate its action *in vivo*. Each well was stimulated with phorbol 12-myristate 13-acetate (PMA) 10 ng/ml and ionomycin 1 µg/ml (Sigma, MO, USA) for 1hr at 37°C and 5% CO_2. The protein transport inhibitor Brefeldin A (10 µg/ml) (Sigma, MO, USA) was added for a further 3 hrs, after which time cells were transferred to FACS tubes and blocked as above. Cells were labelled with antibodies against CD3 PE-eFluor and CD8 PerCP (Miltenyi Biotech, Bergisch Gladbach, Germany), incubated for 30 min at 4°C protected from light. Surface antibodies were fixed using 50 µl solution A (Fix and Perm cell permeabilization kit, Caltag Laboratories, Buckingham, UK) for 15 min at room temperature. 50µl permeabilization solution B was then added together with antibodies specific for IL-17 FITC VioBright, IL-10 PE, IL-4 PEVio770 and IFN-γ VioGreen (Miltenyi Biotech, Bergisch Gladbach, Germany). Cells were vortexed and incubated for 15 min at room temperature in the dark. Cells were then washed and resuspended in 500 µl FACS buffer and analysed immediately by flow cytometry. using a CyAn™ ADP Analyzer (Beckaman Coulter, Brea, CA, USA) using Summit v4.1 and was analysed using FlowJo v7.6.1.

3.3.6 Quantification of soluble proteins by Enzyme-Linked ImmunoSorbent Assay (ELISA)

PBMCs from 6 healthy volunteers were treated with 100 ng/ml of Amitriptyline, Nortriptyline, a combination of both or none (as VC) for 24 hours at 37°C. Supernatants were taken after 24 hours and cryopreserved at -20°C. Supernatants were defrosted to room temperature and analysed immediately using Fractalkine/CX3CL1 ELISA kits from Abcam (Cambridge, UK) and the following multiplex ELISA kits from MesoScale Diagnostics (Rockville, MD, USA) NGF (R-plex), BDNF (R-plex) and Human Cytokine Panel 1 (V-Plex), containing: GM-CSF, IL-1α, IL-5, IL-7, IL-12/IL-23p40 ,IL-15, IL-16, IL-17A, TNF-β , VEGF-A, Human Cytokine Panel 2 (V-plex)(Pro-inflammatory), containing: IFN-γ, IL-1β, IL-2, IL-4, IL-6, IL-8, IL-10, IL-12p70, IL-13 and TNF-α and Panel 3 (V-plex) (Chemokines) containing Eotaxin, MIP-1β, Eotaxin-3, thymus and activation regulated chemokine (TARC), IP-10, MIP-1α, high abundance IL-8, MCP-1, MDC, MCP-4, according to the manufacturer's instructions without dilution. MSD R-Plex plates for NGF and BDNF were all purchased from MesoScale Diagnostics (Rockville, MD, USA).

3.3.7 Ethics

This study was approved by the St James's/AMNCH Research Ethics Committee, Dublin, Ireland.

3.3.8 Statistics

All statistical analysis was performed using Prism Graph Pad version 8.0. One way ANOVA was used for analysing data of multiple comparisons. Correction for multiple comparisons using statistical hypothesis testing was performed using a Dunnett test compared to VC. Results were expressed in means, p values of <0.05 were considered to be significant.

3.4 Results:

3.4.1 Amitriptyline and Nortriptyline do not induce cell death in PBMCs

An initial toxicity screen was performed by examining the effect of the amitriptyline drugs on the viability of PBMCs. Using flow cytometric analyses, lymphocytes were gated on using forward and side scatter properties. No significant increases in cell death were observed (n=3) between the various drug concentrations of amitriptyline (A), nortriptyline (N), the combination of both drugs (AN) and the no treatment (NT) group in early apoptotic cells (Annexin V^+ PI^-), dead cells (Annexin V^+ PI^+) or necrotic cells (Annexin V^- PI^+), suggesting neither drug was toxic at these concentrations (Figure 16). The control subject who was on 25 mg of amitriptyline but was not treated with any drug *in vitro* had 90.6% and 91.6% live PBMCs, 6.32% and 5.97% early apoptotic, 2.97% and 2.31% dead and 0.09% and 0.12% necrotic cells at 24 hours and 48 hours respectively (Figure 16). Based on these results a concentration of 100 ng/ml was deemed non-toxic to PBMCs and selected for the subsequent experiments with an incubation time of 24 hours to reflect plasma concentrations relative for chronic pain patients.

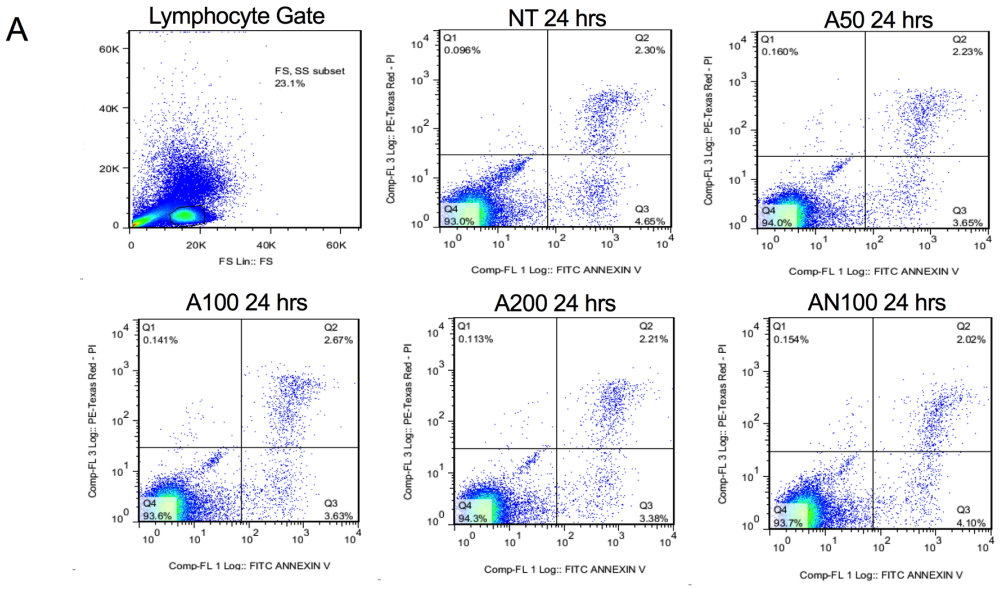
A
Lymphocyte Gate
FS, SS subset
23.1%
FS Lin:: FS
NT 24 hrs
Q1 0.096%
Q2 2.30%
Q4 93.0%
Q3 4.65%
A50 24 hrs
Q1 0.160%
Q2 2.23%
Q4 94.0%
Q3 3.65%
A100 24 hrs
Q1 0.141%
Q2 2.67%
Q4 93.6%
Q3 3.63%
A200 24 hrs
Q1 0.113%
Q2 2.21%
Q4 94.3%
Q3 3.38%
AN100 24 hrs
Q1 0.154%
Q2 2.02%
Q4 93.7%
Q3 4.10%
Comp-FL 3 Log:: PE-Texas Red - PI
Comp-FL 1 Log:: FITC ANNEXIN V

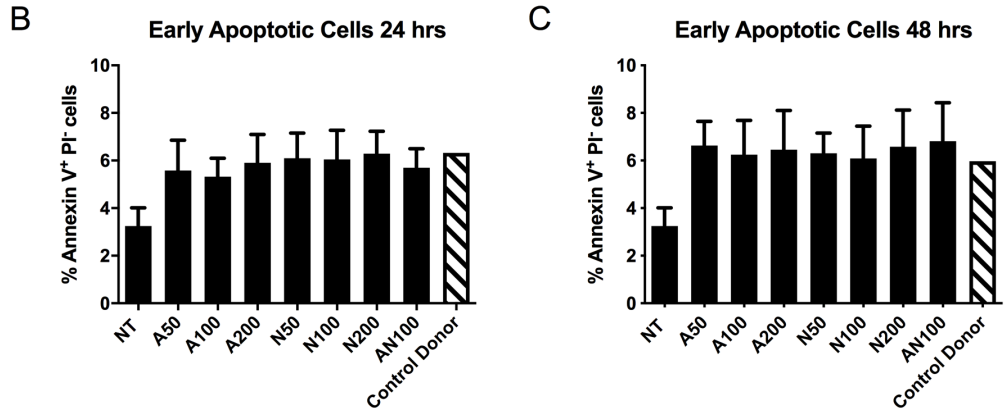
B
Early Apoptotic Cells 24 hrs
% Annexin V+ PI- cells
C
Early Apoptotic Cells 48 hrs
% Annexin V+ PI- cells
NT
A50
A100
A200
N50
N100
N200
AN100
Control Donor

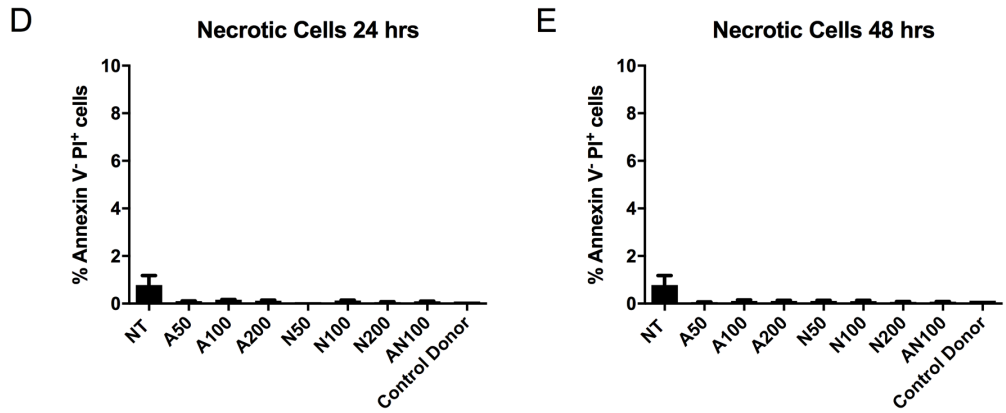
D
Necrotic Cells 24 hrs
% Annexin V- PI+ cells
E
Necrotic Cells 48 hrs
% Annexin V- PI+ cells
NT
A50
A100
A200
N50
N100
N200
AN100
Control Donor

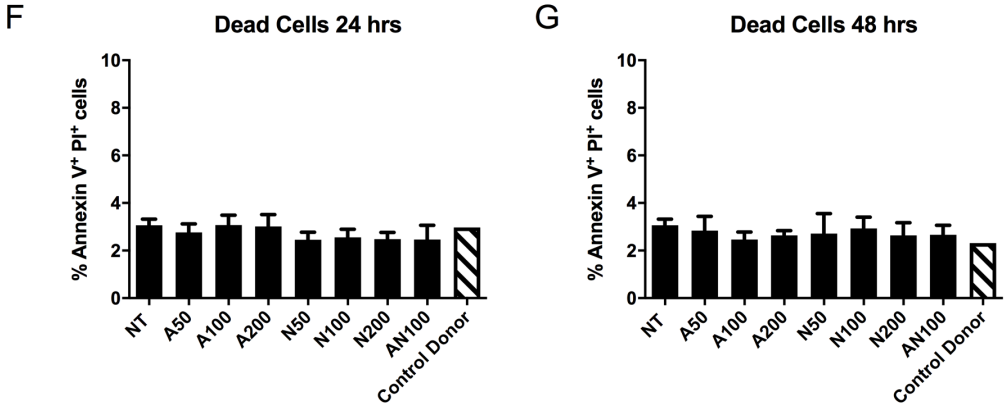
F
Dead Cells 24 hrs
% Annexin V+ PI+ cells
G
Dead Cells 48 hrs
% Annexin V+ PI+ cells
NT
A50
A100
A200
N50
N100
N200
AN100
Control Donor

Figure 16: Amitriptyline and Nortriptyline do not affect PBMC viability: PBMCs isolated from 3 donors were left untreated (NT) or treated with Amitriptyline 50ng (A50), 100 ng (A100) or 200 ng (A200) or Nortriptyline 50 ng (N50), 100 ng (N100) or 200ng (N200), or Amitriptyline 100 ng combined with Nortriptyline 100ng (AN100) at 24 or 48 hours. Following which a cell viability assays using Annexin V and Propidium Iodide staining was carried out by flow cytometry. A control donor (white bars) who was on 25 mg of amitriptyline was also included but was left untreated. Representative dot plots for all treatments (A). Bar charts showing early apoptotic at 24 (B) and 48 hours (C), necrotic at 24 (D) and 48 hours (E) and dead cells at 24 (F) and 48 hours (G). A one-way ANOVA with a Dunnett post-test was used to assess differences across all treatments n=3 donors.

3.4.2 Amitriptyline and Nortriptyline induce significant changes in T cell phenotype

Phenotypic analysis of T cells was carried out following treatment of PBMCs with amitriptyline and nortriptyline. There was no significant change in the frequency of $CD4^+$ T cells when amitriptyline, nortriptyline or a combination of both drugs at 100 ng/ml concentrations were compared to the VC (Figure 17). There were also no significant changes in the frequency of activated $CD69^+$ or naïve ($CD45RA^+$) within the $CD3^+CD4^+$ lymphocyte population compartments following treatment with amitriptyline, nortriptyline or a combination of both drugs compared to the VC group. However, there was a significant decrease in the frequency of $CD27^+$ of the $CD3^+CD4^+$ lymphocyte population following treatment with a combination of both drugs (VC 64.5% versus AN100 39.23%, p=0.027) (Figure 17A). The subsets of the $CD3^+CD4^+$ lymphocyte population according to the Dieli scheme are illustrated in Figure 18. There were no significant changes in the frequency of Naïve ($CD45RA^+CD27^+$) (Figure 18A), effector memory ($CD45RA^-CD27^-$) (Figure 18B) and central memory ($CD45RA^-CD27^+$) (Figure 18C) cells after treatment with amitriptyline, nortriptyline and a combination of both drugs. There was a significant increase in the frequency of terminally differentiated cells ($CD45RA^+CD27^-$) of the $CD3^+CD4^+$ lymphocyte population after a combination of the drugs (VC 6.423% vs AN100 18.07%, p=0.03) but not with amitriptyline or nortriptyline (Figure 18D). The $CD3^+CD8^+$ cells could not be gated according to the Dieli scheme due to the downregulation of the CD8 receptor.

In contrast to $CD4^+$ T cells, there was a significant reduction in the frequency of $CD8^+$ T cell after amitriptyline (A100) (26.4% VC vs 8.181% A100, $p<0.001$), nortriptyline (26.4% VC vs 6.878% N100, $p<0.001$) or treatment with a combination of the two (26.4% VC vs

4.42% AN100, p<0.001) (Figure 17B). There was also a significant reduction in the percentage of naïve $CD8^+$ T cells (%$CD45RA^+$ cells within the $CD3^+CD8^+$ lymphocyte population) after amitriptyline (18.97% VC vs 5.33% A100, p<0.001), nortriptyline (18.97% VC vs 5.94% N100, p<0.001) and a combination of the two (18.97% VC vs 7.61% AN100, p<0.001) (Figure 2B). There was no effect on the percentage of $CD69^+$ cells within the $CD3^+$ $CD8^+$ lymphocyte population, but similar to $CD4^+$ T cells, there was a significant reduction in the expression of $CD27^+$ cells within the $CD3^+CD8^+$ lymphocyte population following treatment with a combination of the drugs (37.8% VC vs 12.27% AN100, p=0.013) (Figure 17B). This data suggests that amitriptyline and nortriptyline may affect $CD8^+$ T cells more profoundly than $CD4^+$ T cells.

Further analysis was performed to investigate if the decrease in frequency of $CD8^+$ T cells resulted in an increased frequency of double-negative T cells (DNT cells) ($CD4^-CD8^-$). There was a significant increase in the expression of DNT cells after amitriptyline (9.11% VC vs 26.48% A100, p=0.02), nortriptyline (9.11% VC vs 38.82% N100, p<0.001) and a combination of both drugs (9.11% VC vs 48.53% AN100, p=0.004) (Figure 19).

While there was no change in the percentage of $CD3^-CD56^+$ cells, there was a significant increase in the frequency of $CD3^+CD56^+$ cells after nortriptyline (1.598% VC vs 5.953% N100, p=0.017) and the drug combination (1.598% VC vs 5.953% AN100, p=0.017) (Figure 18). Interestingly, both amitriptyline and nortriptyline reduced the mean fluorescence intensity of CD4, CD8 and CD56 expression on the cell surface, however these drugs only affected the frequency of $CD8^+$ T cells.

A

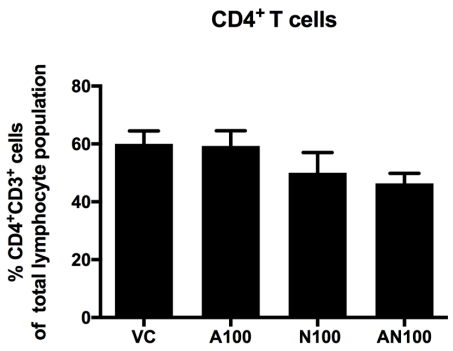
CD4+ T cells
% CD4+CD3+ cells of total lymphocyte population
80
60
40
20
0
VC
A100
N100
AN100

E

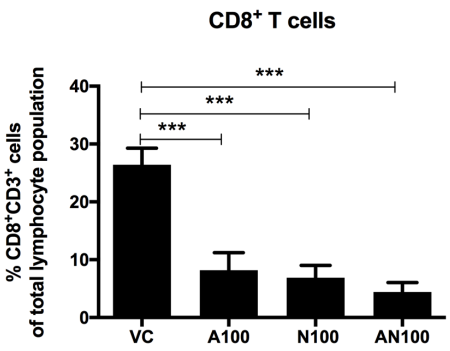
CD8+ T cells
% CD8+CD3+ cells of total lymphocyte population
***
***
***
40
30
20
10
0
VC
A100
N100
AN100

B

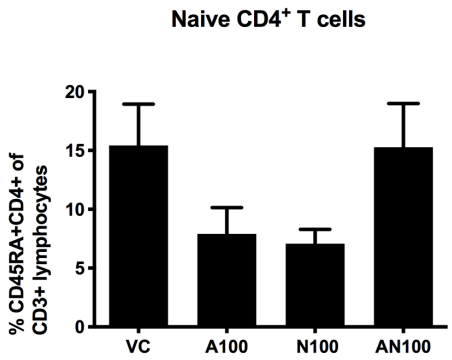
Naive CD4+ T cells
% CD45RA+CD4+ of CD3+ lymphocytes
20
15
10
5
0
VC
A100
N100
AN100

F

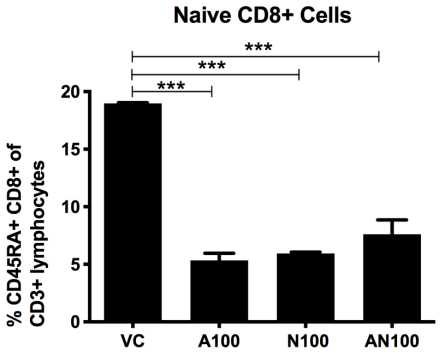
Naive CD8+ Cells
% CD45RA+ CD8+ of CD3+ lymphocytes
***
***
***
20
15
10
5
0
VC
A100
N100
AN100

C

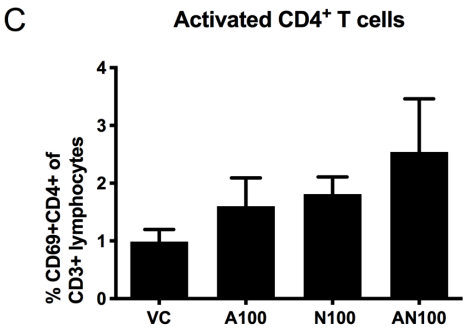
Activated CD4+ T cells
% CD69+CD4+ of CD3+ lymphocytes
4
3
2
1
0
VC
A100
N100
AN100

G

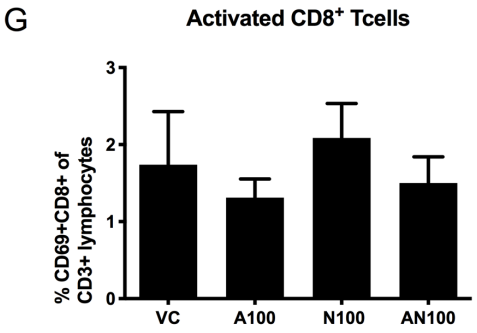
Activated CD8+ Tcells
% CD69+CD8+ of CD3+ lymphocytes
3
2
1
0
VC
A100
N100
AN100

D

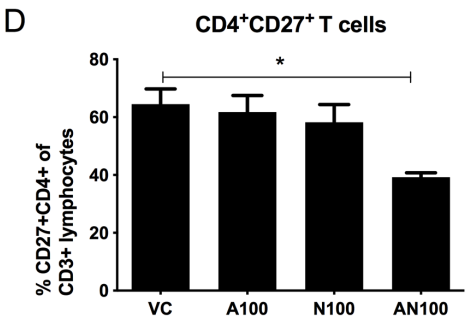
CD4+CD27+ T cells
% CD27+CD4+ of CD3+ lymphocytes
*
80
60
40
20
0
VC
A100
N100
AN100

H

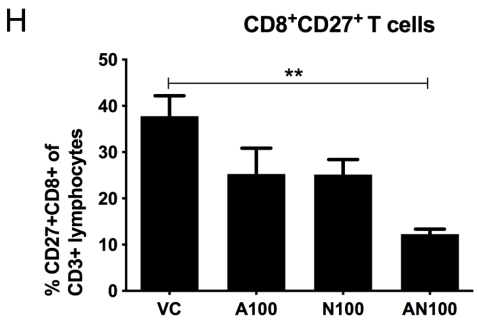
CD8+CD27+ T cells
% CD27+CD8+ of CD3+ lymphocytes
**
50
40
30
20
10
0
VC
A100
N100
AN100

Figure 17: Amitriptyline and Nortriptyline affect $CD8^+$ T cell phenotype: PBMCs were isolated from 6 healthy donors and treated with Amitriptyline 100 ng (A100), Nortriptyline 100 ng (N100) and a combination of the two (AN100) or vehicle control (VC) for 24 hours. Cells were stained for CD3, CD4, CD8, CD45RA, CD69 and CD27 and assessed by flow cytometry. Bar charts of $CD4^+$ T cells and subsets within the $CD3^+CD4^+$ lymphocyte population (A-D). Bar charts of $CD8^+$ T cells and subsets within the $CD3^+CD8^+$ lymphocyte population (E-F). A one-way ANOVA with a Dunnett test was used to assess differences across all treatments. * $p<0.05$, ** $p<0.01$ and *** $p<0.001$.

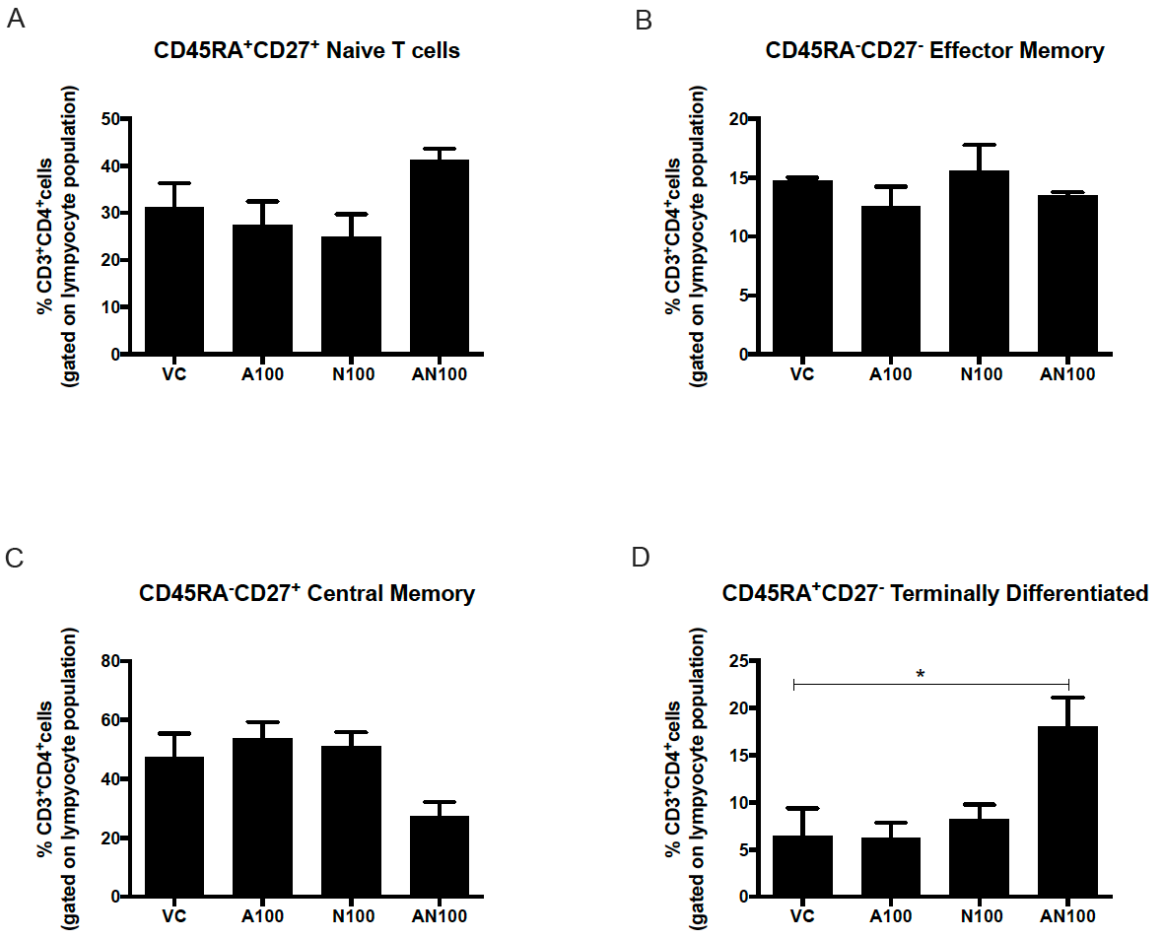

Figure 18: Subsets of different phenotypes of gated $CD3^+CD4^+$ lymphocyte population according to the Dieli scheme: There were no significant changes in the frequency of Naïve ($CD45RA^+CD27^+$) (Figure 18A), effector memory ($CD45RA^-CD27^-$) (Figure 18B) and central memory ($CD45RA^-CD27^+$) (Figure 18C) after treatment with amitriptyline, nortriptyline and a combination of both drugs. There was a significant increase in the frequency of terminally differentiated cells ($CD45RA^+CD27^-$) of the $CD3^+CD4^+$ lymphocyte population after a combination of the drugs (VC 6.423% vs AN100 18.07%, $p=0.03$) but not with amitriptyline or nortriptyline (Figure 18D). A one-way ANOVA with a Dunnett test was used to assess differences across all treatments. * $p<0.05$

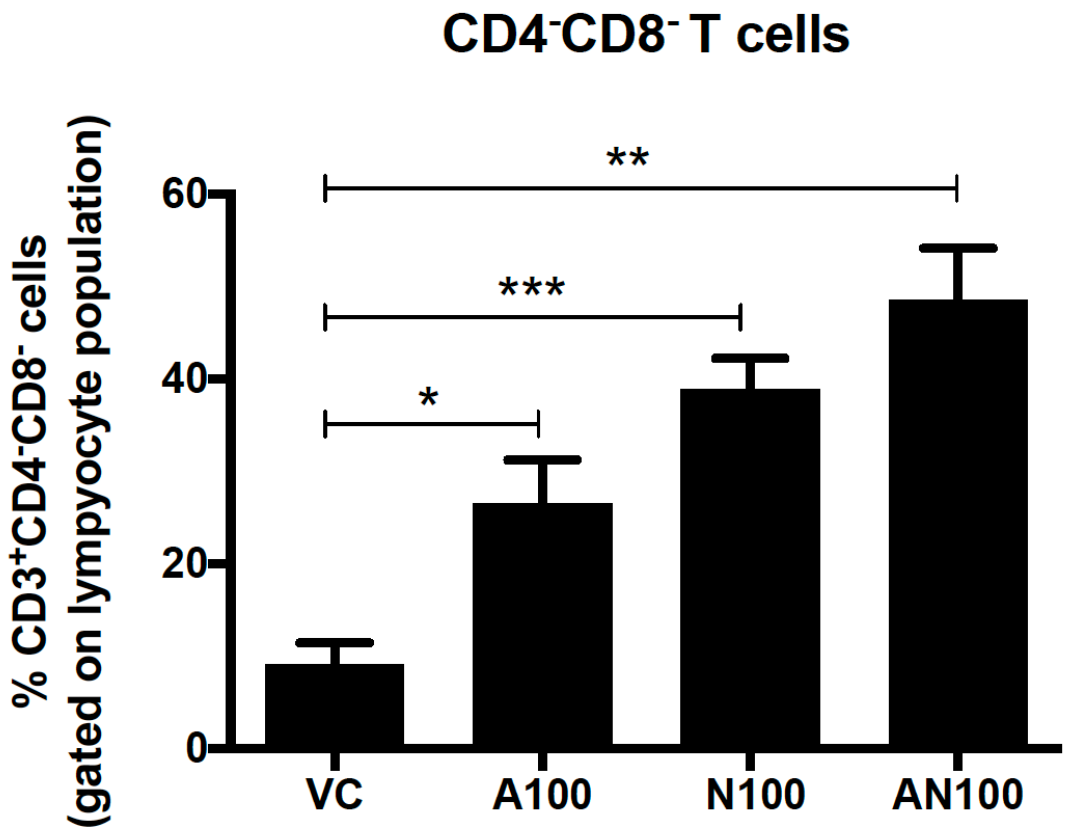

Figure 19: **Amitriptyline and Nortriptyline increased the frequency of double negative T cells (DNT cells) ($CD4^-CD8^-$):** There was a significant increases in the expression of DNT cells after amitriptyline (9.11% VC vs 26.48% A100, p=0.02), nortriptyline (9.11% VC vs 38.82% N100, p<0.001) and a combination of both drugs (9.11% VC vs 48.53% AN100, p=0.004). A one-way ANOVA with a Dunnett test was used to assess differences across all treatments. *p<0.05.

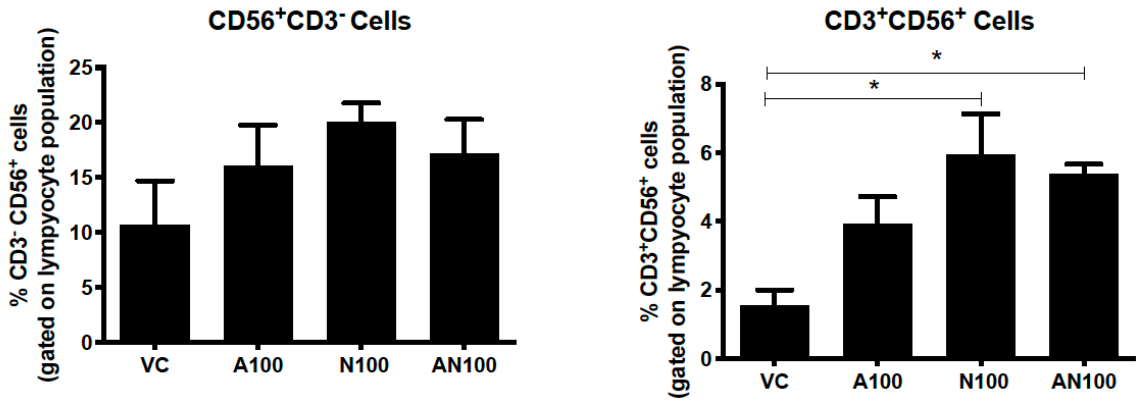

Figure 20: Nortriptyline and drug combination increased the frequency of $CD3^+CD56^+$ cells: PBMCs were isolated from 6 healthy donors and treated with Amitriptyline 100 ng (A100), Nortriptyline 100 ng (N100), a combination of the two (AN100) or vehicle control (VC) for 24 hours. Cells were stained with CD3 and CD56 and assessed by flow cytometry. $CD3^-CD56^+$ cells illustrated in (A) and $CD3^+CD56^+$cells in (B). A one-way ANOVA with a Dunnett test was used to assess differences across all treatments. *$p<0.05$.

3.4.3 Intracellular cytokine expression by T cells is altered following amitriptyline and nortriptyline treatment

Significantly lower frequencies of IFN-γ producing $CD8^+$ cells within the $CD3^+$ lymphocyte population were observed in cells treated with amitriptyline (6.54% VC vs 1.36% A100, p=0.033), nortriptyline (6.54% VC vs 1.42% N100, p=0.033) and a combination of both (6.54% VC vs 1.64% AN100, p=0.033) (Figure 21), but no change was observed in IFN-γ expression by $CD4^+$ cells within the $CD3^+$ lymphocyte population. There was also a significantly decreased frequency of IL-17-producing $CD4^+$ cells within the $CD3^+$ lymphocyte population (1.253% VC v 0.134% A100, $p<0.05$) and $CD8^+$ cells within the $CD3^+$ lymphocyte population (1.18% VC v 0.18% A100, $p<0.05$) following amitriptyline treatment (Figure 21). There was no difference in the expression of IL-4 or IL-10 (Figure 21).

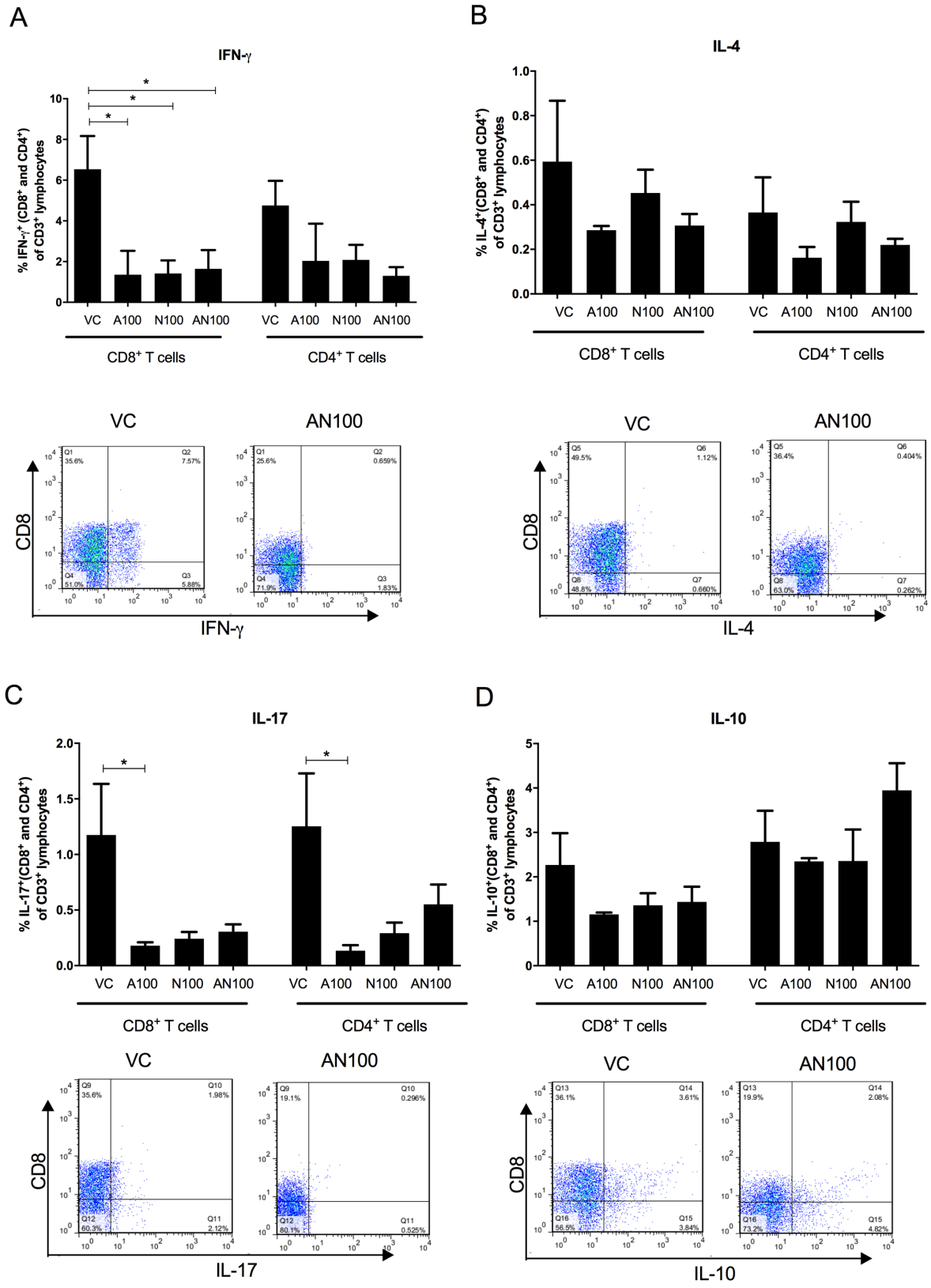

Figure 21: Amitriptyline and nortriptyline significantly reduced the frequency of IFN-γ and IL-17 in T cells: PBMCs were isolated from 6 healthy donors and treated with Amitriptyline 100 ng (A100), Nortriptyline 100 ng (N100), a combination of the two (AN100) or vehicle control (VC) for 24 hours. Cells were stained with CD3, CD8, IFN- γ, IL-4, IL-17 and IL-10 and assessed by flow cytometry. Bar charts show cumulative data

for 6 donors and the representative dot plots show VC and AN100 treated PBMCs. IFN-γ (A), IL-4 (B), IL-17 (C) and IL-10 (D) producing $CD8^+$ and $CD4^+$ cells of the gated $CD3^+$ lymphocytes are illustrated. A one way ANOVA with a Dunnett test was used to assess differences across all treatments.*$p<0.05$.

3.4.4 Supernatant analysis of neurotrophins, chemokines and cytokines after amitriptyline and nortriptyline treatment

There was no significant change in the concentration of neurotrophins, classical T_H2-type cytokines or growth factors (Figure 22). Nerve Growth Factor (NGF) was undetectable in all samples. Amitriptyline and nortriptyline had no effect on the release of a range of chemokines by PBMCs (Figure 23). There was however a significant increase in the concentration of IL-16 with amitriptyline (57 pg/ml VC vs 812.4 pg/ml A100 p=<0.001), nortriptyline (852 pg/ml N100, p<0.0001) and a combination of the two (789 pg/ml AN100, p<0.0001) (Figure 24). There was also a significant decrease in the concentration of TNF-β with amitriptyline (1 pg/ml VC v 0.2 pg/ml A100, p=0.032), nortriptyline (0.2 pg/ml N100, p=0.032) and the combination (0.2 pg/ml AN100, p=0.032) (Figure 24).

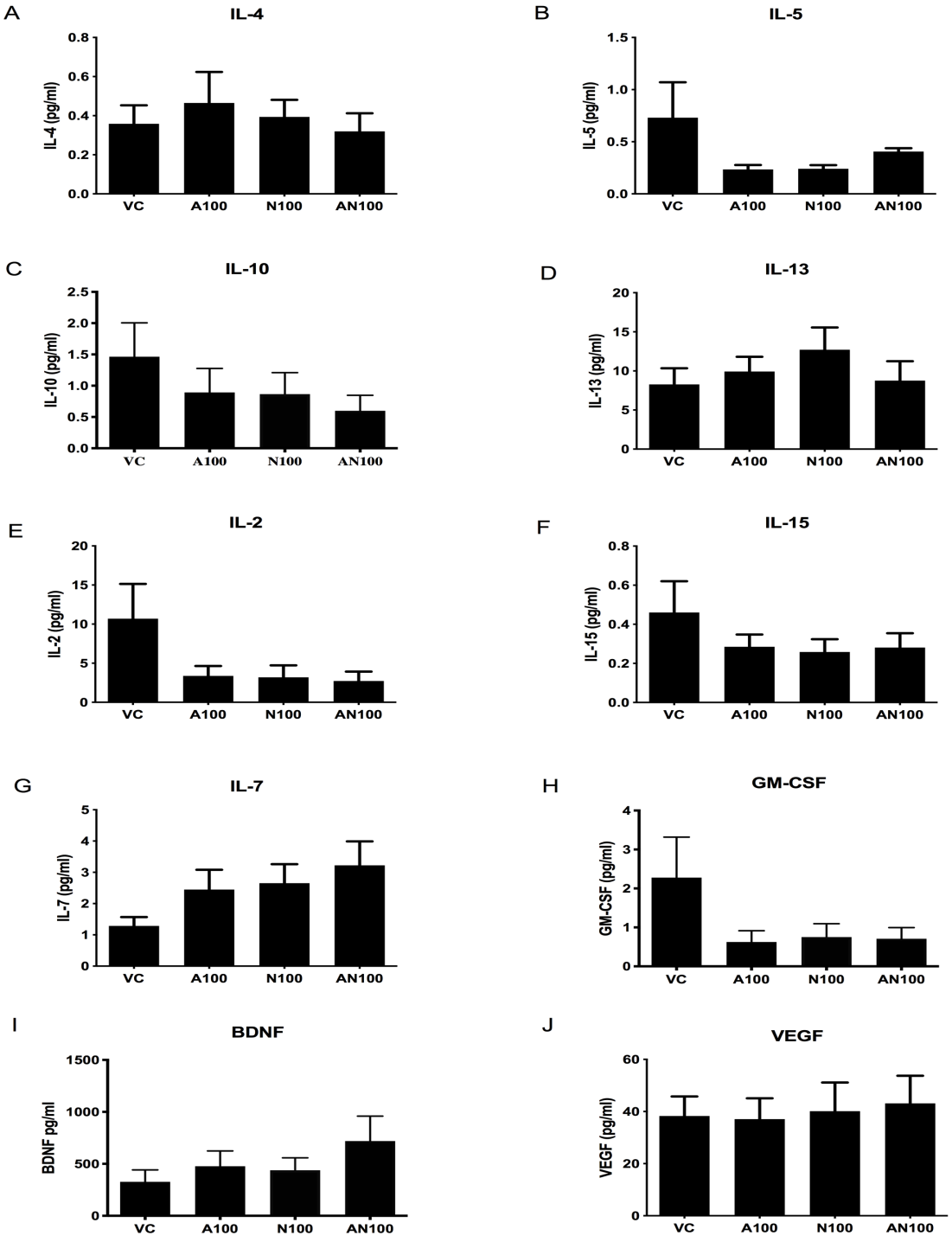

Figure 22: T_H2 type cytokines, growth factors and neurotrophin secretion by PBMCs is not affected by either amitriptyline or nortriptyline treatment. PBMCs were isolated from 6 healthy donors and treated with Amitriptyline 100 ng (A100), Nortriptyline 100 ng (N100), a combination of the two (AN100) or vehicle control (VC) for 24 hours. The supernatants were removed and the concentrations of specific analytes were determined by ELISA. The following are illustrated: IL-4 (A), IL-5 (B), IL-10 (C), IL-13 (D), IL-2 (E), IL-15 (F), Il-7 (G), GM-CSF (H), Brain Derived Neurotrophic factor (BDNF) (I) and Vascular Endothelia Growth Factor (VEGF) (J). A one-way ANOVA with a Dunnett test was used to assess differences across all treatments.

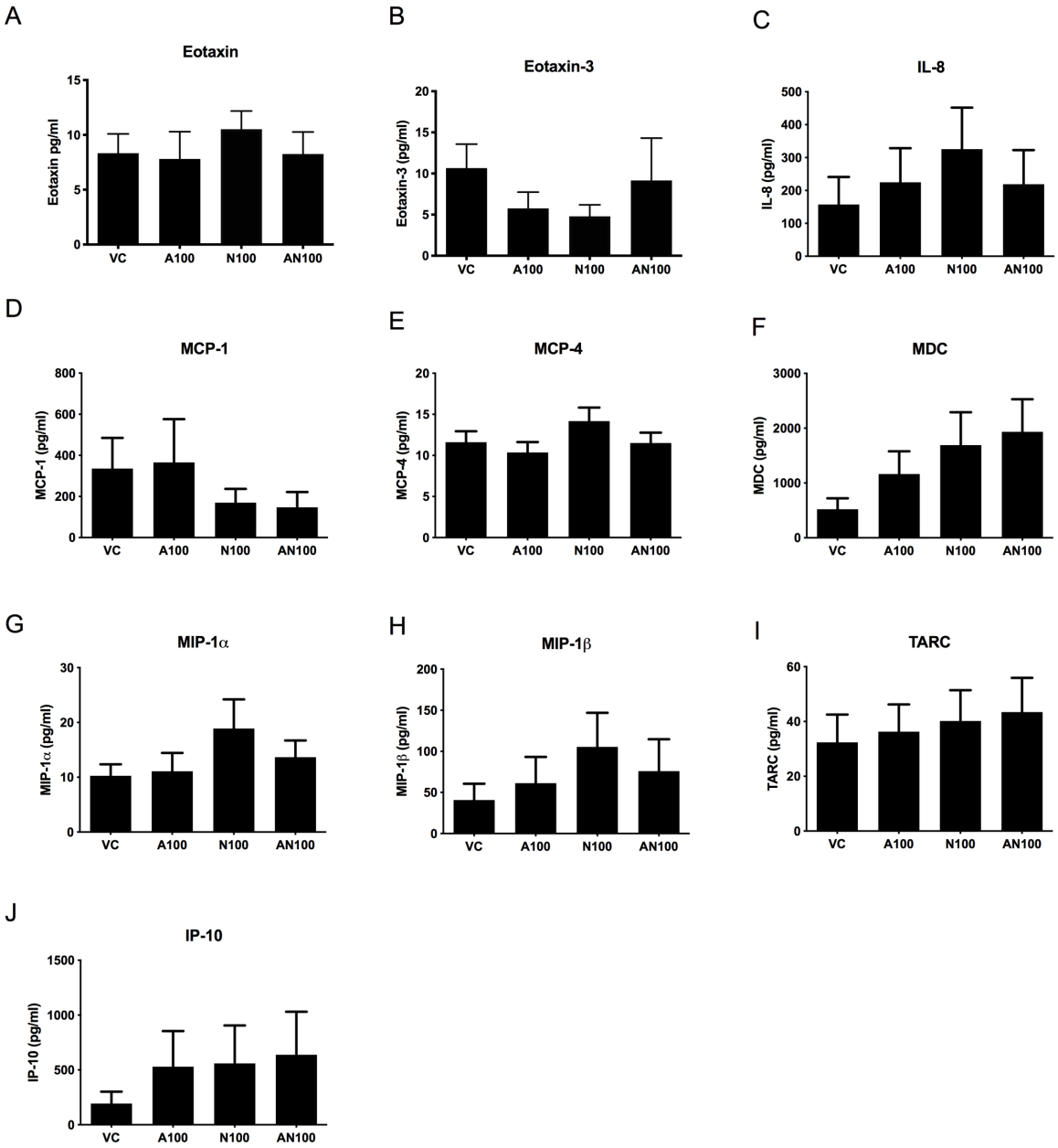

Figure 23: Chemokine secretion by PBMCs is not affected by either amitriptyline or nortriptyline treatment: PBMCs were isolated from 6 healthy donors and treated with Amitriptyline 100 ng (A100), Nortriptyline 100 ng (N100), a combination of the two (AN100) or vehicle control (VC) for 24 hours. The supernatants were removed and the concentration of chemokines were determined by ELISA. The following chemokines are illustrated: Eotaxin (A), Eotaxin-3 (B), IL-8 (C), Monocyte chemoattractant protein-1 (MCP-1) (D), Monocyte chemoattractant protein-4 (MCP-4) (E), Macrophage-derived chemokine (MDC) (F), Macrophage inflammatory protein-1α (MIP-1α) (G), MIP-1β (H), Thymus and activation regulated chemokine (TARC) (I) and Interferon gamma-induced protein 10 (IP-10) (J). A one way ANOVA with a Dunnett test was used to assess differences across all treatments.

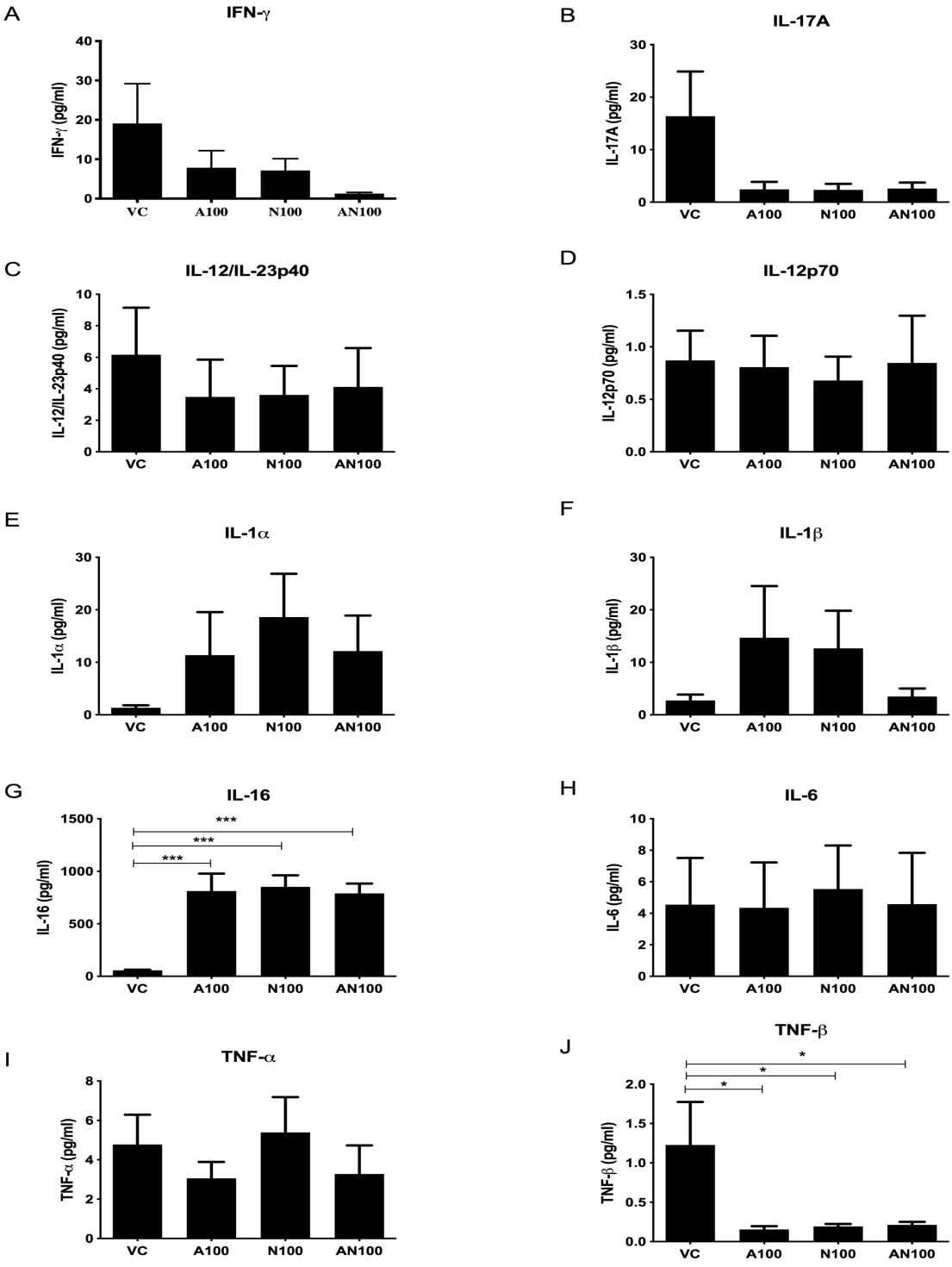

Figure 24: IL-16 and TNF-β concentrations are significantly affected by amitriptyline or nortriptyline treatment: PBMCs were isolated from 6 healthy donors and treated with Amitriptyline 100 ng (A100), Nortriptyline 100 ng (N100), a combination of the two (AN100) or vehicle control for 24 hours. The supernatant was removed and the concentrations of cytokines were determined by ELISA. The following cytokines are illustrated: IFN-γ (A), IL-17A (B), IL-12/IL-23p40 (C), IL-12p70 (D), IL-1α (E), IL-1β (F), IL-16 (G), IL-6 (H), TNF-α (I), TNF-β (J). A one-way ANOVA with a Dunnett test was used to assess differences across all treatments. *p<0.05, ***p<0.001.

3.5 Discussion:

The effect of amitriptyline on T cell activation and cytokine expression was examined in this study, to investigate potential mechanisms for off-label utilisation including neuropathic pain. We have demonstrated dynamic changes in T cell phenotype and cytokine expression. This builds upon the current evidence that amitriptyline has the potential to modulate immune cells and the production of neuropeptides (247, 248, 301, 305, 367). It also contributes to the hypothesis that immune mechanisms are potentially contributory to the pathophysiology of many conditions where amitriptyline is employed with clinical benefit.

Based on reported safe therapeutic levels a range of different drug concentrations were chosen to assess toxicity for PBMCs (229, 231, 235). Viability of PBMCs was not affected by any of the drug concentrations or incubation times tested, suggesting that up to 200 ng/ml of drug is not toxic to circulating immune cells. Peak plasma concentrations of the drug are variable, an old study for depression found levels of 60-200 ng/ml were needed to be clinically effective (229). More recent studies in healthy volunteers on an initial dosing of 25 mg demonstrated low plasma concentrations of 26.8 ng/ml (231). Amitriptyline is highly protein-bound in plasma and tissues however, this leads to an accumulation over time leading to higher tissue concentrations from initial dosing (231). A study using the tricyclic trimipramine in mice illustrated a 5-20 fold increase in concentration in different tissues compared to blood (234, 366). As most chronic pain patients are on 25-75 mg amitriptyline, 100 ng/ml dose was chosen for this study, to reflect the upper limits of plasma concentrations that PBMC would be exposed to *in vivo* (45).

Interestingly, our data shows that amitriptyline and its active metabolite nortriptyline modulate different subsets of $CD8^+$ cells and $CD4^+$ cells but have the most profound impact on $CD8^+$ T cells. These drugs may have different effects in specific tissues, as effector and memory cells are more prevalent in CSF than blood, where naïve subsets are more frequent (291). There is still much debate over whether the generator of chronic neuropathic pain is a central, peripheral or combined phenomenon (368). The percentage of cells expressing CD8 was significantly lower following treatment suggesting that the drug treatment is capable of downregulating the CD8 receptor. The biological implications of this require further study to determine if these cells remain functional or if their numbers are diminished.

$CD8^+$ cells have multiple functions including the attenuation of $CD4^+$ clonal expansion, the secretion of anti-inflammatory cytokine IL-10 and contributing to downregulation of Th17 cells (369, 370). The $CD8^+$ receptor holds the target cell close during antigen specific activation and aids in activation of transcription factors which affect expression of certain genes (370-372). Down regulation of $CD8^+$ is observed when T cells are stimulated by pathogens in vivo (373); this appears to be transient peaking at seven days (374). The effect of downregulation of $CD8^+$ expression in this study by amitriptyline increased the presence of double negative T cells (DNTs). DNTs have distinct cytokine expression patterns based on their environment and despite often being termed pathological in autoimmune diseases, they may carry out many important mechanisms in host defence (375, 376). Interestingly DNTs frequently express characterisation of an exhausted terminally differentiated phenotype and express the inhibitory molecule Programme Cell Death Protein 1 (PD-1) which is associated with suppression of nociceptive neural activity (377). In terms of cytokine expression DNTs spontaneously secrete IL-10 and fail to express Il-2; although we saw a trend in the reduction of IL-2 levels in our supernatant, any correlation should be taken with caution (376).

$CD27^+$ binds to molecules expressed by antigen presenting cells including CD70 which is an important modulator of T cell function (371). $CD27^+$ T cells frequently produce IL-2 and IFN-γ. As the frequency of $CD27^+$ expression was lower in both $CD4^+$ and $CD8^+$ T cell compartments after the combined drug treatment, this may at least in part explain the reduction in these cytokines following drug treatment (378).

T cells are highly influential in the adaptive immune response and implicated in the chronicity of neuropathic pain and multiple sclerosis (81, 128-130, 132, 133, 135, 210, 370). An anti-inflammatory shift has also been observed in patients with chronic neuropathic pain with a T_H17/Treg imbalance [increased regulatory T cells (T regs) and decreased T_H17 cells] (199). Whether associated or causative, there appears to be a loss of equilibrium in T cells in patients with neuroinflammatory disorders (129, 132, 218). $CD8^+$ T cells are altered in patients with autoimmune arthritis where inflammatory environments attenuate their susceptibility to regulation (210). Effector $CD8^+$ T cells in autoimmune diseases also have decreased ability to eliminate diseased cells and have altered cytokine

production (369, 370). The importance of T cells in repair and homeostasis is also emphasised by T cell deficiency, being associated with increased neural damage (379). $CD8^+$ T cells have also been implicated and mediate cytotoxicity to Schwann cells and play a role in the development of peripheral neuropathy with high glucose levels in diabetic neuropathy (133). Although amitriptyline is utilised to treat the symptoms related to all of these pathologies the exact causation of immune modulation remains unclear. There is limited evidence available examining the phenotype of T cells and their true effector functions in chronic neuropathic pain (371, 378). Pre-clinical models to date have provided inconsistent results regarding the role T cells in initiation, maintenance and resolution of neuropathic pain (218). It is likely that the expression and effector function of T cells likely has an influence over pain perception through communication with other immune cells, glia and neuronal pathways (81, 128-130, 132).

The significant increase in relative $CD3^+CD56^+$ cell frequencies, although small, may be relevant. Previous *in vitro* work has demonstrated downregulation of $CD8^+$ and the inducibility of $CD56^+$ cells in the presence of particular cytokines, including IL-2 (380). This same pattern is unlikely however as we observed a trend in the reduction of IL-2 in the supernatant.

We have demonstrated amitriptyline and nortriptyline modulate T cells and other immune cells by affecting cytokine production. There were clear trends observed in many cytokines measured including a significant increase in IL-16 and a significant decrease in TNF-β. Interestingly, there was significantly lower expression of IFN-γ by $CD8^+$ T cells and IL-17 by both $CD4^+$ and $CD8^+$ T cells, but no effect on IL-4 and IL-10 which suggests that these drugs are capable of reducing inflammatory T cells but do not affect T cells with a more anti-inflammatory phenotype. A reduction of IFN-γ in T cells has previously been demonstrated in two *in vitro* studies with tricyclic antidepressants (305, 366). IFN-γ activates macrophages and stimulates cytolytic activity of Natural Killer (NK) cells. IFN-γ has also been implicated in the pathology of neuropathic pain (96, 364), depression (381) and other neuroinflammatory conditions (168). Specifically, in one preclinical study mice lacking IFN-γ had less mechanical sensitivity after sciatic nerve ligation potentially suggesting it carries out a function in immune mediated pain (81). Levels of IL-17A were significantly higher compared to controls in 58 fibromyalgia patients and this correlated with levels of IL-2 (382). Although not significant, levels of IL-2 reduced after all

combinations of the drugs. Other studies have also suggested IL-17A levels correlate with pain levels, depression and anxiety which amitriptyline is frequently used to treat (382). Pre-clinical models have also suggested that IL-17 produced by glia suppresses inhibitory synaptic transmission and drives neuropathic pain (383).

IL-16 exerts its function by binding to the $CD4^+$ receptor where it can exert its signalling pathways (384). IL-16 is produced by T cells, B cells, monocytes, macrophages, dendritic cells and mast cells and can selectively regulate migration of $CD4^+$ cells, expression of CD25 and orchestrate dendritic cell/T cell cooperation. A significant reduction in circulating IL-16 has been observed in patients with chronic fatigue syndrome (CFE) and myalgic encephalomyelitis (ME) compared to controls (365). Profound fatigue, poor sleep, exercise malaise, cognitive dysfunction and chronic pain are symptoms expressed by patients with CFE and ME. These symptoms are also frequently reported in patients with chronic neuropathic pain and are highly prevalent in fibromyalgia (237, 385). Amitriptyline has been utilised to treat the symptoms of both of these conditions thus potentially providing a key mechanism for amitriptyline (237, 385, 386).

TNF-β (lymphotoxin-alpha) levels also significantly reduced following treatment with amitriptyline and is largely produced by lymphocytes (387). Although there is a paucity of evidence in its role in neuropathic pain in humans, there is evidence to suggest that TNF-β may play a role in migraine in specific populations (387). Amitriptyline is prescribed for migraine prophylaxis but is only efficacious in a select group of patients (49, 164). This adds to the available evidence on the potential anti-inflammatory mechanisms of amitriptyline for migraine prophylaxis (49, 164, 387).

There were some clear trends in the altered expression of multiple cytokines and chemokines in our study. The relationship between altered neuropeptide/cytokine expression in chronic pain patients and their normalisation in response to treatment may be too simplistic. Despite this, there is growing evidence that many successful treatments to neuropathic pain generate neuro-immunomodulatory changes *in vivo* (53). There still however remains a gulf in our understanding into the role of how immune cells, glia and neurons interact with each other to generate chronic pain in humans (3).

3.6 Conclusion:

This study provides *in vitro* evidence that amitriptyline modulates immune function via T cell and cytokine regulatory pathways. Neuroimmune aetiologies have been postulated for

the clinical conditions for which amitriptyline is prescribed therefore providing mechanistic information regarding amitriptyline's mechanism of action. We have demonstrated that amitriptyline can attenuate the T_H1/T_H17 immune response and modify immunomodulatory pathways *in vitro*. Amitriptyline has been in use for decades and there is no clear demonstrable morbidity related to immune activity (50). This study supports the clinical use of amitriptyline and the further exploration of the *in vivo* effects of amitriptyline in patients with notoriously difficult to treat conditions in particular chronic neuropathic pain and fibromyalgia.

Chapter 4:

Examination and Characterisation of Burst Spinal Cord Stimulation on Cerebrospinal Fluid Cellular and Protein Constituents in Patient Responders with Chronic Neuropathic Pain- A Pilot Study (321)

Highlights:

- Burst stimulation for chronic pain modulates the proteome of spinal fluid *in vivo*
- Proteins in synapse assembly are altered suggesting a potential mechanism of action
- Immune effectors were the most upregulated proteins after Burst stimulation
- PRL, SST and NUCB2 showed decreased expression suggesting supraspinal effects

Presented as E-poster at EFIC, Valencia, Spain, 2019.

Published in 'Journal of Neuroimmunology' (321)

https://doi.org/10.1016/j.jneuroim.2020.577249

4.1 Abstract

Introduction: Patients with neuropathic pain have altered proteomic and neuropeptide constituents in cerebrospinal fluid (CSF) compared to controls. Tonic spinal cord stimulation (SCS) has demonstrated differential expression of neuropeptides in CSF before and after treatment suggesting potential mechanisms of action. Burst-SCS is an evidence-based paraesthesia free waveform utilised for neuropathic pain with a potentially different mechanistic action to tonic SCS. This study examines the dynamic biological changes of CSF at a cellular and proteome level after Burst-SCS.

Methods: Patients with neuropathic pain selected for SCS had CSF sampled prior to implant of SCS and following 8 weeks of continuous Burst-SCS. Baseline and 8-week pain scores with demographics were recorded. T cell frequencies were analysed by flow cytometry, proteome analysis was performed using mass spectrometry and secreted cytokines, chemokines and neurotrophins were measured by enzyme-linked immunosorbent assay (ELISA).

Results: 4 patients (2 females, 2 males) with a mean age of 51 years (+/-SEM 2.74, SD 5.48) achieved a reduction in pain of >50% following 8 weeks of Burst-SCS. Analysis of the CSF proteome indicated a significant alteration in protein expression most related to synapse assembly and immune regulators. There was significantly lower expression of the proteins: growth hormone A1 (PRL), somatostatin (SST), nucleobindin-2 (NUCB2), Calbindin (CALB1), acyl-CoA binding protein (DBI), proSAAS (PCSK1N), endothelin-3 (END3) and cholecystokinin (CCK) after Burst-SCS. The concentrations of secreted chemokines and cytokines and the frequencies of T cells were not significantly changed following Burst-SCS.

Conclusion: This study characterised the alteration in the CSF proteome in response to burst SCS *in vivo*. Functional analysis indicated that the alterations in the CSF proteome is predominately linked to synapse assembly and immune effectors. Individual protein analysis also suggests potential supraspinal mechanisms.

4.2 Introduction

Burst-DR Spinal Cord Stimulation (SCS) (Abbott, Plano, TX), first introduced by De Ridder, is a paraesthesia-free based waveform utilised in patients with chronic neuropathic pain refractory to medical therapy (8). Burst-SCS has demonstrated non-inferiority to tonic, paraesthesia-based-stimulation in a randomised controlled study in patients with Failed Back Surgery Syndrome (FBSS) (68). Burst-SCS may also be considered when tonic stimulation has intolerable side effects or fails to achieve efficacy (263, 388).

In Burst-SCS, 5 pulses are delivered per burst at a frequency of 500 Hz, with 40 bursts applied per second (10, 265). Pre-clinical and in vitro evidence has portrayed burst neuronal firing (BNF) in sensory transmission as relaying stimuli dependent information. BNF can also improve signal to noise ratio and can increase the reliability of synaptic transmission and efficacy (277). Behaviourally relevant stimulus features may also be involved with BNF and there is evidence to suggest Burst-SCS activates the medial spinothalamic tract and may improve the behavioural and emotional component of chronic neuropathic pain in humans (10, 277, 278). The full extent of Burst-SCS in modulating the sensory information in chronic pain however remains to be defined.

There is growing evidence that the mechanism of action of Spinal Cord Stimulation (SCS) is not dependent solely on neuronal discharge but also on alterations in the Central Nervous System (CNS) cellular function (122, 189, 213, 257, 269, 272, 273, 279). The concept of micro-dosing, now utilised with Burst-SCS, where there is a prolonged period between stimulation doses may also indicate mechanisms beyond neuronal discharge (389). The syncytium of neuronal cells in the spinal cord where SCS is applied for back and leg pain contains predominantly glial cells of a ratio ranging from 11-13:1 compared to neurons (390). BNF has elicited differential effects in neuronal-glia communications in pre-clinical studies further enhancing a wider mechanistic profile (391-393). There is also increasing evidence that chronic neuropathic pain is also not solely related to neuronal pathology but also includes pathological neuronal-glia communications (141, 142, 309, 394).

Examination of CSF has been used in many conditions including chronic neuropathic pain to help determine pathogenesis and mechanisms of treatment (122, 168, 188, 212, 213). We thus carried out a study to examine the effect of Burst-SCS on patients with a diagnosis of neuropathic pain. Examination and characterisation of proteomic and cellular profiles before and after Burst-SCS will help to develop our understanding of the mechanism of action of this modality of spinal cord stimulation and provide much needed information on the pathophysiology of neuropathic pain *in vivo* (189, 395). Neuropathic pain is recognised as the type of chronic pain which has proven most resistant to current pharmacological therapies as a result of the pathological alterations in CNS physiology (45). At present the exact mechanisms underpinning this resistance to treatment remain unclear (23, 368). Although there are no high quality sham/placebo controlled trials, electrical neuromodulation has demonstrated a significant improvement in multidimensional outcomes for chronic neuropathic pain patients (66, 68, 268, 396).

4.2.1 Aims

The aim of this chapter was to explore mechanisms of action of Burst-SCS for the treatment of neuropathic pain by examining the cellular, neuropeptide and proteomic constituents of CSF before and after Burst-SCS.

4.3 Methods

4.3.1 Study design

This was an interventional prospective study performed in St James's Hospital, Dublin 8, Ireland; a tertiary referral centre for patients with chronic pain. Ethical approval was obtained from the St James's and AMNCH Research Ethics Committee, Dublin, Ireland. The study was registered online at http://www.isrctn.com/ISRCTN70120536. Patients were offered inclusion following an outpatient pain clinic assessment to determine whether the patient met the inclusion/exclusion criteria.

Inclusion criteria included (i) patients must be aged between 20 – 65 years, (ii) patients must present with neuropathic pain (iii) patients must have been approved by the Department of Pain Medicine for spinal cord stimulation, (iv) patients must have had an MRI of their spine and finally (v) patients must have achieved a reduction in Numerical Rating Pain score (NRS) of 50% after eight weeks of Burst-SCS. This is the standard method to measure if a patient is classified as a responder in the majority of studies utilising electrical neuromodulation (66, 68, 268, 396).

Exclusion criteria included (i) patient refusal, (ii) if the patient was receiving anticoagulant medication, (iii) if the patient was shown to have an ongoing infection, (iv) if the patient was pregnant or breastfeeding, (v) if the patient had previously had a stroke, (vi) if the patient has a psychiatric history, (vii) if the patient has a cognitive impairment, and finally (viii) if the patient is currently medicated with biologic medication, anti-inflammatory medication or immunosuppressive therapy.

All patients were given an information leaflet about inclusion in the study as per ethics committee. All patients provided a signed a consent form in agreement with the Hospital ethics committee's requirements for study inclusion. Additionally, signed consent forms were required for the lumbar punctures for CSF sampling. Patients were instructed not to reduce their medications until after completion of the study.

4.3.2 CSF Sampling

The baseline CSF sampling occurred between 13:00-14:00 with the patients required to fast for 13-14 hours prior to implant of the SCS device. Under strict asepsis and AAGBI guidelines (319), CSF was obtained between the fourth and fifth lumbar vertebra using Ultrasound or Fluoroscopy. Prior to performing the lumbar puncture (LP), 2-3ml of Lidocaine (1%) was allowed to infiltrate the skin at the site to provide local analgesia. LP was performed with an introducer and 25 Gauge Whittacre needle (B braun®) until resistance entering the dura was felt. The CSF was collected in cryovials for subsequent ELISA and mass spectrometry. The CSF sample intended for flow cytometric analysis was stored in a Transfix/EDTA tube (CaltagMedisystems, Buckingham, UK). The acquired CSF samples were visually inspected for blood contamination. To ensure there was no blood contamination the proteomics aliquots were centrifuged for 10 minutes at 2000 g at 4^{o}C and the supernatant was transferred to a new tube. The Transfix tube was placed in storage at 4^{o}C and the other tubes were immediately frozen at -20 degrees Celsius. A second consented LP sample was obtained in the same manner 8 weeks after the implantation of the SCS.

4.3.3 Pain Measurement

Each patient completed an average 24-hour numerical rating score (NRS) (320) and a Douleur Neuropathique score (DN4) (41) by the investigating physician prior to obtaining the initial CSF sample. The NRS and DN4 assessment was repeated following SCS treatment for 8 weeks. The patients were instructed to remain on their current medications until the second CSF sample was taken. Positive responders were deemed as those who reported a >50% reduction in pain in the NRS questionnaire after 8 weeks of Burst-SCS which is frequently utilised as a responder to therapy in SCS trials (68, 268, 396).

4.3.4 Intervention

Patients were implanted with leads in the epidural space with paraesthesia mapping to ensure the stimulation was covering the affected area of pain. There was no trial period of stimulation and the implantable programme generator (IPG) was placed in the buttock after intra-operative stimulation (397). All of the patients implanted devices were programmed

the day after surgery with a Burst-SCS protocol which was implemented for 8 weeks until the second pain NRS assessment was performed and the second CSF sample was obtained via LP.

4.3.5 Quantification of T cells in CSF:

After collection, samples were stored at 4°C for no longer than 72 hours in TransFix/EDTA CSF Sample Storage Tubes (Caltag Medsystems Ltd, Buckingham, UK). Samples were brought to room temperature and washed in phosphate buffered saline (PBS) solution was added to each tube and the samples were centrifuged at 1500 rpm for 3 minutes. The supernatant was discarded and the Transfix tube vortexed. The pellet in the Transfix tube was re-suspended in 200µl of PBS and stained with fluorochrome-conjugated monoclonal antibodies (mAbs) specific for human surface markers (CD45-APC, CD3-APC-Vio770, CD8-PerCP, CD69-PE, CD45RA-VioGreen, CD27-VioBright FITC) obtained from Miltenyi Biotec (Germany). incubated in the dark for 30 minutes at 4°C. 2mls of PBS were added to each tube and centrifuged at 1500 rpm for 3 minutes., then washed in PBS. Due to the precious nature of the CSF samples and the lower number of cells within each CSF sample, flow cytometry voltage and compensation settings were optimised for this lymphocyte antibody panel using peripheral blood lymphocytes. Patient-matched unstained CSF samples were used as a control for each experiment. Data was acquired using a CyAn™ ADP Analyzer (Beckman Coulter) and Summit v4.1 and analysed using FlowJo v7.6.1 (Tree Star Inc.). An example of the gating method used is demonstrated in **Figure 25**. For every sample, Forward Scatter (FSC) v Side Scatter (SSC) dot plots were used to gate on lymphocytes based on size and granularity **(Figure 25A)**, followed by gating on cells expressing the lymphocyte common antigen CD45 **(Figure 25B)**. All $CD45^+$ cells expressing CD3 were gated to identify the total T cell population **(Figure 25C)**. Subsequent gating within this $CD3^+CD45^+$ population facilitated the identification of $CD8^+$ T cells, $CD69^+$ T cells and the 4 different T cell memory subsets; naive, central memory, effector memory and terminally differentiated, based on CD45RA and CD27 expression **(Figure 25D)**.

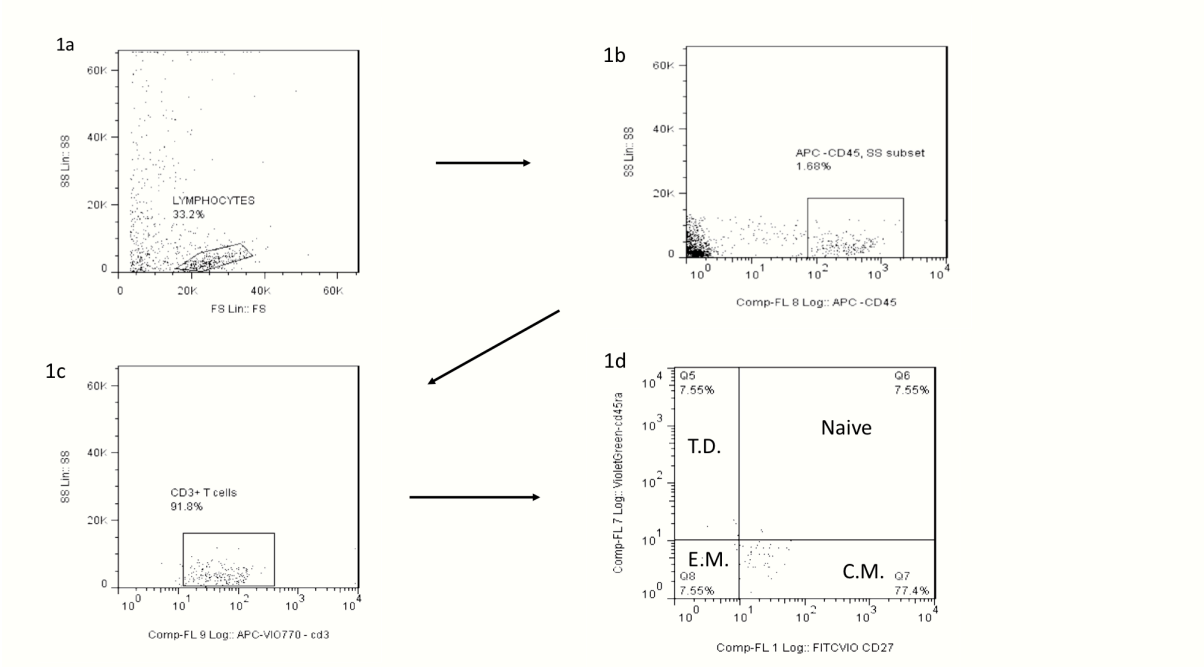

Figure 25: Gating strategy used for T Cells: Forward Scatter (FSC) v Side Scatter (SSC) dot plots were used to gate on lymphocytes based on size and granularity (a), followed by gating on cells expressing the lymphocyte common antigen CD45 (b). All $CD45^+$ cells expressing CD3 were gated to identify the total T cell population (c). Subsequent gating within this $CD3^+CD45^+$ population facilitated the identification of $CD8^+$ T cells, $CD69^+$ T cells and the 4 different T cell memory subsets; naive, central memory (C.M), effector memory (E.M) and terminally differentiated (T.D) (d). Data was acquired using a CyAn™ ADP Analyzer (Beckman Coulter) and Summit v4.1 and analysed using FlowJo v7.6.1.

4.3.6 Quantification of soluble mediators in CSF

Glial Cell Derived Neurotrophic factor (GDNF) and Fractalkine single plex ELISAs (Abcam, Cambridge, UK) were performed according to the manufacturer's guidelines. Mesoscale Diagnostics (MSD, Rockville, MD, USA) V-Plex Human Cytokine 30-Plex kit, R-Plex Human Brain Derived Neurotrophic factor (BDNF) antibody set with MSD Gold 96 SM Spot Streptavidin plate pack, and human Nerve Growth Factor (NGF) ELISAs were performed as per the manufacturer's instructions, using a final CSF dilution of 1:2. MSD plates were read using MesoScale Diagnostics Sector S600. The sensitivities to the kits are available at www.mesoscale.com and www.abcam.com. The limits of detection for the neuropeptides were in pg/ml : GM-CSF 0.842-750, IL-1α 2.85-278, IL-5 4.41-562, IL-7 0.546-563, IL-12/IL-23p40 1.32-2,250, IL-15 0.774-525, IL-16 19.1-1,870, IL-17A 3.19-3650, TNF-β 0.465-458, VEGF-A 7.70-562, IFN-γ 1.76-938, IL-1β 0.646-375, IL-2 0.890-

938, IL-4 0.218-158, IL-6 0.633-488, IL-8 0.591-375, IL-10 0.298-233, IL-12p70 1.22-315, IL-13 4.21-353, TNF-α 0.690-248, Eotaxin 12.3-1120, MIP-1β 1.02-750, Eotaxin-3 10.2-3750, TARC 3.32-1120, IP-10 1.37-500, MIP-1α 13.8-743, IL-8 713-43400, MCP-1 1.09-375, MDC 88.3-7500, MCP-4 5.13-469, NGF 0.05-498, BDNF 0.72-2000pg/mL, GDNF 2.743-2000 , Fractalkine 3.91-250.

4.3.7 Preparation of the CSF samples for mass spectrometry

A shotgun proteomics approach was employed to analyse the CSF proteome, utilising a single-pot solid-phase-enhanced sample preparation (SP3) for sample preparation (322). The SP3 protocol utilizes commercially available beads which carry a carboxylate moiety. For this experiment both hydrophobic and hydrophilic Sera-Mag Speed bead Magnetic carboxylate modified particles were employed in a 1:1 mix (GE Healthcare). Prior to use the beads were combined in a ratio of 1:1 (v/v), rinsed and reconstituted in MS grade water (Fisher Scientific) at a stock concentration of 10µg/ml and stored at 4°C until required.

SP3 preparation was performed according to the protocol of Hughes *et al* (322). Briefly, 200µg CSF was resuspended in 100µl lysis buffer (6M urea, 2M thiourea, 50mM MOPS) and centrifuged for 15 minutes at 15,000 rpm at 4°C to remove any cellular debris. The supernatant was transferred to a fresh Eppendorf tube. The CSF was reduced by adding 0.2M 1,4-dithiothreitol (DTT; Sigma Aldrich) and incubated at 37°C on a shaker at 700 rpm for 15 minutes. Samples were then alkylated by adding 0.4M iodoacetamide (IAA; Sigma Aldrich). Acetonitrile (ACN; Sigma Aldrich) was added to each sample to give a final concentration of 70% acetonitrile (v/v) and the prepared SP3 bead mixture was added to each sample and rotated for 18 minutes at room temperature. Subsequently the beads were immobilized by incubation for 2 minutes on the DynaMag-2™ stand (Thermo Fisher). The supernatant was discarded and the pellet was rinsed with 70% (v/v) Ethanol in water and 100% ACN. Beads were resuspended in 50 mM ammonium bicarbonate (NH_4HCO_3; Sigma Aldrich). Lyophilised sequence grade trypsin (Promega) was resuspended in 50mM ammonium bicarbonate before trypsin was added to each sample. After overnight digestion at 37°C on a thermoshaker at 500rpm, prepared bead mixture was added to the samples and ACN was added to reach a final concentration of 95% (v/v). After mixing and incubation, the supernatant was removed and beads were rinsed with 100% ACN. The peptides bound to the beads were eluted using HPLC grade water with intermittent vortexing. The

supernatant containing the purified peptides was transferred into a fresh tube containing 10% acetic acid. The samples were placed on the DynaMag-2™ for 5 minutes before the supernatant was transferred to MS vials for analysis.

4.3.8 LC-MS/MS analysis:

Each sample was run in duplicate on a Thermo Scientific Q Exactive mass spectrometer connected to a Dionex Ultimate 3000 (RSLCnano) chromatography system. Each sample was loaded onto a fused silica emitter (75µm ID), pulled using a laser puller (Sutter Instruments P2000, Novato, CA, USA), packed with ReprocilPur (Dr Maisch, Ammerbuch-Entringen, Germany) C18 (1.9µm; 12 cm in length) reverse phase media and were separated by an increasing acetonitrile gradient over 60 minutes at a flow rate of 250 nL/min direct into a Q-Exactive mass spectrometer. The mass spectrometer was operated in positive ion mode with a capillary temperature of 320°C, and with a potential of 2300 V applied to the frit. All data was acquired while operating in automatic data dependent switching mode. A high resolution (70,000) MS scan (300-1600 m/z) was performed using the Q Exactive to select the 12 most intense ions prior to MS/MS analysis using high-energy collision dissociation (HCD).

4.3.9 Protein identification and quantification:

Proteins were identified and quantified by MaxLFQ (323) by searching with MaxQuant version 1.5 against the Homo Sapiens reference proteome database which was obtained from Uniprot. LFQ intensities of all technical replicates were averaged and all samples obtained before and after SCS were averaged and expressed as a Log_2 value. The log fold change was calculated as well as a false discovery rate (FDR) and p value. Proteins found to be differentially expressed between groups were subjected to pathway mapping analysis and were distributed into categories according to their cellular component, molecular function, and biological process using Ingenuity Pathway Analysis (IPA) [QIAGEN (Redwood City, CA)] or STRING Database (Version 10.5). STRING (www.string-db.org) was used to generate protein-protein interaction networks, which were then imported into Cytoscape for further editing (Version 3.4.0). The NeuroPep database (islab.info/NeuroPep/) and the neuropeptides database (www.neuropeptides.nl) were employed to identify neuropeptides from mass spectrometry. The Brain RNA-Seq tool

(www.brainrnaseq.org) was used to establish what cells produced specific proteins. UniProt was used to assess Gene Otology (GO) biological and molecular functions.

4.3.10 Statistical analysis:

All statistical analysis was performed on Prism Graph Pad version 7.0. Non-parametric paired and unpaired tests were used where appropriate, Wilcoxon Sign Rank and Mann Whitney respectively. Data was expressed in means with standard error of means (SEM) and standard deviations (SD). P values of <0.05 were considered to be significant for the flow-cytometry and ELISA analysis. A separate analysis for the proteomic data is described in section 3.4.

4.4 Results

4.4.1 Patient enrolment

In accordance with the exclusion and inclusion criteria a total of 4 patients (2 females, 2 males) participated in the study **(Figure 26)**, with a mean age of 51 years (+/- SEM 2.74, SD 5.48) shown in the patient demographics **(Table 13)**. The patients respective pain scores and stimulation parameters were documented **(Table 14)**, with all of the patients deemed to be responders following 8 weeks of Burst-SCS. It was also noted that the patients received no changes in medications between the initial CSF sampling and the follow up sampling after 8 weeks of Burst-SCS treatment.

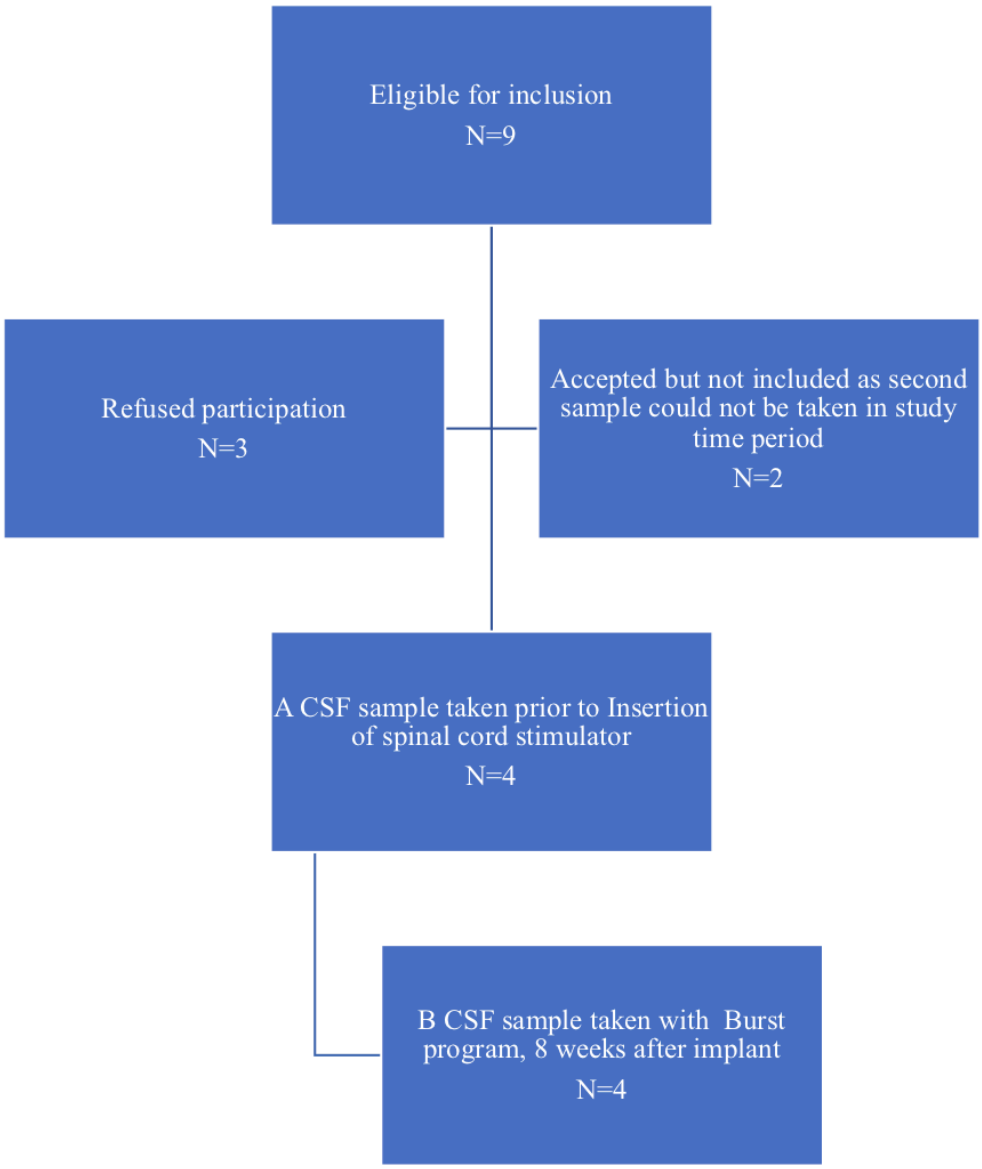

Figure 26: Consort diagram of patients eligible for inclusion in the study and the performance of a second cerebrospinal fluid (CSF) sample: Patients were enrolled if they met inclusion criteria for the study.

Table 13: Distribution of Patient Characteristics prior to implant of Spinal cord Stimulator: Age, Gender, Diagnosis, Douleur Neuropathique score (DN4), Area of Pain, Medications and quantity taken in mg.

Study ID	Age	Gender	Diagnosis	DN4 Score	Area of pain	Medications (per day)
101	45	Male	FNSS (cervical fusion)	4	Left neck and arm	None
102	57	Female	FBSS	9	Left back and leg	Targin 20mg/200mg (oxycodone/naloxone) MME=40mg
103	48	Male	FBSS	9	Left back and leg	None
104	54	Female	Chronic post mastectomy pain	7	T4, 5 dermatomes	Pregabalin 150mg/ day

FBSS: Failed back surgery syndrome; FNSS: Failed Neck Surgery Syndrome; MME: Milligram morphine equivalent

Table 14: Spinal cord stimulator (SCS) settings and 24 hour Numerical Pain Scores (NRS) before and after Burst-SCS Stimulation for 8 weeks

Study ID	Electrode type	Contacts	Burst Rate (Hz)	Intraburst Rate (Hz)	Burst Spike Pulse width (ms)	Target amplitude (mA)	Baseline NRS	NRS with Burst-SCS for 8 weeks
101	Octrode x 1	1- ,3+,5+,6-	40	500	1	0.6	7	0
102	Octrode x 2	14-, 15+, 16-	40	500	1	0.6	8	4
103	Octrode x 2	13+, 14-	40	500	1	0.6	8	3
104	Octrode x 2	7+, 9-, 8+	40	500	1	0.55	8	3

Patients were deemed responders to Burst-SCS stimulation if a 50% reduction in pain ccurred.

4.3.2 Cellular Analysis

There were no significant differences in the percentage (%) frequencies of T cells in the CSF samples obtained prior to and after stimulation. Some higher frequencies were observed in the $CD3^+$ cells (Pre vs Post Burst-SCS: $CD3^+$ cells: 30.7% ±7.7% vs 54.7% ±19.3%, p=0.25), $CD8^+$ T cell frequencies (Pre vs Post Burst-SCS $CD8^+$ T cells: 17.1% ± 5.3 vs 40.6% ± 24.2, p=0.3179) as wells as those of activated ($CD69^+$) T cells (Pre vs Post Burst-SCS $CD69^+CD3^+$ cells: 13.9% ± 5.5% vs 40% ±16.3%, p=0.1448) **(Figure 27)**. However, none of these changes were found to be significant. There was a reversal of effector memory (EM)/central memory (CM) T cell phenotype following Burst-SCS stimulation but this was not significant (EM Pre vs Post Burst-SCS: 51.2% ± 20.7% vs 15.4% ± 9%, p=0.2224) (CM Pre vs Post Burst-SCS: 27.3% ± 18.2% vs 42.3% ± 23.4%, p=0.6281) **(Figure 28)**.

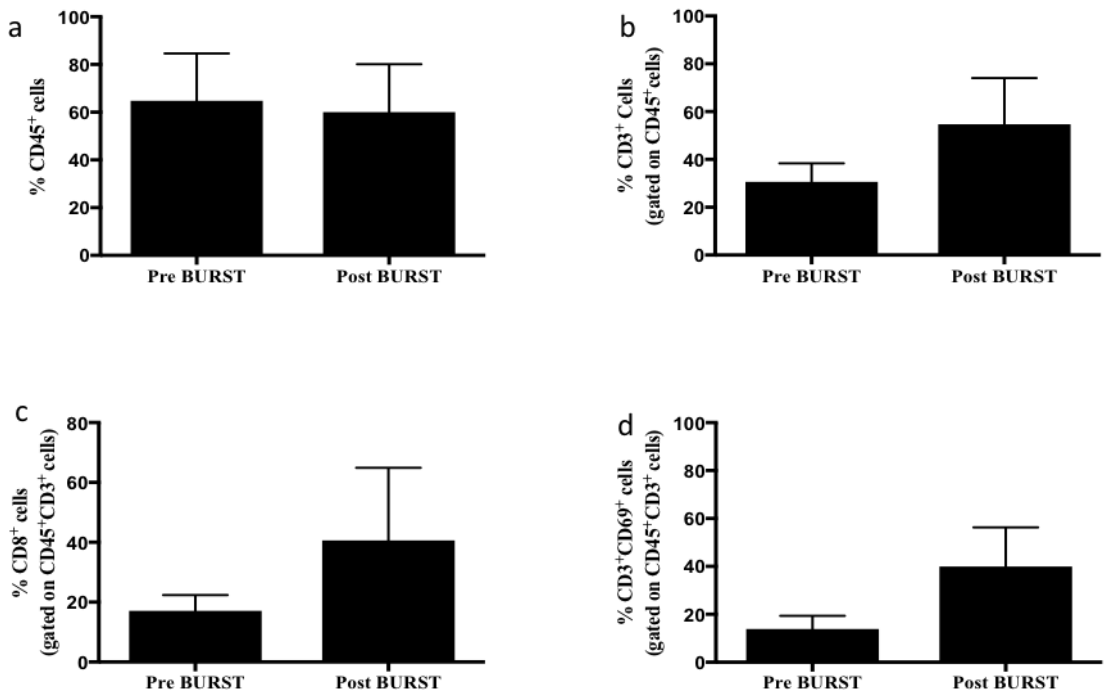

Figure 27: The percentage frequency of T cells in Cerebrospinal fluid (CSF) before and following 8-weeks after Burst stimulation: Columns indicate the sample means, while the error bars represent the Standard error of the mean (SEM). Statistical analysis was performed using the Mann-Whitney U test. Comparison of (a) the percentage of

CD45+ cells prior to and following Burst-SCS (64.83% ±19.79 vs 60% ±20.09, p=0.87), (b) the percentage of CD3+ cells before and after Burst-SCS treatment (30.65% ±7.68 vs 54.73% ±19.29, p=0.25), (c) the percentage of CD8+ before and after Burst-SCS treatment (17.11% ± 5.27 vs 40.63% ± 24.23, p=0.3179) and (d) the percentage of CD3+ CD69+ cells before and after Burst-SCS treatment (13.85% ± 5.517 vs 39.97% ±16.31, p=0.1448).

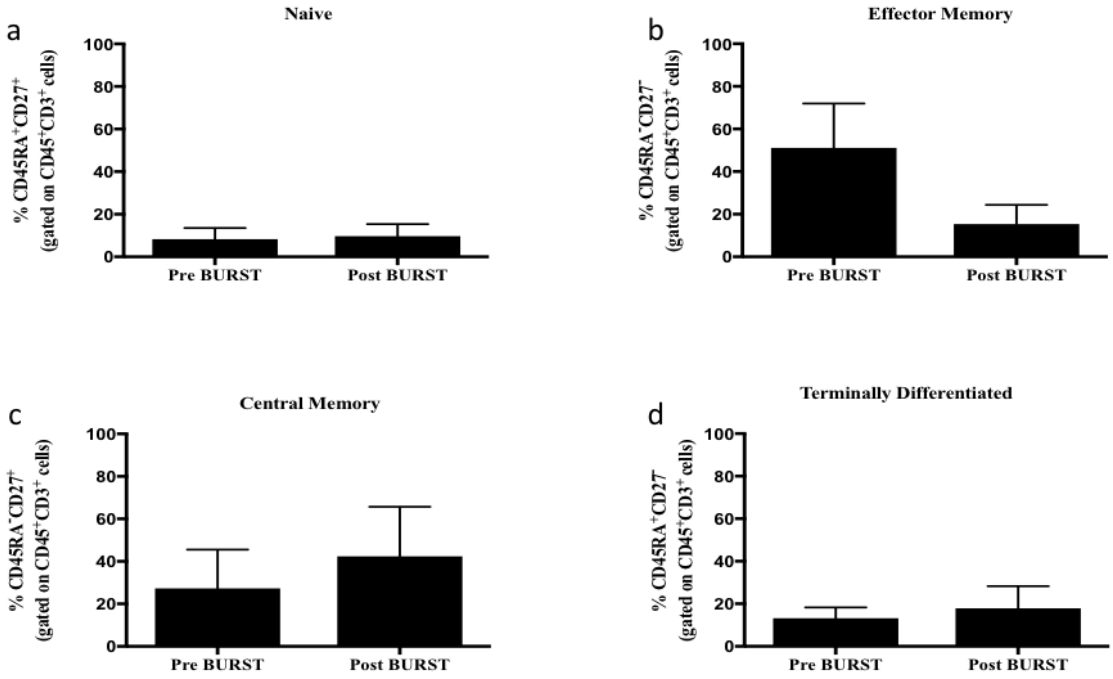

Figure 28: Phenotype of the percentage of CD8+ cells in the CSF before and following an 8-week duration of Burst stimulation, showing the mean ± standard error of the mean (SEM): Statistical analysis was performed using Mann-Whitney U test. Comparisons of the percentage of (a) Naive cells before and after burst stimulation (8.3%± 5.22 vs 9.695%±5.7, p=0.87), (b) Effector Memory cells before and after burst stimulation (51.15% ±20.77 vs 15.35% ±9, p=0.22), (c) Central memory cells before and after burst stimulation (27.33% ± 18.2 vs 42.33% ±23.4, p=0.62) and finally (d) terminally differentiated cells before and after burst stimulation (13.23% ±5.07 vs 17.91% ±10.39, p=0.67).

4.3.3 Cytokines, chemokines and neurotrophins analysis:

There were no significant differences in the concentrations of a panel of cytokines and chemokines analysed within the CSF before and after stimulation **(Table 15, 16 and 17)**. The following neuropeptides were undetectable within the CSF at both time-points for all patients; Nerve growth factor (NGF), brain derived neurotrophic factor (BDNF), glial cell

derived neurotrophic factor (GDNF), GM-CSF, IP-10, TNF-β and IL-2. All other cytokines were within range according to the manufacturer's instructions.

Table 15: Pro-Inflammatory Cytokine Panel in Cerebrospinal fluid (CSF) before and 8 weeks after Burst-SCS Stimulation in (pg/ml), n=4.

	Mean Baseline +/- SEM (pg/ml)	Mean 8 weeks after Burst-SCS +/- SEM (pg/ml)	Mean of differences	SD of differences	SEM of differences	P value Wilcoxon-Sign Rank
IFN-γ	0.1501 ± 0.087	0.1526 ± 0.08826	0.0025	0.1806	0.09	0.99
IL-10	0.1967 ± 0.037	0.2212 ± 0.0278	0.0245	0.0855	0.043	0.625
IL-12p70	0.04869 ± 0.028	0.05026 ± 0.0366	0.0016	0.119	0.0596	1.000
IL-13	2.929 ± 0.5273	1.908 ± 0.6073	-1.022	1.509	0.754	0.375
IL-1β	0.3034 ± 0.086	0.2621 ± 0.05175	-0.041	0.104	0.0522	0.625
IL-4	0.07518 ± 0.027	0.06708 ± 0.0073	-0.0081	0.044	0.022	0.875
IL-6	0.9359 ± 0.159	1.099 ± 0.1141	0.1631	0.134	0.067	0.250
IL-8	21.26 ± 7.367	24.22 ± 4.419	2.958	10.91	5.455	0.625
TNF-α	0.381 ± 0.0339	0.3117 ± 0.0696	-0.069	0.158	0.0794	0.625

Table 16: Cytokine Panel in CSF before and after Burst-SCS Stimulation in (ng/ml), n=4

	Mean Baseline +/- SEM (pg/ml)	Mean 8 weeks after Burst-SCS +/- SEM (pg/ml)	Mean of differences	SD of differences	SEM of differences	P value Wilcoxon-Sign Rank
IL-12/IL-23p40	3.123 ± 0.3642	3.767 ± 0.2125	0.644	0.470	0.235	0.125
IL-15	3.561 ± 0.5049	3.989 ± 0.4214	0.428	0.565	0.283	0.250
IL-16	8.004 ± 1.322	7.883 ± 1.678	-0.121	1.324	0.662	0.875
IL-17A	0.3253 ± 0.07274	0.4078 ± 0.06008	0.0826	0.1441	0.072	0.375
IL-5	0.5925 ± 0.1123	0.6804 ± 0.1104	0.0879	0.0913	0.045	0.250
IL-7	1.115 ± 0.1406	1.273 ± 0.2115	0.158	0.2193	0.109	0.250
VEGF	2.816 ± 1.414	4.129 ± 1.163	1.313	2.096	1.048	0.50

Table 17: Chemokine Panel in CSF before and after Burst-SCS Stimulation in (ng/ml), n=4

	Mean Baseline +/- SEM (pg/ml)	Mean 8 weeks after Burst-SCS +/- SEM (pg/ml)	Mean of differences	SD of differences	SEM of differences	P value Wilcoxon-Sign Rank
MCP-1	417.5 ± 55.8	411.9 ± 34.62	-5.64	68.53	34.27	0.875
MCP-4	9.36 ± 1.681	12.56 ± 2.845	3.198	7.548	3.774	0.625
Eotaxin-3	7.731 ± 4.164	20.79 ± 6.781	13.06	9.793	4.896	0.250
Eotaxin	14.99 ± 2.7	17.53 ± 4.09	2.544	5.583	2.792	0.625
MIP-1α	6.41 ± 1.526	7.366 ± 1.406	0.956	2.658	1.329	0.686
MIP-1β	10.45 ± 2.891	9.862 ± 2.089	-0.5911	3.275	1.637	0.625
MDC	40.43 ± 10.05	52.09 ± 17.61	11.66	30.9	15.45	0.625
TARC	6.893 ± 0.5208	7.445 ± 0.5938	0.5523	1.404	0.7019	0.375
Fractalkine	9.402 ± 7.862	4.758 ± 2.064	-4.644	12.62	6.311	0.875
IP-10	129.8 ± 21.55	189.3 ± 53.5	59.56	92.19	46.09	0.375

4.3.4 Proteomics Analysis:

To determine the effects on protein expression in the CSF, the proteomics data obtained from patients following 8 weeks of Burst-SCS was compared to CSF obtained from the same patients prior to beginning treatment. In total 992 proteins were identified in the CSF obtained from patients, with differential expression of proteins observed in samples obtained prior to and after Burst-SCS stimulation. For the purposes of identifying proteins which were significantly altered following Burst-SCS strict filtering settings were applied to the proteomics data in order identify proteins which were significantly increased (log fold change (LFC)>2, FDR<0.05) **(Table 18)** and decreased (LFC <1, FDR <0.05) **(Table 19)** following Burst-SCS stimulation.

Table 18: Top 25 proteins upregulated (Log fold change >2, FDR<0.05) following 8 weeks of Burst-SCS stimulation in order of log fold change.

Protein	Gene	Log Fold Change	FDR
ATP-dependent zinc metalloprotease YME1L1	YME1L1	23.987	0.0446
Double-stranded RNA-specific editase 1	ADARB1	23.921	0.0362
Proliferation marker protein Ki-67	MKI67	22.088	0.0342
Lipopolysaccharide-binding protein	LBP	21.961	0.0303
C-reactive protein	CRP	21.531	0.0229
COP9 signalosome complex subunit 5	COPS5	21.471	0.0442
Metallothionein	MT3	21.404	0.0148
Immunoglobulin lambda variable 4-60	IGLV4-60	21.072	0.0005
Disintegrin and metalloproteinase domain-containing protein 11	ADAM11	21.003	0.0084
Mitotic spindle assembly checkpoint protein MAD1	MAD1L1	20.887	0.0098

Immunoglobulin lambda variable 5-45	IGLV5-45	20.775	0.0059
Cadherin-5	CDH5	20.555	0.0330
Epithelial discoidin domain-containing receptor 1	DDR1	20.476	0.0373
Kallikrein-7	KLK7	20.342	0.0347
Cartilage oligomeric matrix protein, isoform CRA_b	COMP	20.301	0.0137
Adhesion G protein-coupled receptor B1	ADGRB1	20.133	0.0107
Ephrin-A5	EFNA5	20.081	0.0027
Complement C1q tumor necrosis factor-related protein 5	C1QTNF5	20.074	0.0461
Sia-alpha-2,3-Gal-beta-1,4-GlcNAc-R:alpha 2,8-sialyltransferase	ST8SIA3	20.020	0.0176
Complement factor H-related protein 3	CFHR3	20.017	0.0369
DOMON domain-containing protein FRRS1L	FRRS1L	19.970	0.0478
Adenosine deaminase 2	ADA2	19.958	0.008
Ryanodine receptor 3	RYR3	19.880	0.002
Immunoglobulin heavy variable 1-3	IGHV1-3	19.779	0.005
Immunoglobulin kappa variable 1D-16	IGKV1D-16	19.728	0.021

Table 19: Top 25 proteins downregulated (Log fold change <1, FDR<0.05) following 8 weeks of Burst-SCS stimulation in order of log fold change.

Protein	Gene	Log Fold Change	FDR
Growth hormone A1	PRL	-22.893	0.0207
Titin	TTN	-22.532	0.0039
Myoglobin	MB	-22.249	0.0223
Somatostatin	SST	-22.226	0.0355
Alpha-actinin-2	ACTN2	-22.115	0.0128
Tropomyosin alpha-4 chain	TPM4	-22.078	0.0163
Calsyntenin-3	CLSTN3	-22.076	0.0456
Spectrin beta chain	SPTBN4	-21.998	0.0101
A disintegrin and metalloproteinase with thrombospondin motifs 1	ADAMTS1	-21.799	0.0485
V-type proton ATPase subunit S1	ATP6AP1	-21.579	0.0395
Contactin-6	CNTN6	-21.373	0.0493
Hepatocyte growth factor-like protein	MST1	-21.206	0.0136
Protein disulfide-isomerase A3	PDIA3	-20.785	0.0328

Semaphorin-3G	SEMA3G	-20.739	0.0472
Oral-facial-digital syndrome 1 protein	OFD1	-20.623	0.0184
Serotransferrin	TF	-20.473	0.0100
Calnexin	CANX	-20.450	0.0323
WAP four-disulfide core domain protein 2	WFDC2	-20.299	0.0386
Junction plakoglobin	JUP	-20.186	0.0294
Voltage-dependent calcium channel subunit alpha-2/delta-3	CACNA2D3	-20.063	0.0425
CD320 antigen	CD320	-20.049	0.0166
Plexin-B1	PLXNB1	-19.987	0.0175
OX-2 membrane glycoprotein	CD200	-19.980	0.0338
Neuromodulin	GAP43	-19.953	0.0301
Piezo-type mechanosensitive ion channel component	PIEZO2	-19.844	0.01134

Compared to CSF obtained prior to treatment, CSF obtained following an 8-week course of Burst-SCS resulted in the differential expression of 477 proteins (48.1% of total proteins; FDR<0.05) **(Figure 29a)**. Of these 477 differentially expressed proteins, 346 proteins were upregulated (72.5%) and 131 proteins were downregulated (27.5%) following Burst-SCS (-2 < LFC > 2) **(Figure 29a)**. Focusing on these differentially expressed proteins a total of 38 proteins (8%) were shown to be significantly upregulated while 42 proteins (8.8%) were shown to be significantly downregulated after Burst-SCS (FDR<0.05) **(Figure 29a).**

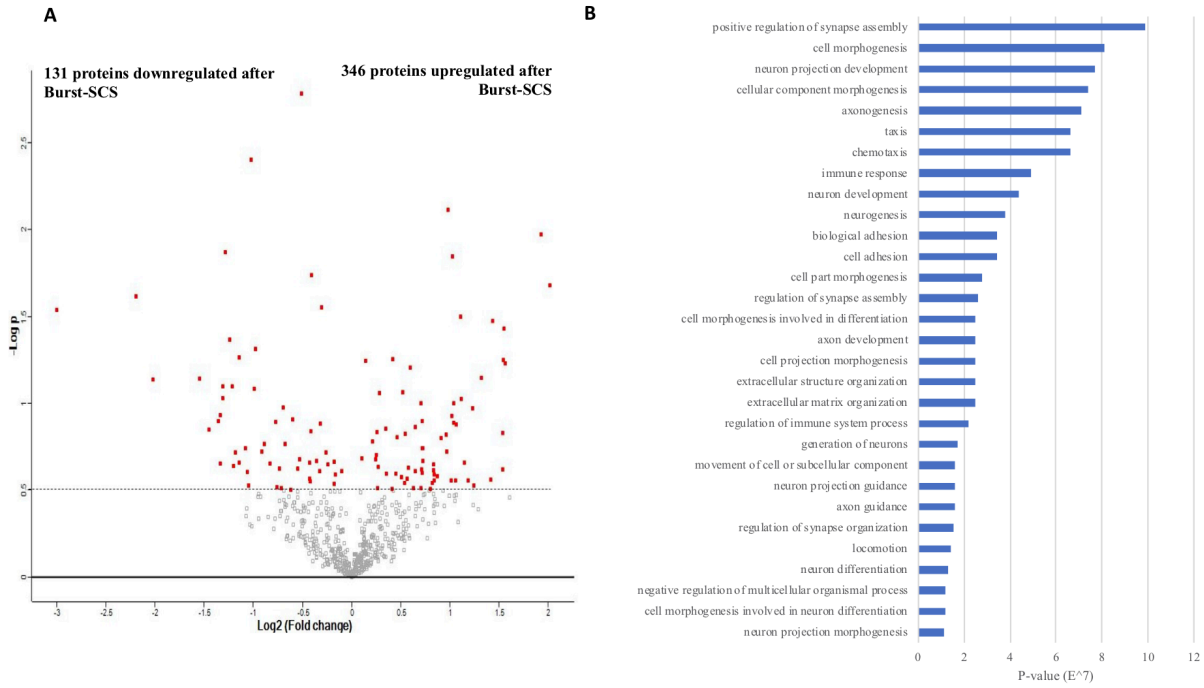

Figure 29: Differential protein expression in Cerebrospinal Fluid (CSF) obtained prior to treatment and following an 8-week course of Burst-SCS: Volcano plot showing protein differential data of the 648 proteins differentially expressed (5A). Of the differentially expressed proteins, 346 proteins were upregulated (53.4%) and 131 proteins were downregulated (20.2%). The significant differentiated proteins are in red: 38 proteins (4.8%) were significantly upregulated and 42 (6.5%) were downregulated after Burst-SCS (Figure 5a). GO biological functional enrichment analysis of 30 biological processes involving the differentially expressed proteins (5B). The top 5 biological processes identified as the positive regulation of synapse assembly ($p<9.9E^{-7}$), cell morphogenesis ($p<8.1E^{-7}$), neuron projection development ($p<7.7E^{-7}$), cellular component morphogenesis ($p< 7.4E^{-7}$) and axonogenesis ($p<7.1E^{-7}$).

GO analysis focusing on the biological functional enrichment identified 30 biological processes involving the differentially expressed proteins, with the top 5 biological processes identified as the positive regulation of synapse assembly ($p<9.9E^{-7}$), cell morphogenesis ($p<8.1E^{-7}$), neuron projection development ($p<7.7E^{-7}$), cellular component morphogenesis ($p< 7.4E^{-7}$) and axonogenesis ($p<7.1E^{-7}$) **(Figure 29b)**. Focusing on the 477 differentially expressed proteins, the proteins could be classified into protein classes (i.e., transporters, enzymes (including kinases and peptidases), receptors (including G protein coupled receptors, transmembrane receptors and ion channels), and immune effectors) as defined by International Union of Basic and Clinical Pharmacology **(Figure 30 a, b)**.

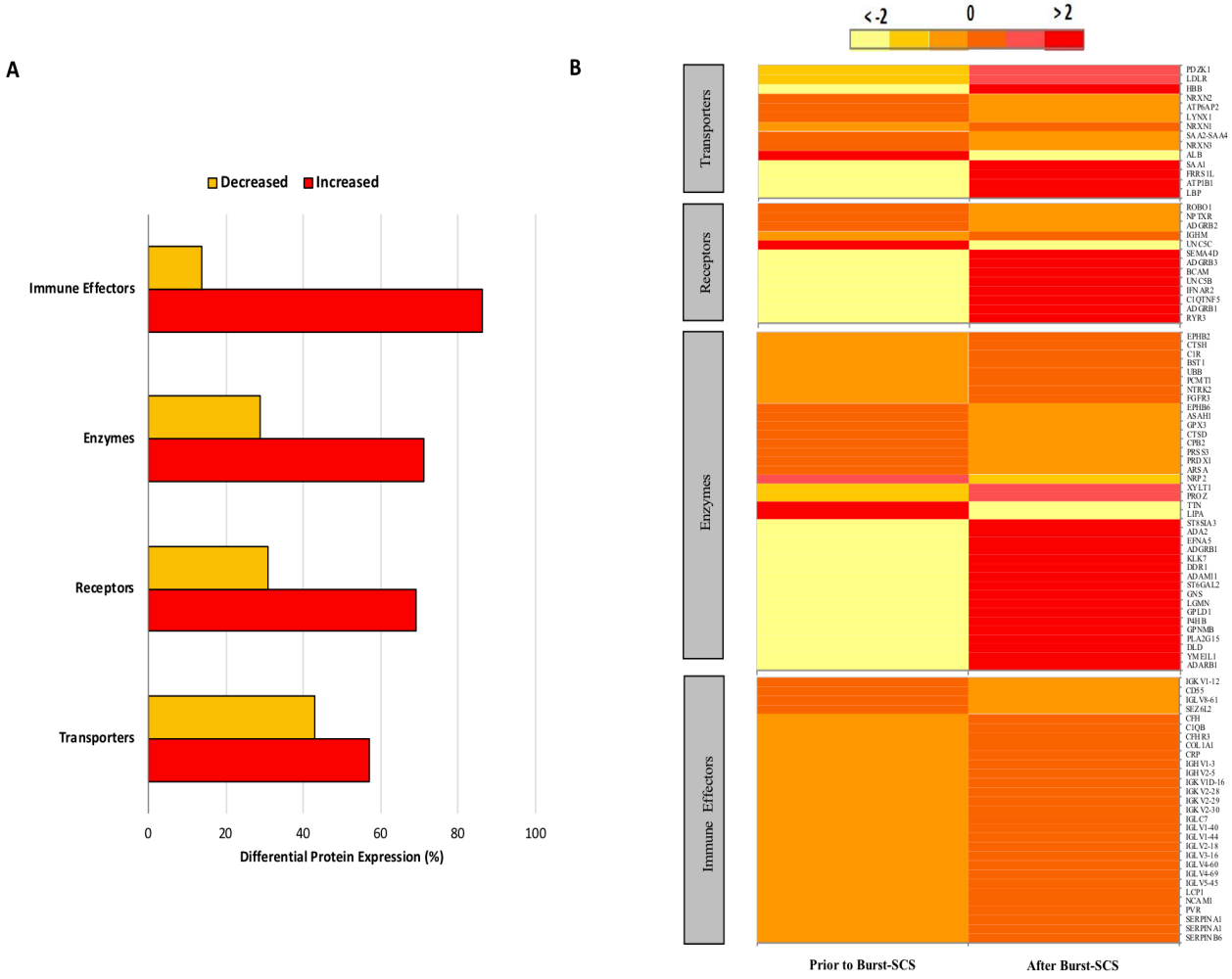

Figure 30: Bar chart of protein classes and heat map of individual proteins: Bar chart showing classification of % of differentially expressed protein classes as defined by International Union of Basic and Clinical Pharmacology (6A): transporters, enzymes (including kinases and peptidases), receptors (including G protein coupled receptors, transmembrane receptors and ion channels), and immune effectors. Relative expression of each protein (gene class) in a bar plot, red representing upregulation and yellow downregulation (6B).

Further analysis focusing on the differentially expressed proteins identified a cohort of 24 known neuropeptides which demonstrated differential analysis following treatment, with the expression of 8 of these identified neuropeptides shown to be significantly changed following treatment (FDR<0.05) **(Figure 31)**. Seven neuropeptides were shown to be increased following Burst-SCS, including proenkephalin-A (PENK), cerebellin-3 (CBLN3), cocaine and amphetamine-regulated transcript protein (CARTPT),

nucleobindin-1 (NUCB1), kininogen-1 (KNG1), cerebellin-1 (CBLN1) and angiotensinogen (AGT), but the changes were found to be nonsignificant when stricter filtering was applied (Log fold change>1, FDR<0.05) **(Table 20)**. In addition, 18 neuropeptides were shown to be decreased following Burst-SCS treatment **(Table 21)**. Neuropeptides demonstrating significant decreases in expression following burst SCS include growth hormone A1 (PRL), somatostatin (SST), nucleobindin-2 (NUCB2), Calbindin (CALB1), acyl-CoA binding protein (DBI), proSAAS (PCSK1N), endothelin-3 (END3) and cholecystokinin (CCK) **(Table 21)**. The GO molecular function and biological processes for each of these significantly altered proteins was assessed **(Table 22)**.

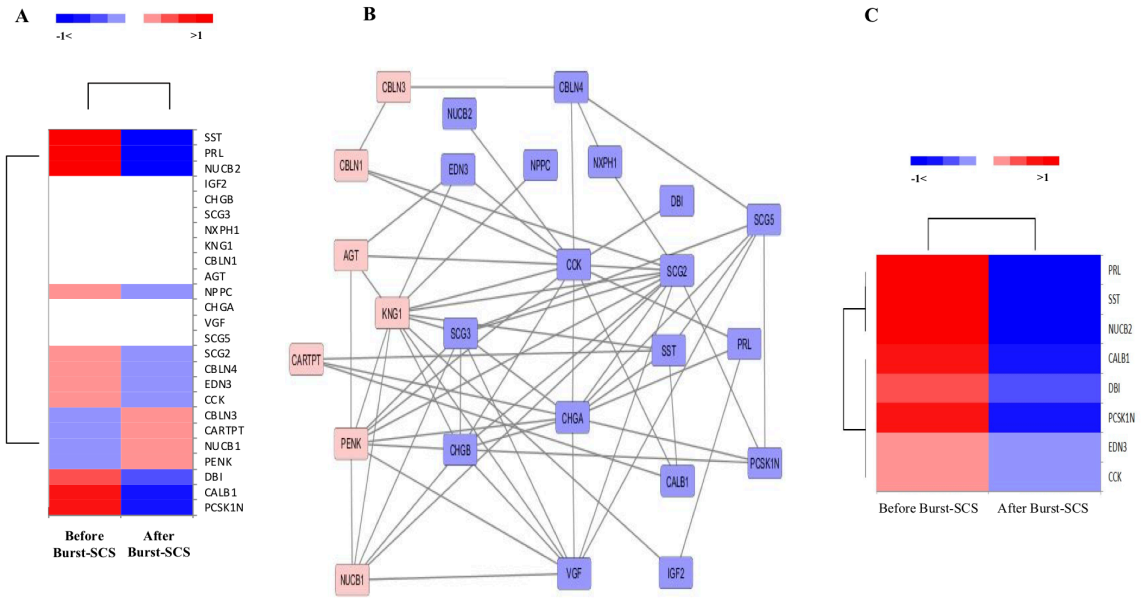

Figure 31: Differential expression of neuropeptides after Burst-SCS: (A) shows the differential expression of 24 neuropeptides. (B) shows the neuropeptide network, with neuropeptides showing increased expression after Burst-SCS shown in blue while neuropeptides showing decreased expression after treatment are shown in pink. (C) shows a heatmap with the expression of 8 of these identified neuropeptides shown to be significantly changed following treatment (FDR<0.05). FDR= false discovery rate

Table 20: Proteomic Mass spectrometry: Neuropeptides increased (Log fold change >0, False discovery rate (FDR) <0.05) in CSF following 8 weeks of Burst-SCS Stimulation. The Brain RNA-Seq tool (www.brainrnaseq.org) was used to establish what cells produced specific proteins. Proteins which were significantly decreased (Log fold change>1, FDR<0.05).

Protein	Gene	Cells that produce in CNS	Log Fold Change	FDR
Proenkephalin-A	PENK	Neurons, Oligodendrocytes Endothelial	0.8554	0.0206
Cerebellin-3	CBLN3	Neurons	0.5484	0.0410
Cocaine- and amphetamine-regulated transcript protein	CARTPT	Astrocytes, Endothelial	0.5464	0.03961
Nucleobindin-1	NUCB1	Astrocytes, Endothelial, Microglia, Oligodendrocytes, Neurons	0.3729	0.0368
Kininogen-1	KNG1	Neurons	0.1052	0.0206
Cerebellin-1	CBLN1	Neurons, Oligodendrocytes	0.0918	0.0315
Angiotensinogen	AGT	Astrocytes, Neurons,	0.0331	0.020

Table 21: Proteomic Mass spectrometry: Neuropeptides decreased (Log fold change <0, False discovery rate (FDR) <0.05) in CSF following 8 weeks of Burst-SCS Stimulation. The specific proteins. Proteins which were significantly decreased (Log fold change<-1, FDR<0.05)

Protein	Gene	Cells that produce in CNS	Log Fold Change	FDR
Growth hormone A1	PRL	Neurons	-22.893	0.0207*
Somatostatin	SST	Neurons, Oligodendrocytes, endothelial, astrocytes	-22.226	0.0355*
Nucleobindin-2	NUCB2	Neurons, astrocytes, , oligodendrocytes, endothelial, microglia	-18.750	0.0012*
ProSAAS	PCSK1N	oligodendrocytes	-1.863	0.0484*
Calbindin	CALB1	Neurons, Astrocytes, endothelial	-1.551	0.0251*
Acyl-CoA-binding protein	DBI	Microglia, astrocytes, Oligodendrocytes, neurons, endothelial	-1.242	0.0038*
Cholecystokinin	CCK	Neurons, Mature Astrocytes, Oligodendrocytes, endothelial	-0.7368	0.0252*
Endothelin-3	EDN3	Endothelial	-0.588	0.0291*
Cerebellin-4	CBLN4	Neurons	-0.495	0.0473
Secretogranin-2	SCG2	Neurons, Oligodendrocytes, Astrocytes, endothelial	-0.491	0.0288
C-type natriuretic peptide	NPPC	astrocytes, neurons	-0.325	0.0317
Chromogranin-A	CHGA	Neurons	-0.273	0.0281
Neurosecretory protein VGF	VGF	Neurons	-0.224	0.0174
Neuroendocrine protein 7B2	SCG5	Neurons, Oligodendrocytes, endothelial, astrocytes, microglia	-0.212	0.0248
Neurexophilin-1	NXPH1	Neurons, oligodendrocytes, astrocytes, , endothelial	-0.120	0.009
Secretogranin-3	SCG3	astrocytes, neurons, oligodendrocytes, endothelial	-0.115	0.0435

Secretogranin-1	CHGB	Neurons, Oloigodendrocytes, endothelial, astrocytes, microglia	-0.0766	0.0245
Insulin-like growth factor II	IGF2	Endothelial	-0.046	0.0207

Table 22: GO Molecular, Biological function and immune activity of proteins downregulated with Burst SCS

Protein	Gene	GO- Molecular Function	GO- Biological process
Growth hormone A1	PRL	Hormone activity	Involved in the prolactin signalling pathway as a positive regulator, Hyperosmotic response, chemical synaptic transmission
Somatostatin	SST	Hormone activity	Involved in the somatostatin signalling pathway, locomotor activity ,cognitive function, chemical synaptic transmission
Nucleobindin-2	NUCB2	DNA and Calcium ion binding	Negative regulation of appetite
ProSAAS	PCSK1N	Signalling receptor binding	Neuropeptide signalling pathway, peptide hormone processing, response to cold and dietary excess
Calbindin	CALB1	Calcium ion binding (involved in regulation of pre and postsynaptic cytosolic calcium ion concentration) Vitamin D and Zinc binding	Regulation of long term synaptic potential, short and long term memory, locomotory behaviour, retina layer formation, cochlea development
Acyl-CoA-binding protein	DBI	Benzodiazepine receptor, lipid, long-chain fatty acyl-CoA binding, protein dimerization acitivity	Acyl-CoA metabolic process, phosphatidylcholine acyl-chain remodelling
Cholecystokinin	CCK	Hormone activity	Axonogensis, memory, signal transduction, positive regulation of sensory perception of pain ,negative regulation of appetite, positive regulation of fear response, positive regulation of glutamate response
Endothelin-3	END3	Endothelin B receptor binding, hormone activity, signal receptor binding	Blood circulation, cellular calcium and magnesium ion homeostasis, neuron differentiation, signal transduction, immune chemotaxis, positive regulation of hormone secretion

4.4 Discussion

We present the results of a pilot study examining the effect of Burst-SCS on the cellular and neuropeptide constituents of CSF in patient responders with neuropathic pain. All of the patients recruited were responders (>50% pain relief) to Burst-SCS in order to give an accurate analysis of the treatment response. This is the first molecular description of the effect of Burst-SCS on CSF constituents *in vivo* potentially validating its ability to target the neural interface in the CNS.

The development of Burst-SCS was based upon information regarding thalamo-cortical firing patterns having the ability to strengthen synaptic connectivity (275-277). The majority of proteins differentiated after Burst-SCS illustrate a modulation in relation to synapse assembly using biological enrichment analysis. Synapse assembly is largely orchestrated by glial cells within the CNS which includes astrocytes (153, 398) and microglia (144, 151). Long term synaptic changes have been previously demonstrated with bursts of stimulation in the hippocampus in rats (399). There is also pre-clinical evidence of BNF being transmitted across synapses more reliably which may be indicative of this alteration in neuronal physiology (277). It is difficult to determine the exact processes of this alteration from the enrichment analysis however. In terms of protein classes, immune effectors were the predominant increased neuropeptides. Immune mediators including pro-inflammatory cytokines also have significant effects on neurotransmission at the synaptic cleft which is frequently referred to as the 'neuroimmune interface' (3). Despite proteomic evidence in the change of immune effectors, no significant differences were identified in the frequency of T cells, or the concentrations of secreted cytokines or chemokines within the CSF before and after 8 weeks of Burst-SCS in this study. There was however a modest, non-significant increase in the percentage of $CD8^+$ T cells which may be related to the increase in immune effectors. Interestingly, the predominant T cell memory phenotype was effector memory prior to stimulation, which is in line with our group's previous report of a series of patients with lumbar radicular neuropathic pain prior to any treatment (60). This is in contrast to T cell populations within the CSF of healthy controls which are predominantly central memory (286, 291). Pre-clinical studies have frequently implicated T cells in the development, maintenance and resolution of neuropathic pain (81, 129, 130, 132, 133, 135, 163, 199, 218). Immune related peptides have also been the most upregulated in spinal cord segments analysed after sciatic nerve ligation in a study in

rodents following tonic SCS (400). The same study also illustrated key transcriptional pathways induced by SCS including decreased efficacy of synaptic signalling mediated via genes that encode scaffold proteins (400).

Proteomic analysis revealed that growth hormone A1 (PRL) and somatostatin (SST) demonstrated significantly lower expression following Burst-SCS. Growth hormone (GH) signalling molecules have been implicated in nociception and the development of neuropathic pain (401). There is also selective evidence of growth hormone reducing neuropathic pain in cases of fibromyalgia and reversing pain behaviour in rodents (401). This would appear contradictory to our findings. SST, an inhibitor of GH release was also significantly lower after Burst-SCS. There are conflicting reports of how SST modulates both pain and pruritis in pre-clinical models with evidence of both attenuation and causative (402-408). NUCB2 was significantly lower following Burst-SCS and this protein is known to have a role in hypothalamic pathways and endocrine function but is potentially expressed by multiple cells within the CNS (409). Given PRL, SST and NUCB2 are involved in hypothalamic functions it may be indicative of supraspinal mechanisms when applying Burst-SCS to the spinal cord. However, the attenuated release of these neuropeptides may occur at a more caudal location in the spinal cord. Despite this uncertainty, a neurophysiological study in humans using fluorodeoxyglucose positron emission tomography (FGD-PET) scanning illustrated activation of the corticolimbic system via the dorsal anterior cingulate cortex with Burst-SCS (278). Similar results were also achieved with electroencephalography (EEG)(10) in patients with Burst-SCS. It must be noted that both of these studies had low numbers of participants and did not illustrate modulation of the hypothalamic-pituitary axis (10, 278). The corticolimbic system, which includes the hypothalamic pituitary axis, is strongly associated with emotional components of chronic pain and depression (410, 411). The hypothalamic-pituitary axis may also have the potential to restore metabolic associated pathological neural transmission and chronic pain in the periphery (412). Somatostatin receptors are present on immune cells and can have an effect on the release of cytokines which can modulate pain transmission (93, 100, 171, 216, 413). Changes to metabolic and immune associated peptides in serum have previously been reported in responders to Burst-SCS (414). These included leptin, indicating central mechanisms can alter differential cytokine/adipokine traffic peripherally; however only the cytokine IL-10 was significantly altered (414). Pre-clinical evidence supports the role of ProSAAS in the control of the neuroendocrine secretory pathway (415, 416). ProSAAS

was also significantly lower after Burst-SCS and has previously been significantly upregulated in the CSF of patients with fibromyalgia compared to healthy controls (417). Given these two findings the role of ProSAAS in chronic neuropathic pain justifies further clinical research.

Calbindin (CALB1) is a calcium binding protein that is involved in many biological processes within the CNS including synaptic plasticity but there is little evidence to date that it has an effect on pain processing (418-420). Burst-SCS is thought to ride on a calcium mediated plateau and NUCB2 also binds calcium and is involved in calcium homeostasis (395). As peripheral neuropathies and chronic pain have implicated calcium dysregulation in their pathologies modulating calcium homeostasis may have positive effects for pain perception (98, 421-424).

Diazepam binding protein (DBI) is classified as an acyl-CoA binding domain containing proteins (ABCD1) that regulates mitochondrial Translocator protein (TSPO) function and is largely expressed in glial cells in the CNS (173). TSPO is a protein expressed in steroid synthesising cells and is involved in the translocation of cholesterol from the outer to the inner mitochondrial membrane (173). It is utilised as a marker of brain and spinal cord inflammation and is involved in autocrine and paracrine signalling responses in glial cells to disease (173, 180, 181, 183). Radiolabelled TSPO is upregulated in the CNS in many chronic pain patients compared to controls with chronic back pain (180, 181), Complex Regional Pain Syndrome (CRPS) (182), fibromyalgia (181) and lumbar radicular pain (183). As DBI was lower following Burst-SCS in our cohort, this potentially indicates a reduction in neuroinflammation in glial cells.

CCK was significantly lower after Burst-SCS and has previously been implicated in the chronicity of neuropathic pain and reducing the anti-nociceptive effect of opioids (425, 426). Increased CCK levels have also been associate with motivational loss, anxiety and panic attacks that are frequently seen in chronic pain patients (425). CCK's reduction may also contribute to the analgesic and psychological improvement observed with Burst-SCS (427).

Endothelin-3 (EDN3) (lower expression after Burst-SCS) is part of the endothelin family that have been heavily implicated in many chronic and acute pain conditions (428, 429).

The majority of research has been performed with EDN1, however EDN3 is known to bind to the same receptors as EDN1. EDN3 is more associated as an agonist to the ET-B receptor which it has a 100-fold higher affinity in comparison to the ET-A receptor. ET-B receptors are upregulated in a sciatic nerve ligation models and antagonism is associated with a reduction of allodynia in pre-clinical models of trigeminal neuralgia (429). The role of EDN3 and the ET-B receptor requires more attention in future clinical and pre-clinical research. There is an isolated case report of a patient with sciatica reporting a reduction in pain after administration of a endothelin-A antagonist for pulmonary hypertension (430). However, to date, there have been no further reports or studies relating to EDN3 and neuropathic pain in humans.

A major limitation of this observational study is the small number of patients and the findings therefore require validation in a larger cohort. Although pathologies were different, patients with the same pathology of neuropathic pain often present with different symptoms and phenotyping in any study remains a challenge (19). What is more important is that all of the patients in this study responded to Burst-SCS. The phenotyping of patients to different waveforms of SCS has yet to be addressed in clinical studies. There is also little evidence to profile and phenotype CSF constituents between different patients with neuropathic pain and is largely confined to individual studies using controls (211, 431). Participants also had CSF taken at different distances to the target therapy, but other proteomic studies have highlighted that rostral-caudal gradient of CNS proteins does not differ along the axis of the spine (213, 351). Some studies using CSF routinely check for contamination by assessing the number of red cells within the sample (205-207, 286, 291). While we did not perform this check the application of a fine gauge needle which was utilised in our study led to minimal contamination in other studies (286, 291). Even in the presence of blood contamination protein level changes within the CNS have been successfully measured but this needs to be taken into account (351). None of the proteins significantly differentially expressed were related to possible blood contamination (351). Although there were no controls in this study, variations in repeated samples in the same individual do not demonstrate significant variation for proteomic analysis (432). Despite this a control group of non-responders to Burst-SCS would provide a stronger analysis. It would also be useful in future studies to use patient-matched blood samples for comparison or to include a sham control group to differentiate from potential placebo responders.

4.5 Conclusion:

Our research in this pilot study provides the first indication that the CSF proteome is altered by Burst-SCS. However, due to the small sample size any results should be considered preliminary in nature. The differential pathways altered in our cohort include those involved in synapse assembly and immune regulation. Significantly lower levels of singular proteins also suggest supraspinal and potential neuroendocrine effects. The ability of Burst-SCS to alter pathways in multiple cells within the CNS suggests that the mechanism of action is not solely dependent upon selective neuronal discharge. More research into the effect of Burst-SCS on CNS cellular function is required to fully elucidate its mechanism of action. We propose that a combination of multiple diagnostic and physiological parameters should be scrutinized to advance our knowledge of Burst-SCS's effects and the pathophysiology of chronic neuropathic pain.

Chapter 5:

An investigation into proteomic constituents of cerebrospinal fluid in patients with chronic peripheral neuropathic pain medicated with opioids- A Pilot Study (433)

Highlights:

- Cerebrospinal fluid proteome is modulated by opioids in chronic neuropathic pain patients
- Proteins related to nervous system development were differentially expressed
- Patients on opioids had increased expression of neural proteins, enzymes and receptors
- Opioids may have immunomodulatory properties via myeloid cell activation, neutrophil mediated immunity and differential expression of immune effectors

Published:

"Journal of Neuroimmune Pharmacology" (433)

https://doi.org/10.1007/s11481-020-09970-3

5.1 Abstract:

Introduction: The pharmacodynamics of opioids for chronic peripheral neuropathic pain are complex and likely extend beyond classical opioid receptor theory. Preclinical evidence of opioid modulation of central immune signalling has not been identified *in vivo* in humans. Examining the cerebrospinal fluid (CSF) of patients medicated with opioids is required to identify potential pharmacodynamic mechanisms.

Methods: We compared CSF samples of chronic peripheral neuropathic pain patients receiving opioids (n=7) versus chronic peripheral neuropathic pain patients not taking opioids (control group, n=13). Baseline pain scores with demographics were recorded. Proteome analysis was performed using mass spectrometry and secreted neuropeptides were measured by enzyme-linked immunosorbent assay.

Results: Based on Gene Ontology analysis, proteins involved in the positive regulation of nervous system development and myeloid leukocyte activation were increased in patients taking opioids versus the control group. The largest decrease in protein expression in patients taking opioids were related to neutrophil mediated immunity. In addition, notably higher expression levels of neural proteins (85%) and receptors (80%) were detected in the opioid group compared to the control group.

Conclusion: This study suggests modulation of CNS homeostasis, possibly attributable to opioids, thus highlighting potential mechanisms for the pharmacodynamics of opioids. We also provide new insights into the immunomodulatory functions of opioids *in vivo.*

5.2 Introduction

Opiates have been used to treat pain for centuries. The modern development of synthetic opioids with different specific properties has led to their extensive use in acute, chronic and cancer pain (434-436). Developments in opioid therapies have focused on reduction in serious side effects and have been largely unsuccessful, particularly in the management of chronic pain (437). The factors that have attenuated the prescription of opioids for chronic pain are related to increased risk of addiction, depression and death (14). These risks are not only focused solely on the individual patient but society as whole, with increased supply in circulation leading to divergence (14). The use of opioids in chronic pain can be made on a case by case basis where improvement in function and pain over the course of 3 months occurs in selected patients (45, 437-439). However, there is a paucity of independent evidence supporting the long-term use of opioids in patients with chronic pain in terms of efficacy and safety, with the development of tolerance, neuroendocrine dysfunction and depression leading to more morbidity than benefit (440-444).

Our understanding of the pharmacodynamic effect of opioids has historically focused on neurons and their opioid receptors. Opioids exert their analgesic effect by binding to opioid receptors mu (MOP), kappa (KOP) delta (DOP) and nociceptin/orphanin FQ (NOP) in primary afferent fibres (445). These G protein linked receptors trigger intracellular messaging systems inhibiting adenylate cyclase activity, inhibiting calcium conductance and aiding potassium influx in neurons (446). Opioids predominantly bind to neurons at the periaqueductal grey matter, rostral ventromedial medulla, amygdala and dorsal horn of the spinal cord (446, 447). Their intracellular actions lead to modulation of excitatory neuropeptides and postsynaptic inhibition of neurons involved in nociception (446). Opioid receptors have also been found in a wide array of cells within the CNS including glial cells and immune cell (447, 448). Pre-clinical studies have demonstrated opioids bind to both astrocytes and microglia inducing dynamic changes in cytokine, chemokine and neuropeptide release at the synaptic cleft (447). Since astrocytes and microglia have a profound influence over synaptic function and neuronal signalling, it is conceivable that opioids may contribute to neural-glial communications (152, 392, 449-451). Opioid receptors MOP, DOP, KOP and NOP have also been identified in macrophages, monocytes, lymphocytes and granulocytes (452).

Cross talk between glia, immune cells and neurons, referred to as the 'neuroimmune interface', occurs via messengers which include cytokines, chemokines, neurotrophins and other neuropeptides (3). A change in the dynamic of these messengers with opioids may enhance our knowledge of their pharmacodynamic properties *in vivo*. The concept of modulating central neuroimmune signalling has long been proposed in an attempt to provide a mechanism for analgesia with opioids (447, 453). There also remains considerable debate regarding whether opioids are immunosuppressive (442, 444, 454-456) and the *in vivo* human opioid neuroimmunopharmacology has remained largely unexplored.

Studying the difference in expression of proteomic and neuropeptide constituents of CSF in patients with neuropathic pain taking opioids versus those who are not taking opioids may give insight into opioid related mechanisms *in vivo* (457, 458). As CSF is composed of metabolites from cells within the CNS, alterations in the composition of this biological fluid is reflective of CNS modulation and pathological processes and represents the biological sample of choice for studying neuronal-glia interactions in humans (283). Numerous studies have been conducted investigating CSF, for the most part focusing on biomarker discovery for common neurodegenerative diseases (432, 459-465). The evolution of mass spectrometry techniques has radically altered the biological and clinical sciences. Label-free quantitative techniques have become more robust over the past decade, offering increased sensitivity and accuracy in conjunction with improved data processing algorithms (466, 467). Label-free approaches can be applied to any biological sample and label-free quantitative methods are based on the correlation that peak area for each peptide is linearly proportional to protein abundance in a single LC-MS run (467). Discovery-based mass proteomic approaches lend themselves to global analyses, whereby a broad analysis of the proteome is conducted across different samples (466). Quantitative label-free mass spectrometry can measure CSF proteins with low technical variability (468); and has been utilised by previous studies to explore the effectiveness of therapies in chronic pain including spinal cord stimulation (213, 321, 469, 470). Studying the differential expression of protein and neuropeptide constituents of CSF in patients medicated with chronic opioids may provide much needed insight into the opioid mechanism of action *in vivo* (457, 458). Previous studies have highlighted significant differences in the proteomic signatures in healthy CSF compared with CSF from chronic pain patients (28, 168, 170, 211, 213, 417, 471). This study focuses on proteomic changes in the CSF resulting from opioid treatment in a background of chronic neuropathic pain. Examination of CSF from the dorsal spinal

cord, where much attention to the genesis of Chronic Peripheral Neuropathic pain (CPNP) is derived, and where opioids exert their effect is compelling to investigate opioid related mechanisms (11, 458).

5.2.1 Aims

The aim of this chapter was to explore mechanisms of opioids in patients with neuropathic pain by comparing the neuropeptide and proteomic constituents of CSF in patients taking and not taking opioids

5.3 Methods

This is a post-hoc analysis of initial baseline CSF samples for studies examining mechanistic actions of medication used in the management of CPNP (321). The study was registered online at http://www.isrctn.com/ISRCTN70120536. Patients were offered inclusion following an outpatient pain clinic assessment to determine whether the patient met the inclusion/exclusion criteria (http://www.isrctn.com/ISRCTN70120536). All patients provided written informed consent prior to enrolment. This study was approved by the St James's and AMNCH Research Ethics Committee, Dublin, Ireland.

5.3.1 CSF Sampling

The CSF sampling occurred between 13:00-14:00 with the patients required to fast for 13-14 hours prior to the initial sample. Under strict asepsis and AAGBI guidelines (319), CSF was obtained between the fourth and fifth lumbar vertebra using Ultrasound or Fluoroscopy. Prior to performing the lumbar puncture (LP), 2-3ml of Lidocaine (1%) was allowed to infiltrate the skin at the site to provide local analgesia. LP was performed with an introducer and 25 Gauge Whittacre needle (B braun®) until resistance entering the dura was felt. The CSF was collected in chilled collection tubes and placed on ice; (2 x 1ml sample volumes) in two separate tubes: one for ELISA and one for mass spectrometry. The acquired CSF samples were visually inspected for blood contamination. To ensure there was no blood contamination and to eliminate any cells and other insoluble material, the

proteomics CSF aliquots were centrifuged immediately for 10 minutes at 2000 RPM at 4ºC. Following centrifugation (472) the supernatant was transferred to a new tube. The tubes were immediately frozen at -20 ºC for ELISA and the tubes for proteomic analysis were stored at -80 ºC at a separate facility until required for subsequent analysis.

5.3.2 Pain Measurement

Each patient completed an average 24-hour numerical rating score (NRS) questionnaire and Douleur Neuropathique score (DN4) prior to acquisition of the initial CSF sample. Daily medications were also recorded with the opioid doses confirmed.

5.3.3 Quantification of soluble mediators in CSF

Glial Cell Derived Neurotrophic factor (GDNF) and Fractalkine single plex ELISAs (Abcam, Cambridge, UK) were performed according to the manufacturer's guidelines. Mesoscale Diagnostics (MSD, Rockville, MD, USA) V-Plex Human Cytokine 30-Plex kit, R-Plex Human Brain Derived Neurotrophic factor (BDNF) antibody set with MSD Gold 96 SM Spot Streptavidin plate pack, and human Nerve Growth Factor (NGF) ELISAs were performed as per the manufacturer's instructions. MSD plates were read using MesoScale Diagnostics Sector S600. The sensitivities to the kits are available at www.abcam.com and www.mesoscale.com, respectively. The following cytokines measured in pg/ml and limits of detection in pg/ml were: GM-CSF 0.842-750, IL-1α 2.85-278, IL-5 4.41-562, IL-7 0.546-563, IL-12/IL-23p40 1.32-2,250, IL-15 0.774-525, IL-16 19.1-1,870, IL-17A 3.19-3650, TNF-β 0.465-458, VEGF-A 7.70-562, IFN-γ 1.76-938, IL-1β 0.646-375, IL-2 0.890-938, IL-4 0.218-158, IL-6 0.633-488, IL-8 0.591-375, IL-10 0.298-233, IL-12p70 1.22-315, IL-13 4.21-353, TNF-α 0.690-248, Eotaxin 12.3-1120, MIP-1β 1.02-750, Eotaxin-3 10.2-3750, TARC 3.32-1120, IP-10 1.37-500, MIP-1α 13.8-743, IL-8 713-43400, MCP-1 1.09-375, MDC 88.3-7500, MCP-4 5.13-469, NGF 0.05-498, BDNF 0.72-2000, GDNF 2.743-2000 and Fractalkine 3.91-250.

5.3.4 Preparation of CSF samples for mass spectrometry

All mass spectrometry (MS) and data analysis of the proteomic data was performed by Dr Hilary Cassidy, Systems Biology Ireland, University College Dublin (UCD). A shotgun proteomics approach was employed to analyse the CSF proteome, utilising a single-pot

solid-phase-enhanced sample preparation (SP3) for sample preparation (322). The SP3 protocol utilizes commercially available beads which carry a carboxylate moiety. For this experiment both hydrophobic and hydrophilic Sera-Mag Speed bead Magnetic carboxylate modified particles were employed in a 1:1 mix (GE Healthcare). Prior to use the beads were combined in a ratio of 1:1 (v/v), rinsed and reconstituted in MS grade water (Fisher Scientific) at a stock concentration of 10µg/ml and stored at 4°C until required.

SP3 preparation was performed according to the protocol of Hughes *et al* (322). Prior to beginning sample preparation for mass spectrometry, the protein content of the CSF samples was measured by BCA assay to ensure that all samples would contain equal amounts of protein at the beginning of the preparation to avoid huge variations in the mass spectrometry results. To begin sample preparation 200µg CSF was resuspended in 100µl lysis buffer [6M urea, 2M thiourea, 50mM MOPS) and centrifuged for 15 minutes at 15,000 RCF at 4^{o}C to remove any cellular debris. The supernatant was transferred to a fresh Eppendorf tube. The CSF was reduced by adding 0.2M 1,4-dithiothreitol (DTT; Sigma Aldrich) and incubated at 37^{o}C on a shaker at 700 rpm for 15 minutes. Samples were then alkylated by adding 0.4M iodoacetamide (IAA; Sigma Aldrich). Next acetonitrile (ACN; Sigma Aldrich) was added to each sample to give a final concentration of 70% acetonitrile (v/v) and the prepared SP3 bead mixture was added to each sample and rotated for 18 minutes at room temperature. Subsequently the beads were immobilized by incubation for 2 minutes on the DynaMag-2™ stand (Thermo Fisher). The supernatant was discarded and the pellet was rinsed with 70% (v/v) ethanol in water and 100% ACN. Beads were resuspended in 50 mM ammonium bicarbonate (NH_4HCO_3; Sigma Aldrich). The pH was adjusted to pH 7. Lyophilised sequence grade trypsin (Promega) was resuspended in 50mM ammonium bicarbonate to a final concentration of 0.5µg/µl before 4µl of trypsin was added to each sample. After overnight digestion at 37°C on a thermoshaker at 500rpm, an additional 8µl of prepared bead mixture was added to the samples. The pH was readjusted, if necessary, to pH 7 and ACN was added to reach a final concentration of 95% (v/v). After mixing and incubation, the sample was placed on a DynaMag-2™ magnetic stand, the supernatant was removed and beads were rinsed with 100% can in the same manner. The peptides bound to the beads were eluted using 20µl HPLC grade water with intermittent vortexing. The sample was placed on the DynaMag-2™ magnetic stand for 5 minutes before the supernatant containing the purified peptides was transferred into a fresh tube containing 2µl of 10% acetic acid. The samples were centrifuged for 15 minutes at 15,000

RCF at 4°C and then placed on the DynaMag-2™ for 5 minutes before the supernatant was transferred to MS vials for analysis.

5.3.5 LC-MS/MS analysis

Each sample was run in duplicate on a Thermo Scientific Q Exactive mass spectrometer connected to a Dionex Ultimate 3000 (RSLCnano) chromatography system. Each sample was loaded onto a fused silica emitter (75µm ID), pulled using a laser puller (Sutter Instruments P2000, Novato, CA, USA), packed with ReprocilPur (Dr Maisch, Ammerbuch-Entringen, Germany) C18 (1.9µm; 12 cm in length) reverse phase media and were separated by an increasing acetonitrile gradient over 60 minutes at a flow rate of 250 nL/min direct into a Q-Exactive mass spectrometer. The mass spectrometer was operated in positive ion mode with a capillary temperature of 320 °C, and with a potential of 2300 V applied to the frit. All data was acquired while operating in automatic data dependent switching mode. A high resolution (70,000) MS scan (300-1600 m/z) was performed using the Q Exactive to select the 12 most intense ions prior to MS/MS analysis using high-energy collision dissociation (HCD).

5.3.6 Protein identification and quantification

Proteins were identified and quantified by MaxLFQ (323) by searching with MaxQuant version 1.5 against the Homo Sapiens reference proteome database which was obtained from Uniprot. Normalisation is conducted through the MaxQuant LFQ algorithm for label-free quantification (323), which has successfully been benchmarked against other software solutions for label-free quantification, independently confirming its performance (324). MaxLFQ is a generic method for label-free quantification that can be combined with standard statistical tests of quantification accuracy for each of thousands of quantified proteins. In brief, protein abundance profiles are assembled using the maximum possible information from MS signals, given that the presence of quantifiable peptides varies from sample to sample. This is based on the assumption that most proteins do not or only minimally change between conditions, to have a constant baseline (the algorithm still works with (quantitative) changes in about one third of all proteins (323). Once the Maxquant analysis is complete, the individual LFQ intensities for all technical replicates were expressed as a Log_2 value and an average Log_2 value was determined for each of the

treatment groups, i.e. control group and Opioid treatment group. The log fold change (LFC ; Log_2(Opioid) -Log_2(Control)) was calculated as well as a false discovery rate (FDR) and p value. This data was utilised for manual filtering of the proteins to identify differentially expressed proteins.

The free program Perseus (obtained from https://maxquant.net/perseus/) (473), was utilised to analyse the proteomic data and generate the volcano plots. The raw data (in the form of a tab separated values file (.tsv)) generated from the Maxquant search was loaded into the program through the generic matrix upload button. All expression columns were transferred into "main" columns window, all other numerical data was uploaded into the "numerical" column and finally all columns containing identifiers such as protein IDs were entered in to "text" column. In the processing tab all rows were filtered based on categorical column to exclude proteins identified by site, matching to the reverse database or contaminants, reducing the matrix. Under the processing tab, select basic and transform to transform to a logarithmic scale (log_2(x)). Missing/zero values were then imputed from the normal distribution. Rows are then filtered based on valid values, keeping the default 70% value for the minimum percentage of values parameter. Next, the rows are annotated selecting "categorical annotation rows", and all samples belonging to the same condition or treatment i.e. opioids or no opioids, were given the same annotation. To graphically represent the t-test data, a volcano plot was created by clicking on analysis and selecting the volcano plot icon and then utilising the default s0 and FDR values. A LFC of more than 2 or less than -2, combined with a -LogP cutoff of greater than 1.13 was deemed significant. The list of significantly differentially expressed proteins were exported from Perseus for additional analysis. Heatmaps of significant global protein expression was carried out using XLSTAT (Addinsoft, NY, USA), an Excel add-in, was utilised to create heatmaps of significant global protein expression with unsupervised analysis.

All proteins found to be differentially expressed between groups (-2< LFC >2) with an FDR<0.05 (equates to LogP >1.13) were subjected to pathway mapping analysis and were distributed into categories according to their cellular component, molecular function, and biological process. Pathway and network analysis of the identified proteins was generated through the use of Ingenuity Pathway Analysis (IPA) [http://www.ingenuity.com QIAGEN Inc. (Redwood City, CA)], taking into consideration whether the proteins were increased or decreased(474). STRING Database (Version 11) (www.string-db.org) was used to

generate protein-protein interaction (PPI) networks. Protein accession numbers (UniProt) for the identified important proteins were entered in the search engine (multiple proteins) with the following parameters: organism was Homo sapiens; the maximum number of interactions was query proteins only; interaction score was set to minimum required interaction score of high confidence (0.700); and an FDR ≤ 0.05. In these PPI network figures, each protein is represented by a colored node, and protein-protein interaction and association are represented by an edge represented by a line. Higher combined confidence scores are represented by thicker lines. The generated network was further investigated to identify a group of proteins that clustered together by selecting the k-mean clustering option and the significant biological process for the cluster was identified. The clustered string network was exported as a .tsv file and imported into the Cytoscape program (Version 3.7.2; https://cytoscape.org/) to further refine the network and generate the protein hubs (475). Panther classification system (http://www.pantherdb.org/genes/batchIdSearch.jsp) was utilised to determine protein classification and identify signalling pathways (476). The NeuroPep database (islab.info/NeuroPep/) and the neuropeptides database (www.neuropeptides.nl) were employed to identify neuropeptides identified by the mass spectrometry analysis. Shiny Go (http://bioinformatics.sdstate.edu/go/) were used to assess GO biological and molecular functions. The list of proteins were submitted to the program by their UniProt identifier.

5.3.7 Statistical analysis:

All statistical analysis was performed on Graph Pad Prism version 8.0. Non-parametric unpaired Mann Whitney tests were used to analyse data sets and Fisher's exact test for contingency data. Data was expressed in means with standard error of means (SEM), p values of <0.05 were considered to be significant. The analysis for proteomics is detailed in the results section.

5.4 Results

5.4.1 Patient enrolment and demographics

A total of 20 patients had a CSF sample taken of which 7/20 (35%) patients were receiving opioids. Each patient had a DN4 score of >4 and was clinically diagnosed with neuropathic pain prior to CSF sampling. The demographics are summarised in **Table 23** and there were no significant differences between each group in relation to age (p=0.6), diagnosis (p=1), DN4 score (p=0.28) and pain scores (p=0.85). One patient was on another analgesic medication (pregabalin) for neuropathic pain and was in the control group. All of the patients taking opioids had been receiving stable doses for >3 months prior to enrolment in the study. The different opioids, doses and the milligram morphine equivalents (MME) of the patients are detailed in **Table 24**.

Table 23: Demographics of the Chronic Peripheral Neuropathic Pain (CPNP) patients taking opioids versus controls with comparison between groups

	CPNP Patients taking Opioids n=7	Control Group n=13	p value
Age	52.86 +/- 2.595	49.54 +/- 3.016	0.6
Gender	Male N=2 Female N=5	Male N=7 Female N=6	0.37
Pain Score (NRS)	7.143 +/- 0.40	6.923 +/- 0.54	0.85
DN4 Score	6.857 +/- 0.63	5.923 +/-0.48	0.28
Diagnosis			
Painful Radiculopathy	6	10	
Failed Back/Neck Surgery Syndrome	1	2	
Post-Surgical Thoracic Pain	0	1	1
Other analgesic medications	0	1 (Pregabalin)	1

Data is presented as means with standard error of means. Non-parametric unpaired Mann Whitney tests were used for analysis to compare data sets and Fisher's exact test for contingency data. Abbreviations: DN4; Douleur Neuropathique 4, NRS; Numerical Rating Score

Table 24: Daily Opioid Use and Morphine milligram equivalents (MME) of the patients taking opioids.

Patient	Daily Opioid Use	MME
1	Oxycodone 60mg	120mg
2	Fentanyl patch 75mcg/hr	270mg
3	Oxycodone 20mg	40mg
4	Tramadol 100mg	20mg
5	Codeine 240mg	24mg
6	Tramadol 200mg	40mg
7	Oxycodone 20mg	40mg

All opioid prescribed had been taken for at least 3 months prior to CSF sampling with compliance confirmed verbally

5.4.2 Proteomics Analysis

The CSF proteome of the patients who were taking opioids was compared to the patients not taking opioids control group. In total 992 proteins were identified in the CSF, with 618 proteins increased (LFC>0) in the CSF of the opioid group versus the control group and 336 were decreased (LFC<0). For the purposes of identifying proteins which were significantly altered in the CSF, strict filtering settings were applied to the proteomics data in order to identify proteins which were significantly increased [log fold change (LFC)>1.5, False Discovery Rate (FDR)<0.05] **(Table 25)** and decreased (LFC <-1.5, FDR <0.05) **(Table 26).**

Perseus (http://www.perseus-framework.org) (477) was employed with stricter filtering to compare the CSF proteomes from the patients taking opioids compared with the control group and it identified a total of 300 significantly differentially expressed proteins (30.2% of total proteins; -2<log fold change (LFC) > 2, FDR<0.05) **(Figure 32A)**. Of these 300 differentially expressed proteins, 246 proteins (82%) were found to be upregulated and 54 proteins (18%) were downregulated in the CSF proteome of the opioid group.

Table 25: All differentially upregulated proteins (Log fold change >1.5, FDR<0.05) in the Cerebrospinal fluid (CSF) proteome of Chronic Peripheral Neuropathic Pain (CPNP) patients taking opioids in order of log fold change

Protein	Gene	Log Fold Change	P Value	FDR
Synaptonemal complex central element protein 1-like	SYCE1L	24.66178	0.174832	0.019304
Somatostatin	SST	22.02115	0.057629	0.008115
Cadherin-5	CDH5	21.90312	0.058012	0.008216
Vesicle-fusing ATPase	NSF	21.90045	0.168521	0.018548
Mesothelin	MSLN	21.73669	0.050855	0.007308
OX-2 membrane glycoprotein	CD200	21.72044	0.026686	0.004385
Protein CASC4	CASC4	21.14383	0.335561	0.029738
Immunoglobulin heavy variable 1-3	IGHV1-3	20.95513	0.335561	0.030091
Immunoglobulin lambda variable 4-60	IGLV4-60	20.81654	0.045904	0.006754
Contactin-3	CNTN3	20.52557	0.164947	0.017137
Receptor-type tyrosine-protein phosphatase-like N	PTPRN	20.50726	0.089628	0.011139
Ephrin type-A receptor 5	EPHA5	20.45295	0.093874	0.011643
Amyloid-like protein 1	APLP1	20.19944	0.165445	0.01749
Neuromodulin	GAP43	20.12438	0.041541	0.005998
ABHD14A-ACY1 readthrough	ABHD14A-ACY1	20.06228	0.169729	0.0188
Nucleobindin-2	NUCB2	20.03563	0.022985	0.003679
Lysosomal acid lipase/cholesteryl ester hydrolase	LIPA	19.93367	0.116871	0.013256
PITH domain-containing protein 1	PITHD1	19.82302	0.042214	0.0062
E3 ubiquitin-protein ligase RNF13	RNF13	19.79703	0.166044	0.017893
Ephrin-A5	EFNA5	19.72318	0.335561	0.030141
Semaphorin-6A	SEMA6A	19.70458	0.166361	0.018095
Paired immunoglobulin-like type 2 receptor alpha	PILRA	19.70236	0.083159	0.010282

Glia maturation factor gamma	GMFG	19.70037	0.335561	0.029536
Proprotein convertase subtilisin/kexin type 9	PCSK9	19.69002	0.029069	0.004536
alpha-1,2-Mannosidase	MAN1B1	19.67396	0.150918	0.015423
Microtubule-actin cross-linking factor 1, isoforms 1/2/3/5	MACF1	19.65628	0.335561	0.029688
N(G),N(G)-dimethylarginine dimethylaminohydrolase 1 (DDAH-1)	DDAH1	19.63079	0.168952	0.0187
Arginyl-tRNA--protein transferase 1	ATE1	19.55463	0.335561	0.02994
Butyrophilin subfamily 2 member A1	BTN2A1	19.5287	0.091234	0.011341
Anthrax toxin receptor 1	ANTXR1	19.49814	0.335561	0.028881
Protein FAM19A2	FAM19A2	19.46422	0.166416	0.018145
Intercellular adhesion molecule 2	ICAM2	19.44359	0.083289	0.010333
Small subunit processome component 20 homolog	UTP20	19.38053	0.335561	0.029435
Netrin receptor UNC5C	UNC5C	19.36692	0.165176	0.017339
Osteoclast-associated immunoglobulin-like receptor	OSCAR	19.32937	0.164952	0.017188
Coactosin-like protein	COTL1	19.30675	0.176319	0.019355
Malectin	MLEC	19.2752	0.082789	0.010181
Voltage-dependent calcium channel subunit alpha-2/delta-3	CACNA2D3	19.25643	0.335561	0.030292
CD320 antigen	CD320	19.24186	0.164896	0.017087
Neurogenic locus notch homolog protein 3	NOTCH3	19.22009	0.16889	0.018599
HCG2044781 (TMEM189-UBE2V1 readthrough)	TMEM189-UBE2V1	19.21095	0.133757	0.014264
Cation-independent mannose-6-phosphate receptor	IGF2R	19.06609	0.098392	0.012046
Arylsulfatase A	ARSA	19.05992	0.165664	0.017692

Protein Z-dependent protease inhibitor	SERPINA10	18.8724	0.335561	0.029788
UPF0454 protein C12orf49	C12orf49	18.78126	0.208433	0.021774
Complement factor H-related protein 3	CFHR3	18.67571	0.335561	0.030343
14-3-3 protein epsilon	YWHAE	18.66739	0.186778	0.02006
Calsyntenin-2	CLSTN2	18.65316	0.165933	0.017792
Tetraspanin	CD81	18.63298	0.335561	0.02999
Acetylcholinesterase	ACHE	18.57476	0.165447	0.01754
Neuroplastin	NPTN	18.53814	0.165247	0.017389
Carboxypeptidase M	CPM	18.46278	0.335561	0.029385
Apolipoprotein	LPA	18.43665	0.335561	0.030393
Cholinesterase	BCHE	18.39827	0.176695	0.019405
Trophoblast glycoprotein	TPBG	18.31723	0.165013	0.017288
Neudesin	NENF	18.31271	0.335561	0.02878
Selenoprotein M	SELENOM	18.29472	0.335561	0.030242
EPH receptor A10, isoform CRA_b (Ephrin type-A receptor 10)	EPHA10	18.19646	0.220252	0.022379
EPHB2 protein (Ephrin type-B receptor 2)	EPHB2	18.15431	0.172098	0.019052
Complement C1q tumor necrosis factor-related protein 4	C1QTNF4	18.08462	0.08692	0.010786
Protocadherin-7	PCDH7	18.04386	0.1689	0.018649
Thioredoxin domain-containing protein 17	TXNDC17	18.03641	0.166534	0.018196
Carbonic anhydrase 14	CA14	18.00228	0.187979	0.020262
Glutathione synthetase	GSS	17.92455	0.170168	0.018901
Chondroadherin	CHAD	17.86976	0.335561	0.029486
Connective tissue growth factor	CTGF	17.80279	0.335561	0.029284
Neuroligin-1	NLGN1	17.79157	0.335561	0.029587
Disintegrin and metalloproteinase domain-containing protein 15	ADAM15	17.68214	0.335561	0.029133

Receptor-type tyrosine-protein phosphatase kappa	PTPRK	17.60872	0.335561	0.029889
Alpha-N-acetylgalactosaminidase	NAGA	17.60573	0.335561	0.029335
Protein disulfide-isomerase	P4HB	17.48053	0.335561	0.029637
Lipolysis-stimulated lipoprotein receptor	LSR	17.41465	0.335561	0.028982
Leucine-rich repeat neuronal protein 1	LRRN1	17.23825	0.098503	0.012097
Leukocyte-associated immunoglobulin-like receptor 1	LAIR1	17.12775	0.335561	0.03004
Transferrin receptor	TFRC	17.05848	0.335561	0.029839
Transmembrane protein 59-like	TMEM59L	16.8833	0.335561	0.028831
Neural cell adhesion molecule 1	NCAM1	16.87903	0.335561	0.030192
TGF-beta receptor type-2	TGFBR2	16.80833	0.335561	0.029234
Cysteine-rich with EGF-like domain protein 1	CRELD1	16.71284	0.335561	0.028931
14-3-3 protein gamma	YWHAG	16.66435	0.335561	0.029183
Desmocollin-3	DSC3	16.52968	0.335561	0.029083
Semaphorin-3B	SEMA3B	16.02421	0.335561	0.030444
Protein FAM19A1	FAM19A1	15.37256	0.335561	0.029032
Interferon alpha/beta receptor 2	IFNAR2	4.817185	0.03645	0.00499
Laminin subunit beta-2	LAMB2	4.529234	0.099933	0.012248
Ectonucleotide pyrophosphatase/phosphodiesterase family member 5	ENPP5	4.463306	0.14266	0.014869
Serum amyloid A-1 protein	SAA1	3.898049	0.204309	0.021522
VPS10 domain-containing receptor SorCS1	SORCS1	3.871786	0.018498	0.003327
Protocadherin-17	PCDH17	3.558703	0.061161	0.008619
Immunoglobulin lambda variable 5-45	IGLV5-45	3.541067	0.128092	0.013911

Soluble scavenger receptor cysteine-rich domain-containing protein SSC5D	SSC5D	3.449979	0.080188	0.01003
Calnexin	CANX	3.377965	0.05638	0.007964
Basal cell adhesion molecule	BCAM	3.293447	0.138492	0.014718
Zona pellucida sperm-binding protein 2	ZP2	3.274105	0.233164	0.023034
Lysosomal alpha-glucosidase	GAA	3.212538	0.173125	0.019153
Protein HEG homolog 1	HEG1	3.079056	9.35E-05	0.000151
Myelin-associated glycoprotein	MAG	3.05987	0.092418	0.011391
WAP four-disulfide core domain protein 2	WFDC2	3.002885	0.008644	0.001663
Ephrin-B1	EFNB1	2.921955	0.00044	0.000252
Sialic acid-binding Ig-like lectin 14	SIGLEC14	2.917524	0.003986	0.000806
Adhesion G protein-coupled receptor B2	ADGRB2	2.905839	0.001948	0.000655
SLIT and NTRK-like protein 5	SLITRK5	2.885452	0.084618	0.010383
Endothelial cell-selective adhesion molecule	ESAM	2.87386	0.007985	0.001512
Netrin receptor DCC	DCC	2.866807	0.166057	0.017994
Cytokine-like protein 1	CYTL1	2.808965	0.011333	0.002117
Leucine-rich repeat transmembrane neuronal protein 2	LRRTM2	2.7566	0.100408	0.012298
Dipeptidyl aminopeptidase-like protein 6	DPP6	2.738209	0.026508	0.004234
Endosialin	CD248	2.733795	0.187215	0.020161
Sortilin-related receptor	SORL1	2.727177	0.02117	0.003528
Ras guanyl-releasing protein 3	RASGRP3	2.727066	0.415735	0.032863
Plexin domain-containing protein 1	PLXDC1	2.691209	0.012608	0.002218
Ryanodine receptor 2	RYR2	2.641703	0.292659	0.025756
Peptidyl-prolyl cis-trans isomerase C	PPIC	2.489816	0.044777	0.006552
Neuroligin-2	NLGN2	2.482087	0.022993	0.00373

cDNA FLJ57652, highly similar to Ephrin-A3		2.373841	0.03736	0.005192
Neuropilin-2	NRP2	2.359144	0.055803	0.007863
Cell growth regulator with EF hand domain protein 1	CGREF1	2.357567	0.015697	0.002722
Serotransferrin	TF	2.334772	0.054418	0.007661
Phosphoserine aminotransferase	PSAT1	2.260868	0.05972	0.008367
Polypeptide N-acetylgalactosaminyltransferase 18	GALNT18	2.255398	0.066608	0.009073
Carbohydrate sulfotransferase 10	CHST10	2.198144	0.078821	0.009929
Noelin	OLFM1	2.175841	0.022525	0.003579
Semaphorin-6D	SEMA6D	2.126839	0.089889	0.01124
C-type mannose receptor 2	MRC2	2.07709	0.034984	0.004788
Contactin-associated protein-like 2	CNTNAP2	2.014482	0.050151	0.007056
Double-stranded RNA-specific editase 1	ADARB1	2.011919	0.120664	0.013357
DOMON domain-containing protein FRRS1L	FRRS1L	2.001758	0.096501	0.011946
Alpha-mannosidase 2	MAN2A1	2.001277	0.047849	0.006956
Eukaryotic translation initiation factor 2 subunit 3B	EIF2S3B	1.956133	0.255061	0.023942
Dihydrolipoyl dehydrogenase	DLD	1.948128	0.484462	0.035081
Twisted gastrulation protein homolog 1	TWSG1	1.934232	0.036844	0.005141
Prosaposin receptor GPR37L1	GPR37L1	1.932018	0.043288	0.006401
Myelin-oligodendrocyte glycoprotein	MOG	1.850306	0.000758	0.000353
Xylosyltransferase 1	XYLT1	1.822795	0.254493	0.023891
Protein disulfide-isomerase A3	PDIA3	1.813008	0.044621	0.006502
UAP56-interacting factor	FYTTD1	1.797307	0.307902	0.026109
Netrin-G1	NTNG1	1.774105	0.045025	0.006603
NAD	NAXE	1.766507	0.237847	0.023236
Cadherin-4	CDH4	1.742451	0.010782	0.002016

Secreted and transmembrane protein 1	SECTM1	1.735821	0.243717	0.023488
AP complex subunit beta	AP2B1	1.72076	0.187722	0.020212
Collagen alpha-1(XV) chain	COL15A1	1.706092	0.00526	0.001058
Xyloside xylosyltransferase 1	XXYLT1	1.661432	0.10619	0.012702
Transmembrane protein 132A	TMEM132A	1.644929	0.088675	0.011038
Thymosin beta-4	TMSB4X	1.630875	0.081281	0.010131
Protein FAM69C	FAM69C	1.615922	0.074445	0.009829
Polypeptide N-acetylgalactosaminyltransferase 6	GALNT6	1.582305	0.162494	0.016633
Immunoglobulin lambda variable 2-18	IGLV2-18	1.57906	0.014436	0.002419
Neuroendocrine convertase 1	PCSK1	1.55933	0.018454	0.003276
Neuronal pentraxin-2	NPTX2	1.543237	0.016344	0.002823
Tropomodulin-1	TMOD1	1.539528	0.40081	0.03246
Mannosyl-oligosaccharide 1,2-alpha-mannosidase IC	MAN1C1	1.53159	0.198058	0.021119

Table 26: All differentially downregulated proteins (Log fold change <-1.5, FDR<0.05) in the Cerebrospinal fluid (CSF) proteome of Chronic Peripheral Neuropathic Pain (CPNP) patients taking opioids in order of log fold change

Protein	**Gene**	**Log Fold Change**	**P Value**	**FDR**
Carbonic anhydrase 1	CA1	-28.4265	0.16222	0.016431
Hemoglobin subunit delta	HBD	-26.9462	0.161655	0.016028
Interferon-induced transmembrane protein 3	IFITM3	-26.8369	0.326892	0.027772
Carbonic anhydrase 2	CA2	-25.6795	0.161407	0.015978
Testis-expressed protein 2	TEX2	-25.3467	0.196323	0.020867
Catalase	CAT	-25.1879	0.161684	0.016079
Flavin reductase	BLVRB	-24.7856	0.165595	0.017591
Hemoglobin subunit gamma-2	HBG2	-23.7095	0.185769	0.02001

Carbonic anhydrase 3	CA3	-23.2549	0.16246	0.016583
Ceruloplasmin	CP	-23.1349	0.161884	0.01628
Ankyrin-1	ANK1	-22.4539	0.164645	0.017036
Protein S100-A4	S100A4	-21.8733	0.159009	0.015776
Immunoglobulin kappa variable 1-12	IGKV1-12	-21.7932	0.038622	0.005393
Immunoglobulin heavy variable 3-64	IGHV3-64	-21.6406	0.095677	0.011895
Nucleoside diphosphate kinase A	NME1	-21.6353	0.161774	0.016179
Bisphosphoglycerate mutase	BPGM	-21.5705	0.165378	0.01744
Growth hormone A1	PRL	-21.2976	0.292487	0.025706
Adenylate kinase isoenzyme 1	AK1	-21.2296	0.166185	0.018044
Transmembrane protein 139	TMEM139	-21.1675	0.161924	0.016331
Immunoglobulin kappa variable 1-27	IGKV1-27	-21.1539	0.104412	0.01255
HLA class I histocompatibility antigen, A-24 alpha chain	HLA-A	-20.8984	0.038807	0.005494
Delta-aminolevulinic acid dehydratase	ALAD	-20.7888	0.164113	0.016885
Eukaryotic translation initiation factor 5A	EIF5A2	-20.6215	0.164074	0.016835
Rho guanine nucleotide exchange factor 18	ARHGEF18	-20.4302	0.326892	0.028327
Msx2-interacting protein	SPEN	-20.408	0.199251	0.02127
Purine nucleoside phosphorylase (PNP)	PNP	-20.3336	0.166725	0.018246
HCG1745306, isoform CRA_a (Hemoglobin subunit alpha)	HBA2	-20.3324	0.326892	0.027571
Creatine kinase M-type	CKM	-20.2597	0.1617	0.016129
Histone H2B	HIST1H2BN	-20.2166	0.092896	0.011542
Hsc70-interacting protein	ST13	-20.1757	0.166887	0.018296
Endothelin-3	EDN3	-20.0723	0.013141	0.002319
Spectrin beta chain, erythrocytic	SPTB	-20.0247	0.326892	0.027218
Mitotic spindle assembly checkpoint protein MAD1	MAD1L1	-19.954	0.326892	0.027823
Spondin-2	SPON2	-19.9432	0.126747	0.01381
Basigin	BSG	-19.79	0.09471	0.011794

Erythrocyte membrane protein band 4.2	EPB42	-19.6468	0.326892	0.027067
Serum albumin	ALB	-19.5729	0.0831	0.010232
Retinal dehydrogenase 1	ALDH1A1	-19.491	0.165614	0.017641
Band 3 anion transport protein	SLC4A1	-19.4468	0.326892	0.027369
Growth/differentiation factor 8	MSTN	-19.4141	0.124666	0.013609
Sodium/potassium-transporting ATPase subunit beta	ATP1B1	-19.2442	0.050952	0.007359
Transmembrane glycoprotein NMB	GPNMB	-19.2396	0.263353	0.024345
Myosin-7	MYH7	-19.0982	0.326892	0.027167
Myosin-2	MYH2	-19.0844	0.18101	0.019708
Phosphoglycerate mutase 1	PGAM1	-18.9889	0.090213	0.01129
Adenosine deaminase 2	ADA2	-18.9464	0.161822	0.01623
Hemoglobin subunit zeta	HBZ	-18.8885	0.166047	0.017944
Legumain	LGMN	-18.7034	0.085974	0.010635
Secretogranin-1	CHGB	-18.65	0.326892	0.028175
Immunoglobulin heavy variable 3/OR16-10	IGHV3OR16-10	-18.589	0.162652	0.016683
GTP-binding nuclear protein Ran	RAN	-18.56	0.326892	0.027873
Junction plakoglobin	JUP	-18.486	0.326892	0.027117
Meteorin-like protein	METRNL	-18.4752	0.167299	0.018397
Beta-galactoside alpha-2,6-sialyltransferase 2	ST6GAL2	-18.4205	0.165998	0.017843
UDP-GalNAc:beta-1,3-N-acetylgalactosaminyltransferase 1	B3GALNT1	-18.4021	0.103632	0.01245
Protein 4.1	EPB41	-18.3599	0.326892	0.028024
Epithelial discoidin domain-containing receptor 1	DDR1	-18.3329	0.326892	0.026865
ADAM DEC1	ADAMDEC1	-18.2416	0.239039	0.023286
Chitinase domain-containing protein 1	CHID1	-18.2385	0.326892	0.026563
Vimentin variant 3	VIM	-18.2288	0.326892	0.027974
Biglycan	BGN	-18.1909	0.326892	0.030998

Histone H1.2	HIST1H1C	-18.19	0.087363	0.010887
Desmoglein-1	DSG1	-18.1229	0.326892	0.026915
Cadherin-10	CDH10	-18.0496	0.167769	0.018498
Immunoglobulin heavy variable 3-20	IGHV3-20	-18.0435	0.326892	0.028125
Ryanodine receptor 3	RYR3	-17.9843	0.326892	0.028427
Prosaposin receptor GPR37	GPR37	-17.8731	0.162428	0.016482
Protein S100-A9	S100A9	-17.7937	0.326892	0.027319
Rho GTPase-activating protein 5	ARHGAP5	-17.7179	0.326892	0.028226
Immunoglobulin heavy variable 1-58	IGHV1-58	-17.7155	0.326892	0.028075
Chitotriosidase-1	CHIT1	-17.6231	0.326892	0.027722
Zinc transporter ZIP12	SLC39A12	-17.5753	0.326892	0.026764
Matrix remodeling-associated protein 8	MXRA8	-17.5013	0.326892	0.045766
Target of Nesh-SH3	ABI3BP	-17.4858	0.181172	0.019758
Apolipoprotein F	APOF	-16.975	0.326892	0.026815
Golgi apparatus protein 1, isoform CRA_c	GLG1	-16.9711	0.326892	0.02752
Palmitoyl-protein thioesterase 1	PPT1	-16.8959	0.326892	0.027621
Ribose-phosphate pyrophosphokinase 1	PRPS1	-16.8957	0.326892	0.027923
Low-density lipoprotein receptor-related protein 11	LRP11	-16.8382	0.326892	0.026714
Leucine zipper protein 1	LUZP1	-16.3551	0.326892	0.026663
Group XV phospholipase A2	PLA2G15	-16.0955	0.326892	0.02747
Procollagen-lysine,2-oxoglutarate 5-dioxygenase 3	PLOD3	-15.9848	0.326892	0.027419
Serglycin	SRGN	-15.9455	0.326892	0.027268
Fatty acid-binding protein 5	FABP5	-15.3405	0.326892	0.026966
Angiopoietin-related protein 2	ANGPTL2	-14.7778	0.326892	0.048841
Hemoglobin subunit alpha	HBA1;	-9.54202	0.132227	0.014113
Hemoglobin subunit beta	HBB	-8.91284	0.136266	0.014466
Myoglobin	MB	-5.61107	0.109928	0.012853

Peroxiredoxin-2	PRDX2	-4.82682	0.162459	0.016532
Immunoglobulin heavy variable 1-2	IGHV1-2	-4.3068	0.190482	0.020514
Immunoglobulin kappa variable 6D-21	IGKV6D-21	-3.8097	0.128453	0.013962
Trypsin-3	PRSS3	-3.43361	0.043011	0.0063
Immunoglobulin heavy variable 1-46	IGHV1-46	-2.91159	0.088311	0.010988
WASH complex subunit 2A	WASHC2A	-2.85609	0.005069	0.001008
Immunoglobulin heavy variable 4-34	IGHV4-34	-2.66284	0.015553	0.002671
Peroxiredoxin-6	PRDX6	-2.48461	0.356017	0.030998
Vitamin D-binding protein	GC	-2.45333	0.046582	0.006855
Protein S100-A6	S100A6	-2.19869	0.136567	0.014516
Immunoglobulin heavy variable 2-70D	IGHV2-70D	-2.18034	0.037998	0.005242
Serine protease inhibitor Kazal-type 6	SPINK6	-2.13905	0.033723	0.004738
Protein shisa-6	SHISA6	-2.13773	0.001095	0.000454
Immunoglobulin heavy variable 3-13	IGHV3-13	-2.11486	0.140565	0.014819
Properdin	CFP	-1.96741	0.252028	0.02379
Sex hormone-binding globulin, isoform CRA_a	SHBG	-1.80155	0.103194	0.012349
VPS10 domain-containing receptor SorCS3	SORCS3	-1.79093	0.067862	0.009123
Semaphorin-3G	SEMA3G	-1.7667	0.15996	0.015927
Immunoglobulin kappa variable 6-21	IGKV6-21	-1.75667	0.157287	0.015575
Neurexin-3-beta	NRXN3	-1.72464	0.256127	0.024042
Immunoglobulin kappa variable 1-16	IGKV1-16	-1.67578	0.131554	0.014063
Neuron-specific vesicular protein calcyon	CALY	-1.62946	0.092729	0.011442
A disintegrin and metalloproteinase with thrombospondin motifs 4	ADAMTS4	-1.6216	0.167224	0.018347
Peroxiredoxin-1	PRDX1	-1.5262	0.243119	0.023438
Heat shock 70 kDa protein 6	HSPA6	-1.50639	0.033205	0.004688
Glutathione hydrolase 7	GGT7	-1.50253	0.37466	0.031552

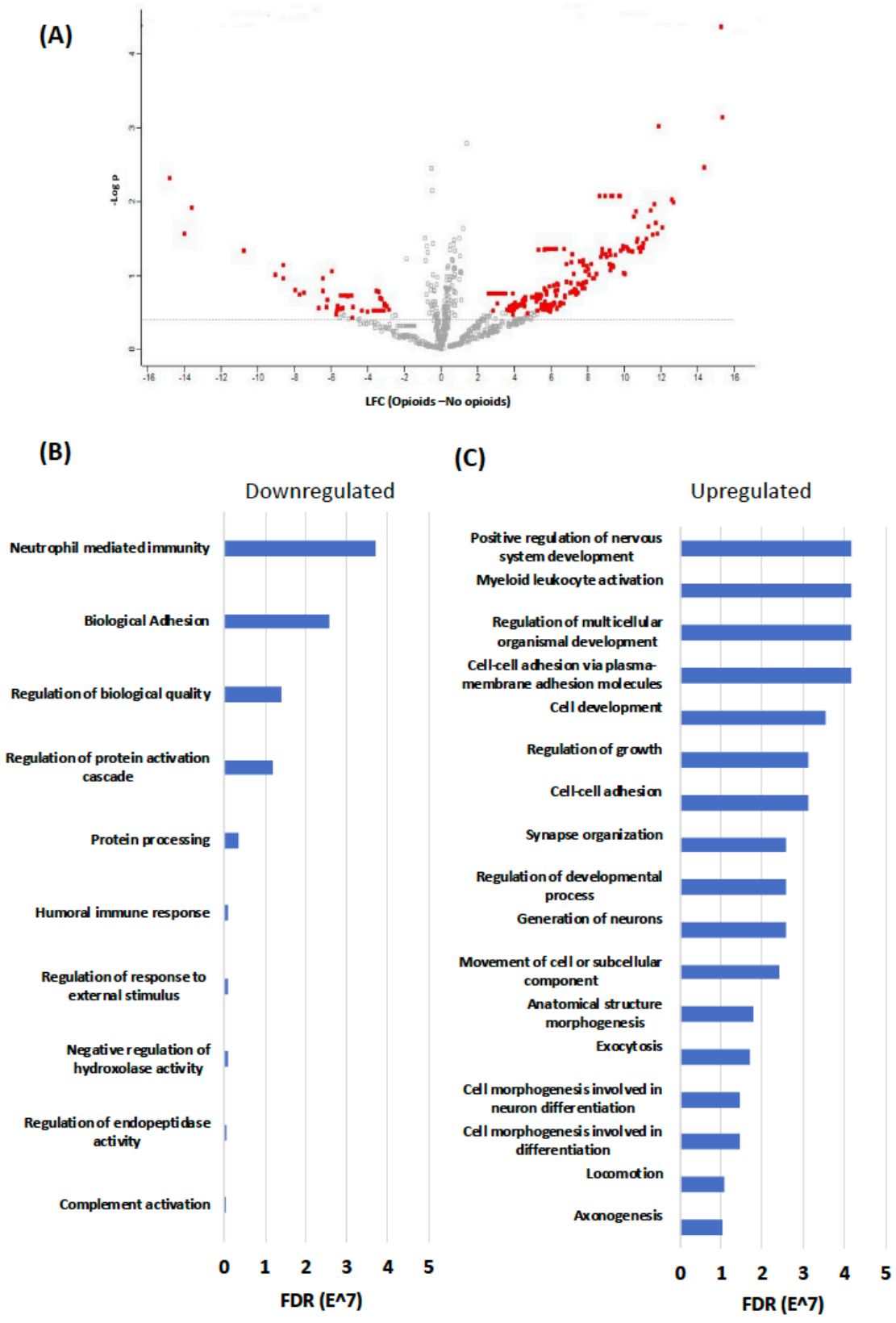

Figure 32: Volcano plot and GO analysis of differentially expressed proteins: (A) Volcano plot showing differential protein signature in the patients' CSF proteome based on their groups. Differentially expressed proteins are designated in red and are defined as differentially expressed genes with a False Discovery rate (FDR)<0.05. (B) Gene Ontology

(GO) biological processes enriched from differentially expressed genes that are downregulated in the CSF proteome of CPNP patients who were taking opioids. The biological processes associated with genes upregulated are illustrated (FDR<0.05) as ranked by FDR (C) GO biological processes enriched from differentially expressed genes that are upregulated in the CSF proteome of CPNP patients who were taking opioids. Abbreviations: LFC; Log-fold change

Gene Ontology (GO) analysis focusing on the biological functional enrichment identified processes involving the differentially expressed proteins, with the top 5 increased biological processes identified as positive regulation of nervous system development (FDR = $4.16E^{-7}$), myeloid leukocyte activation (FDR = $4.16E^{-7}$), regulation of multicellular organismal development (FDR = $4.16E^{-7}$), cell-cell adhesion via plasma-membrane adhesion molecules (FDR = $4.16E^{-7}$) and cell development (FDR = $3.53E^{-7}$) **(Figure 32C)**. The top 5 decreased biological processes were neutrophil mediated immunity (FDR = $3.68E^{-7}$), biological adhesion (FDR = $2.56E^{-7}$), regulation of biological quality (FDR = $1.41E^{-7}$), regulation of protein activation cascade (FDR = $1.17E^{-7}$) and protein processing (FDR = $0.37E^{-7}$) **(Figure 32B)**. Protein to protein interaction clustered networks of the upregulated **(Figure 33)** and downregulated (**Figure 34**) proteins according to GO analysis are in supplementary figures.

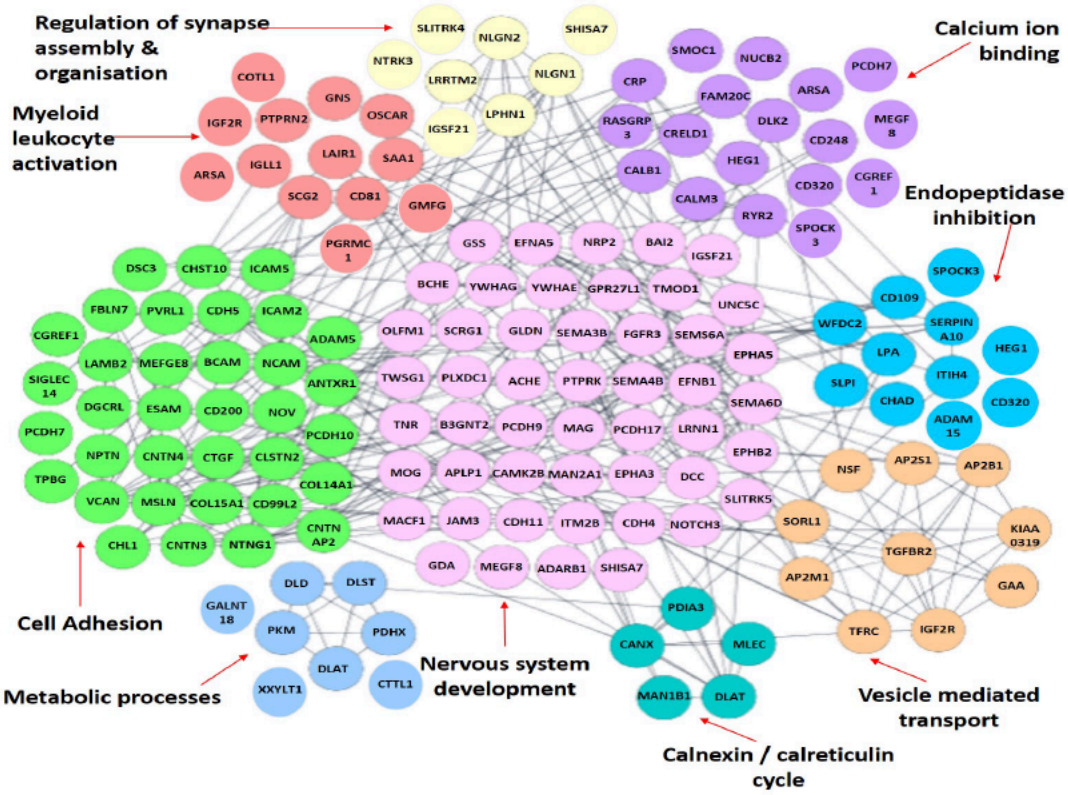

Figure 33: Protein to protein interaction clustered network of significantly increased proteins according to Gene Ontology analysis

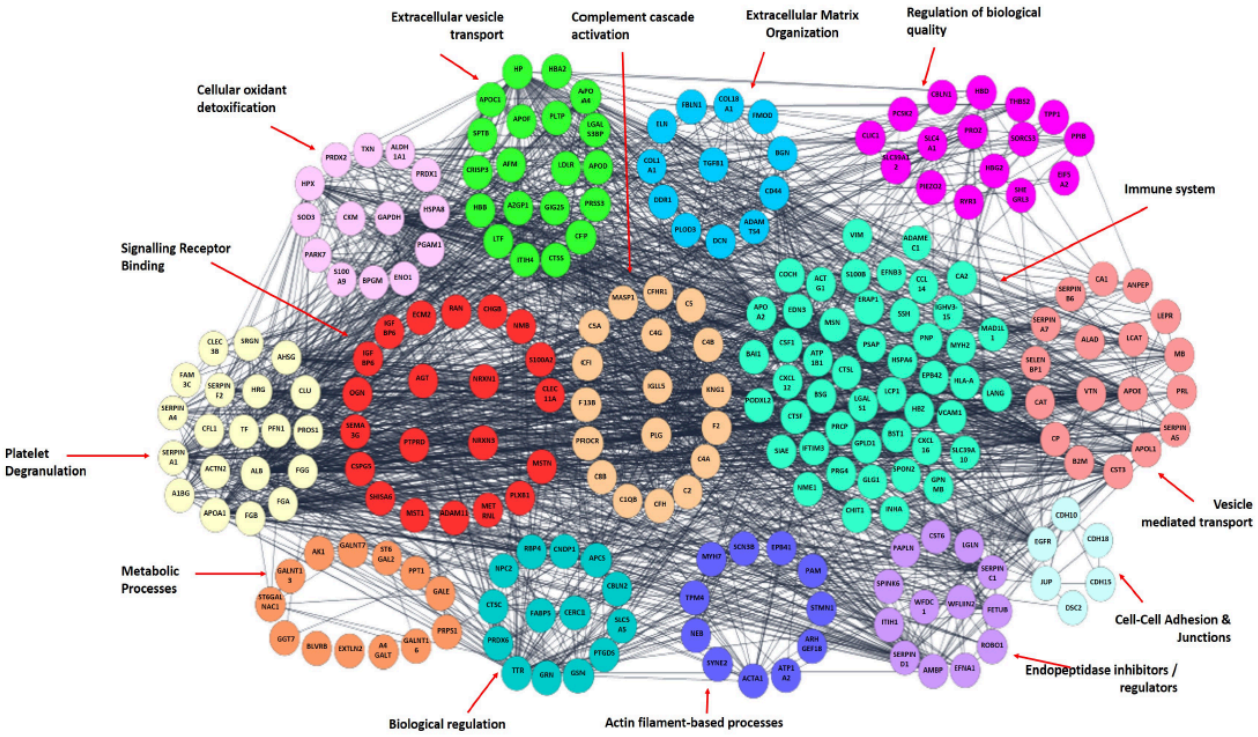

Figure 34: Protein to protein interaction clustered network of significantly decreased proteins according to Gene Ontology analysis

Focusing on these 300 differentially expressed proteins, the proteins could be classified into protein classes: (i) receptors (including G protein coupled and transmembrane receptors), transporters and ion channels **(Figure 35 A, B, C)**, enzymes (including kinases and peptidases) and enzyme inhibitors **(Figure 36 A, B, C)** as defined by International Union of Basic and Clinical Pharmacology. This was based on recommendations of best practice for examining proteomic changes with drug development (478). Finally, immune effectors **(Figure 357A, B)** and proteins related to myeloid leukocyte activation were also

analysed separately **(Figure 37 C, D)**. Further analysis identified 79 known neuronal proteins of the 300 differentially expressed proteins within the CSF of patients receiving opioids versus those who were not **(Figure 38)**.

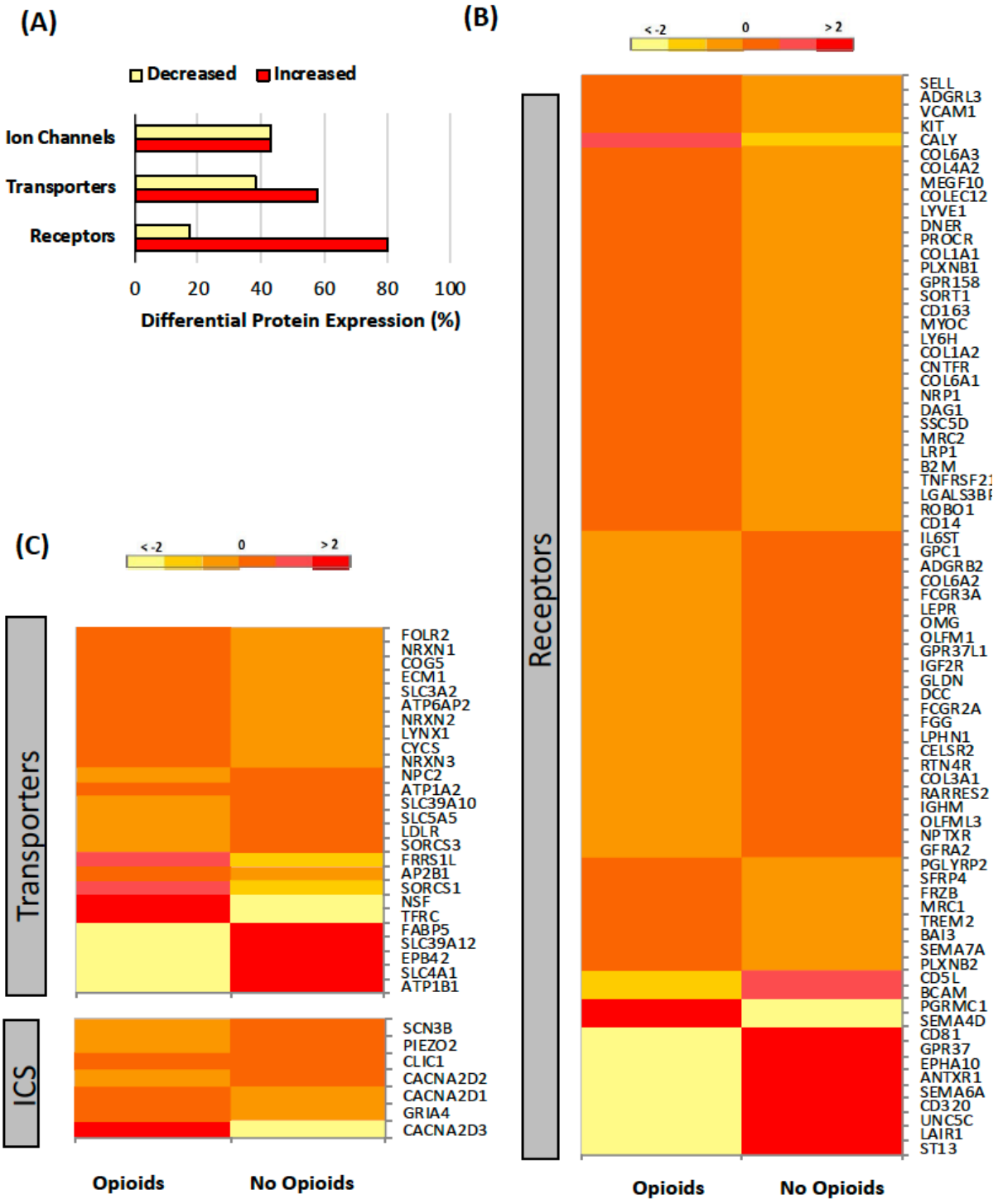

Figure 35: Differential expression of proteins related to ion channels, transporters and receptors in chronic peripheral neuropathic pain (CPNP) patients taking opioids versus controls: (A) Bar plots showing the number of differentially expressed proteins up and downregulated by protein class (receptors, transporters and ion channels), which were identified by ingenuity pathway analysis. (B) & (C) Relative protein expression levels in the CSF samples for the two different treatment groups are shown for each protein class represented in the bar plot. Up and downregulated genes are coloured in yellow and red, respectively. Horizontal bars indicate individual proteins. Abbreviations: ICS; Ion channels

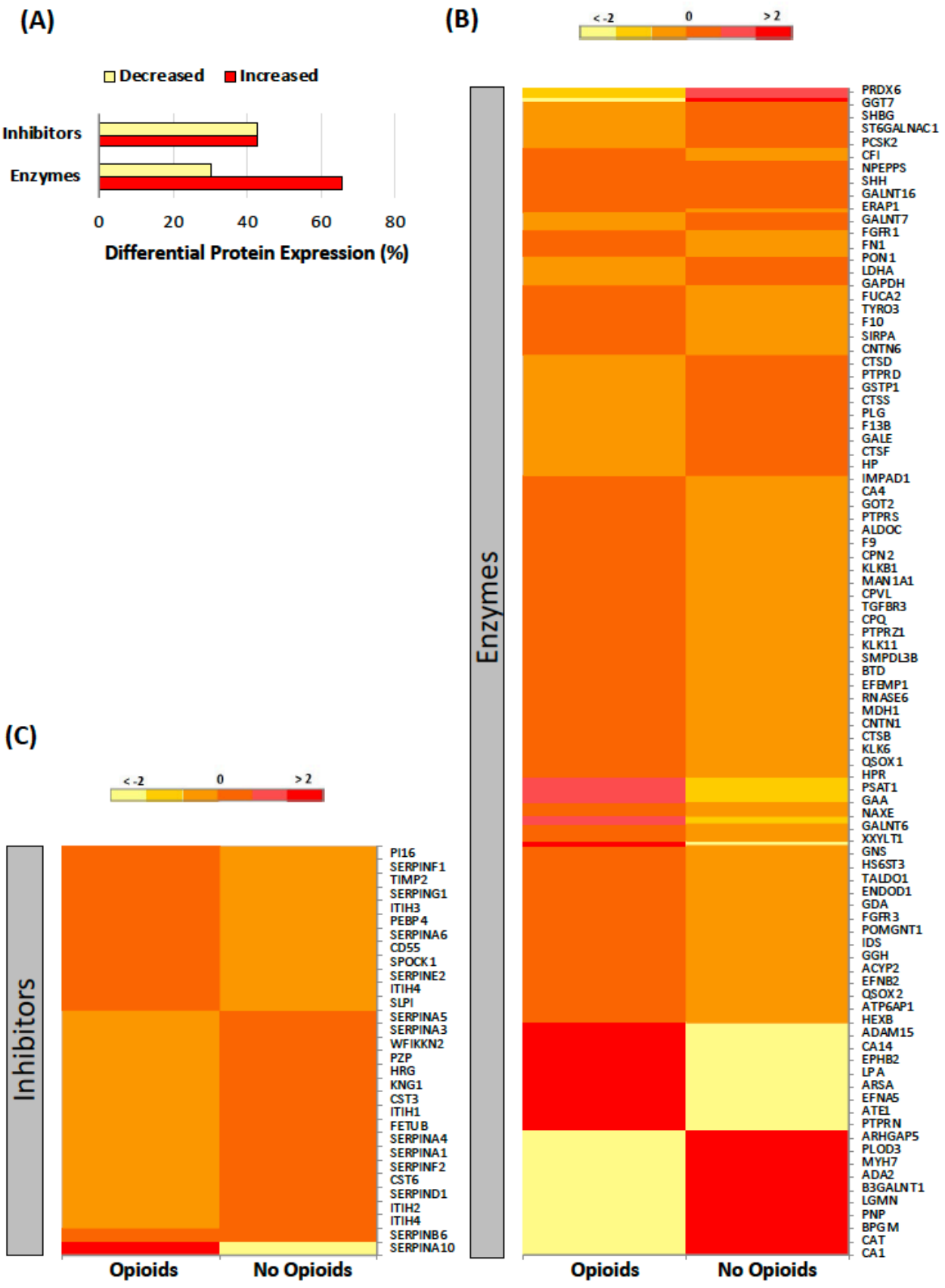
(A)
Decreased
Increased
Inhibitors
Enzymes
0
20
40
60
80
Differential Protein Expression (%)
(B)
< -2
0
> 2
Enzymes
PRDX6
GGT7
SHBG
ST6GALNAC1
PCSK2
CFI
NPEPPS
SHH
GALNT16
ERAP1
GALNT7
FGFR1
FN1
PON1
LDHA
GAPDH
FUCA2
TYRO3
F10
SIRPA
CNTN6
CTSD
PTPRD
GSTP1
CTSS
PLG
F13B
GALE
CTSF
HP
IMPAD1
CA4
GOT2
PTPRS
ALDOC
F9
CPN2
KLKB1
MAN1A1
CPVL
TGFBR3
CPQ
PTPRZ1
KLK11
SMPDL3B
BTD
EFEMP1
RNASE6
MDH1
CNTN1
CTSB
KLK6
QSOX1
HPR
PSAT1
GAA
NAXE
GALNT6
XXYLT1
GNS
HS6ST3
TALDO1
ENDOD1
GDA
FGFR3
POMGNT1
IDS
GGH
ACYP2
EFNB2
QSOX2
ATP6AP1
HEXB
ADAM15
CA14
EPHB2
LPA
ARSA
EFNA5
ATE1
PTPRN
ARHGAP5
PLOD3
MYH7
ADA2
B3GALNT1
LGMN
PNP
BPGM
CAT
CA1
Opioids
No Opioids
(C)
< -2
0
> 2
Inhibitors
PI16
SERPINF1
TIMP2
SERPING1
ITIH3
PEBP4
SERPINA6
CD55
SPOCK1
SERPINE2
ITIH4
SLPI
SERPINA5
SERPINA3
WFIKKN2
PZP
HRG
KNG1
CST3
ITIH1
FETUB
SERPINA4
SERPINA1
SERPINF2
CST6
SERPIND1
ITIH2
ITIH4
SERPINB6
SERPINA10
Opioids
No Opioids

Figure 36: Proteins related to inhibitors and enzymes are differentially expressed in chronic peripheral neuropathic pain (CPNP) patients taking opioids versus controls: (A) Bar plots showing the number of differentially expressed proteins up and downregulated by protein class (enzymes and inhibitors), which were identified by ingenuity pathway analysis. (B) & (C) Relative protein expression levels in the CSF samples for the two different groups [Enzymes (B), Inhibitors (C)] are illustrated for each protein class represented in the bar plot. Up and downregulated genes are coloured in yellow and red, respectively. Horizontal bars indicate individual proteins.

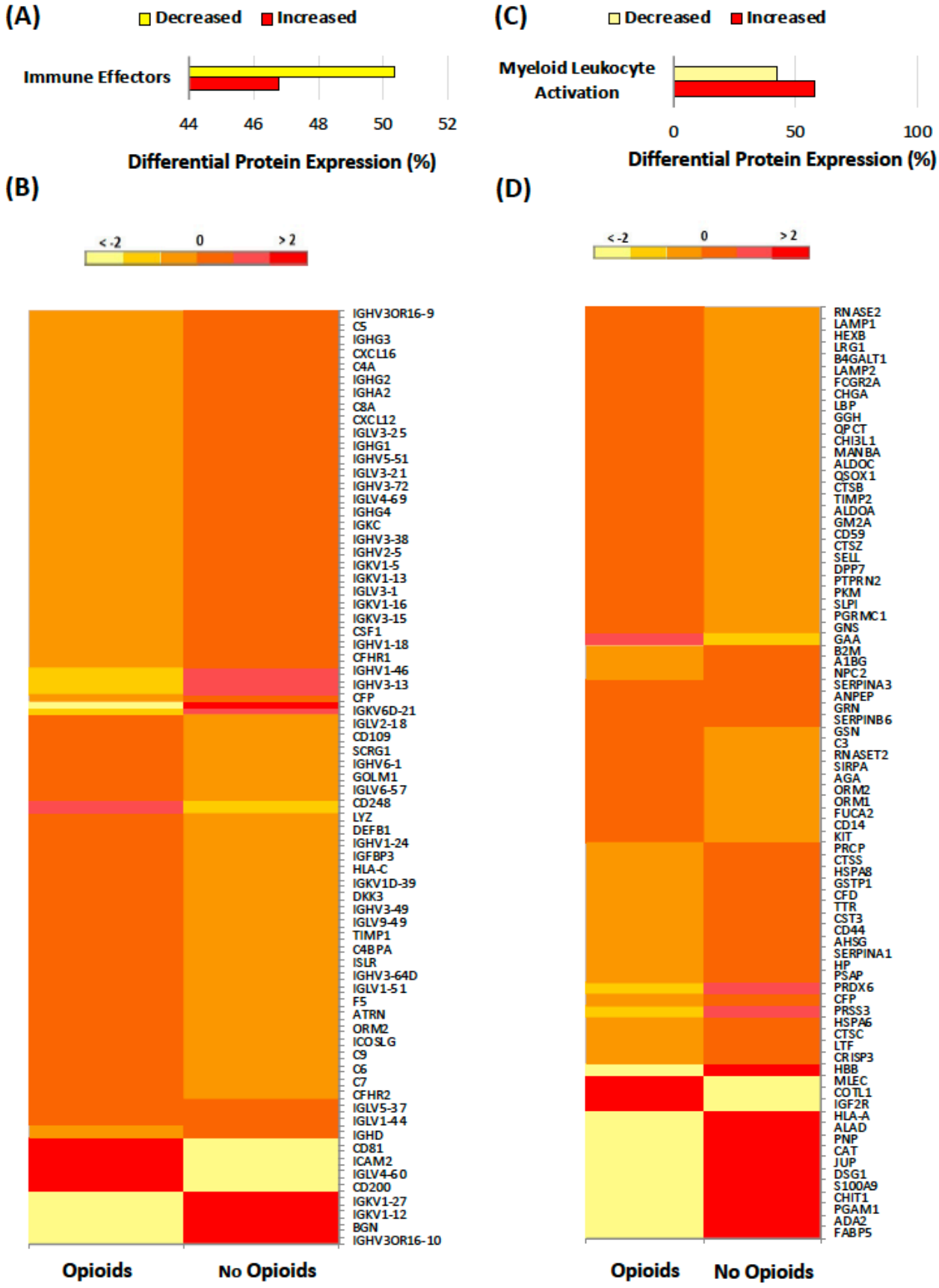
(A)
Decreased
Increased
Immune Effectors
44
46
48
50
52
Differential Protein Expression (%)
(C)
Decreased
Increased
Myeloid Leukocyte Activation
0
50
100
Differential Protein Expression (%)
(B)
< -2
0
> 2
IGHV3OR16-9
C5
IGHG3
CXCL16
C4A
IGHG2
IGHA2
C8A
CXCL12
IGLV3-25
IGHG1
IGHV5-51
IGLV3-21
IGHV3-72
IGLV4-69
IGHG4
IGKC
IGHV3-38
IGHV2-5
IGKV1-5
IGKV1-13
IGLV3-1
IGKV1-16
IGKV3-15
CSF1
IGHV1-18
CFHR1
IGHV1-46
IGHV3-13
CFP
IGKV6D-21
IGLV2-18
CD109
SCRG1
IGHV6-1
GOLM1
IGLV6-57
CD248
LYZ
DEFB1
IGHV1-24
IGFBP3
HLA-C
IGKV1D-39
DKK3
IGHV3-49
IGLV9-49
TIMP1
C4BPA
ISLR
IGHV3-64D
IGLV1-51
F5
ATRN
ORM2
ICOSLG
C9
C6
C7
CFHR2
IGLV5-37
IGLV1-44
IGHD
CD81
ICAM2
IGLV4-60
CD200
IGKV1-27
IGKV1-12
BGN
IGHV3OR16-10
Opioids
No Opioids
(D)
< -2
0
> 2
RNASE2
LAMP1
HEXB
LRG1
B4GALT1
LAMP2
FCGR2A
CHGA
LBP
GGH
QPCT
CHI3L1
MANBA
ALDOC
QSOX1
CTSB
TIMP2
ALDOA
GM2A
CD59
CTSZ
SELL
DPP7
PTPRN2
PKM
SLPI
PGRMC1
GNS
GAA
B2M
A1BG
NPC2
SERPINA3
ANPEP
GRN
SERPINB6
GSN
C3
RNASET2
SIRPA
AGA
ORM2
ORM1
FUCA2
CD14
KIT
PRCP
CTSS
HSPA8
GSTP1
CFD
TTR
CST3
CD44
AHSG
SERPINA1
HP
PSAP
PRDX6
CFP
PRSS3
HSPA6
CTSC
LTF
CRISP3
HBB
MLEC
COTL1
IGF2R
HLA-A
ALAD
PNP
CAT
JUP
DSG1
S100A9
CHIT1
PGAM1
ADA2
FABP5
Opioids
No Opioids

Figure 37: Proteins related to immune effectors are differentially expressed in chronic peripheral neuropathic pain (CPNP) patients taking opioids versus controls: (A) Bar plots showing the number of differentially expressed immune effectors up- and down-regulated identified by ingenuity pathway analysis. (B) Relative protein expression levels in the CSF samples for the two groups are illustrated for each immune effector protein represented in the bar plot. Up and downregulated genes are coloured in yellow and red, respectively. Horizontal bars indicate individual proteins. (C) Bar plots showing the number of differentially expressed proteins related to myeloid leukocyte activation demonstrating up and downregulation which were identified by ingenuity pathway analysis IPA. (D) Relative protein expression levels illustrated for proteins related to myeloid leukocyte activation.

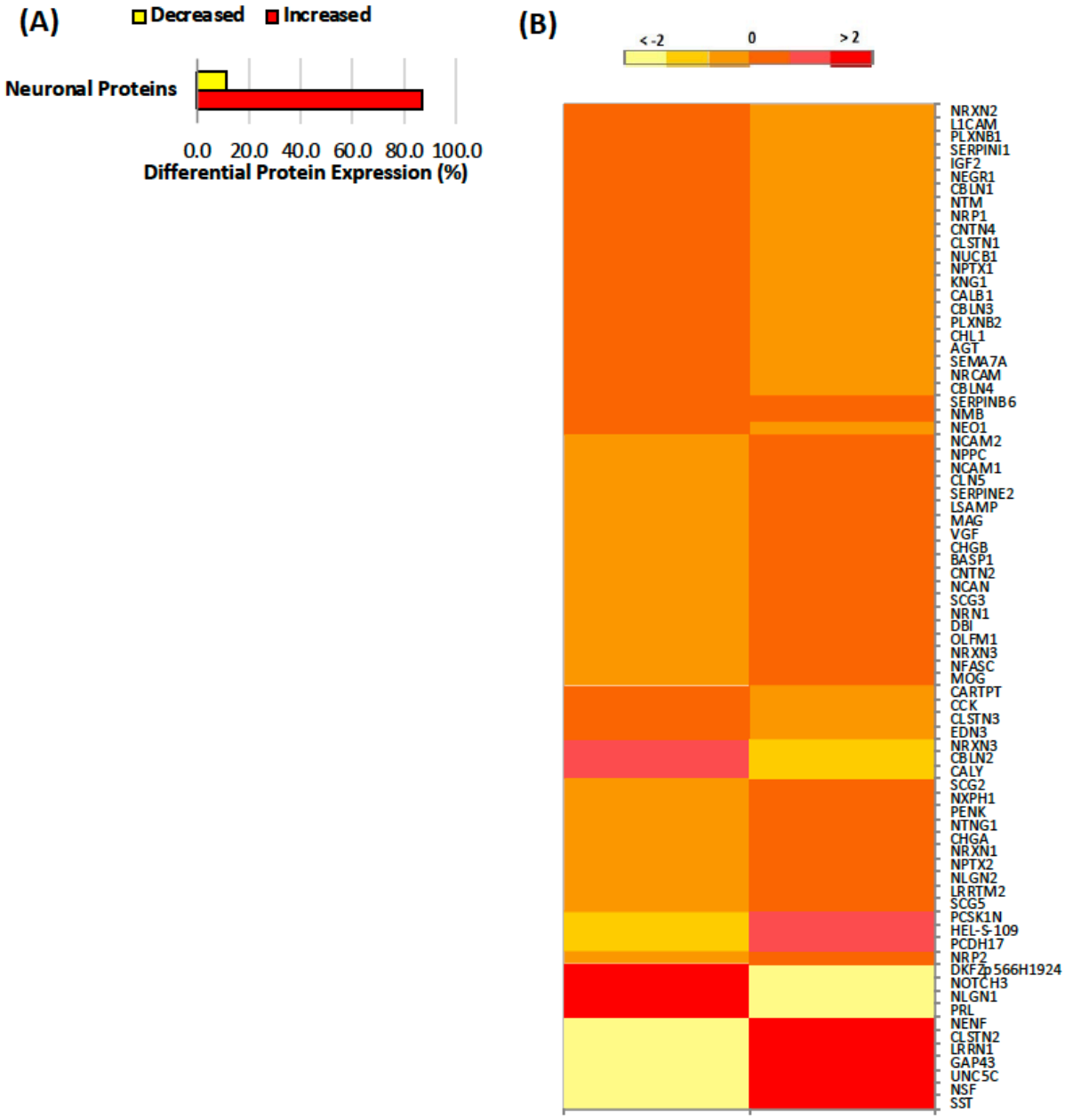

Figure 38: Neural proteins are differentially expressed in chronic peripheral neuropathic pain (CPNP) patients taking opioids versus controls. (A) Bar plots showing the number of differentially expressed neuronal proteins / neuropeptides demonstrating up and downregulation which were identified by ingenuity pathway analysis IPA. (B) Relative protein expression levels in the CSF samples for the two subsequent groups are illustrated for the neuronal proteins represented in the bar plot. Up and downregulated genes are coloured in yellow and red, respectively. Horizontal bars indicate individual proteins.

5.4.3 Cytokine, Chemokine and Neurotrophin analysis

There was no significant difference in the level of cytokines, chemokines or neurotrophins between the two groups. However, IL-16 was notably lower in the patients taking opioids versus the control group [8.75 pg/ml ±0.811 vs 11.09 pg/ml ±0.82 ($p<0.07$)] **(Figure 39),** whereas IL-4 was higher in patients taking opioids [0.1 pg/ml ±0.02 vs 0.06 pg/ml ±0.01 ($p=0.07$)] **(Figure 39)**. The following neuropeptides were undetectable within the CSF of both patient cohorts: Nerve Growth factor (NGF), brain derived neurotrophic factor (BDNF), Glial cell derived neurotrophic factor (GDNF), GM-CSF, IP-10, TNF-β and IL-2 **(Table 27)**.

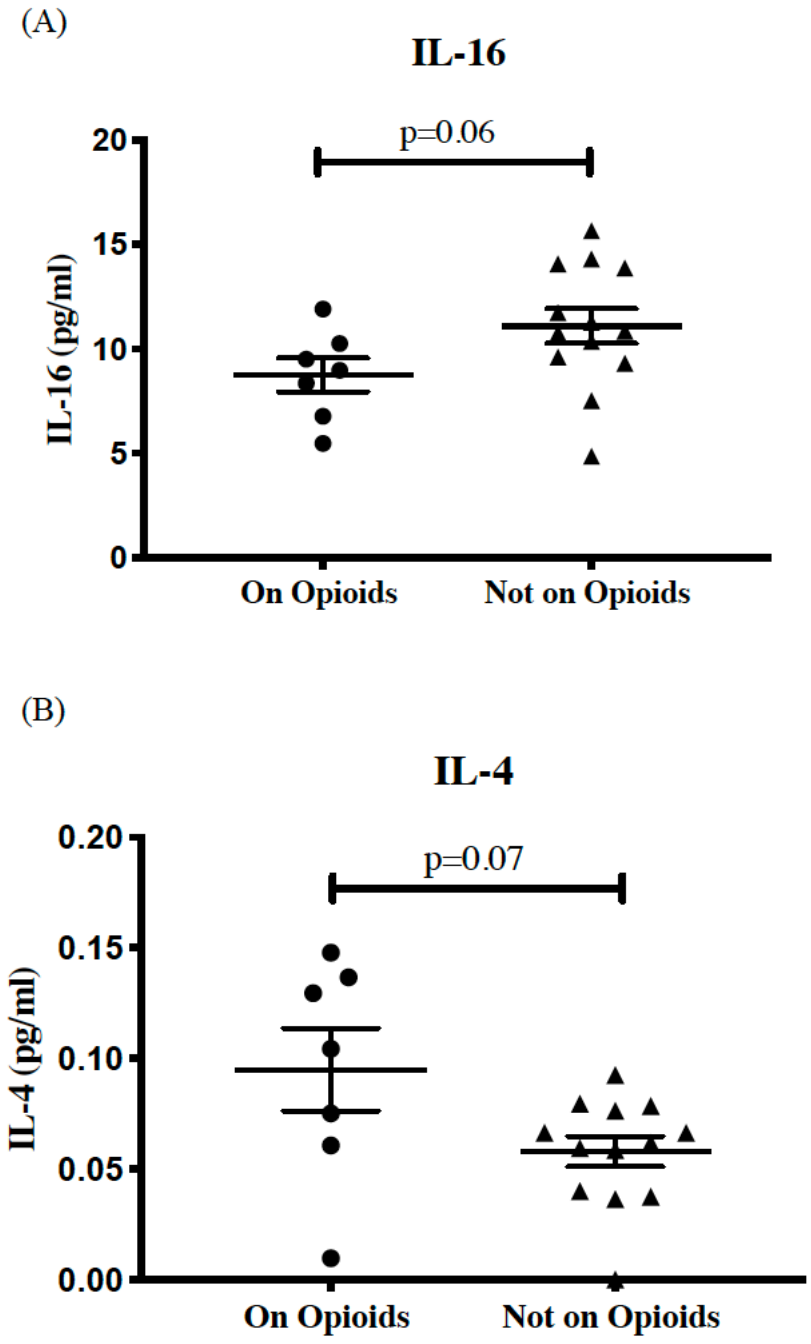

Figure 39: Differential secreted levels of IL-16 and IL-4 in the cerebrospinal fluid (CSF) of chronic peripheral neuropathic pain (CPNP) patients taking opioids versus controls: Individual scatter plots illustrating the difference concentrations of (A) IL-16 [8.75 pg/ml ±0.811 (Opioid Group) vs 11.09 pg/ml ±0.82 (Control group) ($p<0.07$)] & (B) IL-4 [0.1 pg/ml ±0.02 (Opioid Group) vs 0.06 pg/ml ±0.01 (Control Group) ($p=0.07$)] in CSF. Non-parametric unpaired Mann Whitney tests were used for analysis to compare data sets and is illustrated in means with standard error of means (SEM).

Table 27: Measurement of cytokine, chemokine and neurotrophin levels secreted in the Cerebrospinal fluid (CSF) of Chronic Peripheral Neuropathic Pain (CPNP) patients taking opioids versus controls

	Patients taking Opioids Mean +/- SEM (pg/ml)	**Controls Mean +/- SEM (pg/ml)**	**P value**
MCP-1	410 ±44.14	403.5 ±39.75	0.54
MCP-4	10.55 ±2.5	9.338 ±1.798	0.49
Eotaxin-3	5.051 ±1.367	7.251 ±1.653	0.58
Eotaxin	29.69 ±8.88	19.46 ± 3.27	0.39
MIP-1α	8.605 ±1.478	6.154 ±0.637	0.14
MIP-1β	11.69 ±2.43	12.22 ±2.33	0.94
MDC	53.66 ±11.6	47.24 ±6.58	0.82
TARC	9.201 ±0.93	9.378 ±0.84	0.99
Fractalkine	6 ±1.864	8.959 ±2.528	0.66
IP-10	208.2 ±41.64	219.4 ±33.61	0.69
VEGF-A	2.82 ±0.49	3.83 ±0.76	0.58
IL-12/IL-23p40	4 ±0.39	5.28 ±0.79	0.57
IL-15	4.69 ±0.42	4.57 ±0.59	0.69
IL-16	8.75 ±0.811	11.09 ±0.82	0.06
IL-17A	0.26 ±0.09	0.34 ±0.08	0.68
IL-5	0.73 ±0.1	0.69 ±0.08	0.55
IL-7	1.399 ±0.18	1.053 ±0.1	0.09
IFN-γ	0.6 ±0.31	0.334 ±0.06	0.99
IL-10	0.12 ±0.03	0.12 ±0.02	0.98
IL-12p70	0.04 ±0.007	0.05 ±0.02	0.7
IL-13	2.65 ±0.34	3.11 ±0.24	0.28
IL-1β	0.216 ±0.03	0.286 ±0.03	0.27
IL-4	0.1 ±0.02	0.06 ±0.01	0.07
IL-6	1.2 ±0.24	1.24 ±0.18	0.94
IL-8	13.8 ±3.02	17.17 ±3.39	0.54
TNF-α	0.48 ±0.04	0.51 ±0.04	0.47

Statistical significance was determined by the Mann-Whitney test with significant differential expression identified.

5.5 Discussion

This *ex vivo* study has demonstrated significant differences in CSF constituents in CPNP patients on chronic opioid therapy versus controls with neuropathic pain. These alterations in CNS neurophysiology suggest potential pharmacodynamic insights into opioid therapy in chronic pain patients. The findings from our GO analysis also differ from many other proteomic studies of CSF examining treatments for chronic pain including spinal cord stimulation (213, 321). We have demonstrated differences in the expression of cell receptors, enzymes, transporters and neuronal proteins. The effects of opioids have largely been attributed to modulation of receptors (479, 480), transporters (481) and ion channels (482) within the CNS. Previous studies exploring the precise mechanisms of opioid activity on CNS function in humans have largely been confined to imaging studies in acute pain, healthy volunteers and animal models which vary in outcomes (483).

Our GO analysis of CSF from CPNP patients receiving chronic opioid therapy has indicated a significantly increased modulation of CSF proteins related to the nervous system development. Long term exposure to opioids is an established concept in modulating the developing and maturing human brain in terms of connectivity and cognition (484). Many studies have demonstrated how opioids modulate nervous system proliferation and development but these studies are confined to rodents and *in vitro* studies (447, 485, 486). Proliferation of cells within the CNS is site and cell type specific and dependent on the expression of different opioid receptors (485). A detailed review of opioid related proliferation focusing on non-neuronal cells from pre-clinical and *in vitro* models has been addressed in a review by Hutchinson and colleagues (447). The majority of studies examining neurons have largely demonstrated a decrease in neurogenesis with opioids (487). Despite this, non-neuronal cells in particular astrocytes and oligodendrocytes have more definitive evidence of proliferation (447, 485). This suggests increased expression of proteins involved in nervous system development from our data is more likely due to gliogenesis (447, 485). Kappa opioid agonism leads to exclusive proliferation of spinal astrocytes (488), which correlates with our findings, as our samples were more representative of fluid drained from the spinal cord (203). Increased spinal astrocytes have also been identified from a cadaver study in a patient with complex regional pain syndrome taking chronic opioids versus controls (31). Notably this patient also had neuronal loss on the ipsilateral side to the CRPS (31). This suggests increased astrocyte proliferation in the spinal cord may be a phenomenon observed in patients with CPNP taking opioids.

Furthermore, these cells are the most abundant in the posterior aspect of the human spinal cord where we took our CSF samples (390). Future studies would need to be performed to verify these findings, with the use of neuroimaging of ligands for specific cell types in the brain and spinal cord.

The concept of central immune signalling being attributable for many of the effects of opioids have been reported but there is little *in vivo* evidence in humans to support this (447, 489). For the first time, our GO enrichment of differentially expressed proteins identified the largest alterations in pathways related to myeloid leukocyte activation. Myeloid cells arise from clonogenic myeloid-primed precursors giving rise to neutrophils, basophils, mast cells, eosinophils, granulocytes, monocytes, macrophages and dendritic cells (490). Many of these cells are influential in the persistence and attenuation of neuropathic pain within the neuroimmune interface (218) and express opioid receptors (442, 444, 452). The myeloid cells found within the CSF include monocytes, granulocytes and dendritic cells (286, 291). Microglia mimic the action of macrophages in the CNS but are not routinely found in CSF; invading macrophages in the spinal cord have also been observed in neuropathic pain models (94, 136, 137). Myeloid leukocyte activation is more likely to represent activation of monocytes, microglia (142) and possibly dendritic cells (491, 492) from studies in neuropathic pain and opioids in the CNS. The activation of these cells, their phenotypes and dynamics with other cells emphasises their role in opioid related phenomena which has been described in pre-clinical studies (158, 159, 452, 493).

Myeloid cell development and effector profiles are complex and influenced by their microenvironment but are potent regulators of T lymphocytes (490). While we did not observe any cytokine patterns specific to myeloid leukocyte activation, one of the largest differences from the secretome analysis was the Th2 cytokine IL-4. Opioid exposure skews T cells towards a Th2 lineage that is IL-4 dependent in a positive feedback loop (443). IL-4 is a predominantly anti-inflammatory cytokine which functions as a potent regulator of immunity and has been demonstrated to be antinociceptive in inflammatory pain models but its role in neuropathic pain has yet to be investigated(92). Studies have reported increased IL-4 expression within the spinal cord with the reversal of neuropathic hypersensitivity following treatment with glatiramer acetate (494). In addition, decreased CSF levels of IL-4 have been reported in complex regional pain syndrome (CRPS) patients (186). IL-4 is produced by basophils and mast cells but the higher levels detected in CPNP patients receiving opioids might also represent a downstream T cell mediated effect of

myeloid cell activation. Our observations of higher IL-4 in CSF from patients taking opioids is in line with previous *in vitro* work demonstrating morphine induces naïve $CD4^+$ T cells to differentiate into Th2 effector cells with significantly increased IL-4 cytokine production and IL-4 RNA expression (495). As $CD4^+$ T cells are predominant within the CSF this may explain a source of IL-4 (291). There is also *in vitro* evidence of IL-4 being induced by fentanyl and methadone in a study of human T cells from blood (496).

Interestingly, decreased levels of IL-16 in the CSF of patients taking opioids may indicate a further trend from a Th1 to Th2 profile in this cohort. IL-16, also referred to as lymphocyte chemoattractant factor (LCF), is a Th1 cytokine which has been implicated in modulating the inflammatory environment in multiple sclerosis (384), HIV encephalitis (497) and spinal cord injury (498). The difference in the expression and secretion of immune mediators within the CSF presented here contributes to the evidence that opioids have immunomodulatory properties (442, 444, 499). However, the microenvironmental function and cytokine profile of many of the immune cells within the CNS still requires more research and would necessitate a more specific cytokine panel and in-depth flow cytometric analysis (76, 490). Zin and colleagues previously examined cytokines in the CSF of patients with intrathecal opioid pumps, providing evidence to correlate the intensity of pain to IL-6 and IL-10 levels (350). However, neither of these two cytokines were significantly altered with our cohort of patients receiving opioids.

The largest decrease in proteins according to GO enrichment were related to neutrophil mediated immunity. Neutrophils, part of the innate immune response also influence neuroimmune interactions (500). Although neutrophil infiltration has been reported within the spinal cord in rodent models of neuropathic pain there is no evidence in humans(90). Neutrophils can be present within the CSF, meninges and pia membrane and as a result their mediators including acetylcholine, catecholamines and cytokines can modulate neural networks (500). Neutrophils can also migrate to the leptomeninges in cases of neuroinflammation, specifically stroke in humans (501). The leptomeninges has been highlighted as an important site for the genesis and attenuation of neuropathic pain by immune mediators, specifically T cells (502, 503). From our data, neutrophils may also play a role in the attenuation of neuropathic pain and possibly hyperalgesia at a later stage by secretion of their mediators at specific sites (504). Morphine can exclusively attenuate migration of neutrophils to the site of inflammation and opioids can also decrease neutrophil bactericidal function (443). This may indicate a mechanism of opioids in attenuating neuropathic pain in the acute and sub-acute stage as neuroinflammation in the

neuroforamina has been reported in chronic radicular pain patients that make up the majority of patients within this cohort (183).

The findings of this novel pilot study are observational. Although there are different aetiologies of peripheral neuropathic pain, they are classified according to second level diagnosis for ICD-11 (505). In this study, each patient had been medicated with opioids for more than 3 months prior to inclusion and each patient had reported a reduction in pain, however, this reduction in pain was not quantified. Examining for opioid related phenomena was beyond the scope of this work. Different opioids have also clearly demonstrated contrasting and distinct cellular mechanisms *in vitro* and from pre-clinical studies (447, 489, 496, 506). The differences in efficacy with individual opioids in humans and the ability for patients to tolerate one over the other also suggests humans metabolise opioids differently (507-509). Molar concentrations of drugs within the CNS are also not quantifiable. These variables support the rationale to focus on patients who have achieved a reduction in pain to different opioids. Other medications including analgesics are also variables that may alter the CSF proteome but only one of the patients in this study was on another medication for neuropathic pain.

Researchers must be aware of the limitations of proteomic approaches (213, 321, 351). Until recently, technological limitations prevented full characterization of the CSF proteome, with analysis made challenging by low protein concentrations, inter-sample protein variability, potential masking of neuronal specific proteins by high abundant proteins and limited accessibility to an adequate number of appropriate biological samples, specifically the barriers to recruiting true controls or healthy patients for lumbar puncture (432). Based on these challenges, most CSF proteomic studies employed pooled samples from patient populations with the disease of interest or pooled samples from people who underwent lumbar puncture for the investigation of neurological conditions and who were subsequently found to have no pathology (432). These CSF samples were subsequently used in studies as a substitute for true healthy volunteers due to the issues encountered with obtaining healthy CSF samples(432). The most comprehensive studies of the normal healthy CSF composition were conducted by Schutzer and colleagues (n=11) and later by Guldbransen and colleagues (n=21) (432, 510), with both studies pooling the patient samples prior to analysis. These studies identified 1489 common protein constituents of normal CSF and these studies provide this analysis with key information on the proteins which should be expected to be detected by mass spectrometry.

Proteomic analysis is vulnerable to contamination from environmental proteins such as keratins which can be derived from the patient's skin during sample acquisition or from skin cells shed by the laboratory researcher performing the sample preparation for mass spectrometry. Therefore, efforts must be made to remove any contaminants from the downstream analysis. Additionally, sampling by lumbar puncture can result in blood protein contamination in the CSF. This issue can be overcome using standard centrifugation clean-up techniques, such as those employed in this study, thus limiting the potential contamination. When choosing CSF as a biological sample, researchers must also consider the effects of rostral/caudal gradients on protein expression levels. Some proteins will decrease in concentration if a sample is taken from a more caudal location, similarly proteins can also enter the CSF from blood at a more caudal location. The effect of these proteins however is minimal and only 13 proteins have been identified as potentially coming from blood if CSF is taken at the base of the lumbar spine (351). Aside from the potential issues with biological samples, interpatient variability (352, 432) and environmental contaminants, one must also be aware of the limitations of the mass spectrometry approach itself. Protein analysis is limited by its substrate, with studies showing that the less-abundant, large, hydrophobic proteins, e.g. transmembrane proteins, are frequently missed in mass spectrometry studies. However, the SP3 protocol counteracts this common shortcoming of many proteomic sample preparation techniques by using both hydrophilic and hydrophobic paramagnetic beads which allow for unbiased protein retrieval and purification and offers extensive proteome coverage (322, 511). Furthermore, it is acknowledged that proteins can undergo numerous post-translational modifications (PTMs) such as carbonylation and phosphorylation, which subsequently impact on the function of the protein. The specific types of PTMs which occur are clinically relevant. However, PTMs require special analytical processing to capture these minute changes to a protein and standard processing techniques are inadequate in their detection of PTMs. Unfortunately, without a targeted approach to the mass spectrometric analysis to focus specifically on phosphorylated proteins these modifications are not recognised, and the analysis does not distinguish between different versions of the protein due to their similarities in size. Enrichment strategies and advanced MS algorithms are improving the identification of PTMs, however the approach utilised in this study has not focused on the occurrence of PTMs.

Despite limitations, this study has generated evidence to support further investigations into the alterations to the CSF proteome in CPNP and provide new insights into the

immunomodulatory and cellular alterations in response to opioid treatment in CPNP patients. Further work will uncover the cellular mediators and immune networks underpinning these alterations with specific opioid related phenomena.

5.6 Conclusion

This is the first observational study to provide new data on both the CSF proteome and secretome in patients with CPNP medicated with opioids providing analgesia versus CPNP patients receiving no opioids. Differences in CNS development proteins, enzymes and receptors suggest a modulation of homeostasis attributable to opioids. Observed differences in immunomodulation and central immune signalling proteins also suggest that opioids may exert their analgesic and adverse effects via immune-mediated mechanisms. The novel data presented here should be considered when performing future explorative CSF studies and comparing different populations. Larger targeted studies are required to confirm the aforementioned observations and comment on opioid related phenomena and their mechanisms in future research.

Chapter 6: Discussion

6.1 Overview

This thesis aimed to explore mechanisms of action to common therapies used in neuropathic pain through analysis of CSF. The central hypothesis was that neuroimmune dysfunction is one of the proposed pathogenesis implicated in the development of chronic neuropathic pain and thus effective treatments will have to target these processes. Neuroplasticity, or more appropriately pathological neuroplasticity, is a term utilised to explain the development of neuropathic pain and central sensitisation within the CNS (512). Neuroplasticity is heavily orchestrated by glia-neuronal interactions resulting in changes in synapse assembly and neuropeptide concentrations (11, 153, 451, 512). Glia-neuronal interactions are also influenced by resident and infiltrating immune cells and are thus key players in the function of the central nervous system and pathological pain (3). Studying CSF remains one of the best methods to study the metabolites of the neuroimmune interface *in vivo.*

Many of the common therapies used for chronic pain lack a global consensual mechanism of action and are thus explored using many utilities. Functional MRI may suggest anatomical locations of neuroplasticity for the development of chronic pain and suggest mechanistic pathways in treatments (513-515). Electrical neurophysiology studies also indicate the recruitment of specific nerve fibres but there is a paucity of data on the molecular basis of many therapies *in vivo* (201, 516). Identification and characterisation of the molecular pathophysiology of chronic pain and mechanisms of therapies will enable more accurate diagnostic tools to be developed, will improve phenotyping and substantially increase effective treatment options. This will inevitably lead to better outcomes for patients. Many therapies currently utilised for chronic pain lead to more morbidity than benefit including pregabalin for radicular pain and opioids when prescribed without phenotyping and physician led follow-up (17, 517). The three therapeutic modalities examined in this thesis differ in terms of proposed mechanisms. This may explain the different results we achieved and thus making parallels between the different therapeutic options challenging. It also suggests that chronic neuropathic pain has many pathophysiological dimensions and genetic variability thus explaining why remission remains a rare happening. Despite this, the work from this thesis has envisaged and verified many mechanisms of action for amitriptyline, Burst-SCS and opioid therapy. We have also

suggested, within the amitriptyline study, why patients with neuropathic pain remain refractory to treatment.

6.3 Summary of Findings

Our initial hypothesis implicated neuroimmune dysfunction as a mechanism for the chronicity of neuropathic pain and also postulated that current treatments modulated this interface. The body of evidence to support this hypothesis in humans was limited and thus this hypothesis may be described as speculative (53). There is however very limited evidence supporting most proposed hypotheses regarding chronic pain and mechanisms of treatment (293). The quest for biomarkers and definitive pathways has been highlighted as particularly important to aid the development of safe and effective pain therapeutics (293). Neuronal glia communications within humans, particularly where immune cells and glia are in a reactive phenotype, have remained a challenge to study effectively. Despite this, we have demonstrated pathways that are modulated with amitriptyline, Burst-SCS and opioids relating to immune activity. Amitriptyline demonstrated the greatest involvement of immune mediated characteristics in terms of therapeutic mechanisms. GO and KEGG analysis illustrated modulation of immune system process and a decrease in MAPK and PI3K-Akt pathways. These pathways have also been described in many *in-vitro* and pre-clinical studies which provides convincing validating evidence of amitriptyline's mechanism of action (248, 518). This is the first-time immune system process interaction has been validated *in vivo* in humans. Although the implication of T cells in the chronicity of pain is not definitive, we also demonstrated amitriptyline modulates the phenotype of T cells *in vitro* that correlate with many cytokines previously reported to be implicated in pain chronicity.

Immune effectors were also modulated by Burst-SCS, although the evidence from GO analysis was not as convincing as amitriptyline in terms of immunomodulation. Although much of the evidence regarding the mechanism of action of Burst-SCS is industry sponsored and has focused on the activation of the medial pain pathway (8, 10, 519). A factor that remains unique about Burst-SCS is the prolonged wash in and washout times and new duty cycling dosing regimens which brings into question the hypothesis of a pure neuronal mechanism of action (520). We have demonstrated new concepts into the mechanism of action of Burst-SCS and identified a possible molecular basis of action for Burst-SCS in humans for the first time.

Finally, for patients medicated with opioids, proteins related to myeloid leukocyte activation had increased expression in comparison to patients not receiving opioids. There was also an associated cytokine pattern suggesting amplification of a Th2 response. This provides potential evidence that opioids play a role in neuroimmune processes. Whether the changes illustrated in patients receiving opioids are related to analgesia remains inconclusive as the differences highlighted may also relate to the initiation of sequelae and detrimental effects including opioid induced hyperalgesia.

6.3 Amitriptyline's effect on cellular function

From the *in vitro* experiment there was a clear change in frequency of $CD8^+$ cells particularly the naïve subset. The same was also noted with $CD3^+CD56^+$ cells and $CD27^+CD4^+$ T cells. Although our cellular data from CSF was not conclusive, it was clear the same dynamic change in expression was not observed with the CSF samples after amitriptyline administration. There are a number of reasons why this may be the case. Naïve T cells are significantly underrepresented in CSF and constitute the lowest frequency of cells, while in peripheral circulation they are the highest (291). $CD3^+CD56^+$ cells are also in low abundance in CSF and were not detected in many of our samples(291). The environment within the CNS and CSF is also heavily influenced by microglia and astrocytes and different to systemic circulation (521). Although amitriptyline and nortriptyline can easily penetrate the BBB, the CNS also has many factors that contribute to immune privilege, which also contributes to a different climate of immune related peptides (522, 523). The significantly altered CSF neuropeptides eotaxin-1 and VEGF-A in our data, in responders to amitriptyline would likely have come from microglia and astrocytes based on RNA analysis (342). We did not observe any evidence to suggest T-cell function is modulated in CSF after amitriptyline treatment. However, dynamic changes in neuropeptides from other cells may modulate T cells if present within the dorsal horn. If T cells are the pathophysiological reason for chronic neuropathic pain (81), the trafficking of T cells within the dorsal horn to CSF may be small in number and not sufficient enough to significantly alter the overall phenotype of T cells within CSF. This small localised effect in the dorsal horn would be difficult to illustrate without a specific type of neuroimaging. If, however a patient's neuropathic pain is peripherally mediated it is possible that amitriptyline's mechanism lies in T cell modulation. Whether T cells are implicated in the pathogenesis of chronic neuropathic pain or not, their modulation will

have an effect on other immune cells and their respective peptides which may be pathognomonic (129, 198). These theories are all highly speculative. The source of neuropathic pain may be based in primary afferent nerves, centrally mediated or both; there is still considerable debate over this issue (368).

The way in which T cells were activated with PMA *in vitro* may not also mimic their activation in chronic neuropathic pain. Translation of many *in vitro* experiments correlate poorly to *in vivo* studies due to inaccurate models or other unidentified variables in pathophysiology (175, 524, 525). An example within pre-clinical models is a study by Costigan *et al*, implicating T cells in a chronic neuropathic pain model (81). However, a more recent rodent model demonstrated no T cell infiltration at all (146). Timing and methodology are different between these two experiments and the accuracy of translation from pre-clinical pain models to humans has so far been disappointing (53, 76). There is a need to develop a better understanding of the role of T cells in neuropathic pain in humans. A study in CRPS patients by Russo and colleagues demonstrated there is expansion of $CD8^+$ and $CD4^+$ central memory T cells in blood compared to controls with increased phosphorylation of NF-κB and STAT1 pathways (198). There were also increased number of Th1 and Treg cells in the CRPS cohort. While the authors accepted the limitations of this study on the pathogenesis of CRPS, it may explain why amitriptyline rarely improves the symptoms of CRPS (71, 198). None of the pathways and cellular changes described match our *in vitro* data directly, although NF-κB is a transcription factor in IFNγ production in $CD8^+$ T lymphocytes (198). From our data, $CD8^+$ cells demonstrated an intracellular reduction of IFNγ after amitriptyline and nortriptyline.

Other cellular targets that may be of interest for amitriptyline are monocytes and macrophages. Macrophage function will to a degree mimic microglia activity (142). Reduced IFNγ expression was observed in peritoneal macrophages in a model of allergic neuritis after tricyclic antidepressants (526). The tricyclic compound clomipramine also inhibits both *in vitro* and *in vivo* migration and chemotaxis of both spontaneous and stimulated macrophages (527). Tricyclics may even influence the differentiation of monocytes into macrophages in inflamed tissues which was demonstrated in an *in vitro* experiment (314). Tricyclic's actions on microglia and astrocytes cultures have demonstrated partial alteration of NF-κB and p38 MAPK pathways as well as neuroprotective effects via inhibition of neurodegeneration (528). Other pathways in microglia and astrocytes identified by pre-clinical and *in vitro* models include MAPK/ERK,

CREB and A3AR activation by reducing pro-inflammatory cytokines TNFα , MCP-1 and MIP2 (248). We have in part verified that amitriptyline reduces proteins related to the MAPK pathway in humans from our *in vivo* experiment.

The presumed effect of eotaxin-1 in the CNS comes from astrocyte-microglial interactions promoting microglial migration and activation with reactive oxygen species potentiating glutamate mediated cell death (330, 336). Eotaxin-1 has not been verified as having an effect on neurons directly (330), but pre-clinical evidence has associated eotaxin-1 in decreased neurogenesis and age related degeneration of the hippocampus, a region of the brain associated with memory and emotion (529). Microglial activation with LPS in rat retinal microglial cells demonstrated a significant increase in eotaxin mRNA expression emphasising the pro-inflammatory association of eotaxin-1 (334). Drawing a definitive conclusion on a mechanism related to eotaxin-1 directly from our data would not be prudent as it likely represents evidence of dysfunctional neuroinflammatory processes with many other neuropeptides in chronic pain patients. Indeed, from our data many chemokines reduced in responders to amitriptyline but did not meet statistical significance. Minocycline (microglia pro-inflammatory inhibitor) attenuated the expression of eotaxin mRNA pathway in microglia with an associated decrease in p38 MAPK expression in a rat model (334). As proteins related to MAPK processes demonstrated decreased expression after amitriptyline, this suggests it may be the pathway attenuated by amitriptyline from our data (334).

Amitriptyline, through activation of TrkA aids neuronal growth in DRG neurons in a study in rats (346). Interestingly the associated increase in VEGF-A in CSF could also potentially be associated with neuronal growth within the spinal cord. A study in mice revealed VEGF stimulated axonal growth in the DRG and promoted survival of neurons and satellite cells in culture(530). In the same experiment blockade of VEGF signaling in culture lead to neuronal apoptosis. Conversely, VEGF elevation is associated with proliferation and migration of astrocytes and microglia (339). However, the role of VEGF in the nervous system is globally portrayed as neuroprotective (117, 118). Low VEGF levels and other neurotrophic factors are heavily related to depression from multiple studies leading to structural and functional changes in the nervous system (synaptic plasticity) (119). *In vitro* experiments in the hippocampus of rodents have demonstrated increased VEGF expression after amitriptyline, however, this has not been demonstrated in the spinal cord (312). As

many neuropeptides in CSF are believed to be re-absorbed into systemic or lymph circulation from the brain prior to entering the spinal canal from a pre-clinical study (531), the production of VEGF may be more localized to the spinal cord than the brain. Glial cells significantly outnumber neurons within the spinal cord compared to the brain (390), and based on RNA analysis VEGF-A is predominately secreted by microglia and astrocytes (342). VEGF levels have increased in a spinal cord injury model and lead to activation of neural stem cells (340). This provides potential evidence that the site of action of amitriptyline may also be in the spinal cord and not solely in the brain.

6.4 Mechanism of action of Burst spinal cord stimulation:

Burst-SCS was devised from thalamo-cortical firing patterns that have the ability to strengthen synaptic connectivity (275-277). However, an initial proof of concept study revealed an improvement in pain scores in patients who had functioning efficacious tonic SCS systems (8). This was followed by a number of case series demonstrating further proof of concept (263, 279, 388, 532) and a randomised controlled trial that was powered for non-inferiority versus tonic stimulation but suggested superiority (68). The concepts proposed for improved efficacy of Burst-SCS include a higher level of charge per second compared to tonic stimulation, activation of more neurons, and opioid release from the dorsal horn (8). Our proteomic analysis demonstrated the majority of proteins altered are related to synapse assembly after Burst-SCS. This would correlate with initial experiments with burst firing which lead to strengthening of synaptic activity (275-277, 399). Electromyography (EMG) analysis subsequently demonstrated activation of areas of the brain connected to the medial spinothalamic tract including the anterior cingulate cortex with burst but not with tonic stimulation in 5 patients, thus suggesting supraspinal effects (10). The hypothalamic-pituitary axis has been associated with impacting chronic pain related neural transmission by means of metabolic markers improving with vagal nerve stimulation and Burst-SCS (412). This may all be epiphenomenal or more associated with an improvement in exercise and sleep demonstrated in many of the studies (412). For this reason, this theory should be taken as preliminary in nature. There is also the possibility none of the significant proteins altered came from the hypothalamus and were produced by neurons locally. Other phenomena observed in patients treated with Burst-SCS in a clinical study of 150 patients were decreased catastrophising although this may be purely associated

with pain relief (533). This may however be related to modulation of supraspinal targets associated with the medial spinothalamic tract pain pathway. We did not measure catastrophising scales within our cohort of patients but one of the proteins significant downregulated after Burst-SCS was CCK which is associated with symptoms suggestive of catastrophising including motivational loss, anxiety and panic attacks (425). This emphasises that some of the theories proposed for Burst-SCS have in part been verified with molecular evidence.

6.5 CSF as a valid tool to explore pharmacodynamics

6.5.1 Cells

Measuring CSF gives a representation of the biochemical changes within the CNS and contains immune cells, signalling peptides, metabolites and proteins. We measured T cells as these are the most predominant within the CSF and are amenable to analysis via flow-cytometry (205, 286, 291). Other cells including microglia, macrophages, oligodendrocytes, astrocytes and endothelial cells are not as amenable to analysis. The possibility of taking biopsies of neuronal structures has not been attempted and would likely cause significant morbidity. The roles of each cell in the development and the chronicity of chronic pain are not entirely clear (27, 76, 129, 152, 163, 198, 534). Analysis of our cellular data could not determine if T cells were modulated after amitriptyline within the *in vivo* study. Flow-cytometry in the Burst-SCS cohort were all analysed within the 3-day window (which was later updated by the company supplying the tubes) together with functioning antibodies. However, no significant differences were observed in samples after Burst-SCS. Significant changes in T cell phenotype within CSF would be difficult to implicate directly in chronic pain and mechanisms to treatment. This is due to the possibility that neuropeptides secreted from the spinal cord alter their effector functions. Thus, we would not be able to state a specific T cell phenotype in the CSF causes neuropathic pain or a dynamic change is responsible for efficacy to medication. What would be more compelling is studying any infiltrating T cells within the dorsal horn of the spinal cord. Whether specific populations of T cells migrate from the spinal cord into CSF would need further clarification. In patients with peripheral neuropathy and HIV infection, increased $CD8^+$ T cells in the CSF have been implicated in neuropathy but examination of the spinal cord was not carried out to verify the source of these cells (32). The CNS and

immune privilege is the term given to an organ in which implanted tissue grafts are incapable of provoking immunity (523). However, activated circulating T cells can cross the blood brain barrier without inflammation so the exact mechanism of immune privilege is yet to be fully characterised(522). In cases of neuroinflammation, cells within the CSF have correlated with infiltrating brain parenchymal immune cells (535, 536). There is evidence to suggest neuroinflammation is synonymous with neuropathic pain in the brain (174, 180, 182), focally within the spinal cord and neuroforamina of individual nerve roots in radicular pain (183). Despite this, there is no direct evidence to demonstrate infiltrating immune cells enter the spinal cord of patients with neuropathic pain. Myeloid cells including microglia and monocytes have demonstrated a strong correlation with chronic pain but remain a challenge to study. Pre-clinical models in mice have demonstrated exclusive infiltration of microglia into the dorsal horn of the spinal cord, 21 days after nerve injury (146). More advanced techniques will likely be required to study other cells within the CNS and implicate them in the chronicity of pain.

6.5.2 Neuropeptides

The ELISA sets chosen for our study were based on previous work with CSF (122, 168, 170, 171, 187, 188, 301), however the cytokine and chemokine networks within the CNS are likely to be considerably more advanced. The plates chosen for ELISA allowed us to measure the most cytokines with 1ml of CSF. The neurotrophins NGF, BDNF and GDNF have all been successfully measured in other studies (110, 115, 188), however we were not able to measure any of these in our cohort and this was using the ELISA sets with the lowest detectable ranges.

The ability to link neuropeptide changes to specific cellular structures within the CNS also remains a considerable challenge. Human astrocytes have been analysed using RNA sequences compared to rodent astrocytes demonstrating clear physiological differences (342). Human astrocytes with LPS stimulation have also been mapped in terms of a secretome but these were foetal cells (335). Remarkably, one of the chemokines highlighted in the secretome was eotaxin-1, which was downregulated after amitriptyline in our cohort of responders (335). More research into pathological phenotypes and exosome of specific cells in humans within the CNS needs to be performed.

Proteomics and cluster analysis likely represent the most compelling part of this thesis and has been the centre of most research with CSF in recent scientific literature (211, 213, 294, 417, 463, 537). Although the pathways identified in this thesis may be associative or consistent with normal variation, each study highlighted mechanisms concordant with other work previously published which further validates mechanistic pathways. A valid question is the variability of proteins within the CSF on an individual subject over time and how this impacts results. A study examining this variability concluded that individual variability over a short period of time is relatively small (432). This would indicate any changes from dual sampling before and after the interventions described in this thesis were likely related to that intervention. The question of inter-subject variability is more complex. A study looking at variability of proteins in CSF in healthy controls identified 81 proteins that have variability between healthy subjects (468). These proteins have a different degree of variability and excluding them was not recommended by the authors (468). For this reason, our analysis in the opioid study may be more open to criticism as differential proteins may not have been attributable to the effect of opioids alone. More work in the future needs to be performed to determine which proteins vary and are not synonymous with pathological sequelae. Despite these limitations, proteomic work with CSF has resulted in progress in many fields of neurodegenerative diseases. Proteomic analysis of CSF in Alzheimer's has led to the development of identifying at risk populations and tracking treatment response (293). More studies in specific cohorts of patients with chronic pain may enable similar progression of our understanding of the condition.

The challenges in proteomic and biomarker discovery remain the inability to validate the findings of specific proteins. Although proteomic methods have improved, particularly with CSF (211), many studies have not validated the findings of significant proteins with ELISA (211, 417, 537). The use of label-free proteomics lack the ability to validate specific proteins with antibody tests to determine if they can be true biomarkers of efficacy or mechanisms(538), this is related to the availability of an antibody set and the combined quality of both tests. What is recommended is an untargeted approach followed by a targeted approach (539). Working with large patient cohorts and a high statistical power remains paramount. The importance of appropriate control samples is also contentious as healthy subjects may not necessarily be available for sample analysis. Healthy controls with CSF have largely come from headache patients with no confirmed pathology and patients undergoing spinal anaesthesia (211, 351, 468, 510). It is therefore not really appropriate to call these patients 'healthy' controls.

6.5.3 Comparison between proteomic, cellular and cytokine data

The chapters within this thesis have attempted in part to connect cellular, cytokine and proteomic data. Due to the many different cells and phenotypes within the CNS and CSF it remains a considerable challenge to identify where the proteins or neuropeptides have been produced. *In-vitro* stimulation of specific cells and RNA analysis allows some proteins and neuropeptides to be matched to specific cells and phenotypes (335, 342).
It is notable however, that there is no identification of the neuropeptides in the proteomics results and there are a number of reasons for this. Low abundance proteins create a significant challenge to MS techniques (540). Cytokines generally are low abundance proteins and while it is possible to detect these using MS, detection is hindered by matrix interferences and suppression (540, 541). Digestion processes and dilution in sample preparation are also a factor (540). One example of this is where interferon spiked proteins using specific MS techniques could not detect interferons below 1ng/mL (542). All of our cytokines and chemokines were in the pg range. Antibody techniques need to be used to capture specific low abundance proteins and it is better to use more established techniques that include ELISA.
Mass spectrometry has limitations as it also cannot detect many neuronal signalling molecules including GABA and glycine which are important to chronic pain and neuronal signalling (213). We did not perform ELISA on signalling neuropeptides as it was central to the thesis to focus on immune neuropeptides. Future studies should ideally be more focused and have CSF stored in enough aliquots to validate the proteomic findings or test more specific proteins and neuropeptides.

6.6 Future and Follow up studies:

The primary limitation was the low number of participants within these studies. We also cannot account for placebo responders, which may distort the results, and can be as high as 30% in trials within chronic pain (543). Pain is also multidimensional, and we only used pain scores without assessments of mood, function and quality of life which are frequently

required for large multicentre trials. The use of a control group may also have been useful to compare neuropeptides to healthy controls. Repeated samples in control groups or in the subjects may have also been able to account for proteins that have significant variation between samples without intervention using our protocols.

Studies examining CSF in the future should envisage as many patients as possible and phenotype them according to diagnosis and medication. Mechanisms explored for intervention or medication need to be analysed in larger patient cohorts and more importantly in placebo-controlled trials. The establishment of a CSF Bio Bank are appealing across many centres combined with novel neuroimaging studies (174, 293). The information gained from these measures may not be able to draw firm conclusions to mechanisms but may phenotype patients to an appropriate treatment. A combination of investigations will increase the ability to recognise if neuroinflammation and the phenomena of gliosis are pathognomonic of chronic neuropathic pain.

Cellular analysis can be improved with FACS to gain more information of the effector function of cells within the CSF and how processes within the brain and spinal cord modulate their intracellular processes(76). It may also be possible to capture microglia within the CSF in specific patient cohorts which has already been achieved (208).

Proteomic data and RNA analysis has already been architectural in the genesis of new treatments which include spinal cord stimulation with analysis of the spinal cord in rodents (400, 544). The findings of one study have developed into the creation of a novel waveform for SCS that has demonstrated glia specific modulation in mice using the sciatic nerve ligation model (545). Interestingly, the pre-clinical experiments focused more on sensomes or identified genes and proteins from specific cells within the CNS (544, 545). The exact same sensomes or biosignatures may not necessarily transfer well to humans however with only astrocytes mapped from foetal tissue being analysed thus far (335). Although this waveform termed “Differential target multiplex” claims uniquely to target glial cells, many of the initial experiments did not use many of the novel waveforms including Burst-SCS (544, 545). Initial results in humans with this waveform have demonstrated a superior reduction in pain scores compared to tonic stimulation but the *in vivo* modulation of glia in humans have yet to be validated (546). Our analysis of Burst-SCS suggested that many of altered proteome were from glial cells, although this has not been concordant with the mechanisms proposed in other studies thus far (395). Studies with proteomic or RNA analysis with multiple waveforms with suitable washout periods would an interesting study to perform. It is important to measure dynamic changes *in vivo* to determine if the pre-

clinical studies translate. Moreover, with many waveforms of spinal cord stimulation available, being able to prescribe a waveform for a particular phenotype of chronic neuropathic pain will benefit patients and reduce healthcare costs.

The quest for biomarkers or predictors of treatment for chronic pain needs to be established and correlated with subjective outcomes in order to justify treatments. Placebo responders in many studies emphasise that we are still unsure of the true efficacy of many treatments in chronic pain. There is evidence of disease remission in some cases and examining the biomarker profile of these patients would be interesting to observe if any biomarker or set of biomarkers (biosignature) return to a physiological norm of a control population.

Observation from prospective and retrospective studies clearly identifies patient populations that lose efficacy to a given treatment. The reasons for this remain uncertain and may be multifactorial. There may be disease progression or the genesis of a novel pain condition that is independent from the treated condition. A better understanding of many of these phenomena would need to be matched with biomarkers or neuroimaging as it is currently challenging for physicians to identify one pathology from another.

Furthermore, the study of non-responders in clinical studies with biomarker profiles may enhance our knowledge of treatment resistance. The ability to inform patients of treatment failure remains important and prevents exposure to risk of interventions and side effects from drugs. We still lack specificity in selecting many patients for chronic pain treatments. The study of patients with a definitive diagnosis after treatment failure will provide a map for new therapeutic targets.

6.7 Implications and Recommendations for Clinical Practice

This thesis demonstrates that CSF can provide mechanistic evidence of action for therapeutic strategies employed in the management of chronic neuropathic pain in patients. This may lead to the identification of biomarkers which is required for the development of effective therapies and will allow identification of the placebo response in patients with chronic neuropathic pain which is notoriously high. This is already practiced in oncological treatment regimens (547). Placebo responders within clinical trials for chronic pain frequently distort outcomes (543, 548, 549). It is therefore also important to identify if the proposed pharmacodynamic response is not present in placebo responders. This level of scrutiny remains important as prescribing of opioids in chronic pain has developed into a

societal issue with crime and deaths attributed to the liberal prescribing of opioids on a daily basis (14, 17, 550). Future phased studies of novel pharmacological and device innovations should strongly consider using CSF to identify biomarkers and pathways of mechanisms to treatment.

6.8 Conclusions

The strengths of this thesis include *in vivo* methodology in humans in well selected patients with dual sample analysis (with the exception of the opioid chapter) to determine mechanisms of action of pain therapeutics. Furthermore, analysis and conclusions were drawn only from responders when assessing amitriptyline and Burst-SCS. The results of this thesis have provided important information on mechanisms of action of therapies that are commonly used within the field of chronic pain and in many other specialities. This validates, with certain limitations, molecular evidence of effectiveness of amitriptyline and Burst-SCS for chronic pain. There have also been multiple novel findings in the pharmacodynamics of the treatments discussed. These novel findings will encourage more research with CSF and in the development of therapeutics for chronic neuropathic pain. An improvement in treatment options for the highly refractory condition of chronic neuropathic pain will benefit patients, physicians and society.

Appendix:

Appendix I: Patient information leaflet Amitriptyline study

Study:

An investigation of the effect of amitriptyline on Cerebrospinal Fluid concentrations of TNF-α, NGF, BDNF, VEGF and MCP-1 and quantification of cellularity of CSF in patients with chronic lumbar radicular pain.

Introduction:

You have been offered inclusion in this study because you have radicular pain (nerve pain, sciatica). This is treated with tablets like amitriptyline and a procedure called pulsed radiofrequency (prf), which is standard practice. We are doing this study to find out how the tablet amitriptyline works in nerve pain.

Procedure:

During the first procedure of prf we will take a small sample of spinal fluid using a very thin needle. This is done in our day surgery and you can go home on the same day. It will add 1-2 minutes on to the procedure time. The risk involved in this is very small and includes a 1/400 chance of a headache and a lower chance of infection and bleeding. You will then be started on the tablet called amitriptyline for 6 weeks and take it at night time until the second procedure of prf on a different affected nerve. We will take a second small sample of spinal fluid during the second procedure.

Benefits:

PRF and amitriptyline are treatments we use as standard for nerve pain. You can still receive either of these treatments or alternatives if you do not wish to participate in this study. Inclusion in this study offers no benefits other than to progress our understanding of the use of amitrityline in chronic pain.

Risks:

There is risk of infection, bleeding, nerve damage and headache related to pain procedure and spinal fluid sampling. However, this is rare. The methods used are well established in the St. James Pain Medicine unit and have already been demonstrated to be safe.

The tablet amitriptyline has some side effects like drowsiness and dry mouth. You can stop taking this medication at any time; you can also refuse to have the second prf treatment.

Exclusion from participation:

You cannot be included in this study if you are pregnant, breast- feeding, on anticoagulation or corticosteroid therapy, having active infection, have history of stroke and significant psychiatric problem.

Alternative treatment:

All patients with radicular pain are offered amitriptyline and/or PRF therapy. You do not have to be a part of this study to be treated.

Confidentiality:

Your identity will remain confidential. Your name will not be published and will not be disclosed to anyone outside the hospital.

Compensation:

Your doctors are covered by standard medical malpractice insurance. Nothing in this document restricts or curtails your rights.

Voluntary Participation:

If you have volunteered to participate in this study, you may quit at any time. If you decide not to participate, or if you quit, you will not be penalised and will not give up any benefits, which you had before entering the study.

Stopping the study:

You understand that your doctor may stop your participation in the study at any time without your consent but you will never be deprived of treatment.

Permission:

This study has hospital Research Ethics Committee approval.

Further information:

You can get more information or answers to your questions about the study, your participation in the study, and your rights, from Dr Jonathan Royds who can be contacted via the hospital switchboard. If your doctor learns of important new information that might affect your desire to remain in the study, he or she will tell you.

Risks of Lumbar Puncture:

Risks:

Common >5%:

- You may have mild backache for a few days; this would be similar if having PRF alone
- Shooting pain down legs during the procedure is common but resolves after the needle is withdrawn

Uncommon 1-5%:

- Headache with the needles we use is rare but can be severe and last for a few days. It may require intervention if persists

Rare:

- Nerve damage is between 1/10,000 – 1/30,000, this may result in numbness or loss of power in your legs. This will likely improve over 6 months.
- Infection occurs in roughly 1/100,000 patients and would require antibiotics and/or surgery
- Bleeding and clots can occur in 1/200,000 patients and requires urgent surgery

References:
Cook TM, Counsell D, Wildsmith JA. Major complications of central neuraxial block: report on the Third National Audit Project of the Royal College of Anaesthetists†. British journal of anaesthesia. 2009 Feb 1;102(2):179-90.

Appendix II Patient Information Leaflet Burst SCS study

Title of Study: An investigation of the effect of different methods neuromodulation on Cerebrospinal Fluid concentrations of TNF-α, NGF, BDNF, VEGF and MCP-1 and quantification of cellularity of CSF in patients with failed back surgery syndrome and complex regional pain syndrome.

Introduction:
You have been selected to take place in this study because you are going to have a spinal cord stimulator. This study is being done to see how the stimulator works and affects proteins in the spine using different settings. We will also be looking at how the different settings improve your pain and function.

Procedure:
If you a agree to participate you will come in to the day ward as planned. We will take a small sample of spinal fluid from your back (before the stimulator is put in) using a thin needle. We will then take a second sample of spinal fluid from your back during your follow up visit. The risk of any complications is low for this procedure and includes a 1/400 chance of headache and much lower risk of nerve damage.

Benefits: Inclusion in this study offers no benefits other than to progress our understanding of the use of spinal cord stimulators in chronic pain.

Risks:

There is risk of bleeding, nerve damage and headache related to spinal fluid sampling. However, this is rare (see risks of lumbar puncture below). The methods used are well established in the St. James Pain Medicine unit and have already been demonstrated to be safe.

Exclusion from participation:

You cannot be included in this study if you are pregnant, breast- feeding, on anticoagulation or corticosteroid therapy, having active infection, have history of stroke and significant psychiatric problem.

Confidentiality:

Your identity will remain confidential. Your name will not be published and will not be disclosed to anyone outside the hospital.

Compensation:

Your doctors are covered by standard medical malpractice insurance. Nothing in this document restricts or curtails your rights.

Voluntary Participation:

If you have volunteered to participate in this study, you may quit at any time. If you decide not to participate, or if you quit, you will not be penalised and will not give up any benefits, which you had before entering the study.

Stopping the study:

You understand that your doctor may stop your participation in the study at any time without your consent but you will never be deprived of treatment.

Permission:

This study has hospital Research Ethics Committee approval.

Further information:

You can get more information or answers to your questions about the study, your participation in the study, and your rights, from Dr Jonathan Royds who can be contacted via the hospital switchboard. If your doctor learns of important new information that might affect your desire to remain in the study, he or she will tell you.

Risks of Lumbar Puncture:

Risks:

Common >5%:

- You may have mild backache for a few days; this would be similar if having PRF alone
- Shooting pain down legs during the procedure is common but resolves after the needle is withdrawn

Uncommon 1-5%:

- Headache with the needles we use is rare but can be severe and last for a few days. It may require intervention if persists

Rare:

- Nerve damage is between 1/10,000 – 1/30,000, this may result in numbness or loss of power in your legs. This will likely improve over 6 months.
- Infection occurs in roughly 1/100,000 patients and would require antibiotics and/or surgery
- Bleeding and clots can occur in 1/200,000 patients and requires urgent surgery

References:

Cook TM, Counsell D, Wildsmith JA. Major complications of central neuraxial block: report on the Third National Audit Project of the Royal College of Anaesthetists†. British journal of anaesthesia. 2009 Feb 1;102(2):179-90.

Appendix III: Numerical rating scale to assess pain intensity

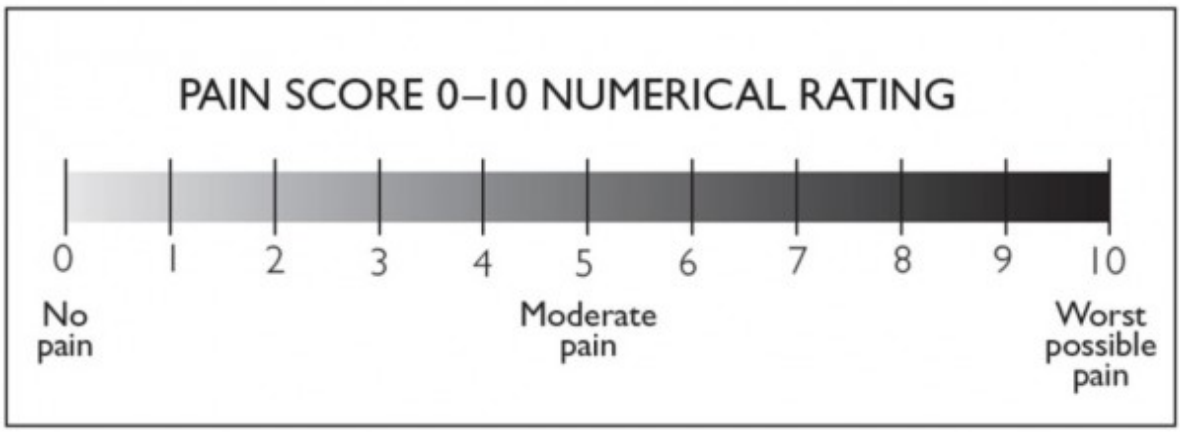

Appendix IV : Doleur Neuropathique 4 questionnaire to assess neuropathic pain

DN4 Questionnaire

Please complete this questionnaire by ticking one answer for each item in the 4 questions below:

INTERVIEW OF THE PATIENT

Question 1: Does the pain have one or more of the following characteristics?

	Yes	No
1 – Burning		
2 – Painful cold		
3 – Electric shocks		

Question 2: Is the pain associated with one of more of the following symptoms in the same area?

	Yes	No
4 – Tingling		
5 – Pins and needles		
6 – Numbness		
7 – Itching		

EXAMINATION OF THE PATIENT

Question 3: Is the pain located in an area where the physical examination may reveal one or more of the following characteristics?

	Yes	No
8 – Hypoesthesia to touch		
9 – Hypoesthesia to prick		

Question 4: In the painful area, can the pain be caused or increased by:

	Yes	No
10 – Brushing		

The total score is calculated as the sum of the 10 items and the cut-off value for the diagnosis of neuropathic pain is a total score of 4/10.

Total

Bouhassira D, Attal N, Alchaar H, et al. "Comparison of pain syndromes associated with nervous or somatic lesions and development of a new neuropathic pain diagnostic questionnaire (DN4)." Pain 114.1-2 (2005): 29-36.

References:

1. Treede RD, Rief W, Barke A, Aziz Q, Bennett MI, Benoliel R, et al. A classification of chronic pain for ICD-11. Pain. 2015;156(6):1003-7.
2. Cordero-Erausquin M, Inquimbert P, Schlichter R, Hugel S. Neuronal networks and nociceptive processing in the dorsal horn of the spinal cord. Neuroscience. 2016;338:230-47.
3. Grace PM, Hutchinson MR, Maier SF, Watkins LR. Pathological pain and the neuroimmune interface. Nat Rev Immunol. 2014;14(4):217-31.
4. Dubin AE, Patapoutian A. Nociceptors: the sensors of the pain pathway. J Clin Invest. 2010;120(11):3760-72.
5. Costigan M, Scholz J, Woolf CJ. Neuropathic pain: a maladaptive response of the nervous system to damage. Annual review of neuroscience. 2009;32:1-32.
6. Wooten M, Weng HJ, Hartke TV, Borzan J, Klein AH, Turnquist B, et al. Three functionally distinct classes of C-fibre nociceptors in primates. Nat Commun. 2014;5:4122.
7. D'Mello R, Dickenson AH. Spinal cord mechanisms of pain. Br J Anaesth. 2008;101(1):8-16.
8. De Ridder D, Vanneste S, Plazier M, van der Loo E, Menovsky T. Burst spinal cord stimulation: toward paresthesia-free pain suppression. Neurosurgery. 2010;66(5):986-90.
9. Geha PY, Baliki MN, Harden RN, Bauer WR, Parrish TB, Apkarian AV. The brain in chronic CRPS pain: abnormal gray-white matter interactions in emotional and autonomic regions. Neuron. 2008;60(4):570-81.
10. De Ridder D, Vanneste S. Burst and Tonic Spinal Cord Stimulation: Different and Common Brain Mechanisms. Neuromodulation. 2016;19(1):47-59.
11. Woolf CJ. Central sensitization: implications for the diagnosis and treatment of pain. Pain. 2011;152(3 Suppl):S2-15.
12. Breivik H, Eisenberg E, O'Brien T. The individual and societal burden of chronic pain in Europe: the case for strategic prioritisation and action to improve knowledge and availability of appropriate care. BMC public health. 2013;13:1229.
13. Volkow ND, McLellan AT. Opioid Abuse in Chronic Pain--Misconceptions and Mitigation Strategies. N Engl J Med. 2016;374(13):1253-63.
14. Rudd RA, Aleshire N, Zibbell JE, Gladden RM. Increases in Drug and Opioid Overdose Deaths--United States, 2000-2014. MMWR Morb Mortal Wkly Rep. 2016;64(50-51):1378-82.
15. Chou R, Turner JA, Devine EB, Hansen RN, Sullivan SD, Blazina I, et al. The effectiveness and risks of long-term opioid therapy for chronic pain: a systematic review for a National Institutes of Health Pathways to Prevention Workshop. Ann Intern Med. 2015;162(4):276-86.
16. Christie MJ. Cellular neuroadaptations to chronic opioids: tolerance, withdrawal and addiction. Br J Pharmacol. 2008;154(2):384-96.
17. Dowell D, Haegerich TM, Chou R. CDC Guideline for Prescribing Opioids for Chronic Pain--United States, 2016. JAMA. 2016;315(15):1624-45.
18. Vardeh D, Mannion RJ, Woolf CJ. Toward a Mechanism-Based Approach to Pain Diagnosis. The journal of pain : official journal of the American Pain Society. 2016;17(9 Suppl):T50-69.

19. van Hecke O, Kamerman PR, Attal N, Baron R, Bjornsdottir G, Bennett DL, et al. Neuropathic pain phenotyping by international consensus (NeuroPPIC) for genetic studies: a NeuPSIG systematic review, Delphi survey, and expert panel recommendations. Pain. 2015;156(11):2337-53.
20. Yekkirala AS, Roberson DP, Bean BP, Woolf CJ. Breaking barriers to novel analgesic drug development. Nature reviews Drug discovery. 2017;16(8):545-64.
21. Hurst H, Bolton J. Assessing the clinical significance of change scores recorded on subjective outcome measures. J Manipulative Physiol Ther. 2004;27(1):26-35.
22. Cruccu G, Truini A. Tools for assessing neuropathic pain. PLoS Med. 2009;6(4):e1000045.
23. Colloca L, Ludman T, Bouhassira D, Baron R, Dickenson AH, Yarnitsky D, et al. Neuropathic pain. Nat Rev Dis Primers. 2017;3:17002.
24. Gilron I, Baron R, Jensen T. Neuropathic pain: principles of diagnosis and treatment. Mayo Clin Proc. 2015;90(4):532-45.
25. Cobos EJ, Nickerson CA, Gao F, Chandran V, Bravo-Caparros I, Gonzalez-Cano R, et al. Mechanistic Differences in Neuropathic Pain Modalities Revealed by Correlating Behavior with Global Expression Profiling. Cell reports. 2018;22(5):1301-12.
26. Bridges D, Thompson SW, Rice AS. Mechanisms of neuropathic pain. Br J Anaesth. 2001;87(1):12-26.
27. Scholz J, Woolf CJ. The neuropathic pain triad: neurons, immune cells and glia. Nature Neuroscience. 2007;10(11):1361-8.
28. Sisignano M, Lotsch J, Parnham MJ, Geisslinger G. Potential biomarkers for persistent and neuropathic pain therapy. Pharmacol Ther. 2019.
29. Haberberger RV, Barry C, Dominguez N, Matusica D. Human Dorsal Root Ganglia. Front Cell Neurosci. 2019;13:271.
30. Talbot S, Foster SL, Woolf CJ. Neuroimmunity: Physiology and Pathology. Annual review of immunology. 2016;34:421-47.
31. Del Valle L, Schwartzman RJ, Alexander G. Spinal cord histopathological alterations in a patient with longstanding complex regional pain syndrome. Brain Behav Immun. 2009;23(1):85-91.
32. Wang SX, Ho EL, Grill M, Lee E, Peterson J, Robertson K, et al. Peripheral neuropathy in primary HIV infection associates with systemic and central nervous system immune activation. J Acquir Immune Defic Syndr. 2014;66(3):303-10.
33. Chapman CR, Vierck CJ. The Transition of Acute Postoperative Pain to Chronic Pain: An Integrative Overview of Research on Mechanisms. The journal of pain : official journal of the American Pain Society. 2017;18(4):359 e1- e38.
34. Apkarian AV, Baliki MN, Farmer MA. Predicting transition to chronic pain. Curr Opin Neurol. 2013;26(4):360-7.
35. Latremoliere A, Woolf CJ. Central sensitization: a generator of pain hypersensitivity by central neural plasticity. The journal of pain : official journal of the American Pain Society. 2009;10(9):895-926.
36. Fairless R, Williams SK, Diem R. Dysfunction of neuronal calcium signalling in neuroinflammation and neurodegeneration. Cell Tissue Res. 2014;357(2):455-62.
37. Austin PJ, Fiore NT. Supraspinal neuroimmune crosstalk in chronic pain states. Current Opinion in Physiology. 2019;11:7-15.
38. Walker AK, Kavelaars A, Heijnen CJ, Dantzer R. Neuroinflammation and comorbidity of pain and depression. Pharmacol Rev. 2014;66(1):80-101.
39. Baumgärtner U, Magerl W, Klein T, Hopf HC, Treede R-D. Neurogenic hyperalgesia versus painful hypoalgesia: two distinct mechanisms of neuropathic pain. Pain. 2002;96(1-2):141-51.

40. Freynhagen R, Baron R, Gockel U, Tolle TR. painDETECT: a new screening questionnaire to identify neuropathic components in patients with back pain. Curr Med Res Opin. 2006;22(10):1911-20.
41. Bouhassira D, Attal N, Alchaar H, Boureau F, Brochet B, Bruxelle J, et al. Comparison of pain syndromes associated with nervous or somatic lesions and development of a new neuropathic pain diagnostic questionnaire (DN4). Pain. 2005;114(1-2):29-36.
42. Koes BW, Van Tulder M, Peul W. Diagnosis and treatment of sciatica. Bmj. 2007;334(7607):1313-7.
43. Ergun T, Lakadamyali H. CT and MRI in the evaluation of extraspinal sciatica. The British journal of radiology. 2010;83(993):791-803.
44. Baron R, Binder A, Wasner G. Neuropathic pain: diagnosis, pathophysiological mechanisms, and treatment. Lancet Neurol. 2010;9(8):807-19.
45. Finnerup NB, Attal N, Haroutounian S, McNicol E, Baron R, Dworkin RH, et al. Pharmacotherapy for neuropathic pain in adults: a systematic review and meta-analysis. The Lancet Neurology. 2015;14(2):162-73.
46. Van Boxem K, Cheng J, Patijn J, van Kleef M, Lataster A, Mekhail N, et al. 11. Lumbosacral radicular pain. Pain Pract. 2010;10(4):339-58.
47. Gatchel RJ, Peng YB, Peters ML, Fuchs PN, Turk DC. The biopsychosocial approach to chronic pain: scientific advances and future directions. Psychol Bull. 2007;133(4):581-624.
48. Parkitny L, Wand BM, Graham C, Quintner J, Moseley GL. Interdisciplinary Management of Complex Regional Pain Syndrome of the Face. Phys Ther. 2016;96(7):1067-73.
49. Couch JR, Amitriptyline Versus Placebo Study G. Amitriptyline in the prophylactic treatment of migraine and chronic daily headache. Headache. 2011;51(1):33-51.
50. Moore RA, Derry S, Aldington D, Cole P, Wiffen PJ. Amitriptyline for neuropathic pain in adults. Cochrane Database Syst Rev. 2015(7):CD008242.
51. van den Driest JJ, Bierma-Zeinstra SMA, Bindels PJE, Schiphof D. Amitriptyline for musculoskeletal complaints: a systematic review. Family Practice. 2017;34(2):138-46.
52. Shepherd AJ, Copits BA, Mickle AD, Karlsson P, Kadunganattil S, Haroutounian S, et al. Angiotensin II Triggers Peripheral Macrophage-to-Sensory Neuron Redox Crosstalk to Elicit Pain. The Journal of neuroscience : the official journal of the Society for Neuroscience. 2018;38(32):7032-57.
53. Royds J, McCrory C. Neuroimmunity and chronic pain. Bja Education. 2018;18(12):377-83.
54. Brooks K, Kessler T. Treatments for neuropathic pain. Clin Pharm. 2017;9:12.
55. Deer TR, Malinowski M, Varshney V, Pope J. Choice of intrathecal drug in the treatment of neuropathic pain-new research and opinion. Expert review of clinical pharmacology. 2019(just-accepted).
56. Zhu B, Zhou X, Zhou Q, Wang H, Wang S, Luo K. INTRA-VENOUS LIDOCAINE TO RELIEVE NEUROPATHIC PAIN: A SYSTEMATIC REVIEW AND META-ANALYSIS. Frontiers in Neurology. 2019;10:954.
57. Quintão NL, Santin JR, Stoeberl LC, Corrêa TP, Melato J, Costa R. PHARMACOLOGICAL TREATMENT OF CHEMOTHERAPY-INDUCED NEUROPATHIC PAIN: PPAR AGONISTS AS A PROMISING TOOL. Frontiers in Neuroscience. 2019;13:907.

58. Falco FJ, Manchikanti L, Datta S, Wargo BW, Geffert S, Bryce DA, et al. Systematic review of the therapeutic effectiveness of cervical facet joint interventions: an update. Pain Physician. 2012;15(6):E839-68.
59. Kwak SG, Lee DG, Chang MC. Effectiveness of pulsed radiofrequency treatment on cervical radicular pain: A meta-analysis. Medicine (Baltimore). 2018;97(31):e11761.
60. Das B, Conroy M, Moore D, Lysaght J, McCrory C. Human dorsal root ganglion pulsed radiofrequency treatment modulates cerebrospinal fluid lymphocytes and neuroinflammatory markers in chronic radicular pain. Brain Behav Immun. 2018;70:157-65.
61. Lee DG, Ahn SH, Lee J. Comparative Effectivenesses of Pulsed Radiofrequency and Transforaminal Steroid Injection for Radicular Pain due to Disc Herniation: a Prospective Randomized Trial. J Korean Med Sci. 2016;31(8):1324-30.
62. Diwan S, Manchikanti L, Benyamin RM, Bryce DA, Geffert S, Hameed H, et al. Effectiveness of cervical epidural injections in the management of chronic neck and upper extremity pain. Pain Physician. 2012;15(4):E405-34.
63. Cohen SP, Peterlin BL, Fulton L, Neely ET, Kurihara C, Gupta A, et al. Randomized, double-blind, comparative-effectiveness study comparing pulsed radiofrequency to steroid injections for occipital neuralgia or migraine with occipital nerve tenderness. Pain. 2015;156(12):2585-94.
64. North RB, Campbell JN, James CS, Conover-Walker MK, Wang H, Piantadosi S, et al. Failed back surgery syndrome: 5-year follow-up in 102 patients undergoing repeated operation. Neurosurgery. 1991;28(5):685-90; discussion 90-1.
65. North RB, Kidd DH, Farrokhi F, Piantadosi SA. Spinal cord stimulation versus repeated lumbosacral spine surgery for chronic pain: a randomized, controlled trial. Neurosurgery. 2005;56(1):98-106; discussion -7.
66. Deer TR, Levy RM, Kramer J, Poree L, Amirdelfan K, Grigsby E, et al. Dorsal root ganglion stimulation yielded higher treatment success rate for complex regional pain syndrome and causalgia at 3 and 12 months: a randomized comparative trial. Pain. 2017;158(4):669-81.
67. Liem L, Russo M, Huygen FJ, Van Buyten JP, Smet I, Verrills P, et al. A multicenter, prospective trial to assess the safety and performance of the spinal modulation dorsal root ganglion neurostimulator system in the treatment of chronic pain. Neuromodulation. 2013;16(5):471-82; discussion 82.
68. Deer T, Slavin KV, Amirdelfan K, North RB, Burton AW, Yearwood TL, et al. Success Using Neuromodulation With BURST (SUNBURST) Study: Results From a Prospective, Randomized Controlled Trial Using a Novel Burst Waveform. Neuromodulation. 2018;21(1):56-66.
69. Al-Kaisy A, Palmisani S, Smith TE, Pang D, Lam K, Burgoyne W, et al. 10 kHz High-Frequency Spinal Cord Stimulation for Chronic Axial Low Back Pain in Patients With No History of Spinal Surgery: A Preliminary, Prospective, Open Label and Proof-of-Concept Study. Neuromodulation. 2017;20(1):63-70.
70. Baber Z, Erdek MA. Failed back surgery syndrome: current perspectives. J Pain Res. 2016;9:979-87.
71. Birklein F, Dimova V. Complex regional pain syndrome-up-to-date. Pain Rep. 2017;2(6):e624.
72. Harden RN, Maihofner C, Abousaad E, Vatine JJ, Kirsling A, Perez R, et al. A prospective, multisite, international validation of the Complex Regional Pain Syndrome Severity Score. Pain. 2017;158(8):1430-6.

73. Eldabe S, Buchser E, Duarte RV. Complications of Spinal Cord Stimulation and Peripheral Nerve Stimulation Techniques: A Review of the Literature. Pain Med. 2016;17(2):325-36.
74. Al-Kaisy A, Palmisani S, Pang D, Sanderson K, Wesley S, Tan Y, et al. Prospective, Randomized, Sham-Control, Double Blind, Crossover Trial of Subthreshold Spinal Cord Stimulation at Various Kilohertz Frequencies in Subjects Suffering From Failed Back Surgery Syndrome (SCS Frequency Study). Neuromodulation. 2018;21(5):457-65.
75. Watkins LR, Maier SF. Beyond neurons: evidence that immune and glial cells contribute to pathological pain states. Physiol Rev. 2002;82(4):981-1011.
76. Hore Z, Denk F. Neuroimmune interactions in chronic pain - An interdisciplinary perspective. Brain Behav Immun. 2019.
77. McMahon SB, La Russa F, Bennett DL. Crosstalk between the nociceptive and immune systems in host defence and disease. Nat Rev Neurosci. 2015;16(7):389-402.
78. Waldburger J-M, Firestein GS. Regulation of Peripheral Inflammation by the Central Nervous System. Current Rheumatology Reports. 2010;12(5):370-8.
79. Coraggio V, Guida F, Boccella S, Scafuro M, Paino S, Romano D, et al. Neuroimmune-Driven Neuropathic Pain Establishment: A Focus on Gender Differences. Int J Mol Sci. 2018;19(1).
80. Karshikoff B, Tadros MA, Mackey S, Zouikr I. Neuroimmune modulation of pain across the developmental spectrum. Current Opinion in Behavioral Sciences. 2019;28:85-92.
81. Costigan M, Moss A, Latremoliere A, Johnston C, Verma-Gandhu M, Herbert TA, et al. T-cell infiltration and signaling in the adult dorsal spinal cord is a major contributor to neuropathic pain-like hypersensitivity. The Journal of neuroscience : the official journal of the Society for Neuroscience. 2009;29(46):14415-22.
82. White FA, Jung H, Miller RJ. Chemokines and the pathophysiology of neuropathic pain. Proc Natl Acad Sci U S A. 2007;104(51):20151-8.
83. Gao YJ, Ji RR. Chemokines, neuronal-glial interactions, and central processing of neuropathic pain. Pharmacol Ther. 2010;126(1):56-68.
84. Turner MD, Nedjai B, Hurst T, Pennington DJ. Cytokines and chemokines: At the crossroads of cell signalling and inflammatory disease. Biochim Biophys Acta. 2014;1843(11):2563-82.
85. Jung H, Toth PT, White FA, Miller RJ. Monocyte chemoattractant protein-1 functions as a neuromodulator in dorsal root ganglia neurons. J Neurochem. 2008;104(1):254-63.
86. Mika J, Zychowska M, Popiolek-Barczyk K, Rojewska E, Przewlocka B. Importance of glial activation in neuropathic pain. Eur J Pharmacol. 2013;716(1-3):106-19.
87. Zhang JM, An J. Cytokines, inflammation, and pain. Int Anesthesiol Clin. 2007;45(2):27-37.
88. Garcia-Zepeda EA, Rothenberg ME, Ownbey RT, Celestin J, Leder P, Luster AD. Human eotaxin is a specific chemoattractant for eosinophil cells and provides a new mechanism to explain tissue eosinophilia. Nat Med. 1996;2(4):449-56.
89. Miller RJ, Jung H, Bhangoo SK, White FA. Cytokine and chemokine regulation of sensory neuron function. Handb Exp Pharmacol. 2009(194):417-49.
90. Ren K, Dubner R. Interactions between the immune and nervous systems in pain. Nat Med. 2010;16(11):1267-76.
91. Audet M-C, Anisman H. Interplay between pro-inflammatory cytokines and growth factors in depressive illnesses. Frontiers in Cellular Neuroscience. 2013;7.

92. Clark AK, Old EA, Malcangio M. Neuropathic pain and cytokines: current perspectives. J Pain Res. 2013;6:803-14.
93. Hung AL, Lim M, Doshi TL. Targeting cytokines for treatment of neuropathic pain. Scand J Pain. 2017;17:287-93.
94. Skaper SD, Giusti P, Facci L. Microglia and mast cells: two tracks on the road to neuroinflammation. FASEB J. 2012;26(8):3103-17.
95. Matsuda M, Huh Y, Ji RR. Roles of inflammation, neurogenic inflammation, and neuroinflammation in pain. J Anesth. 2019;33(1):131-9.
96. Sonekatsu M, Taniguchi W, Yamanaka M, Nishio N, Tsutsui S, Yamada H, et al. Interferon-gamma potentiates NMDA receptor signaling in spinal dorsal horn neurons via microglia-neuron interaction. Mol Pain. 2016;12.
97. Verkhratsky A, Chvatal A. NMDA Receptors in Astrocytes. Neurochem Res. 2019.
98. Navarrete M, Perea G, Maglio L, Pastor J, Garcia de Sola R, Araque A. Astrocyte calcium signal and gliotransmission in human brain tissue. Cereb Cortex. 2013;23(5):1240-6.
99. Sibille J, Zapata J, Teillon J, Rouach N. Astroglial calcium signaling displays short-term plasticity and adjusts synaptic efficacy. Front Cell Neurosci. 2015;9:189.
100. Cook AD, Christensen AD, Tewari D, McMahon SB, Hamilton JA. Immune Cytokines and Their Receptors in Inflammatory Pain. Trends Immunol. 2018;39(3):240-55.
101. Benedetti B, Matyash V, Kettenmann H. Astrocytes control GABAergic inhibition of neurons in the mouse barrel cortex. J Physiol. 2011;589(Pt 5):1159-72.
102. Mariotti L, Losi G, Sessolo M, Marcon I, Carmignoto G. The inhibitory neurotransmitter GABA evokes long-lasting Ca(2+) oscillations in cortical astrocytes. Glia. 2016;64(3):363-73.
103. Skaper SD. Nerve growth factor: a neuroimmune crosstalk mediator for all seasons. Immunology. 2017;151(1):1-15.
104. Kelleher JH, Tewari D, McMahon SB. Neurotrophic factors and their inhibitors in chronic pain treatment. Neurobiol Dis. 2017;97(Pt B):127-38.
105. Anisman H, Merali Z, Hayley S. Neurotransmitter, peptide and cytokine processes in relation to depressive disorder: comorbidity between depression and neurodegenerative disorders. Prog Neurobiol. 2008;85(1):1-74.
106. Tsuda M, Inoue K, Salter MW. Neuropathic pain and spinal microglia: a big problem from molecules in "small" glia. Trends Neurosci. 2005;28(2):101-7.
107. Croft W, Dobson KL, Bellamy TC. Plasticity of Neuron-Glial Transmission: Equipping Glia for Long-Term Integration of Network Activity. Neural Plast. 2015;2015:765792.
108. Piccinni A, Marazziti D, Catena M, Domenici L, Del Debbio A, Bianchi C, et al. Plasma and serum brain-derived neurotrophic factor (BDNF) in depressed patients during 1 year of antidepressant treatments. J Affect Disord. 2008;105(1-3):279-83.
109. Suliman S, Hemmings SMJ, Seedat S. Brain-Derived Neurotrophic Factor (BDNF) protein levels in anxiety disorders: systematic review and meta-regression analysis. Frontiers in Integrative Neuroscience. 2013;7.
110. Monteleone F, Nicoletti CG, Stampanoni Bassi M, Iezzi E, Buttari F, Furlan R, et al. Nerve growth factor is elevated in the CSF of patients with multiple sclerosis and central neuropathic pain. J Neuroimmunol. 2018;314:89-93.
111. Chang DS, Hsu E, Hottinger DG, Cohen SP. Anti-nerve growth factor in pain management: current evidence. J Pain Res. 2016;9:373-83.

112. Zhang W, Shi Y, Peng Y, Zhong L, Zhu S, Zhang W, et al. Neuron activity-induced Wnt signaling up-regulates expression of brain-derived neurotrophic factor in the pain neural circuit. J Biol Chem. 2018;293(40):15641-51.
113. Merighi A, Salio C, Ghirri A, Lossi L, Ferrini F, Betelli C, et al. BDNF as a pain modulator. Progress in neurobiology. 2008;85(3):297-317.
114. Obata K, Noguchi K. BDNF in sensory neurons and chronic pain. Neuroscience research. 2006;55(1):1-10.
115. Pillai A, Kale A, Joshi S, Naphade N, Raju MS, Nasrallah H, et al. Decreased BDNF levels in CSF of drug-naive first-episode psychotic subjects: correlation with plasma BDNF and psychopathology. Int J Neuropsychopharmacol. 2010;13(4):535-9.
116. Boucher TJ, Okuse K, Bennett DL, Munson JB, Wood JN, McMahon SB. Potent analgesic effects of GDNF in neuropathic pain states. Science. 2000;290(5489):124-7.
117. Ruiz de Almodovar C, Lambrechts D, Mazzone M, Carmeliet P. Role and therapeutic potential of VEGF in the nervous system. Physiol Rev. 2009;89(2):607-48.
118. Mackenzie F, Ruhrberg C. Diverse roles for VEGF-A in the nervous system. Development. 2012;139(8):1371-80.
119. Nowacka MM, Obuchowicz E. Vascular endothelial growth factor (VEGF) and its role in the central nervous system: a new element in the neurotrophic hypothesis of antidepressant drug action. Neuropeptides. 2012;46(1):1-10.
120. Isung J, Mobarrez F, Nordstrom P, Asberg M, Jokinen J. Low plasma vascular endothelial growth factor (VEGF) associated with completed suicide. World J Biol Psychiatry. 2012;13(6):468-73.
121. Isung J, Aeinehband S, Mobarrez F, Martensson B, Nordstrom P, Asberg M, et al. Low vascular endothelial growth factor and interleukin-8 in cerebrospinal fluid of suicide attempters. Transl Psychiatry. 2012;2:e196.
122. McCarthy KF, Connor TJ, McCrory C. Cerebrospinal fluid levels of vascular endothelial growth factor correlate with reported pain and are reduced by spinal cord stimulation in patients with failed back surgery syndrome. Neuromodulation. 2013;16(6):519-22; discussion 22.
123. Hohman TJ, Bell SP, Jefferson AL, Alzheimer's Disease Neuroimaging I. The role of vascular endothelial growth factor in neurodegeneration and cognitive decline: exploring interactions with biomarkers of Alzheimer disease. JAMA Neurol. 2015;72(5):520-9.
124. Levy D, Burstein R, Kainz V, Jakubowski M, Strassman AM. Mast cell degranulation activates a pain pathway underlying migraine headache. Pain. 2007;130(1-2):166-76.
125. Rudick CN, Bryce PJ, Guichelaar LA, Berry RE, Klumpp DJ. Mast cell-derived histamine mediates cystitis pain. PLoS One. 2008;3(5):e2096.
126. Folgueras AR, Valdes-Sanchez T, Llano E, Menendez L, Baamonde A, Denlinger BL, et al. Metalloproteinase MT5-MMP is an essential modulator of neuro-immune interactions in thermal pain stimulation. Proc Natl Acad Sci U S A. 2009;106(38):16451-6.
127. Lewin GR, Rueff A, Mendell LM. Peripheral and central mechanisms of NGF-induced hyperalgesia. Eur J Neurosci. 1994;6(12):1903-12.
128. Moalem G, Xu K, Yu L. T lymphocytes play a role in neuropathic pain following peripheral nerve injury in rats. Neuroscience. 2004;129(3):767-77.
129. Duffy SS, Keating BA, Perera CJ, Moalem-Taylor G. The role of regulatory T cells in nervous system pathologies. J Neurosci Res. 2018;96(6):951-68.

130. Austin PJ, Kim CF, Perera CJ, Moalem-Taylor G. Regulatory T cells attenuate neuropathic pain following peripheral nerve injury and experimental autoimmune neuritis. Pain. 2012;153(9):1916-31.
131. Davies AJ, Kim HW, Gonzalez-Cano R, Choi J, Back SK, Roh SE, et al. Natural Killer Cells Degenerate Intact Sensory Afferents following Nerve Injury. Cell. 2019;176(4):716-28 e18.
132. Yang M, Shi XQ, Peyret C, Oladiran O, Wu S, Chambon J, et al. Effector/memory CD8(+) T cells synergize with co-stimulation competent macrophages to trigger autoimmune peripheral neuropathy. Brain Behav Immun. 2018;71:142-57.
133. Tang W, Lv Q, Chen XF, Zou JJ, Liu ZM, Shi YQ. CD8(+) T cell-mediated cytotoxicity toward Schwann cells promotes diabetic peripheral neuropathy. Cell Physiol Biochem. 2013;32(4):827-37.
134. Meuth SG, Herrmann AM, Simon OJ, Siffrin V, Melzer N, Bittner S, et al. Cytotoxic CD8+ T cell-neuron interactions: perforin-dependent electrical silencing precedes but is not causally linked to neuronal cell death. The Journal of neuroscience : the official journal of the Society for Neuroscience. 2009;29(49):15397-409.
135. Krukowski K, Eijkelkamp N, Laumet G, Hack CE, Li Y, Dougherty PM, et al. CD8+ T Cells and Endogenous IL-10 Are Required for Resolution of Chemotherapy-Induced Neuropathic Pain. The Journal of neuroscience : the official journal of the Society for Neuroscience. 2016;36(43):11074-83.
136. Hu P, McLachlan EM. Macrophage and lymphocyte invasion of dorsal root ganglia after peripheral nerve lesions in the rat. Neuroscience. 2002;112(1):23-38.
137. Kiguchi N, Maeda T, Kobayashi Y, Fukazawa Y, Kishioka S. Macrophage inflammatory protein-1alpha mediates the development of neuropathic pain following peripheral nerve injury through interleukin-1beta up-regulation. Pain. 2010;149(2):305-15.
138. Cui JG, Holmin S, Mathiesen T, Meyerson BA, Linderoth B. Possible role of inflammatory mediators in tactile hypersensitivity in rat models of mononeuropathy. Pain. 2000;88(3):239-48.
139. Shubayev VI, Angert M, Dolkas J, Campana WM, Palenscar K, Myers RR. TNFalpha-induced MMP-9 promotes macrophage recruitment into injured peripheral nerve. Mol Cell Neurosci. 2006;31(3):407-15.
140. Verri WA, Jr., Cunha TM, Parada CA, Wei XQ, Ferreira SH, Liew FY, et al. IL-15 mediates immune inflammatory hypernociception by triggering a sequential release of IFN-gamma, endothelin, and prostaglandin. Proc Natl Acad Sci U S A. 2006;103(25):9721-5.
141. Zhao H, Alam A, Chen Q, Eusman MA, Pal A, Eguchi S, et al. The role of microglia in the pathobiology of neuropathic pain development: what do we know? British Journal of Anaesthesia. 2017;118(4):504-16.
142. Inoue K, Tsuda M. Microglia in neuropathic pain: cellular and molecular mechanisms and therapeutic potential. Nat Rev Neurosci. 2018;19(3):138-52.
143. Aguzzi A, Barres BA, Bennett ML. Microglia: scapegoat, saboteur, or something else? Science. 2013;339(6116):156-61.
144. Salter MW, Beggs S. Sublime microglia: expanding roles for the guardians of the CNS. Cell. 2014;158(1):15-24.
145. Vallejo R, Tilley DM, Vogel L, Benyamin R. The role of glia and the immune system in the development and maintenance of neuropathic pain. Pain Pract. 2010;10(3):167-84.

146. Denk F, Crow M, Didangelos A, Lopes Douglas M, McMahon Stephen B. Persistent Alterations in Microglial Enhancers in a Model of Chronic Pain. Cell reports. 2016;15(8):1771-81.
147. Calvo M, Zhu N, Grist J, Ma Z, Loeb JA, Bennett DL. Following nerve injury neuregulin-1 drives microglial proliferation and neuropathic pain via the MEK/ERK pathway. Glia. 2011;59(4):554-68.
148. Kawasaki Y, Xu ZZ, Wang X, Park JY, Zhuang ZY, Tan PH, et al. Distinct roles of matrix metalloproteases in the early- and late-phase development of neuropathic pain. Nat Med. 2008;14(3):331-6.
149. Tanga FY, Nutile-McMenemy N, DeLeo JA. The CNS role of Toll-like receptor 4 in innate neuroimmunity and painful neuropathy. Proc Natl Acad Sci U S A. 2005;102(16):5856-61.
150. Lacagnina MJ, Watkins LR, Grace PM. Toll-like receptors and their role in persistent pain. Pharmacol Ther. 2018;184:145-58.
151. Kettenmann H, Kirchhoff F, Verkhratsky A. Microglia: new roles for the synaptic stripper. Neuron. 2013;77(1):10-8.
152. Hansen RR, Malcangio M. Astrocytes--multitaskers in chronic pain. Eur J Pharmacol. 2013;716(1-3):120-8.
153. Chung W-S, Allen NJ, Eroglu C. Astrocytes control synapse formation, function, and elimination. Cold Spring Harbor perspectives in biology. 2015;7(9):a020370.
154. Liddelow SA, Barres BA. Reactive Astrocytes: Production, Function, and Therapeutic Potential. Immunity. 2017;46(6):957-67.
155. Ji RR, Donnelly CR, Nedergaard M. Astrocytes in chronic pain and itch. Nat Rev Neurosci. 2019.
156. Smith K. Neuroscience: Settling the great glia debate. Nature. 2010;468(7321):160-2.
157. Alfonso Romero-Sandoval E, Sweitzer S. Nonneuronal central mechanisms of pain: glia and immune response. Prog Mol Biol Transl Sci. 2015;131:325-58.
158. Roeckel LA, Le Coz GM, Gaveriaux-Ruff C, Simonin F. Opioid-induced hyperalgesia: Cellular and molecular mechanisms. Neuroscience. 2016;338:160-82.
159. Lacagnina MJ, Rivera PD, Bilbo SD. Glial and Neuroimmune Mechanisms as Critical Modulators of Drug Use and Abuse. Neuropsychopharmacology. 2017;42(1):156-77.
160. Correale J, Farez MF. The role of astrocytes in multiple sclerosis progression. Frontiers in neurology. 2015;6:180.
161. Rosen S, Ham B, Mogil JS. Sex differences in neuroimmunity and pain. J Neurosci Res. 2017;95(1-2):500-8.
162. Mogil JS, Davis KD, Derbyshire SW. The necessity of animal models in pain research. Pain. 2010;151(1):12-7.
163. Sorge RE, Mapplebeck JC, Rosen S, Beggs S, Taves S, Alexander JK, et al. Different immune cells mediate mechanical pain hypersensitivity in male and female mice. Nat Neurosci. 2015;18(8):1081-3.
164. Sprenger T, Viana M, Tassorelli C. Current Prophylactic Medications for Migraine and Their Potential Mechanisms of Action. Neurotherapeutics. 2018;15(2):313-23.
165. Backonja M, Williams L, Miao X, Katz N, Chen C. Safety and efficacy of neublastin in painful lumbosacral radiculopathy: a randomized, double-blinded, placebo-controlled phase 2 trial using Bayesian adaptive design (the SPRINT trial). Pain. 2017;158(9):1802-12.

166. Ransohoff RM, Schafer D, Vincent A, Blachere NE, Bar-Or A. Neuroinflammation: Ways in Which the Immune System Affects the Brain. Neurotherapeutics. 2015;12(4):896-909.
167. Yang QQ, Zhou JW. Neuroinflammation in the central nervous system: Symphony of glial cells. Glia. 2019;67(6):1017-35.
168. Kothur K, Wienholt L, Brilot F, Dale RC. CSF cytokines/chemokines as biomarkers in neuroinflammatory CNS disorders: A systematic review. Cytokine. 2016;77:227-37.
169. Tommasin S, Giannì C, De Giglio L, Pantano P. Neuroimaging techniques to assess inflammation in multiple sclerosis. Neuroscience. 2019;403:4-16.
170. Backryd E, Lind AL, Thulin M, Larsson A, Gerdle B, Gordh T. High levels of cerebrospinal fluid chemokines point to the presence of neuroinflammation in peripheral neuropathic pain: a cross-sectional study of 2 cohorts of patients compared with healthy controls. Pain. 2017;158(12):2487-95.
171. Backonja MM, Coe CL, Muller DA, Schell K. Altered cytokine levels in the blood and cerebrospinal fluid of chronic pain patients. J Neuroimmunol. 2008;195(1-2):157-63.
172. Schmidt-Wilcke T. Neuroimaging of chronic pain. Best Practice & Research Clinical Rheumatology. 2015;29(1):29-41.
173. Rupprecht R, Papadopoulos V, Rammes G, Baghai TC, Fan J, Akula N, et al. Translocator protein (18 kDa) (TSPO) as a therapeutic target for neurological and psychiatric disorders. Nature reviews Drug discovery. 2010;9(12):971-88.
174. Jung C, Ichesco E, Ratai EM, Gonzalez RG, Burdo T, Loggia ML, et al. Magnetic resonance imaging of neuroinflammation in chronic pain: a role for astrogliosis? Pain. 2020;161(7):1555-64.
175. Grace PM. A backbone for reverse-translation: Evidence for neuroinflammation in patients with low back pain. Brain Behav Immun. 2019;75:8-9.
176. Plaven-Sigray P, Schain M, Zanderigo F, Karolinska PBRsg, Rabiner EA, Gunn RN, et al. Accuracy and reliability of [(11)C]PBR28 specific binding estimated without the use of a reference region. Neuroimage. 2019;188:102-10.
177. McNeela AM, Bernick C, Hines RM, Hines DJ. TSPO regulation in reactive gliotic diseases. J Neurosci Res. 2018;96(6):978-88.
178. Li H, Sagar AP, Keri S. Translocator protein (18kDa TSPO) binding, a marker of microglia, is reduced in major depression during cognitive-behavioral therapy. Prog Neuropsychopharmacol Biol Psychiatry. 2018;83:1-7.
179. Richards EM, Zanotti-Fregonara P, Fujita M, Newman L, Farmer C, Ballard ED, et al. PET radioligand binding to translocator protein (TSPO) is increased in unmedicated depressed subjects. EJNMMI Res. 2018;8(1):57.
180. Loggia ML, Chonde DB, Akeju O, Arabasz G, Catana C, Edwards RR, et al. Evidence for brain glial activation in chronic pain patients. Brain. 2015;138(Pt 3):604-15.
181. Albrecht DS, Normandin MD, Shcherbinin S, Wooten DW, Schwarz AJ, Zurcher NR, et al. Pseudoreference Regions for Glial Imaging with (11)C-PBR28: Investigation in 2 Clinical Cohorts. J Nucl Med. 2018;59(1):107-14.
182. Jeon SY, Seo S, Lee JS, Choi SH, Lee DH, Jung YH, et al. [11C]-(R)-PK11195 positron emission tomography in patients with complex regional pain syndrome: A pilot study. Medicine (Baltimore). 2017;96(1):e5735.
183. Albrecht DS, Ahmed SU, Kettner NW, Borra RJH, Cohen-Adad J, Deng H, et al. Neuroinflammation of the spinal cord and nerve roots in chronic radicular pain patients. Pain. 2018;159(5):968-77.

184. Talbot RM, McCarthy KF, McCrory C. Central and systemic inflammatory responses to thoracotomy - potential implications for acute and chronic postsurgical pain. J Neuroimmunol. 2015;285:147-9.
185. Ohtori S, Suzuki M, Koshi T, Takaso M, Yamashita M, Inoue G, et al. Proinflammatory cytokines in the cerebrospinal fluid of patients with lumbar radiculopathy. Eur Spine J. 2011;20(6):942-6.
186. Alexander GM, Perreault MJ, Reichenberger ER, Schwartzman RJ. Changes in immune and glial markers in the CSF of patients with Complex Regional Pain Syndrome. Brain Behav Immun. 2007;21(5):668-76.
187. Alexander GM, van Rijn MA, van Hilten JJ, Perreault MJ, Schwartzman RJ. Changes in cerebrospinal fluid levels of pro-inflammatory cytokines in CRPS. Pain. 2005;116(3):213-9.
188. McCarthy KF, McCrory C. Cerebrospinal fluid levels of glial cell-derived neurotrophic factor correlate with spinal cord stimulation frequency in patients with neuropathic pain: a preliminary report. Spinal Cord. 2014;52 Suppl 2:S8-10.
189. Caylor J, Reddy R, Yin S, Cui C, Huang M, Huang C, et al. Spinal cord stimulation in chronic pain: evidence and theory for mechanisms of action. Bioelectronic Medicine. 2019;5(1).
190. Zhang TC, Janik JJ, Grill WM. Mechanisms and models of spinal cord stimulation for the treatment of neuropathic pain. Brain Res. 2014;1569:19-31.
191. Linderoth B, Foreman RD. Conventional and Novel Spinal Stimulation Algorithms: Hypothetical Mechanisms of Action and Comments on Outcomes. Neuromodulation. 2017;20(6):525-33.
192. Chakravarthy K, Richter H, Christo PJ, Williams K, Guan Y. Spinal Cord Stimulation for Treating Chronic Pain: Reviewing Preclinical and Clinical Data on Paresthesia-Free High-Frequency Therapy. Neuromodulation. 2018;21(1):10-8.
193. Lees JG, Duffy SS, Moalem-Taylor G. Immunotherapy targeting cytokines in neuropathic pain. Front Pharmacol. 2013;4:142.
194. Osuka K, Suzuki Y, Saito K, Takayasu M, Shibuya M. Changes in serum cytokine concentrations after neurosurgical procedures. Acta neurochirurgica. 1996;138(8):970-6.
195. Berger M, Ponnusamy V, Greene N, Cooter M, Nadler JW, Friedman A, et al. The effect of propofol vs. isoflurane anesthesia on postoperative changes in cerebrospinal fluid cytokine levels: results from a randomized trial. Frontiers in immunology. 2017;8:1528.
196. Markovic-Bozic J, Karpe B, Potocnik I, Jerin A, Vranic A, Novak-Jankovic V. Effect of propofol and sevoflurane on the inflammatory response of patients undergoing craniotomy. BMC anesthesiology. 2015;16(1):18.
197. Shi Y, Gelman BB, Lisinicchia JG, Tang SJ. Chronic-pain-associated astrocytic reaction in the spinal cord dorsal horn of human immunodeficiency virus-infected patients. The Journal of neuroscience : the official journal of the Society for Neuroscience. 2012;32(32):10833-40.
198. Russo MA, Fiore NT, van Vreden C, Bailey D, Santarelli DM, McGuire HM, et al. Expansion and activation of distinct central memory T lymphocyte subsets in complex regional pain syndrome. J Neuroinflammation. 2019;16(1):63.
199. Luchting B, Rachinger-Adam B, Heyn J, Hinske LC, Kreth S, Azad SC. Anti-inflammatory T-cell shift in neuropathic pain. J Neuroinflammation. 2015;12:12.
200. Nascimento AI, Mar FM, Sousa MM. The intriguing nature of dorsal root ganglion neurons: Linking structure with polarity and function. Prog Neurobiol. 2018;168:86-103.

201. Morgalla MH, de Barros Filho MF, Chander BS, Soekadar SR, Tatagiba M, Lepski G. Neurophysiological Effects of Dorsal Root Ganglion Stimulation (DRGS) in Pain Processing at the Cortical Level. Neuromodulation. 2019;22(1):36-43.
202. Oreskovic D, Klarica M. The formation of cerebrospinal fluid: nearly a hundred years of interpretations and misinterpretations. Brain Res Rev. 2010;64(2):241-62.
203. Sakka L, Coll G, Chazal J. Anatomy and physiology of cerebrospinal fluid. Eur Ann Otorhinolaryngol Head Neck Dis. 2011;128(6):309-16.
204. Van Boxem K, Huntoon M, Van Zundert J, Patijn J, van Kleef M, Joosten EA. Pulsed radiofrequency: a review of the basic science as applied to the pathophysiology of radicular pain: a call for clinical translation. Reg Anesth Pain Med. 2014;39(2):149-59.
205. Subira D, Castanon S, Aceituno E, Hernandez J, Jimenez-Garofano C, Jimenez A, et al. Flow cytometric analysis of cerebrospinal fluid samples and its usefulness in routine clinical practice. Am J Clin Pathol. 2002;117(6):952-8.
206. Maxeiner HG, Rojewski MT, Schmitt A, Tumani H, Bechter K, Schmitt M. Flow cytometric analysis of T cell subsets in paired samples of cerebrospinal fluid and peripheral blood from patients with neurological and psychiatric disorders. Brain Behav Immun. 2009;23(1):134-42.
207. Hummert MW, Alvermann S, Gingele S, Gross CC, Wiendl H, Mirenska A, et al. Immunophenotyping of cerebrospinal fluid cells by Chipcytometry. J Neuroinflammation. 2018;15(1):160.
208. Farhadian SF, Mehta SS, Zografou C, Robertson K, Price RW, Pappalardo J, et al. Single-cell RNA sequencing reveals microglia-like cells in cerebrospinal fluid during virologically suppressed HIV. JCI Insight. 2018;3(18).
209. Fuggle NR, Howe FA, Allen RL, Sofat N. New insights into the impact of neuro-inflammation in rheumatoid arthritis. Front Neurosci. 2014;8:357.
210. Petrelli A, van Wijk F. CD8(+) T cells in human autoimmune arthritis: the unusual suspects. Nat Rev Rheumatol. 2016;12(7):421-8.
211. Khoonsari PE, Ossipova E, Lengqvist J, Svensson CI, Kosek E, Kadetoff D, et al. The human CSF pain proteome. Journal of Proteomics. 2019;190:67-76.
212. Korvela M, Lind AL, Wetterhall M, Gordh T, Andersson M, Pettersson J. Quantification of 10 elements in human cerebrospinal fluid from chronic pain patients with and without spinal cord stimulation. J Trace Elem Med Biol. 2016;37:1-7.
213. Lind AL, Emami Khoonsari P, Sjodin M, Katila L, Wetterhall M, Gordh T, et al. Spinal Cord Stimulation Alters Protein Levels in the Cerebrospinal Fluid of Neuropathic Pain Patients: A Proteomic Mass Spectrometric Analysis. Neuromodulation. 2016;19(6):549-62.
214. Dantzer R, Kelley KW. Twenty years of research on cytokine-induced sickness behavior. Brain Behav Immun. 2007;21(2):153-60.
215. McCusker RH, Kelley KW. Immune-neural connections: how the immune system's response to infectious agents influences behavior. J Exp Biol. 2013;216(Pt 1):84-98.
216. Zhang J-M, An J. Cytokines, inflammation and pain. International anesthesiology clinics. 2007;45(2):27.
217. Capuron L, Miller AH. Cytokines and psychopathology: lessons from interferon-α. Biological psychiatry. 2004;56(11):819-24.
218. Totsch SK, Sorge RE. Immune System Involvement in Specific Pain Conditions. Mol Pain. 2017;13:1744806917724559.
219. Vezzani A, Viviani B. Neuromodulatory properties of inflammatory cytokines and their impact on neuronal excitability. Neuropharmacology. 2015;96:70-82.

220. Viviani B, Bartesaghi S, Gardoni F, Vezzani A, Behrens M, Bartfai T, et al. Interleukin-1β enhances NMDA receptor-mediated intracellular calcium increase through activation of the Src family of kinases. Journal of Neuroscience. 2003;23(25):8692-700.
221. Hidese S, Hattori K, Sasayama D, Tsumagari T, Miyakawa T, Matsumura R, et al. Cerebrospinal fluid neuroplasticity-associated protein levels in patients with psychiatric disorders: a multiplex immunoassay study. Transl Psychiatry. 2020;10(1):161.
222. Troubat R, Barone P, Leman S, Desmidt T, Cressant A, Atanasova B, et al. Neuroinflammation and depression: A review. Eur J Neurosci. 2020.
223. Dhabhar FS, Burke HM, Epel ES, Mellon SH, Rosser R, Reus VI, et al. Low serum IL-10 concentrations and loss of regulatory association between IL-6 and IL-10 in adults with major depression. J Psychiatr Res. 2009;43(11):962-9.
224. Gonul AS, Akdeniz F, Taneli F, Donat O, Eker C, Vahip S. Effect of treatment on serum brain-derived neurotrophic factor levels in depressed patients. Eur Arch Psychiatry Clin Neurosci. 2005;255(6):381-6.
225. Hisaoka-Nakashima K, Kajitani N, Kaneko M, Shigetou T, Kasai M, Matsumoto C, et al. Amitriptyline induces brain-derived neurotrophic factor (BDNF) mRNA expression through ERK-dependent modulation of multiple BDNF mRNA variants in primary cultured rat cortical astrocytes and microglia. Brain Res. 2016;1634:57-67.
226. Paumier KL, Sortwell CE, Madhavan L, Terpstra B, Daley BF, Collier TJ. Tricyclic antidepressant treatment evokes regional changes in neurotrophic factors over time within the intact and degenerating nigrostriatal system. Exp Neurol. 2015;266:11-21.
227. Warner-Schmidt JL, Duman RS. VEGF as a potential target for therapeutic intervention in depression. Curr Opin Pharmacol. 2008;8(1):14-9.
228. Segi-Nishida E, Warner-Schmidt JL, Duman RS. Electroconvulsive seizure and VEGF increase the proliferation of neural stem-like cells in rat hippocampus. Proc Natl Acad Sci U S A. 2008;105(32):11352-7.
229. Vandel S, Vandel B, Sandoz M, Allers G, Bechtel P, Volmat R. Clinical response and plasma concentration of amitriptyline and its metabolite nortriptyline. Eur J Clin Pharmacol. 1978;14(3):185-90.
230. Finnerup NB, Sindrup SH, Jensen TS. The evidence for pharmacological treatment of neuropathic pain. Pain. 2010;150(3):573-81.
231. Gupta SK, Shah JC, Hwang SS. Pharmacokinetic and pharmacodynamic characterization of OROS and immediate-release amitriptyline. Br J Clin Pharmacol. 1999;48(1):71-8.
232. Brosen K. Some aspects of genetic polymorphism in the biotransformation of antidepressants. Therapie. 2004;59(1):5-12.
233. Ryu S, Park S, Lee JH, Kim YR, Na HS, Lim HS, et al. A Study on CYP2C19 and CYP2D6 Polymorphic Effects on Pharmacokinetics and Pharmacodynamics of Amitriptyline in Healthy Koreans. Clin Transl Sci. 2017;10(2):93-101.
234. Uhr M, Grauer MT. abcb1ab P-glycoprotein is involved in the uptake of citalopram and trimipramine into the brain of mice. Journal of Psychiatric Research. 2003;37(3):179-85.
235. Hulten BA, Heath A, Knudsen K, Nyberg G, Starmark JE, Martensson E. Severe amitriptyline overdose: relationship between toxicokinetics and toxicodynamics. J Toxicol Clin Toxicol. 1992;30(2):171-9.
236. Miyake K, Fukuchi H, Kitaura T, Kimura M, Sarai K, Nakahara T. Pharmacokinetics of amitriptyline and its demethylated metabolite in serum and specific brain regions of rats after acute and chronic administration of amitriptyline. Journal of pharmaceutical sciences. 1990;79(4):288-91.

237. Lawson K. A Brief Review of the Pharmacology of Amitriptyline and Clinical Outcomes in Treating Fibromyalgia. Biomedicines. 2017;5(2).
238. Kremer M, Salvat E, Muller A, Yalcin I, Barrot M. Antidepressants and gabapentinoids in neuropathic pain: Mechanistic insights. Neuroscience. 2016;338:183-206.
239. Kremer M, Yalcin I, Goumon Y, Wurtz X, Nexon L, Daniel D, et al. A Dual Noradrenergic Mechanism for the Relief of Neuropathic Allodynia by the Antidepressant Drugs Duloxetine and Amitriptyline. The Journal of neuroscience : the official journal of the Society for Neuroscience. 2018;38(46):9934-54.
240. Potter WZ, Scheinin M, Golden RN, Rudorfer MV, Cowdry RW, Calil HM, et al. Selective antidepressants and cerebrospinal fluid. Lack of specificity on norepinephrine and serotonin metabolites. Arch Gen Psychiatry. 1985;42(12):1171-7.
241. Sindrup SH, Otto M, Finnerup NB, Jensen TS. Antidepressants in the treatment of neuropathic pain. Basic Clin Pharmacol Toxicol. 2005;96(6):399-409.
242. Reynolds IJ, Miller RJ. Tricyclic antidepressants block N-methyl-D-aspartate receptors: similarities to the action of zinc. Br J Pharmacol. 1988;95(1):95-102.
243. Wang GK, Russell C, Wang SY. State-dependent block of voltage-gated Na+ channels by amitriptyline via the local anesthetic receptor and its implication for neuropathic pain. Pain. 2004;110(1-2):166-74.
244. Wolff M, Czorlich P, Nagaraj C, Schnobel-Ehehalt R, Li Y, Kwapiszewska G, et al. Amitriptyline and carbamazepine utilize voltage-gated ion channel suppression to impair excitability of sensory dorsal horn neurons in thin tissue slice: An in vitro study. Neurosci Res. 2016;109:16-27.
245. Hisaoka K, Tsuchioka M, Yano R, Maeda N, Kajitani N, Morioka N, et al. Tricyclic antidepressant amitriptyline activates fibroblast growth factor receptor signaling in glial cells: involvement in glial cell line-derived neurotrophic factor production. J Biol Chem. 2011;286(24):21118-28.
246. Jang S-W, Liu X, Chan C-B, Weinshenker D, Hall RA, Xiao G, et al. Amitriptyline is a TrkA and TrkB Receptor Agonist that Promotes TrkA/TrkB Heterodimerization and Has Potent Neurotrophic Activity. Chemistry & Biology. 2009;16(6):644-56.
247. Obuchowicz E, Kowalski J, Labuzek K, Krysiak R, Pendzich J, Herman ZS. Amitriptyline and nortriptyline inhibit interleukin-1 release by rat mixed glial and microglial cell cultures. Int J Neuropsychopharmacol. 2006;9(1):27-35.
248. Kim Y, Kwon SY, Jung HS, Park YJ, Kim YS, In JH, et al. Amitriptyline inhibits MAPK/ERK, CREB pathway and proinflammatory cytokines through A3AR activation in rat neuropathic pain models. Korean J Anesthesiol. 2018.
249. Hannestad J, DellaGioia N, Bloch M. The effect of antidepressant medication treatment on serum levels of inflammatory cytokines: a meta-analysis. Neuropsychopharmacology. 2011;36(12):2452-9.
250. Hutchinson MR, Loram LC, Zhang Y, Shridhar M, Rezvani N, Berkelhammer D, et al. Evidence that tricyclic small molecules may possess toll-like receptor and myeloid differentiation protein 2 activity. Neuroscience. 2010;168(2):551-63.
251. Melzack R, Wall PD. Pain mechanisms: a new theory. Science. 1965;150(3699):971-9.
252. Nathan PW. The gate-control theory of pain. A critical review. Brain. 1976;99(1):123-58.
253. Harrison C, Epton S, Bojanic S, Green AL, FitzGerald JJ. The Efficacy and Safety of Dorsal Root Ganglion Stimulation as a Treatment for Neuropathic Pain: A Literature Review. Neuromodulation. 2018;21(3):225-33.

254. Linderoth B, Foreman RD. Physiology of spinal cord stimulation: review and update. Neuromodulation. 1999;2(3):150-64.
255. Shealy CN, Mortimer JT, Reswick JB. Electrical inhibition of pain by stimulation of the dorsal columns: preliminary clinical report. Anesth Analg. 1967;46(4):489-91.
256. Kumar K, North R, Taylor R, Sculpher M, Van den Abeele C, Gehring M, et al. Spinal Cord Stimulation vs. Conventional Medical Management: A Prospective, Randomized, Controlled, Multicenter Study of Patients with Failed Back Surgery Syndrome (PROCESS Study). Neuromodulation. 2005;8(4):213-8.
257. Kriek N, Schreurs MWJ, Groeneweg JG, Dik WA, Tjiang GCH, Gultuna I, et al. Spinal Cord Stimulation in Patients With Complex Regional Pain Syndrome: A Possible Target for Immunomodulation? Neuromodulation. 2018;21(1):77-86.
258. Kemler MA, de Vet HC, Barendse GA, van den Wildenberg FA, van Kleef M. Effect of spinal cord stimulation for chronic complex regional pain syndrome Type I: five-year final follow-up of patients in a randomized controlled trial. J Neurosurg. 2008;108(2):292-8.
259. Perruchoud C, Eldabe S, Batterham AM, Madzinga G, Brookes M, Durrer A, et al. Analgesic efficacy of high-frequency spinal cord stimulation: a randomized double-blind placebo-controlled study. Neuromodulation. 2013;16(4):363-9; discussion 9.
260. Schu S, Slotty PJ, Bara G, von Knop M, Edgar D, Vesper J. A prospective, randomised, double-blind, placebo-controlled study to examine the effectiveness of burst spinal cord stimulation patterns for the treatment of failed back surgery syndrome. Neuromodulation. 2014;17(5):443-50.
261. Zucco F, Ciampichini R, Lavano A, Costantini A, De Rose M, Poli P, et al. Cost-Effectiveness and Cost-Utility Analysis of Spinal Cord Stimulation in Patients With Failed Back Surgery Syndrome: Results From the PRECISE Study. Neuromodulation. 2015;18(4):266-76; discussion 76.
262. Grider JS, Manchikanti L, Carayannopoulos A, Sharma ML, Balog CC, Harned ME, et al. Effectiveness of Spinal Cord Stimulation in Chronic Spinal Pain: A Systematic Review. Pain Physician. 2016;19(1):E33-54.
263. Courtney P, Espinet A, Mitchell B, Russo M, Muir A, Verrills P, et al. Improved Pain Relief With Burst Spinal Cord Stimulation for Two Weeks in Patients Using Tonic Stimulation: Results From a Small Clinical Study. Neuromodulation. 2015;18(5):361-6.
264. Wille F, Breel JS, Bakker EW, Hollmann MW. Altering Conventional to High Density Spinal Cord Stimulation: An Energy Dose-Response Relationship in Neuropathic Pain Therapy. Neuromodulation. 2017;20(1):71-80.
265. Bocci T, De Carolis G, Paroli M, Barloscio D, Parenti L, Tollapi L, et al. Neurophysiological Comparison Among Tonic, High Frequency, and Burst Spinal Cord Stimulation: Novel Insights Into Spinal and Brain Mechanisms of Action. Neuromodulation. 2018;21(5):480-8.
266. Kriek N, Groeneweg JG, Stronks DL, Huygen FJ. Comparison of tonic spinal cord stimulation, high-frequency and burst stimulation in patients with complex regional pain syndrome: a double-blind, randomised placebo controlled trial. BMC Musculoskelet Disord. 2015;16:222.
267. Van Buyten JP, Al-Kaisy A, Smet I, Palmisani S, Smith T. High-frequency spinal cord stimulation for the treatment of chronic back pain patients: results of a prospective multicenter European clinical study. Neuromodulation. 2013;16(1):59-65; discussion -6.
268. Kapural L, Yu C, Doust MW, Gliner BE, Vallejo R, Sitzman BT, et al. Comparison of 10-kHz High-Frequency and Traditional Low-Frequency Spinal Cord Stimulation for the Treatment of Chronic Back and Leg Pain: 24-Month Results From a Multicenter, Randomized, Controlled Pivotal Trial. Neurosurgery. 2016;79(5):667-77.

269. Chakravarthy K, Kent AR, Raza A, Xing F, Kinfe TM. Burst Spinal Cord Stimulation: Review of Preclinical Studies and Comments on Clinical Outcomes. Neuromodulation. 2018;21(5):431-9.
270. Wallin J, Fiskå A, Tjølsen A, Linderoth B, Hole K. Spinal cord stimulation inhibits long-term potentiation of spinal wide dynamic range neurons. Brain research. 2003;973(1):39-43.
271. Kamieniak P, Bielewicz J, Kurzepa J, Daniluk B, Kocot J, Trojanowski T. Serum Level of Metalloproteinase-2 but not Metalloproteinase-9 Rises in Patients With Failed Back Surgery Syndrome After Spinal Cord Stimulation. Neuromodulation. 2019.
272. Ahmed S, Yearwood T, De Ridder D, Vanneste S. Burst and high frequency stimulation: underlying mechanism of action. Expert Rev Med Devices. 2018;15(1):61-70.
273. Vallejo R, Bradley K, Kapural L. Spinal Cord Stimulation in Chronic Pain: Mode of Action. Spine (Phila Pa 1976). 2017;42 Suppl 14:S53-S60.
274. Crosby ND, Weisshaar CL, Smith JR, Zeeman ME, Goodman-Keiser MD, Winkelstein BA. Burst and Tonic Spinal Cord Stimulation Differentially Activate GABAergic Mechanisms to Attenuate Pain in a Rat Model of Cervical Radiculopathy. IEEE Trans Biomed Eng. 2015;62(6):1604-13.
275. Swadlow HA, Gusev AG. The impact of 'bursting' thalamic impulses at a neocortical synapse. Nat Neurosci. 2001;4(4):402-8.
276. Sherman SM. Tonic and burst firing: dual modes of thalamocortical relay. Trends in neurosciences. 2001;24(2):122-6.
277. Krahe R, Gabbiani F. Burst firing in sensory systems. Nat Rev Neurosci. 2004;5(1):13-23.
278. Yearwood T, De Ridder D, Yoo HB, Falowski S, Venkatesan L, Ting To W, et al. Comparison of Neural Activity in Chronic Pain Patients During Tonic and Burst Spinal Cord Stimulation Using Fluorodeoxyglucose Positron Emission Tomography. Neuromodulation. 2019.
279. Kinfe TM, Muhammad S, Link C, Roeske S, Chaudhry SR, Yearwood TL. Burst Spinal Cord Stimulation Increases Peripheral Antineuroinflammatory Interleukin 10 Levels in Failed Back Surgery Syndrome Patients With Predominant Back Pain. Neuromodulation. 2017;20(4):322-30.
280. Wright BL, Lai JT, Sinclair AJ. Cerebrospinal fluid and lumbar puncture: a practical review. J Neurol. 2012;259(8):1530-45.
281. Cserr HF, Cooper DN, Suri PK, Patlak CS. Efflux of radiolabeled polyethylene glycols and albumin from rat brain. Am J Physiol. 1981;240(4):F319-28.
282. Spector R, Robert Snodgrass S, Johanson CE. A balanced view of the cerebrospinal fluid composition and functions: Focus on adult humans. Exp Neurol. 2015;273:57-68.
283. Davson H, Welch K, Segal M. Physiology and pathophysiology of the cerebrospinal fluid. 1987. New York: Churchill Livingstone.
284. Hladky SB, Barrand MA. Mechanisms of fluid movement into, through and out of the brain: evaluation of the evidence. Fluids and Barriers of the CNS. 2014;11(1):26.
285. Qaddoumi I, Sane M, Li S, Kocak M, Pai-Panandiker A, Harreld J, et al. Diagnostic utility and correlation of tumor markers in the serum and cerebrospinal fluid of children with intracranial germ cell tumors. Childs Nerv Syst. 2012;28(7):1017-24.
286. de Graaf MT, de Jongste AH, Kraan J, Boonstra JG, Sillevis Smitt PA, Gratama JW. Flow cytometric characterization of cerebrospinal fluid cells. Cytometry B Clin Cytom. 2011;80(5):271-81.

287. Cherry JD, Stein TD, Tripodis Y, Alvarez VE, Huber BR, Au R, et al. CCL11 is increased in the CNS in chronic traumatic encephalopathy but not in Alzheimer's disease. PLoS One. 2017;12(9):e0185541.
288. Pan S, Zhu D, Quinn JF, Peskind ER, Montine TJ, Lin B, et al. A combined dataset of human cerebrospinal fluid proteins identified by multi-dimensional chromatography and tandem mass spectrometry. Proteomics. 2007;7(3):469-73.
289. Guo Z, Zhang Y, Zou L, Wang D, Shao C, Wang Y, et al. A Proteomic Analysis of Individual and Gender Variations in Normal Human Urine and Cerebrospinal Fluid Using iTRAQ Quantification. PLoS One. 2015;10(7):e0133270.
290. Nascimento JM, Martins-de-Souza D. The proteome of schizophrenia. NPJ Schizophr. 2015;1:14003.
291. de Graaf MT, Smitt PA, Luitwieler RL, van Velzen C, van den Broek PD, Kraan J, et al. Central memory CD4+ T cells dominate the normal cerebrospinal fluid. Cytometry B Clin Cytom. 2011;80(1):43-50.
292. Schwarz JM, Smith SH, Bilbo SD. FACS analysis of neuronal–glial interactions in the nucleus accumbens following morphine administration. Psychopharmacology. 2013;230(4):525-35.
293. Davis KD, Aghaeepour N, Ahn AH, Angst MS, Borsook D, Brenton A, et al. Discovery and validation of biomarkers to aid the development of safe and effective pain therapeutics: challenges and opportunities. Nat Rev Neurol. 2020;16(7):381-400.
294. Rotunno MS, Lane M, Zhang W, Wolf P, Oliva P, Viel C, et al. Cerebrospinal fluid proteomics implicates the granin family in Parkinson's disease. Sci Rep. 2020;10(1):2479.
295. Hall S, Janelidze S, Surova Y, Widner H, Zetterberg H, Hansson O. Cerebrospinal fluid concentrations of inflammatory markers in Parkinson's disease and atypical parkinsonian disorders. Sci Rep. 2018;8(1):13276.
296. Denk J, Boelmans K, Siegismund C, Lassner D, Arlt S, Jahn H. MicroRNA Profiling of CSF Reveals Potential Biomarkers to Detect Alzheimer`s Disease. PLoS One. 2015;10(5):e0126423.
297. Royds J, Cassidy H, Conroy MJ, Dunne MR, Lysaght J, McCrory C. Examination and characterisation of the effect of amitriptyline therapy for chronic neuropathic pain on neuropeptide and proteomic constituents of human cerebrospinal fluid. Brain, Behavior, & Immunity - Health. 2021;10.
298. Fangmann P, Assion HJ, Juckel G, Gonzalez CA, Lopez-Munoz F. Half a century of antidepressant drugs: on the clinical introduction of monoamine oxidase inhibitors, tricyclics, and tetracyclics. Part II: tricyclics and tetracyclics. J Clin Psychopharmacol. 2008;28(1):1-4.
299. Hyttel J, Christensen AV, Fjalland B. Neuropharmacological properties of amitriptyline, nortriptyline and their metabolites. Acta pharmacologica et toxicologica. 1980;47(1):53-7.
300. Valera E, Ubhi K, Mante M, Rockenstein E, Masliah E. Antidepressants reduce neuroinflammatory responses and astroglial alpha-synuclein accumulation in a transgenic mouse model of multiple system atrophy. Glia. 2014;62(2):317-37.
301. Tai YH, Wang YH, Wang JJ, Tao PL, Tung CS, Wong CS. Amitriptyline suppresses neuroinflammation and up-regulates glutamate transporters in morphine-tolerant rats. Pain. 2006;124(1-2):77-86.
302. Rambe AS, Sjahrir H, Machfoed MH. Amitriptyline Effect on Tumor Necrosis Factor-α, Interleukin-1 and Interleukin-6 Serum Level and its Correlation with Pain Severity in Chronic Tension-Type Headache Patients. International Journal of Scientific and Research Publications. 2015:19.

303. Kajitani N, Hisaoka-Nakashima K, Morioka N, Okada-Tsuchioka M, Kaneko M, Kasai M, et al. Antidepressant acts on astrocytes leading to an increase in the expression of neurotrophic/growth factors: differential regulation of FGF-2 by noradrenaline. PLoS One. 2012;7(12):e51197.
304. Jeanson T, Duchene A, Richard D, Bourgoin S, Picoli C, Ezan P, et al. Potentiation of Amitriptyline Anti-Hyperalgesic-Like Action By Astroglial Connexin 43 Inhibition in Neuropathic Rats. Sci Rep. 2016;6:38766.
305. Himmerich H, Fulda S, Sheldrick AJ, Plumakers B, Rink L. IFN-gamma reduction by tricyclic antidepressants. Int J Psychiatry Med. 2010;40(4):413-24.
306. Guan Y, Li X, Umetani M, Boini KM, Li PL, Zhang Y. Tricyclic antidepressant amitriptyline inhibits autophagic flux and prevents tube formation in vascular endothelial cells. Basic Clin Pharmacol Toxicol. 2018.
307. Freysoldt A, Fleckenstein J, Lang PM, Irnich D, Grafe P, Carr RW. Low concentrations of amitriptyline inhibit nicotinic receptors in unmyelinated axons of human peripheral nerve. Br J Pharmacol. 2009;158(3):797-805.
308. Onghena P, Van Houdenhove B. Antidepressant-induced analgesia in chronic non-malignant pain: a meta-analysis of 39 placebo-controlled studies. Pain. 1992;49(2):205-19.
309. Ji RR, Nackley A, Huh Y, Terrando N, Maixner W. Neuroinflammation and Central Sensitization in Chronic and Widespread Pain. Anesthesiology. 2018;129(2):343-66.
310. Hisaoka-Nakashima K, Miyano K, Matsumoto C, Kajitani N, Abe H, Okada-Tsuchioka M, et al. Tricyclic Antidepressant Amitriptyline-induced Glial Cell Line-derived Neurotrophic Factor Production Involves Pertussis Toxin-sensitive Galphai/o Activation in Astroglial Cells. J Biol Chem. 2015;290(22):13678-91.
311. Baranov PY, Sukhanova T, Yerov O, Lin H, James C, Morrow D, et al. Amitriptyline induces glial-cell line derived neurotrophic factor in retinal cells in vivo and in vitro. Investigative Ophthalmology & Visual Science. 2014;55(13):5744-.
312. Greene J, Banasr M, Lee B, Warner-Schmidt J, Duman RS. Vascular endothelial growth factor signaling is required for the behavioral actions of antidepressant treatment: pharmacological and cellular characterization. Neuropsychopharmacology. 2009;34(11):2459-68.
313. Royds J, Conroy MJ, Dunne MR, McCrory C, Lysaght J. An investigation into the modulation of T cell phenotypes by amitriptyline and nortriptyline. Eur Neuropsychopharmacol. 2019.
314. Ying G, Karlsson H, DePierre J, Nässberger L. Tricyclic antidepressants prevent the differentiation of monocytes into macrophage-like cells in vitro. Cell biology and toxicology. 2002;18(6):425-37.
315. Ho EL, Ronquillo R, Altmeppen H, Spudich SS, Price RW, Sinclair E. Cellular Composition of Cerebrospinal Fluid in HIV-1 Infected and Uninfected Subjects. PLoS One. 2013;8(6):e66188.
316. Dworkin RH, O'Connor AB, Backonja M, Farrar JT, Finnerup NB, Jensen TS, et al. Pharmacologic management of neuropathic pain: evidence-based recommendations. Pain. 2007;132(3):237-51.
317. Gelijkens V, Van Zundert J, De Vooght P, Laenen VM, Heylen R, Vanelderen P. The effectiveness of amitriptyline in the treatment of subacute lumbar radicular pain: 14AP7-3. European Journal of Anaesthesiology (EJA). 2014;31:232.
318. Vanelderen P, Van Zundert J, Kozicz T, Puylaert M, De Vooght P, Mestrum R, et al. Effect of Minocycline on Lumbar Radicular Neuropathic PainA Randomized, Placebo-controlled, Double-blind Clinical Trial with Amitriptyline as a Comparator.

Anesthesiology: The Journal of the American Society of Anesthesiologists. 2015;122(2):399-406.
319. Association of Anaesthetists of Great B, Ireland, Obstetric Anaesthetists A, Regional Anaesthesia UK, Association of Paediatric Anaesthetists of Great B, Ireland, et al. Safety guideline: skin antisepsis for central neuraxial blockade. Anaesthesia. 2014;69(11):1279-86.
320. Hawker GA, Mian S, Kendzerska T, French M. Measures of adult pain: Visual Analog Scale for Pain (VAS Pain), Numeric Rating Scale for Pain (NRS Pain), McGill Pain Questionnaire (MPQ), Short-Form McGill Pain Questionnaire (SF-MPQ), Chronic Pain Grade Scale (CPGS), Short Form-36 Bodily Pain Scale (SF-36 BPS), and Measure of Intermittent and Constant Osteoarthritis Pain (ICOAP). Arthritis Care Res (Hoboken). 2011;63 Suppl 11:S240-52.
321. Royds J, Conroy MJ, Dunne MR, Cassidy H, Matallanas D, Lysaght J, et al. Examination and characterisation of burst spinal cord stimulation on cerebrospinal fluid cellular and protein constituents in patient responders with chronic neuropathic pain-A Pilot Study. Journal of Neuroimmunology. 2020:577249.
322. Hughes CS, Foehr S, Garfield DA, Furlong EE, Steinmetz LM, Krijgsveld J. Ultrasensitive proteome analysis using paramagnetic bead technology. Molecular systems biology. 2014;10(10):757.
323. Cox J, Hein MY, Luber CA, Paron I, Nagaraj N, Mann M. MaxLFQ allows accurate proteome-wide label-free quantification by delayed normalization and maximal peptide ratio extraction. Molecular & cellular proteomics. 2014:mcp. M113. 031591.
324. Weisser H, Nahnsen S, Grossmann J, Nilse L, Quandt A, Brauer H, et al. An automated pipeline for high-throughput label-free quantitative proteomics. Journal of proteome research. 2013;12(4):1628-44.
325. Baron R, Maier C, Attal N, Binder A, Bouhassira D, Cruccu G, et al. Peripheral neuropathic pain: a mechanism-related organizing principle based on sensory profiles. Pain. 2017;158(2):261.
326. Xie S, Chen M, Yan B, He X, Chen X, Li D. Identification of a role for the PI3K/AKT/mTOR signaling pathway in innate immune cells. PLoS One. 2014;9(4):e94496.
327. Brunet A, Datta SR, Greenberg ME. Transcription-dependent and-independent control of neuronal survival by the PI3K–Akt signaling pathway. Current opinion in neurobiology. 2001;11(3):297-305.
328. Chen SP, Zhou YQ, Liu DQ, Zhang W, Manyande A, Guan XH, et al. PI3K/Akt Pathway: A Potential Therapeutic Target for Chronic Pain. Curr Pharm Des. 2017;23(12):1860-8.
329. Xu B, Guan XH, Yu JX, Lv J, Zhang HX, Fu QC, et al. Activation of spinal phosphatidylinositol 3-kinase/protein kinase B mediates pain behavior induced by plantar incision in mice. Exp Neurol. 2014;255:71-82.
330. Teixeira AL, Gama CS, Rocha NP, Teixeira MM. Revisiting the Role of Eotaxin-1/CCL11 in Psychiatric Disorders. Front Psychiatry. 2018;9:241.
331. Huber AK, Giles DA, Segal BM, Irani DN. An emerging role for eotaxins in neurodegenerative disease. Clin Immunol. 2018;189:29-33.
332. Mishra A, Hogan SP, Lee JJ, Foster PS, Rothenberg ME. Fundamental signals that regulate eosinophil homing to the gastrointestinal tract. J Clin Invest. 1999;103(12):1719-27.
333. Fulkerson DH, Boaz JC. Cerebrospinal fluid eosinophilia in children with ventricular shunts. J Neurosurg Pediatr. 2008;1(4):288-95.

334. Yang LP, Zhu XA, Tso MO. Minocycline and sulforaphane inhibited lipopolysaccharide-mediated retinal microglial activation. Mol Vis. 2007;13:1083-93.
335. Choi SS, Lee HJ, Lim I, Satoh J, Kim SU. Human astrocytes: secretome profiles of cytokines and chemokines. PLoS One. 2014;9(4):e92325.
336. Parajuli B, Horiuchi H, Mizuno T, Takeuchi H, Suzumura A. CCL11 enhances excitotoxic neuronal death by producing reactive oxygen species in microglia. Glia. 2015;63(12):2274-84.
337. Ji RR, Xu ZZ, Gao YJ. Emerging targets in neuroinflammation-driven chronic pain. Nature reviews Drug discovery. 2014;13(7):533-48.
338. Zhuang ZY, Gerner P, Woolf CJ, Ji RR. ERK is sequentially activated in neurons, microglia, and astrocytes by spinal nerve ligation and contributes to mechanical allodynia in this neuropathic pain model. Pain. 2005;114(1-2):149-59.
339. Storkebaum E, Lambrechts D, Carmeliet P. VEGF: once regarded as a specific angiogenic factor, now implicated in neuroprotection. Bioessays. 2004;26(9):943-54.
340. Liu SM, Xiao ZF, Li X, Zhao YN, Wu XM, Han J, et al. Vascular endothelial growth factor activates neural stem cells through epidermal growth factor receptor signal after spinal cord injury. CNS Neurosci Ther. 2019;25(3):375-85.
341. Warner-Schmidt JL, Duman RS. VEGF is an essential mediator of the neurogenic and behavioral actions of antidepressants. Proc Natl Acad Sci U S A. 2007;104(11):4647-52.
342. Zhang Y, Sloan SA, Clarke LE, Caneda C, Plaza CA, Blumenthal PD, et al. Purification and Characterization of Progenitor and Mature Human Astrocytes Reveals Transcriptional and Functional Differences with Mouse. Neuron. 2016;89(1):37-53.
343. Schratzberger P, Walter DH, Rittig K, Bahlmann FH, Pola R, Curry C, et al. Reversal of experimental diabetic neuropathy by VEGF gene transfer. J Clin Invest. 2001;107(9):1083-92.
344. Simovic D, Isner JM, Ropper AH, Pieczek A, Weinberg DH. Improvement in chronic ischemic neuropathy after intramuscular phVEGF165 gene transfer in patients with critical limb ischemia. Arch Neurol. 2001;58(5):761-8.
345. Murakami T, Arai M, Sunada Y, Nakamura A. VEGF 164 gene transfer by electroporation improves diabetic sensory neuropathy in mice. J Gene Med. 2006;8(6):773-81.
346. Zheng X, Chen F, Zheng T, Huang F, Chen J, Tu W. Amitriptyline Activates TrkA to Aid Neuronal Growth and Attenuate Anesthesia-Induced Neurodegeneration in Rat Dorsal Root Ganglion Neurons. Medicine (Baltimore). 2016;95(18):e3559.
347. Nicoletti F, Patti F, Cocuzza C, Zaccone P, Nicoletti A, Di Marco R, et al. Elevated serum levels of interleukin-12 in chronic progressive multiple sclerosis. Journal of neuroimmunology. 1996;70(1):87-90.
348. Narikawa K, Fujihara K, Misu T, Feng J, Fujimori J, Nakashima I, et al. CSF-chemokines in HTLV-I-associated myelopathy: CXCL10 up-regulation and therapeutic effect of interferon-alpha. J Neuroimmunol. 2005;159(1-2):177-82.
349. Conaghan PG, Cook AD, Hamilton JA, Tak PP. Therapeutic options for targeting inflammatory osteoarthritis pain. Nat Rev Rheumatol. 2019;15(6):355-63.
350. Zin CS, Nissen LM, O'Callaghan JP, Moore BJ, Smith MT. Preliminary study of the plasma and cerebrospinal fluid concentrations of IL-6 and IL-10 in patients with chronic pain receiving intrathecal opioid infusions by chronically implanted pump for pain management. Pain Med. 2010;11(4):550-61.
351. Aasebo E, Opsahl JA, Bjorlykke Y, Myhr KM, Kroksveen AC, Berven FS. Effects of blood contamination and the rostro-caudal gradient on the human cerebrospinal fluid proteome. PLoS One. 2014;9(3):e90429.

352. Hu Y, Malone JP, Fagan AM, Townsend RR, Holtzman DM. Comparative proteomic analysis of intra- and interindividual variation in human cerebrospinal fluid. Mol Cell Proteomics. 2005;4(12):2000-9.
353. Moore D, Galvin D, Conroy MJ, Das B, Dunne M, Lysaght J, et al. Characterisation of the effects of pulsed radio frequency treatment of the dorsal root ganglion on cerebrospinal fluid cellular and peptide constituents in patients with chronic radicular pain: A randomised, triple-blinded, controlled trial. J Neuroimmunol. 2020;343:577219.
354. Royds J, Conroy MJ, Dunne MR, McCrory C, Lysaght J. An investigation into the modulation of T cell phenotypes by amitriptyline and nortriptyline. European Neuropsychopharmacology. 2020;31:131-44.
355. Obata H. Analgesic Mechanisms of Antidepressants for Neuropathic Pain. Int J Mol Sci. 2017;18(11).
356. Segal JP, Tresidder KA, Bhatt C, Gilron I, Ghasemlou N. Circadian control of pain and neuroinflammation. Journal of Neuroscience Research. 2018;96(6):1002-20.
357. Kieseier BC, Mathey EK, Sommer C, Hartung HP. Immune-mediated neuropathies. Nat Rev Dis Primers. 2018;4(1):31.
358. Cahill CM, Taylor AM. Neuroinflammation-a co-occurring phenomenon linking chronic pain and opioid dependence. Curr Opin Behav Sci. 2017;13:171-7.
359. Backryd E, Tanum L, Lind AL, Larsson A, Gordh T. Evidence of both systemic inflammation and neuroinflammation in fibromyalgia patients, as assessed by a multiplex protein panel applied to the cerebrospinal fluid and to plasma. J Pain Res. 2017;10:515-25.
360. Makker PG, Duffy SS, Lees JG, Perera CJ, Tonkin RS, Butovsky O, et al. Characterisation of Immune and Neuroinflammatory Changes Associated with Chemotherapy-Induced Peripheral Neuropathy. PLoS One. 2017;12(1):e0170814.
361. Lenz M, Uceyler N, Frettloh J, Hoffken O, Krumova EK, Lissek S, et al. Local cytokine changes in complex regional pain syndrome type I (CRPS I) resolve after 6 months. Pain. 2013;154(10):2142-9.
362. Birklein F, Schmelz M. Neuropeptides, neurogenic inflammation and complex regional pain syndrome (CRPS). Neurosci Lett. 2008;437(3):199-202.
363. Bartosik-Psujek H, Stelmasiak Z. Correlations between IL-4, IL-12 levels and CCL2, CCL5 levels in serum and cerebrospinal fluid of multiple sclerosis patients. J Neural Transm (Vienna). 2005;112(6):797-803.
364. Ernberg M, Christidis N, Ghafouri B, Bileviciute-Ljungar I, Lofgren M, Bjersing J, et al. Plasma Cytokine Levels in Fibromyalgia and Their Response to 15 Weeks of Progressive Resistance Exercise or Relaxation Therapy. Mediators Inflamm. 2018;2018:3985154.
365. Landi A, Broadhurst D, Vernon SD, Tyrrell DL, Houghton M. Reductions in circulating levels of IL-16, IL-7 and VEGF-A in myalgic encephalomyelitis/chronic fatigue syndrome. Cytokine. 2016;78:27-36.
366. Diamond M, Kelly JP, Connor TJ. Antidepressants suppress production of the Th1 cytokine interferon-gamma, independent of monoamine transporter blockade. Eur Neuropsychopharmacol. 2006;16(7):481-90.
367. Xia BT, Beckmann N, Winer LK, Pugh AM, Pritts TA, Nomellini V, et al. Amitriptyline Reduces Inflammation and Mortality in a Murine Model of Sepsis. Cell Physiol Biochem. 2019;52(3):565-79.
368. Meacham K, Shepherd A, Mohapatra DP, Haroutounian S. Neuropathic Pain: Central vs. Peripheral Mechanisms. Curr Pain Headache Rep. 2017;21(6):28.

369. Kasela S, Kisand K, Tserel L, Kaleviste E, Remm A, Fischer K, et al. Pathogenic implications for autoimmune mechanisms derived by comparative eQTL analysis of CD4+ versus CD8+ T cells. PLoS Genet. 2017;13(3):e1006643.
370. Gravano DM, Hoyer KK. Promotion and prevention of autoimmune disease by CD8+ T cells. J Autoimmun. 2013;45:68-79.
371. Larbi A, Fulop T. From "truly naive" to "exhausted senescent" T cells: when markers predict functionality. Cytometry A. 2014;85(1):25-35.
372. Carrasco J, Godelaine D, Van Pel A, Boon T, van der Bruggen P. CD45RA on human CD8 T cells is sensitive to the time elapsed since the last antigenic stimulation. Blood. 2006;108(9):2897-905.
373. Slifka MK, Whitton JL. Functional avidity maturation of CD8(+) T cells without selection of higher affinity TCR. Nat Immunol. 2001;2(8):711-7.
374. Xiao Z, Mescher MF, Jameson SC. Detuning CD8 T cells: down-regulation of CD8 expression, tetramer binding, and response during CTL activation. J Exp Med. 2007;204(11):2667-77.
375. Meng H, Zhao H, Cao X, Hao J, Zhang H, Liu Y, et al. Double-negative T cells remarkably promote neuroinflammation after ischemic stroke. Proc Natl Acad Sci U S A. 2019;116(12):5558-63.
376. Brandt D, Hedrich CM. TCRαβ + CD3 + CD4 − CD8 − (double negative) T cells in autoimmunity. Autoimmunity Reviews. 2018;17(4):422-30.
377. Chen G, Kim YH, Li H, Luo H, Liu DL, Zhang ZJ, et al. PD-L1 inhibits acute and chronic pain by suppressing nociceptive neuron activity via PD-1. Nat Neurosci. 2017;20(7):917-26.
378. Mahnke YD, Brodie TM, Sallusto F, Roederer M, Lugli E. The who's who of T-cell differentiation: human memory T-cell subsets. Eur J Immunol. 2013;43(11):2797-809.
379. Yoles E, Hauben E, Palgi O, Agranov E, Gothilf A, Cohen A, et al. Protective autoimmunity is a physiological response to CNS trauma. The Journal of neuroscience : the official journal of the Society for Neuroscience. 2001;21(11):3740-8.
380. Kelly-Rogers J, Madrigal-Estebas L, O'Connor T, Doherty DG. Activation-induced expression of CD56 by T cells is associated with a reprogramming of cytolytic activity and cytokine secretion profile in vitro. Hum Immunol. 2006;67(11):863-73.
381. Campos AC, Vaz GN, Saito VM, Teixeira AL. Further evidence for the role of interferon-gamma on anxiety- and depressive-like behaviors: involvement of hippocampal neurogenesis and NGF production. Neurosci Lett. 2014;578:100-5.
382. Pernambuco AP, Schetino LP, Alvim CC, Murad CM, Viana RS, Carvalho LS, et al. Increased levels of IL-17A in patients with fibromyalgia. Clin Exp Rheumatol. 2013;31(6 Suppl 79):S60-3.
383. Luo H, Liu H-Z, Luo X, Bang S, Wang Z-L, Chen G, et al. 2018.
384. Skundric DS, Cruikshank WW, Montgomery PC, Lisak RP, Tse HY. Emerging role of IL-16 in cytokine-mediated regulation of multiple sclerosis. Cytokine. 2015;75(2):234-48.
385. Pae CU, Marks DM, Patkar AA, Masand PS, Luyten P, Serretti A. Pharmacological treatment of chronic fatigue syndrome: focusing on the role of antidepressants. Expert Opin Pharmacother. 2009;10(10):1561-70.
386. Baumer JH. Management of chronic fatigue syndrome/myalgic encephalopathy (CFS/ME). Archives of Disease in Childhood - Education and Practice. 2005;90(2):ep46-ep50.

387. Schurks M, Rist PM, Zee RY, Chasman DI, Kurth T. Tumour necrosis factor gene polymorphisms and migraine: a systematic review and meta-analysis. Cephalalgia. 2011;31(13):1381-404.
388. Tjepkema-Cloostermans MC, de Vos CC, Wolters R, Dijkstra-Scholten C, Lenders MW. Effect of Burst Stimulation Evaluated in Patients Familiar With Spinal Cord Stimulation. Neuromodulation. 2016;19(5):492-7.
389. Vesper J, Slotty P, Schu S, Poeggel-Kraemer K, Littges H, Van Looy P, et al. Burst SCS Microdosing Is as Efficacious as Standard Burst SCS in Treating Chronic Back and Leg Pain: Results From a Randomized Controlled Trial. Neuromodulation. 2019;22(2):190-3.
390. Ruiz-Sauri A, Orduna-Valls JM, Blasco-Serra A, Tornero-Tornero C, Cedeno DL, Bejarano-Quisoboni D, et al. Glia to neuron ratio in the posterior aspect of the human spinal cord at thoracic segments relevant to spinal cord stimulation. J Anat. 2019.
391. Cui Y, Yang Y, Ni Z, Dong Y, Cai G, Foncelle A, et al. Astroglial Kir4.1 in the lateral habenula drives neuronal bursts in depression. Nature. 2018;554(7692):323-7.
392. Fields RD, Burnstock G. Purinergic signalling in neuron-glia interactions. Nat Rev Neurosci. 2006;7(6):423-36.
393. Cacace F, Mineo D, Viscomi MT, Latagliata EC, Mancini M, Sasso V, et al. Intermittent theta-burst stimulation rescues dopamine-dependent corticostriatal synaptic plasticity and motor behavior in experimental parkinsonism: Possible role of glial activity. Mov Disord. 2017;32(7):1035-46.
394. Tsuda M, Koga K, Chen T, Zhuo M. Neuronal and microglial mechanisms for neuropathic pain in the spinal dorsal horn and anterior cingulate cortex. Journal of Neurochemistry. 2017;141(4):486-98.
395. Chakravarthy K, Fishman MA, Zuidema X, Hunter CW, Levy R. Mechanism of Action in Burst Spinal Cord Stimulation: Review and Recent Advances. Pain Med. 2019;20(Supplement_1):S13-S22.
396. Mekhail N, Levy RM, Deer TR, Kapural L, Li S, Amirdelfan K, et al. Long-term safety and efficacy of closed-loop spinal cord stimulation to treat chronic back and leg pain (Evoke): a double-blind, randomised, controlled trial. The Lancet Neurology. 2019.
397. Weinand ME, Madhusudan H, Davis B, Melgar M. Acute vs. Prolonged Screening for Spinal Cord Stimulation in Chronic Pain. Neuromodulation. 2003;6(1):15-9.
398. Ullian EM, Christopherson KS, Barres BA. Role for glia in synaptogenesis. Glia. 2004;47(3):209-16.
399. Remy S, Spruston N. Dendritic spikes induce single-burst long-term potentiation. Proc Natl Acad Sci U S A. 2007;104(43):17192-7.
400. Stephens KE, Chen Z, Sivanesan E, Raja SN, Linderoth B, Taverna SD, et al. RNA-seq of spinal cord from nerve-injured rats after spinal cord stimulation. Mol Pain. 2018;14:1744806918817429.
401. Xu J, Casserly E, Yin Y, Cheng J. A Systematic Review of Growth Hormone in Pain Medicine: From Rodents to Humans. Pain Med. 2019.
402. Seybold V, Hylden J, Wilcox G. Intrathecal substance P and somatostatin in rats: behaviors indicative of sensation. Peptides. 1982;3(1):49-54.
403. Wiesenfeld-Hallin Z. Intrathecal somatostatin modulates spinal sensory and reflex mechanisms: behavioral and electrophysiological studies in the rat. Neuroscience letters. 1985;62(1):69-74.
404. Chapman V, Dickenson A. The effects of sandostatin and somatostatin on nociceptive transmission in the dorsal horn of the rat spinal cord. Neuropeptides. 1992;23(3):147-52.

405. Carlton SM, Du J, Zhou S, Coggeshall RE. Tonic control of peripheral cutaneous nociceptors by somatostatin receptors. Journal of Neuroscience. 2001;21(11):4042-9.
406. Carlton SM, Zhou S, Du J, Hargett GL, Ji G, Coggeshall RE. Somatostatin modulates the transient receptor potential vanilloid 1 (TRPV1) ion channel. Pain. 2004;110(3):616-27.
407. Huang J, Polgar E, Solinski HJ, Mishra SK, Tseng PY, Iwagaki N, et al. Circuit dissection of the role of somatostatin in itch and pain. Nat Neurosci. 2018;21(5):707-16.
408. Shi TJ, Xiang Q, Zhang MD, Barde S, Kai-Larsen Y, Fried K, et al. Somatostatin and its 2A receptor in dorsal root ganglia and dorsal horn of mouse and human: expression, trafficking and possible role in pain. Mol Pain. 2014;10:12.
409. Tagaya Y, Miura A, Okada S, Ohshima K, Mori M. Nucleobindin-2 Is a Positive Modulator of EGF-Dependent Signals Leading to Enhancement of Cell Growth and Suppression of Adipocyte Differentiation. Endocrinology. 2012;153(7):3308-19.
410. Blackburn-Munro G. Hypothalamo-pituitary-adrenal axis dysfunction as a contributory factor to chronic pain and depression. Current Pain and Headache Reports. 2004;8(2):116-24.
411. Vachon-Presseau E. Effects of stress on the corticolimbic system: implications for chronic pain. Prog Neuropsychopharmacol Biol Psychiatry. 2018;87(Pt B):216-23.
412. Kinfe TM, Buchfelder M, Chaudhry SR, Chakravarthy KV, Deer TR, Russo M, et al. Leptin and Associated Mediators of Immunometabolic Signaling: Novel Molecular Outcome Measures for Neurostimulation to Treat Chronic Pain. Int J Mol Sci. 2019;20(19).
413. ten Bokum AM, Hofland L, van Hagen PM. Somatostatin and somatostatin receptors in the immune system: a review. European cytokine network. 2000;11(2):161-76.
414. Muhammad S, Chaudhry SR, Yearwood TL, Krauss JK, Kinfe TM. Changes of Metabolic Disorders Associated Peripheral Cytokine/Adipokine Traffic in Non-Obese Chronic Back Patients Responsive to Burst Spinal Cord Stimulation. Neuromodulation. 2018;21(1):31-7.
415. Mzhavia N, Qian Y, Feng Y, Che FY, Devi LA, Fricker LD. Processing of proSAAS in neuroendocrine cell lines. Biochem J. 2002;361(Pt 1):67-76.
416. Mzhavia N, Berman Y, Che F-Y, Fricker LD, Devi LA. ProSAAS processing in mouse brain and pituitary. Journal of Biological Chemistry. 2001;276(9):6207-13.
417. Khoonsari PE, Musunri S, Herman S, Svensson CI, Tanum L, Gordh T, et al. Systematic analysis of the cerebrospinal fluid proteome of fibromyalgia patients. J Proteomics. 2019;190:35-43.
418. Berg EM, Bertuzzi M, Ampatzis K. Complementary expression of calcium binding proteins delineates the functional organization of the locomotor network. Brain Struct Funct. 2018;223(5):2181-96.
419. Ren K, Ruda MA. A comparative study of the calcium-binding proteins calbindin-D28K, calretinin, calmodulin and parvalbumin in the rat spinal cord. Brain Res Brain Res Rev. 1994;19(2):163-79.
420. Schwaller B, Meyer M, Schiffmann S. 'New' functions for 'old' proteins: the role of the calcium-binding proteins calbindin D-28k, calretinin and parvalbumin, in cerebellar physiology. Studies with knockout mice. Cerebellum. 2002;1(4):241-58.
421. Perea G, Araque A. Glial calcium signaling and neuron-glia communication. Cell Calcium. 2005;38(3-4):375-82.
422. Fernyhough P, Calcutt NA. Abnormal calcium homeostasis in peripheral neuropathies. Cell Calcium. 2010;47(2):130-9.

423. Hagenston AM, Simonetti M. Neuronal calcium signaling in chronic pain. Cell Tissue Res. 2014;357(2):407-26.
424. Mei Y, Barrett JE, Hu H. Calcium release-activated calcium channels and pain. Cell Calcium. 2018;74:180-5.
425. Hebb AL, Poulin J-F, Roach SP, Zacharko RM, Drolet G. Cholecystokinin and endogenous opioid peptides: interactive influence on pain, cognition, and emotion. Progress in Neuro-Psychopharmacology and Biological Psychiatry. 2005;29(8):1225-38.
426. Rowlingson JC. Cholecystokinin and Its Antagonists in Pain Management. Anesthesia & Analgesia. 2007;104(3):750.
427. Kirketeig T, Schultheis C, Zuidema X, Hunter CW, Deer T. Burst Spinal Cord Stimulation: A Clinical Review. Pain Med. 2019;20(Supplement_1):S31-S40.
428. Khodorova A, Montmayeur JP, Strichartz G. Endothelin receptors and pain. The journal of pain : official journal of the American Pain Society. 2009;10(1):4-28.
429. Smith TP, Haymond T, Smith SN, Sweitzer SM. Evidence for the endothelin system as an emerging therapeutic target for the treatment of chronic pain. J Pain Res. 2014;7:531-45.
430. Murphy DM, O'Callaghan DS, Gaine SP. Relief of chronic neuropathic pain through endothelin antagonism. Am J Med. 2010;123(3):e7.
431. Bjurstrom MF, Giron SE, Griffis CA. Cerebrospinal Fluid Cytokines and Neurotrophic Factors in Human Chronic Pain Populations: A Comprehensive Review. Pain Pract. 2016;16(2):183-203.
432. Schutzer SE, Liu T, Natelson BH, Angel TE, Schepmoes AA, Purvine SO, et al. Establishing the proteome of normal human cerebrospinal fluid. PLoS One. 2010;5(6):e10980.
433. Royds J, Cassidy H, Conroy MJ, Dunne MR, Matallanas D, Lysaght J, et al. An Investigation into Proteomic Constituents of Cerebrospinal Fluid in Patients with Chronic Peripheral Neuropathic Pain Medicated with Opioids- a Pilot Study. J Neuroimmune Pharmacol. 2020.
434. O'Brien T, Christrup LL, Drewes AM, Fallon MT, Kress HG, McQuay HJ, et al. European Pain Federation position paper on appropriate opioid use in chronic pain management. Eur J Pain. 2017;21(1):3-19.
435. Rosenblum A, Marsch LA, Joseph H, Portenoy RK. Opioids and the treatment of chronic pain: controversies, current status, and future directions. Exp Clin Psychopharmacol. 2008;16(5):405-16.
436. Ballantyne JC. Chronic pain following treatment for cancer: the role of opioids. Oncologist. 2003;8(6):567-75.
437. Meske DS, Lawal OD, Elder H, Langberg V, Paillard F, Katz N. Efficacy of opioids versus placebo in chronic pain: a systematic review and meta-analysis of enriched enrollment randomized withdrawal trials. J Pain Res. 2018;11:923-34.
438. Ballantyne JC, Shin NS. Efficacy of opioids for chronic pain: a review of the evidence. Clin J Pain. 2008;24(6):469-78.
439. Furlan AD, Sandoval JA, Mailis-Gagnon A, Tunks E. Opioids for chronic noncancer pain: a meta-analysis of effectiveness and side effects. CMAJ. 2006;174(11):1589-94.
440. Scherrer JF, Salas J, Schneider FD, Bucholz KK, Sullivan MD, Copeland LA, et al. Characteristics of new depression diagnoses in patients with and without prior chronic opioid use. J Affect Disord. 2017;210:125-9.
441. Richards GC, Lluka LJ, Smith MT, Haslam C, Moore B, O'Callaghan J, et al. Effects of long-term opioid analgesics on cognitive performance and plasma cytokine

concentrations in patients with chronic low back pain: a cross-sectional pilot study. Pain Rep. 2018;3(4):e669.
442. Boland JW, Pockley AG. Influence of opioids on immune function in patients with cancer pain: from bench to bedside. Br J Pharmacol. 2018;175(14):2726-36.
443. Roy S, Ninkovic J, Banerjee S, Charboneau RG, Das S, Dutta R, et al. Opioid drug abuse and modulation of immune function: consequences in the susceptibility to opportunistic infections. J Neuroimmune Pharmacol. 2011;6(4):442-65.
444. Plein LM, Rittner HL. Opioids and the immune system - friend or foe. Br J Pharmacol. 2018;175(14):2717-25.
445. Heinke B, Gingl E, Sandkühler J. Multiple targets of μ-opioid receptor-mediated presynaptic inhibition at primary afferent Aδ-and C-fibers. Journal of Neuroscience. 2011;31(4):1313-22.
446. Pathan H, Williams J. Basic opioid pharmacology: an update. Br J Pain. 2012;6(1):11-6.
447. Hutchinson MR, Shavit Y, Grace PM, Rice KC, Maier SF, Watkins LR. Exploring the neuroimmunopharmacology of opioids: an integrative review of mechanisms of central immune signaling and their implications for opioid analgesia. Pharmacol Rev. 2011;63(3):772-810.
448. Chao CC, Gekker G, Hu S, Sheng WS, Shark KB, Bu D-F, et al. Kappa opioid receptors in human microglia downregulate human immunodeficiency virus 1 expression. Proceedings of the National Academy of Sciences. 1996;93(15):8051-6.
449. Araque A, Parpura V, Sanzgiri RP, Haydon PG. Tripartite synapses: glia, the unacknowledged partner. Trends Neurosci. 1999;22(5):208-15.
450. Perea G, Navarrete M, Araque A. Tripartite synapses: astrocytes process and control synaptic information. Trends Neurosci. 2009;32(8):421-31.
451. Perea G, Sur M, Araque A. Neuron-glia networks: integral gear of brain function. Front Cell Neurosci. 2014;8:378.
452. Machelska H, Celik MO. Opioid Receptors in Immune and Glial Cells-Implications for Pain Control. Front Immunol. 2020;11:300.
453. Grace PM, Maier SF, Watkins LR. Opioid-induced central immune signaling: implications for opioid analgesia. Headache. 2015;55(4):475-89.
454. Amodeo G, Bugada D, Franchi S, Moschetti G, Grimaldi S, Panerai A, et al. Immune function after major surgical interventions: the effect of postoperative pain treatment. J Pain Res. 2018;11:1297-305.
455. Ninkovic J, Roy S. Role of the mu-opioid receptor in opioid modulation of immune function. Amino Acids. 2013;45(1):9-24.
456. Dublin S, Walker RL, Jackson ML, Nelson JC, Weiss NS, Von Korff M, et al. Use of opioids or benzodiazepines and risk of pneumonia in older adults: a population-based case-control study. J Am Geriatr Soc. 2011;59(10):1899-907.
457. M Moore D, McCrory C. The proteomics of intrathecal analgesic agents for chronic pain. Current neuropharmacology. 2017;15(2):198-205.
458. Gomez-Varela D, Barry AM, Schmidt M. Proteome-based systems biology in chronic pain. J Proteomics. 2019;190:1-11.
459. Hale JE, Gelfanova V, You J-S, Knierman MD, Dean RA. Proteomics of cerebrospinal fluid: methods for sample processing. 2D PAGE: Sample Preparation and Fractionation: Springer; 2008. p. 53-66.
460. Yuan X, Desiderio DM. Proteomics analysis of human cerebrospinal fluid. Journal of Chromatography B. 2005;815(1-2):179-89.

461. Zougman A, Pilch B, Podtelejnikov A, Kiehntopf M, Schnabel C, Kumar C, et al. Integrated analysis of the cerebrospinal fluid peptidome and proteome. Journal of proteome research. 2008;7(01):386-99.
462. D'Ascenzo M. Alzheimer'S Disease Biomarker Discovery And Data Visualization Using Proteomics And Bioinformatics Approaches. 2013.
463. Zhang Y, Guo Z, Zou L, Yang Y, Zhang L, Ji N, et al. A comprehensive map and functional annotation of the normal human cerebrospinal fluid proteome. J Proteomics. 2015;119:90-9.
464. Zhang J, Goodlett DR, Montine TJ. Proteomic biomarker discovery in cerebrospinal fluid for neurodegenerative diseases. Journal of Alzheimer's Disease. 2005;8(4):377-86.
465. Zhang J, Goodlett DR, Quinn JF, Peskind E, Kaye JA, Zhou Y, et al. Quantitative proteomics of cerebrospinal fluid from patients with Alzheimer disease. Journal of Alzheimer's Disease. 2005;7(2):125-33.
466. Lardinois O, Kirby P, Morgan D, Sills R, Tomer K, Deterding L. Mass spectrometric analysis of rat cerebrospinal fluid proteins following exposure to the neurotoxicant carbonyl sulfide. Rapid Communications in Mass Spectrometry. 2014;28(23):2531-8.
467. Craft GE, Chen A, Nairn AC. Recent advances in quantitative neuroproteomics. Methods. 2013;61(3):186-218.
468. Perrin RJ, Payton JE, Malone JP, Gilmore P, Davis AE, Xiong C, et al. Quantitative label-free proteomics for discovery of biomarkers in cerebrospinal fluid: assessment of technical and inter-individual variation. PLoS One. 2013;8(5):e64314.
469. Ericson H, Abu Hamdeh S, Freyhult E, Stiger F, Backryd E, Svenningsson A, et al. Cerebrospinal fluid biomarkers of inflammation in trigeminal neuralgia patients operated with microvascular decompression. Pain. 2019.
470. Zsigmond P, Ljunggren SA, Ghafouri B. Proteomic Analysis of the Cerebrospinal Fluid in Patients With Essential Tremor Before and After Deep Brain Stimulation Surgery: A Pilot Study. Neuromodulation: Technology at the Neural Interface. 2020;23(4):502-8.
471. Olausson P, Ghafouri B, Backryd E, Gerdle B. Clear differences in cerebrospinal fluid proteome between women with chronic widespread pain and healthy women - a multivariate explorative cross-sectional study. J Pain Res. 2017;10:575-90.
472. Bergquist J, Palmblad M, Wetterhall M, Håkansson P, Markides KE. Peptide mapping of proteins in human body fluids using electrospray ionization Fourier transform ion cyclotron resonance mass spectrometry. Mass spectrometry reviews. 2002;21(1):2-15.
473. Cox J, Mann M. 1D and 2D annotation enrichment: a statistical method integrating quantitative proteomics with complementary high-throughput data. BMC bioinformatics. 2012;13(S16):S12.
474. Krämer A, Green J, Pollard Jr J, Tugendreich S. Causal analysis approaches in ingenuity pathway analysis. Bioinformatics. 2014;30(4):523-30.
475. Shannon P, Markiel A, Ozier O, Baliga NS, Wang JT, Ramage D, et al. Cytoscape: a software environment for integrated models of biomolecular interaction networks. Genome research. 2003;13(11):2498-504.
476. Mi H, Muruganujan A, Casagrande JT, Thomas PD. Large-scale gene function analysis with the PANTHER classification system. Nature protocols. 2013;8(8):1551-66.
477. Tyanova S, Temu T, Sinitcyn P, Carlson A, Hein MY, Geiger T, et al. The Perseus computational platform for comprehensive analysis of (prote)omics data. Nature Methods. 2016;13(9):731-40.

478. El-Khateeb E, Vasilogianni AM, Alrubia S, Al-Majdoub ZM, Couto N, Howard M, et al. Quantitative mass spectrometry-based proteomics in the era of model-informed drug development: Applications in translational pharmacology and recommendations for best practice. Pharmacol Ther. 2019;203:107397.
479. Feng Y, He X, Yang Y, Chao D, H Lazarus L, Xia Y. Current research on opioid receptor function. Current drug targets. 2012;13(2):230-46.
480. Chan HS, McCarthy D, Li J, Palczewski K, Yuan S. Designing safer analgesics via μ-opioid receptor pathways. Trends in pharmacological sciences. 2017;38(11):1016-37.
481. Gharavi R, Hedrich W, Wang H, Hassan HE. Transporter-mediated disposition of opioids: implications for clinical drug interactions. Pharmaceutical research. 2015;32(8):2477-502.
482. Kanjhan R. Opioids and pain. Clinical and Experimental Pharmacology and Physiology. 1995;22(6-7):397-403.
483. Lee MC, Wanigasekera V, Tracey I. Imaging opioid analgesia in the human brain and its potential relevance for understanding opioid use in chronic pain. Neuropharmacology. 2014;84:123-30.
484. Boggess T, Risher WC. Clinical and basic research investigations into the long-term effects of prenatal opioid exposure on brain development. Journal of Neuroscience Research. 2020.
485. Stiene-Martin A, Knapp PE, Martin K, Gurwell JA, Ryan S, Thornton SR, et al. Opioid system diversity in developing neurons, astroglia, and oligodendroglia in the subventricular zone and striatum: impact on gliogenesis in vivo. Glia. 2001;36(1):78-88.
486. Zagon IS, McLaughlin PJ. Identification of opioid peptides regulating proliferation of neurons and glia in the developing nervous system. Brain research. 1991;542(2):318-23.
487. Eisch AJ, Harburg GC. Opiates, psychostimulants, and adult hippocampal neurogenesis: Insights for addiction and stem cell biology. Hippocampus. 2006;16(3):271-86.
488. Xu M, Bruchas MR, Ippolito DL, Gendron L, Chavkin C. Sciatic nerve ligation-induced proliferation of spinal cord astrocytes is mediated by κ opioid activation of p38 mitogen-activated protein kinase. Journal of Neuroscience. 2007;27(10):2570-81.
489. Hutchinson MR, Bland ST, Johnson KW, Rice KC, Maier SF, Watkins LR. Opioid-induced glial activation: mechanisms of activation and implications for opioid analgesia, dependence, and reward. ScientificWorldJournal. 2007;7:98-111.
490. Mortha A, Burrows K. Cytokine Networks between Innate Lymphoid Cells and Myeloid Cells. Front Immunol. 2018;9:191.
491. Messmer D, Hatsukari I, Hitosugi N, Schmidt-Wolf IG, Singhal PC. Morphine reciprocally regulates IL-10 and IL-12 production by monocyte-derived human dendritic cells and enhances T cell activation. Mol Med. 2006;12(11-12):284-90.
492. Russo M, Georgius P, Santarelli DM. A new hypothesis for the pathophysiology of complex regional pain syndrome. Med Hypotheses. 2018;119:41-53.
493. Horvath RJ, DeLeo JA. Morphine enhances microglial migration through modulation of P2X4 receptor signaling. The Journal of neuroscience : the official journal of the Society for Neuroscience. 2009;29(4):998-1005.
494. Leger T, Grist J, D'Acquisto F, Clark AK, Malcangio M. Glatiramer acetate attenuates neuropathic allodynia through modulation of adaptive immune cells. Journal of neuroimmunology. 2011;234(1-2):19-26.

495. Han C, Lei D, Liu L, Xie S, He L, Wen S, et al. Morphine induces the differentiation of T helper cells to Th2 effector cells via the PKC-theta-GATA3 pathway. Int Immunopharmacol. 2020;80:106133.
496. Borner C, Lanciotti S, Koch T, Hollt V, Kraus J. mu opioid receptor agonist-selective regulation of interleukin-4 in T lymphocytes. J Neuroimmunol. 2013;263(1-2):35-42.
497. Zhao ML, Si Q, Lee S. IL-16 expression in lymphocytes and microglia in HIV-1 encephalitis. Neuropathology and applied neurobiology. 2004;30(3):233-42.
498. Mueller CA, Schluesener HJ, Conrad S, Pietsch T, Schwab JM. Spinal cord injury-induced expression of the immune-regulatory chemokine interleukin-16 caused by activated microglia/macrophages and CD8+ cells. J Neurosurg Spine. 2006;4(3):233-40.
499. Diasso PDK, Birke H, Nielsen SD, Main KM, Hojsted J, Sjogren P, et al. The effects of long-term opioid treatment on the immune system in chronic non-cancer pain patients: A systematic review. Eur J Pain. 2020;24(3):481-96.
500. Kanashiro A, Hiroki CH, da Fonseca DM, Birbrair A, Ferreira RG, Bassi GS, et al. The role of neutrophils in neuro-immune modulation. Pharmacol Res. 2020;151:104580.
501. Perez-de-Puig I, Miró-Mur F, Ferrer-Ferrer M, Gelpi E, Pedragosa J, Justicia C, et al. Neutrophil recruitment to the brain in mouse and human ischemic stroke. Acta neuropathologica. 2015;129(2):239-57.
502. Davoli-Ferreira M, de Lima KA, Fonseca MM, Guimarães RM, Gomes FI, Cavallini MC, et al. Regulatory T cells counteract neuropathic pain through inhibition of the Th1 response at the site of peripheral nerve injury. Pain. 2020;161(8):1730-43.
503. Du B, Ding YQ, Xiao X, Ren HY, Su BY, Qi JG. CD4+ alphabeta T cell infiltration into the leptomeninges of lumbar dorsal roots contributes to the transition from acute to chronic mechanical allodynia after adult rat tibial nerve injuries. J Neuroinflammation. 2018;15(1):81.
504. Cunha T, Verri Jr W. Neutrophils: are they hyperalgesic or anti-hyperalgesic? Journal of leukocyte biology. 2006;80(4):727-8.
505. Scholz J, Finnerup NB, Attal N, Aziz Q, Baron R, Bennett MI, et al. The IASP classification of chronic pain for ICD-11: chronic neuropathic pain. Pain. 2019;160(1):53-9.
506. von Zastrow M. Regulation of opioid receptors by endocytic membrane traffic: mechanisms and translational implications. Drug Alcohol Depend. 2010;108(3):166-71.
507. Riley III JL, Hastie BA. Individual differences in opioid efficacy for chronic noncancer pain. The Clinical journal of pain. 2008;24(6):509-20.
508. Smith HS, Peppin JF. Toward a systematic approach to opioid rotation. Journal of pain research. 2014;7:589.
509. Branford R, Droney J, Ross J. Opioid genetics: the key to personalized pain control? Clinical genetics. 2012;82(4):301-10.
510. Guldbrandsen A, Vethe H, Farag Y, Oveland E, Garberg H, Berle M, et al. In-depth characterization of the cerebrospinal fluid (CSF) proteome displayed through the CSF proteome resource (CSF-PR). Molecular & cellular proteomics. 2014;13(11):3152-63.
511. Hughes CS, Moggridge S, Müller T, Sorensen PH, Morin GB, Krijgsveld J. Single-pot, solid-phase-enhanced sample preparation for proteomics experiments. Nature protocols. 2019;14(1):68-85.
512. Boadas-Vaello P, Castany S, Homs J, Alvarez-Perez B, Deulofeu M, Verdu E. Neuroplasticity of ascending and descending pathways after somatosensory system

injury: reviewing knowledge to identify neuropathic pain therapeutic targets. Spinal Cord. 2016;54(5):330-40.
513. De Groote S, Goudman L, Peeters R, Linderoth B, Vanschuerbeek P, Sunaert S, et al. Magnetic Resonance Imaging Exploration of the Human Brain During 10 kHz Spinal Cord Stimulation for Failed Back Surgery Syndrome: A Resting State Functional Magnetic Resonance Imaging Study. Neuromodulation. 2019.
514. Kuttikat A, Noreika V, Shenker N, Chennu S, Bekinschtein T, Brown CA. Neurocognitive and Neuroplastic Mechanisms of Novel Clinical Signs in CRPS. Front Hum Neurosci. 2016;10:16.
515. Wise RG, Preston C. What is the value of human FMRI in CNS drug development? Drug Discov Today. 2010;15(21-22):973-80.
516. Falowski SM. An Observational Case Series of Spinal Cord Stimulation Waveforms Visualized on Intraoperative Neuromonitoring. Neuromodulation. 2019;22(2):219-28.
517. Mathieson S, Maher CG, McLachlan AJ, Latimer J, Koes BW, Hancock MJ, et al. Trial of Pregabalin for Acute and Chronic Sciatica. N Engl J Med. 2017;376(12):1111-20.
518. O'Neill E, Kwok B, Day JS, Connor TJ, Harkin A. Amitriptyline protects against TNF-alpha-induced atrophy and reduction in synaptic markers via a Trk-dependent mechanism. Pharmacol Res Perspect. 2016;4(2):e00195.
519. Yearwood T, De Ridder D, Yoo HB, Falowski S, Venkatesan L, Ting To W, et al. Comparison of neural activity in chronic pain patients during tonic and burst spinal cord stimulation using Fluorodeoxyglucose positron emission tomography. Neuromodulation: Technology at the Neural Interface. 2020;23(1):56-63.
520. Deer TR, Patterson DG, Baksh J, Pope JE, Mehta P, Raza A, et al. Novel Intermittent Dosing Burst Paradigm in Spinal Cord Stimulation. Neuromodulation: Technology at the Neural Interface. 2020.
521. Engelhardt B, Carare RO, Bechmann I, Flugel A, Laman JD, Weller RO. Vascular, glial, and lymphatic immune gateways of the central nervous system. Acta Neuropathol. 2016;132(3):317-38.
522. Engelhardt B, Ransohoff RM. Capture, crawl, cross: the T cell code to breach the blood-brain barriers. Trends Immunol. 2012;33(12):579-89.
523. Engelhardt B, Vajkoczy P, Weller RO. The movers and shapers in immune privilege of the CNS. Nat Immunol. 2017;18(2):123-31.
524. Mak IW, Evaniew N, Ghert M. Lost in translation: animal models and clinical trials in cancer treatment. American journal of translational research. 2014;6(2):114.
525. Gidday JM. Pharmacologic preconditioning: translating the promise. Transl Stroke Res. 2010;1(1):19-30.
526. Zhu J, Bengtsson B-O, Mix E, Thorell L-H, Olsson T, Link H. Effect of monoamine reuptake inhibiting antidepressants on major histocompatibility complex expression on macrophages in normal rats and rats with experimental allergic neuritis (EAN). Immunopharmacology. 1994;27(3):225-44.
527. Sacerdote P, Bianchi M, Panerai AE. In vivo and in vitro clomipramine treatment decreases the migration of macrophages in the rat. European journal of pharmacology. 1997;319(2-3):287-90.
528. Hwang J, Zheng LT, Ock J, Lee MG, Kim SH, Lee HW, et al. Inhibition of glial inflammatory activation and neurotoxicity by tricyclic antidepressants. Neuropharmacology. 2008;55(5):826-34.
529. Villeda SA, Luo J, Mosher KI, Zou B, Britschgi M, Bieri G, et al. The ageing systemic milieu negatively regulates neurogenesis and cognitive function. Nature. 2011;477(7362):90.

530. Ogunshola OO, Antic A, Donoghue MJ, Fan S-Y, Kim H, Stewart WB, et al. Paracrine and autocrine functions of neuronal vascular endothelial growth factor (VEGF) in the central nervous system. Journal of Biological Chemistry. 2002;277(13):11410-5.
531. Louveau A, Herz J, Alme MN, Salvador AF, Dong MQ, Viar KE, et al. CNS lymphatic drainage and neuroinflammation are regulated by meningeal lymphatic vasculature. Nat Neurosci. 2018;21(10):1380-91.
532. de Vos CC, Bom MJ, Vanneste S, Lenders MW, de Ridder D. Burst spinal cord stimulation evaluated in patients with failed back surgery syndrome and painful diabetic neuropathy. Neuromodulation. 2014;17(2):152-9.
533. Falowski SM, Moore GA, Cornidez EG, Hutcheson JK, Candido K, Peña I, et al. Improved Psychosocial and Functional Outcomes and Reduced Opioid Usage Following Burst Spinal Cord Stimulation. Neuromodulation: Technology at the Neural Interface. 2020.
534. Raoof R, Willemen H, Eijkelkamp N. Divergent roles of immune cells and their mediators in pain. Rheumatology (Oxford). 2018;57(3):429-40.
535. Lovato L, Willis SN, Rodig SJ, Caron T, Almendinger SE, Howell OW, et al. Related B cell clones populate the meninges and parenchyma of patients with multiple sclerosis. Brain. 2011;134(2):534-41.
536. Stern JN, Yaari G, Vander Heiden JA, Church G, Donahue WF, Hintzen RQ, et al. B cells populating the multiple sclerosis brain mature in the draining cervical lymph nodes. Science translational medicine. 2014;6(248):248ra107-248ra107.
537. Zsigmond P, Ljunggren SA, Ghafouri B. Proteomic Analysis of the Cerebrospinal Fluid in Patients With Essential Tremor Before and After Deep Brain Stimulation Surgery: A Pilot Study. Neuromodulation. 2019.
538. Sobsey CA, Ibrahim S, Richard VR, Gaspar V, Mitsa G, Lacasse V, et al. Targeted and Untargeted Proteomics Approaches in Biomarker Development. Proteomics. 2020;20(9):e1900029.
539. Sobsey CA, Ibrahim S, Richard VR, Gaspar V, Mitsa G, Lacasse V, et al. Targeted and Untargeted Proteomics Approaches in Biomarker Development. Proteomics. 2020;20(9):1900029.
540. Stenken JA, Poschenrieder AJ. Bioanalytical chemistry of cytokines--a review. Anal Chim Acta. 2015;853:95-115.
541. Mendoza-Porras O, Pires PR, Goswami H, Meirelles FV, Colgrave ML, Wijffels G. Cytokines in the grass, a lesson learnt: Measuring cytokines in plasma using multiple reaction monitoring mass spectrometry. Rapid Communications in Mass Spectrometry. 2020;34(9):e8723.
542. Izrael-Tomasevic A, Phu L, Phung QT, Lill JR, Arnott D. Targeting interferon alpha subtypes in serum: a comparison of analytical approaches to the detection and quantitation of proteins in complex biological matrices. Journal of proteome research. 2009;8(6):3132-40.
543. Duarte RV, Nevitt S, McNicol E, Taylor RS, Buchser E, North RB, et al. Systematic review and meta-analysis of placebo/sham controlled randomised trials of spinal cord stimulation for neuropathic pain. Pain. 2020;161(1):24-35.
544. Vallejo R, Gupta A, Kelley CA, Vallejo A, Rink J, Williams JM, et al. Effects of Phase Polarity and Charge Balance Spinal Cord Stimulation on Behavior and Gene Expression in a Rat Model of Neuropathic Pain. Neuromodulation. 2019.
545. Vallejo R, Kelley CA, Gupta A, Smith WJ, Vallejo A, Cedeño DL. Modulation of neuroglial interactions using differential target multiplexed spinal cord stimulation in an animal model of neuropathic pain. Molecular Pain. 2020;16.

546. Fishman MA, Calodney A, Kim P, Slezak J, Benyamin R, Rehman A, et al. Prospective, Multicenter Feasibility Study to Evaluate Differential Target Multiplexed Spinal Cord Stimulation Programming in Subjects With Chronic Intractable Back Pain With or Without Leg Pain. Pain Pract. 2020.
547. André N, Carré M, Pasquier E. Metronomics: towards personalized chemotherapy? Nature reviews Clinical oncology. 2014;11(7):413.
548. Quessy SN, Rowbotham MC. Placebo response in neuropathic pain trials. Pain. 2008;138(3):479-83.
549. Beard DJ CM, Blazeby JM et al. Considerations and Methods for Placebo Controls in Surgical Trials: State of the Art Review and ASPIRE Guidance. The Lancet. 2019;EPUB.
550. Schechter NL, Walco GA. The Potential Impact on Children of the CDC Guideline for Prescribing Opioids for Chronic Pain: Above All, Do No Harm. JAMA Pediatr. 2016;170(5):425-6.